

**Institut für Nutzpflanzenwissenschaften und Ressourcenschutz  
- Fachbereich Pflanzenernährung -**

---

**Genetic and physiological factors of ozone tolerance  
in rice (*Oryza sativa* L.)**

**Inaugural – Dissertation  
zur  
Erlangung des Grades**

**Doktor der Agrarwissenschaften  
(Dr. agr.)**

**der  
Landwirtschaftlichen Fakultät**

**der  
Rheinischen Friedrich-Wilhelms-Universität Bonn**

**von  
Yoshiaki Ueda**

**aus  
Okayama, Japan**

Referent:	Prof. Dr. Michael Frei
Koreferent:	Prof. Dr. Florian M. W. Grundler
Koreferent:	Prof. Dr. Kazuhiko Kobayashi
Fachnahes Mitglied:	Prof. Dr. Lukas Schreiber
Vorsitzender:	Prof. Dr. Mathias Becker
Tag der mündlichen Prüfung:	21.08.2015
Erscheinungsjahr:	2015

**Abstract**

Intensive human activities have contributed to the increase of tropospheric ozone. Ozone is toxic to plants and causes serious damage to crop production and global food supply. Therefore it is necessary to adapt crops to high ozone concentration to cope with increasing ozone concentrations and a growing demand for food. To investigate the tolerance mechanisms and genetic factors conferring ozone stress tolerance, reverse-genetic and forward-genetic studies have been conducted in rice (*Oryza sativa* L.), which serves as the staple crop for more than half of the global population.

In the reverse-genetics approach, a previously suggested candidate gene, an *OZONE-RESPONSIVE APOPLASTIC PROTEINI* (*OsORAPI*), was characterized regarding its involvement in ozone stress tolerance. Knock-out of *OsORAPI* led to the mitigation of leaf visible symptoms and lipid peroxidation formation under ozone stress. Gene expression levels of jasmonic acid (JA) marker genes were higher in the knock-out line. These results showed that *OsORAPI* is involved in the formation of leaf visible symptoms partly together with JA, which negatively regulates the cell death. Apoplastic localization of the protein was confirmed by transient expression of an *OsORAPI/GFP* fusion construct in *Nicotiana benthamiana* leaf epidermal cells. Sequence analysis revealed substantial polymorphisms in promoter sequences between susceptible Nipponbare and tolerant Kasalath cultivars. It reinforced the possibility that different promoter sequences were responsible for differential regulation of *OsORAPI* expression, which eventually led to contrasting ozone stress tolerance.

A genome-wide association study was conducted to explore novel genetic factors related to ozone stress tolerance. A mapping population comprising 328 rice accessions was subjected to season-long ozone fumigation, and nine traits were evaluated. A broad range of responses was observed among the population, as well as significant ozone effect. The subsequent mapping with more than 30,000 genetic markers yielded 16 significant markers applying the threshold of  $P < 0.0001$ . Detailed sequence analysis for the candidate genes for leaf visible symptom formation revealed significant linkage between amino acid polymorphisms in a conserved motif in *RING* gene and detected genetic markers.

In conclusion, a novel mechanism and candidate genetic loci for ozone tolerance in rice were identified. It will open the way for ozone-tolerant crop breeding.

## **Kurzfassung**

Intensive menschliche Aktivität hat zu erhöhter troposphärischer Ozonkonzentration geführt. Ozon verursacht verminderte Ernteerträge und bedroht folglich die Nahrungsmittelversorgung. Daher ist es dringend nötig Nutzpflanzen zu züchten, die tolerant gegen hohe Ozonkonzentrationen sind, um die stetig steigenden Ozonkonzentrationen und den wachsenden Bedarf an Nahrungsmitteln zu bewältigen. Um Toleranzmechanismen und genetische Faktoren zu erforschen, wurden reverse-genetische und forward-genetische Untersuchungen in Reispflanzen (*Oryza sativa* L.) durchgeführt, die das Hauptnahrungsmittel für mehr als die Hälfte der Weltbevölkerung darstellen.

In der reverse-genetischen Methode wurde ein auf Ozon reagierendes apoplastisches Protein1 (OsORAP1) im Rahmen von Ozontoleranz charakterisiert, das zuvor als ein Kandidat für Ozontoleranz vorgeschlagen wurde. Die Knockout-Linie zeigte weniger Blattschäden und eine niedrigere Bildung von reaktiven Sauerstoffspezies und damit höhere Ozontoleranz als der Wildtyp. Jasmonsäure (JA)-verwandte Gene wurden in der Knockout-Linie hochreguliert. Diese Ergebnisse implizierten, dass OsORAP1 an der Bildung von Blattschäden (d. h. Zelltod) beteiligt sein könnte, teilweise mit JA, die unter Ozon den Zelltod unterdrückt hat. Eine transiente Expression eines GFP Fusionproteins in *Nicotiana benthamiana* lokalisierte OsORAP1 im Apoplast. Eine Sequenzanalyse offenbarte, dass Promotorsequenzen von *OsORAP1* zwischen Nipponbare und Kasalath Kultursorten eventuell der Grund für die unterschiedlichen Ozontoleranzen sein könnten.

Eine genomweite Assoziationskartierung (GWAS) wurde durchgeführt um nach neuen genetischen Faktoren für die Ozonstresstoleranz zu suchen. Insgesamt wurden 328 Reissorten aus 77 Ländern einer erhöhten Ozonkonzentration ausgesetzt. Ein breites Spektrum von Phenotypen und signifikanten Ozoneffekten wurde beobachtet. Die folgende Kartierung mit mehr als 30.000 genetischen Markern identifizierte 16 signifikante Marker. Eine Sequenzanalyse von Kandidatengenomen deckte einen signifikanten Zusammenhang zwischen detektierten Markern und Aminosäure-Polymorphismen im konservierten Motiv des *RING* Gens auf.

Zusammenfassend lässt sich sagen, dass neue Mechanismen sowie Kandidatenloci für die Ozontoleranz aufgedeckt wurden. Diese Ergebnisse werden sehr hilfreich für die Züchtung ozontoleranter Nutzpflanzen sein.

## **Dedication**

I dedicate my thesis to my dearest family, who supported and encouraged me during my doctoral study in Germany. I would also like to dedicate my thesis to the late Prof. Dr. Haruto Sasaki (The University of Tokyo), who gave me great scientific inspirations and motivation on my research.

## Acknowledgments

Foremost, I would like to sincerely thank Prof. Dr. Michael Frei for providing me with the great opportunity to work under his supervision, as well as guiding me throughout the research and sharing scientific knowledge with me. I would also like to thank Prof. Dr. Florian Grundler for being my co-supervisor. I also thank him for sharing experimental facilities with me. I would like to thank Prof. Dr. Kazuhiko Kobayashi for reading and giving comments on my thesis, despite a short notice. My gratitude also goes to Prof. Dr. Lukas Schreiber for accepting my request to be in the committee. I also would like to thank Prof. Dr. Mathias Becker for his contribution as the chairman.

My sincere thank also goes to the workers and students of Molecular Phytomedicine group, especially Dr. Shahid Siddique, for sharing their experimental technique and knowledge. Philipp Gutbrod helped me with cloning and bacteria transformation. Zoran Radakovic showed me basic handling of *Arabidopsis* plants. Julia Holbein helped me with confocal microscopy. I would like to thank many other people that I could not mention here due to the limitations of space.

I would also like to express my warm thanks to Prof. Dr. Thorsten Kraska and the technical staffs at the Campus Klein-Altendorf of University of Bonn. The genome-wide association study would not have been possible without the most-advanced facility and their continuous support.

Prof. Dr. Matthias Wissuwa helped me during my stay in IRRI and field phenotyping training. I would also like to send my thanks to him for the introduction of the association mapping. I would also like to thank Jae-Sung Lee, who worked with me in the laboratory and field at IRRI and supported my stay.

My gratitude also goes to Prof. Dr. Andreas Meyer and Dr. Isabel Aller, who helped me with bioinformatic and phylogenetic analyses.

I would like to express my sincere appreciation to Benedict Chijioke Oyiga and Shree Pariyar, with whom I made many discussions about the association mapping. We also exchanged our knowledge and ideas, through which I obtained some new inspirations on my study.

Finally but not least, I would like to thank the workers in Pflanzenernährung for support in experiments and facility. Especially I would like to send gratitude to the colleagues in our group, Dr. João Abreu Neto, Dr. Stefanie Höller and Linbo Wu, for

## Acknowledgments

---

scientific discussions, supports with experiments and critical comments on my thesis. I really appreciate this small, hard-working and efficient group. Elsa Matthus gave me precious comments with deep insight. Felix Frimpong, Yitao Qi and Shangkun Lai made enormous contribution for the mapping study. Vitalij Dombinov shared his experiences with *Arabidopsis* transformation with me. Asis Shrestha conducted a biochemical analysis for me. David Sayaogo also helped me in the laboratory and the greenhouse. I am really grateful for the help that I received during my study.

## **Erklärung**

Ich versichere, dass ich diese Arbeit selbständig verfasst habe, keine anderen als die angegebenen Hilfsmittel benutzt und die Stellen der Arbeit, die anderen Werken dem Wortlaut oder dem Sinn nach entnommen sind, kenntlich gemacht habe.

Diese Arbeit hat in gleicher oder ähnlicher Form keiner anderen Prüfungsbehörde vorgelegen.

Bonn, den

Yoshiaki Ueda

Unterschrift



---

## Table of Contents

Abstract.....	i
Acknowledgments .....	iv
Erklärung .....	vi
Table of Contents.....	vii
List of Figures.....	ix
List of Tables .....	xi
List of Abbreviations .....	xiii
Chapter 1 General Introduction .....	1
1. The threat of tropospheric ozone .....	1
2. Rice: the most important staple crop with great diversity .....	5
3. Ozone tolerance mechanisms .....	8
4. Genetic mapping of ozone stress tolerance .....	15
5. Aims of this study.....	18
References.....	23
Chapter 2 Comparison of two high-throughput ascorbate measurements.....	32
Abstract.....	32
1. Introduction.....	33
2. Materials and Methods .....	35
3. Results and Discussion .....	39
4. Conclusions .....	48
References.....	49
Chapter 3 A novel gene <i>OsORAPI</i> enhances cell death in ozone stress in rice.....	52
Abstract.....	52
1. Introduction.....	53

## Table of Contents

---

2. Materials and Methods .....	56
3. Results .....	63
4. Discussion.....	79
5. Conclusions and Outlook.....	83
References.....	86
Chapter 4 Identification of novel loci involved in ozone stress tolerance in rice.....	93
Abstract.....	93
1. Introduction.....	94
2. Materials and Methods .....	96
3. Results .....	101
4. Discussion.....	114
References.....	119
Chapter 5 General Discussion .....	124
1. Novel mechanisms and genetic loci for ozone tolerance in rice .....	124
2. Future perspectives .....	131
3. How can crop breeding contribute to future global food security? .....	134
References.....	150
Summary of the thesis .....	154
Appendices .....	168
Peer-review publications .....	250
Other scientific activities .....	252
Curriculum Vitae .....	253

---

## List of Figures

Figure 1-1: Estimated increase of ozone concentration by 2050 compared with that of 2005 in the worst scenario. ....	2
Figure 1-2: Subpopulation structure of <i>Oryza sativa</i> . ....	7
Figure 1-3: Scheme of Halliwell-Asada cycle and other antioxidant systems in cytosol and apoplast. ....	10
Figure 1-4: Two QTLs affecting leaf symptom formation under ozone stress and their effect in rice. ....	17
Figure 1-5: Rice population used for the mapping in Zhao <i>et al.</i> (2011). ....	21
Figure 2-1: Correlation between standard AsA concentration and measured AsA concentration. ....	41
Figure 2-2: Standard curve generated by the DPD method. ....	41
Figure 2-3: Absorbance spectrum of red cabbage sample and three AsA standards subjected to the DPD assay compared with blank samples. ....	44
Figure 2-4: Correlation of reduced and total AsA values of rice samples obtained from an iron stress experiment using two analysis methods. ....	46
Figure 3-1: Bioinformatic and physiological analysis of OsORAP1. ....	65
Figure 3-2: Expression analysis of <i>OsORAP1</i> , two other ascorbate oxidase (AO) genes, and a microRNA, <i>Osmir528</i> . ....	67
Figure 3-3: Formation of leaf visible symptoms and biochemical parameters in three rice lines. ....	69
Figure 3-4: Effects of ozone on stomatal conductance and growth characteristics. ....	70
Figure 3-5: Measures of oxidative stress in three rice lines. ....	72
Figure 3-6: Ascorbate oxidase (AO) activity. ....	73
Figure 3-7: Apoplastic ascorbate content and redox status. ....	76
Figure 3-8: Involvement of OsORAP1 in phytohormone signalling. ....	78
Figure 3-9: Sequence comparison of OsORAP1 of Nipponbare and Kasalath rice cultivars. ....	76
Figure 3-10: Proposed mode of action of OsORAP1 in rice. ....	83
Figure 4-1: Box plots for relative phenotypic values. ....	102
Figure 4-2: Association mapping result for square-root transformed leaf bronzing score (t-LBS). ....	105

List of Figures

---

Figure 4-3: Association mapping result for relative dry weight (DW). ..... 107

Figure 4-4: Association mapping results for relative single panicle weight (SPW)... 108

Figure 4-5: Sequence variation of *EREBP* (*LOC\_Os05g29810*). ..... 110

Figure 4-6: Analysis of *RING* (*LOC\_Os05g29710*)..... 112

Figure 5-1: History of subpopulation divergence of rice..... 128

Figure 5-2: Manhattan plots in the neighbouring regions of previously identified QTLs.  
..... 130

Figure 5-3: Transition of production and prices of rice since 1961 (adopted from  
Khush, 2001)..... 135

Figure 5-4: Correlation between relative shoot dry weight (x-axis) and relative total  
panicle weight (y-axis). ..... 137

---

## List of Tables

Table 2-1: Effects of different extraction solvents on the consistency between two ascorbate analysis methods and the stability of ascorbate during storage on ice. ....	40
Table 2-2: Recovery rates of reduced and total AsA in samples spiked with internal standards. ....	42
Table 2-3: AsA concentration measured with two analysis methods. ....	43
Table 2-4: Effects of interfering pigments on ascorbate analysis in red cabbage samples using two analysis methods. ....	44
Table 2-5: Effects of iron on the consistency of ascorbate measurements in dilution experiments. ....	47
Table 2-6: Recovery rates in spiking experiments using AsA extracts obtained from rice plants exposed to iron stress and control plants. ....	47
Table 4-1: Effect of ozone stress on phenotypic values. ....	102
Table 4-2: Correlation coefficient and <i>P</i> value of pair-wise comparison of each phenotype. ....	103
Table 5-1: Origin of accessions in each subpopulation in the mapping population used in Chapter 4. ....	129
Table 5-2: Number of differentially regulated genes between Nipponbare and SL41. ....	133
Table 5-3: Number of differentially regulated genes between Nipponbare and SL46. ....	133
Table 5-4 Enriched gene ontology (GO) terms from the genes down-regulated in SL41. ....	138
Table 5-5 Enriched gene ontology (GO) terms from the genes up-regulated in SL41. ....	141
Table 5-6 Enriched gene ontology (GO) terms from the genes showing a significant interaction between genotype and treatment between Nipponbare and SL41. ....	142
Table 5-7 Enriched gene ontology (GO) terms from the genes down-regulated in SL46. ....	145
Table 5-8 Enriched gene ontology (GO) terms from the genes up-regulated in SL46. ....	147

Table 5-9 Enriched gene ontology (GO) terms from the genes showing a significant interaction between genotype and treatment between Nipponbare and SL46..... 148

**List of Abbreviations**

ACO	aminocyclopropane-1-carboxylic acid oxidase
ACS	aminocyclopropane-1-carboxylic acid synthase
AO	ascorbate oxidase
AOT40	accumulated ozone exposure over a threshold of 40 ppb
AsA	ascorbate
CSSL	chromosome segment substitution line
DHA	dehydroascorbate
DMF	dimethylformamide
DPD	2, 2'-dipyridyl
DTT	dithiothreitol
DW	dry weight
EREBP	ethylene-responsive element binding protein
ET	ethylene
FW	fresh weight
GLM	general linear model
GO	gene ontology
GWAS	genome-wide association study
HR	hypersensitive response
IWF	intercellular washing fluid
JA	jasmonic acid
KO	knock-out line
LBS	leaf bronzing score
LD	linkage disequilibrium
MAF	minor allele frequency
MDA	malondialdehyde

## List of Abbreviations

---

MLM	mixed linear model
MPA	metaphosphoric acid
NEM	<i>N</i> -ethylmaleimide
OE	over-expression line
ORAP1	OZONE-RESPONSIVE APOPLASTIC PROTEIN1
PCA	principal component analysis
PCD	programmed cell death
PSII	photosystem II
RING	really interesting new gene
ROS	reactive oxygen species
Rubisco	1,5-bisphosphate carboxylase/oxygenase
QQ plot	quantile-quantile plot
QTL	quantitative trait locus
SA	salicylic acid
SNP	single-nucleotide polymorphism
TCA	trichloroacetic acid
TGAL	thioglycolic acid lignin
TKW	thousand kernel weight
t-LBS	square-root transformed leaf bronzing score
TPW	total panicle weight
SPW	single panicle weight



# Chapter 1

## General Introduction

### 1. The threat of tropospheric ozone

Human activity causes many effects on the surrounding environment. Since the industrial era, water, soil and air have been changing in an unprecedented speed ever in the human history. Most of the consequences of human activities lead to unfavourable effect, which is acknowledged as environmental pollution, and this in turn causes serious problems to human life. One of the most serious environmental pollutions emerging these years is tropospheric ozone (Akimoto, 2003).

Ozone is formed by photochemical reactions from oxidized nitrogen ( $\text{NO}_x$ , including  $\text{NO}$  and  $\text{NO}_2$ ), carbon monoxide ( $\text{CO}$ ) and volatile organic compounds (VOCs) such as methane, all of which are contained in exhaust gas from transportations and industries (Yamaji *et al.*, 2006). While ozone concentration in the stratosphere (which is termed ‘good ozone’ due to the capacity to block harmful ultraviolet-B radiation from the space) is decreasing, the ozone concentration in the troposphere (termed ‘bad ozone’) has been rising since the last century, which is ascribed to the elevated anthropogenic gas emission (Donahue, 2011). For instance, the emission of  $\text{NO}_x$  is estimated to double by 2020 compared with 1990 in some areas (Streets and Waldhoff, 2000), and this increase of  $\text{NO}_x$  emission is considered to be the main contributor to the increase of ozone concentration in the troposphere. This elevated anthropogenic gas emission has led to the current background concentration of nearly 90 ppb in some areas in the summer season (Yamaji *et al.*, 2006), which is considerably higher than that of the beginning of the 20th century (less than 20 ppb) (Vingarzan, 2004). The current anthropogenic gas emission will further exacerbate the situation in the future. Dentener *et al.* (2006) estimated the current and future increase of ozone concentration in the troposphere as 2 to 4 ppb per year depending on the extent of anthropogenic gas emission and air quality legislations. Large increase of ozone concentration is

expected in Asian countries, especially in South Asia and China (Fig. 1-1). These are highly developing areas and the precursor gas emission is also dramatically growing.

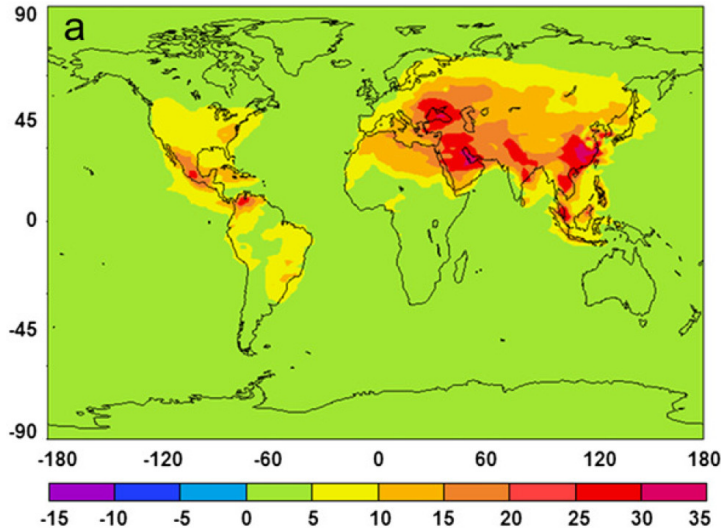


Figure 1-1: Estimated increase of ozone concentration by 2050 compared with that of 2005 in the worst scenario (Lei *et al.*, 2013). The below bar shows the extent of concentration shift (unit, ppb).

Tropospheric ozone is harmful for living organisms. For human bodies, high tropospheric ozone concentration causes respiratory diseases, asthma, increased allergy and higher mortality rate (Sheffield *et al.*, 2011; Shiraiwa *et al.*, 2011; Orru *et al.*, 2013). For plants and natural vegetation, negative effects caused by ozone encompass multiple levels. At the plant community and ecosystem level, elevated tropospheric ozone causes lower biomass production, which derives from impaired CO<sub>2</sub> assimilation rate due to closure of stomata and dysfunction of photosynthetic apparatus (Ainsworth *et al.*, 2012). This loss of CO<sub>2</sub> fixation, together with impaired carbon sequestration to the soil (Loya *et al.*, 2003), affects the global carbon cycle. It leads to the increase of CO<sub>2</sub> in the atmosphere, which might accelerate global warming and further climate change (Ainsworth *et al.*, 2012). At the individual plant level, ozone causes cell death and alteration in the chemical composition, as well as negative effects on the biomass production (Frei *et al.*, 2011; Wang and Frei, 2011). These affected plants, especially in case of agricultural crops, cause decline of crop quality and hence detrimental economic losses (discussed later). For example, cereals and legume crops generally have higher protein concentration in the harvested fraction

under ozone stress compared with the control condition (Wang and Frei, 2011). This is not favourable since high protein content in grain leads to the deterioration of the taste, for example, in rice (Matsuzaki *et al.*, 1973).

The impacts of elevated tropospheric ozone concentration on plants have been estimated by modelling studies. It has been known that the dose of ozone and the effects on plants have positive correlation. In crop fields and forest, an index which shows a good applicability for the assessment of the extent of impact caused by ozone is ‘accumulated ozone exposure over a threshold 40 ppb (AOT40)’. The index AOT40 and the relative crop yield show strong negative correlations (Mills *et al.*, 2007), and therefore, is used frequently for the modelling. In this model, ozone concentration up to 40 ppb is not considered to have any effects on plants, and the concentration above 40 ppb is summed up over time to estimate the impact of ozone. In other words, it is deduced that the critical effect of ozone begins to emerge above 40 ppb. In recent years, the average concentration has by far exceeded this threshold, which readily implies the presence of toxicity to vegetation. Indeed, in urban areas, one can already see detrimental effects of tropospheric ozone on vegetation (Feng *et al.*, 2014). Teixeira *et al.* (2011) conducted yield prediction modelling in four major crops. In their research, it was illustrated that more than 10% of crop yield might be lost because of high tropospheric ozone in some areas. Especially in China and India, which are responsible for almost 50% of world’s rice production, more than 10 million t is estimated to be lost every year in each country. These crop losses lead to economic damage, as well as food shortage. Van Dingenen *et al.* (2009) estimated that the global economic loss of crops caused by elevated tropospheric ozone is 14-26 billion USD annually.

In the light of global population growth and increasing hunger, it is becoming of utmost importance to keep enough supply of food for the growing demands. Due to the shift of dieting habits and increasing population, which is expected to reach 9 billion (FAO STAT, <http://faostat3.fao.org/home/E>, as of November 2014), the demand for food supply is expected to double by 2050 (Tilman *et al.*, 2011). Moreover, the demand for high yield is growing also because of the shrinking area of the earth surface suitable for cropping. Many adverse environmental conditions (*e.g.* drought and nutrient toxicity/deficiency) and too intensive agricultural systems have been limiting the productivity and lessening the available land surface for agriculture (Foley

*et al.*, 2005). Current rice production is only achieved less than 45% of the maximum capacity, partly due to environmental constraints (Mueller *et al.*, 2012). Considering the large amount of crop loss due to elevated tropospheric ozone, much potential is left to improve food supply by coping with the huge impact of ozone on cropping or mitigating the effect of tropospheric ozone on farms. Therefore, the adaptation of agricultural crops for high tropospheric ozone concentration, which accounts for fairly large amount of crop losses, is becoming urgently necessary.

## **2. Rice: the most important staple crop with great diversity**

Rice is classified in genus *Oryza* in the grass family (Wang *et al.*, 2006). Among the *Oryza* genus, two species, namely Asian rice (*O. sativa*) and African rice (*O. glaberrima*), are two domesticated species (Wang *et al.*, 2006). *O. sativa* is widespread around the world and constitutes most of the cultivated rice. On the other hand, *O. glaberrima* is a perennial species grown only in West Africa\* (Juliano, 1993; Linares, 2002). Rice has been grown as a crop since prehistoric time for approximately 10,000 years (Jiang and Liu, 2006), feeding people longer than any other crop species (Maclean *et al.*, 2002). It is suitable as a staple crop for many reasons: (i) it has high yield capacity (reaching nearly 10 t/ha in optimal conditions), implying that a large number of people can be fed with smaller field area; (ii) it has many diverse cultivars adapted to many climate conditions, enabling the cultivation in many parts of the world; and (iii) it is abundant in protein (around 7 to 8% in milled rice) and micronutrients such as vitamin B, vitamin E, zinc and iron, providing people with sufficient nutrients (Juliano, 1993). The annual production of rice sums up to 750 million t in 2013 (FAO STAT), which is the third greatest yield among the cereal crops, next to wheat and maize. Nowadays, grown in more than 110 countries in the world, it stands as the staple crop for more than half of the world's population (Maclean *et al.*, 2002). It is an important crop also because of usability of the straw. The rice straw can be used as a material for handcrafts or houses, and it also plays a role as feed for livestock. For example, the rice straw is fed to more than 90% of ruminants in Asia (Devendra and Sevilla, 2002), which demonstrates a highly important role of rice straw in livestock farming in this area. Thus, it is clear that rice is the most important crop in the world, not only as a food supporting a huge population in large area of the Earth but also as an important resource for humans and livestock.

The origin of the cultivated rice is estimated to be South China, near the middle area of the Pearl River, considering the genetic architectures of the wild rice and domesticated rice (Huang *et al.*, 2012). First, a certain group of wild rice (*O. rufipogon*) acquired/lost some important traits, such as self-crossing habit, grain size

---

\* Therefore 'rice' refers to *O. sativa* hereafter unless otherwise mentioned.

and shattering habit. Hereby the domestication began, which is the origin of, as currently known, the *japonica* subgroup of rice. After that, these *japonica* rice cultivars were crossed with another type of *O. rufipogon* in South and Southeast Asia and developed into the currently known *indica* subgroup. Subsequently, each of the *japonica* and *indica* subgroups developed into several subpopulations (discussed later). Nowadays, more than 100,000 types of rice are stored in the gene bank of the International Rice Research Institute (IRRI) (IRRI website, <http://irri.org/our-work/research/genetic-diversity/international-rice-genebank>, as of November 2014). This number is considerably greater than the current maize seed bank resources (28,000 samples, CYMMT website, <http://www.cimmyt.org/en/germplasm-bank>, as of November 2014). Hence, rice is one of the most diverse crop species, which was probably achieved by the outcrossing habit of ancestor species (Kovach *et al.*, 2007), broad geographical distribution and long history of cultivation.

In addition to the fact that rice is a staple crop with utmost importance, it has relatively small genome size. The rice genome is diploid and has a total genome size of 389 Mb (in the cultivar Nipponbare), which is considerably smaller compared with other crops; tetraploid maize (*Zea mays*) has 2,500 Mb, and hexaploid wheat (*Triticum aestivum*) has 17,000 Mb (Feuillet *et al.*, 2011). It urged the researchers to determine the complete genomic code of rice for the first time in any crop species in 2005 (International Rice Genome Sequencing Project, 2005). It opened the era for functional genomics research in rice. Nowadays, in the time of post-genome era, population genetics and exploitation of diverse cultivars have been acknowledged as highly important for deeper understanding of the species (Li and Zhang, 2013). In 2005, 234 rice cultivars were genotyped by simple sequence repeats markers and it revealed existence of five subpopulations in rice: *aus*, *indica*, *aromatic*, *temperate japonica*, and *tropical japonica* (Fig. 1-2, the first two belong to *indica* subgroup and the latter three belong to *japonica* subgroup; Garris *et al.*, 2005). Recently, approximately 3,000 rice cultivars were completely *de novo* sequenced, through which complex genetic architecture, genetic diversity and evolutionary history have been elucidated (The 3,000 rice genomes project, 2014).

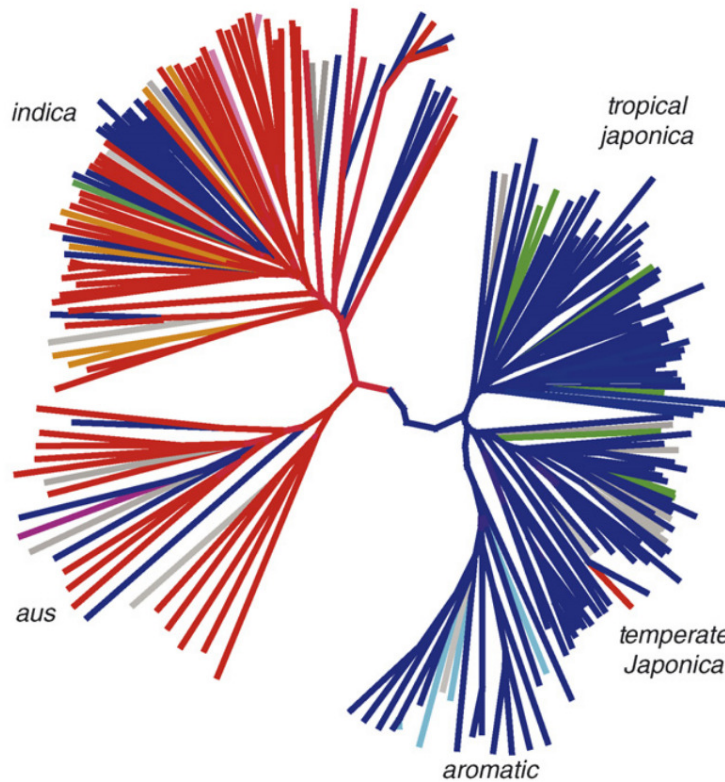


Figure 1-2: Subpopulation structure of *Oryza sativa* (taken from Kovach *et al.*, 2007). Unrooted neighbour-joining tree was constructed based on 169 markers from 234 *O. sativa* cultivars. Five main subpopulations of rice are shown. The subpopulations *indica* and *aus* belong to *indica* subgroup, and the subpopulations *aromatic*, *tropical japonica* and *temperate japonica* belong to *japonica* subgroup. The branch colour represents the chloroplast haplotype.

Thus, rice is the most important crop in the world with great genetic diversity, which implies the large potential for investigations and exploitation of resources. Moreover, many diverse sources of information and tools to handle rice genomics and genetics have become available, and it opened the ways for in-depth investigations. Therefore, rice also serves as a crop with the most powerful and suitable material for investigations of genetic information, not to mention the importance as the food which supports a large population.

### 3. Ozone tolerance mechanisms

The effect of ozone on plants has been investigated for more than a century. It was more than 150 years ago that the toxicity of ozone was first acknowledged in plants. Lea (1864) observed that barley seedlings grew more slowly and the gravitropism was disrupted under an ozone atmosphere. Nearly a century later, a significant impact of tropospheric ozone on crop vegetation was proposed by Middleton (1956) and Middleton *et al.* (1958), when atmospheric pollution was becoming a serious problem in developed countries, causing substantial economic losses. At this point, major important findings were already made: (i) there were differences in the extent of damage among cultivars (*i.e.* genotypic differences); (ii) the effect on biomass and leaf visible symptom formation did not necessarily correlate (*i.e.* they are under different regulations); and (iii) the extent of symptoms and ozone concentration showed positive linear correlation (*i.e.* dose-dependency of ozone effect) (Middleton, 1956), all of which are the basis for the present-day research.

Investigations on the molecular level have been also conducted since the end of the 20th century. Since ozone is a gaseous substance, it is mainly taken up by plants through the stomata (Omasa *et al.*, 2002). Ozone in the stomatal pore is quickly degraded into other substances, as shown by quasi-0 ozone concentration in the stomatal pore (Laisk *et al.*, 1989). The toxicity of ozone derives from the free radicals formed after the degradation of ozone in the apoplast. Upon deposition of ozone in the apoplast, many kinds of highly reactive substances are produced. These molecules are termed reactive oxygen species (ROS). ROS include hydrogen peroxide ( $H_2O_2$ ), superoxide anion radical ( $O_2^{\bullet-}$ ), hydroxyl radical ( $OH^{\bullet}$ ) and many other reactive molecules including ozone itself. As the name implies, these molecules are highly reactive and cause changes in the chemical and physical composition of attacked molecules. For instance, ozone damages the lipids constituting cell membranes (Luwe *et al.*, 1993), thus leading to loss of membrane functions such as fluidity and permeability (Nouchi, 2002). ROS are also capable of degrading proteins and cleaving DNA (Thompson *et al.*, 1987). These types of damage do not only originate from incoming ozone itself, since ozone causes accumulation of secondary ROS, which further damage biomolecules (Ueda *et al.*, 2013). ROS also react with other molecules in the apoplast such as lignin precursors. ROS deprive lignin precursors of hydrogen, thus enabling coupling of these precursors into polymers (Frei, 2013). The increase of



lignin gives rigidity to cell walls, but it also leads to brittleness of the plant tissue. It may affect a plant's susceptibility to mechanical damage (Frei, 2013).

Considering these facts, it is highly important to efficiently scavenge ROS under ozone stress to cope with the incoming stress through both enzymatic and non-enzymatic pathways. Molecules reducing oxidative stress are termed antioxidants. Antioxidants usually deprive ROS of excessive electrons, thereby rendering more stable molecules and removing the toxicity of ROS. One of the most important antioxidants is ascorbate (AsA). AsA has two hydroxyl groups (–OH) and is capable of donating two electrons, producing two keton groups (=O). It is hydrophilic and soluble in water, and exists in many compartments of the cells. AsA has higher reactivity to ozone than lipids, which means that AsA can exhibit a protective role against the damage to lipid caused by ozone (Urbach *et al.*, 1990). It functions as an effective radical scavenger by being a part of 'Halliwell-Asada cycle' (also termed 'ascorbate-glutathione cycle'), which is a system in living organisms to avoid excessive oxidative stress (Fig. 1-3; Asada, 1999). It is a cycle in which toxic H<sub>2</sub>O<sub>2</sub> can be detoxified to water via the aid of AsA and glutathione, which was proposed by Foyer and Halliwell in 1976 (Foyer and Halliwell, 1976), and has been considered one of the most important metabolite cycles to remove excessive ROS under a variety of stress conditions (Asada, 1999).

The importance of AsA as a factor conferring stress tolerance to ozone has been known for a long time. It was already shown in the middle of the last century that exogenous application of AsA to plants resulted in partial or complete mitigation of foliar injury under elevated ozone concentrations (Freebairn, 1960; Menser, 1964), implying a positive effect of AsA for ozone tolerance in plant species. Later on, the importance of AsA under ozone stress was also demonstrated by the use of forward genetics. One *Arabidopsis* (*Arabidopsis thaliana*) mutant showing extreme sensitivity to ozone, which was named *SOZI* (sensitive to ozone), was shown to have lower AsA content compared with the wildtype (Conklin *et al.*, 1996). Later, *SOZI* locus, which was renamed *VTCl* (vitamin C), turned out to code a GDP-D-mannose pyrophosphorylase, which is one of the enzymes involved in AsA biosynthesis (Conklin *et al.*, 1997). The subsequent analyses using other AsA deficient mutants, *vtc2*, *vtc3* and *vtc4*, showed higher susceptibility to ozone in these mutants, which all had less than 50% of AsA content compared with the wildtype (Conklin *et al.*, 2000).

This further proved the importance of AsA to cope with ozone stress. The capacity of AsA to confer ozone stress tolerance has also been confirmed in other plant species by altering AsA concentration via reverse-genetic approaches (Frei *et al.*, 2012).

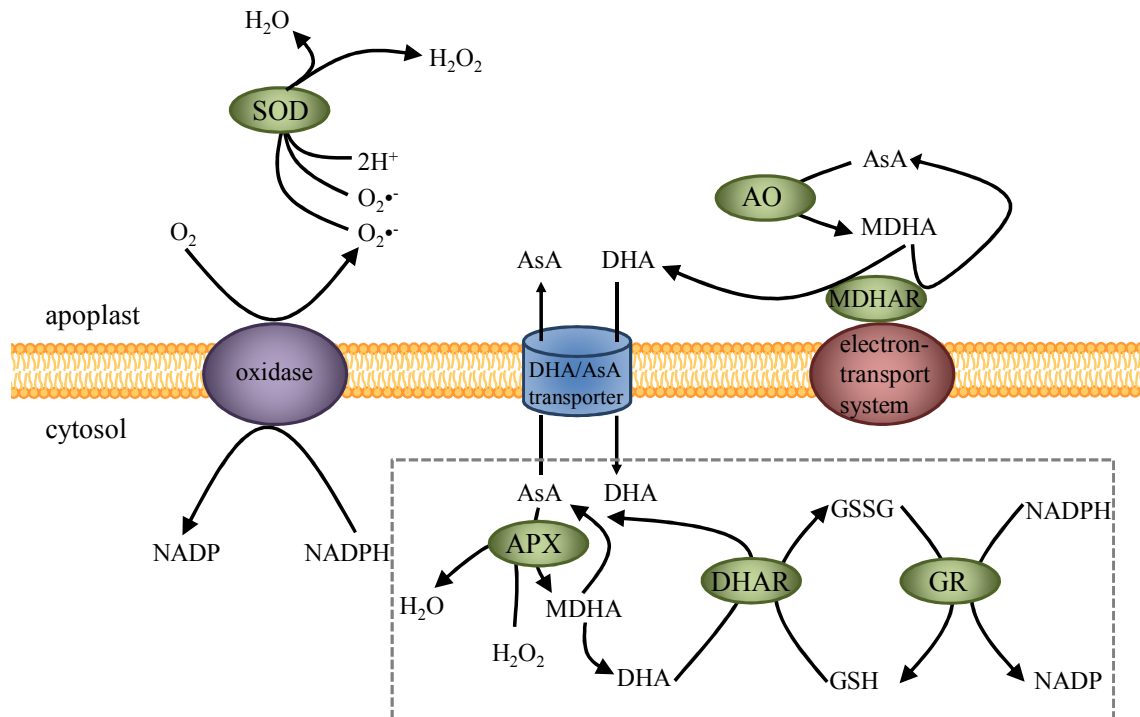


Figure 1-3: Scheme of Halliwell-Asada cycle (surrounded by the gray dashed square) and other antioxidant systems in cytosol and apoplast (modified after Pignocchi and Foyer, 2003). AO, ascorbate oxidase; APX, ascorbate peroxidase; AsA, reduced ascorbate; DHA, dehydroascorbate; DHAR, dehydroascorbate reductase; GR, glutathione reductase; GSH, reduced glutathione; GSSG, oxidized glutathione; MDHA, monodehydroascorbate; MDHAR, monodehydroascorbate reductase; and SOD, superoxide dismutase.

AsA exists in many compartments of plant cells. The apoplast also contains fairly high concentration (mM order) of AsA (Horemans *et al.*, 2000). Moreover, the apoplastic space is void of NADPH, which is an indispensable factor in Halliwell-Asada cycle, although other ROS scavenging enzymes such as superoxide dismutase, ascorbate peroxidase, monodehydroascorbate reductase, dehydroascorbate reductase and glutathione reductase seem to be present in the apoplast (Vanacker *et al.*, 1998; Pignocchi and Foyer, 2003). Therefore, it can be deduced that AsA, not glutathione or other antioxidant enzymes, determines the extent of ozone detoxification in the

apoplast because Halliwell-Asada cycle apparently is not functional in the apoplast due to lack of NADPH. Together with the fact that ozone enters plants through stomata and that the apoplastic space is the first cellular compartment to encounter ozone, it is conceivable that the apoplastic AsA could be a crucial factor determining ozone stress tolerance. This concept has been confirmed by many different approaches. From the physiological aspect, Luwe *et al.* (1993) experimentally showed that apoplastic AsA was oxidized after ozone fumigation and that reduced AsA detoxified the incoming ozone in the apoplast. In a more recent physiological study, Feng *et al.* (2010) compared two wheat cultivars showing contrasting tolerance to elevated ozone concentration. Through this study, it was found that the cultivar with higher apoplastic AsA showed higher tolerance to chronic ozone stress, demonstrating the role of apoplastic AsA as a determinant factor for ozone stress tolerance. Turcsányi *et al.* (2000) employed a physicochemical modelling approach and demonstrated that 30 to 40% of incoming ozone was detoxified by apoplastic AsA in *Vicia faba*. In another approach using reverse-genetics, Sanmartin *et al.* (2003) successfully modified the content and the redox status of apoplastic AsA by introducing an ascorbate oxidase (AO) gene into tobacco plants. The over-expression plants showed increase of AO activity and depletion of reduced AsA in the apoplast, which led to higher susceptibility to ozone in terms of leaf visible injury and photosynthetic activity. All these studies have led to the current consensus; the ozone is detoxified in the apoplast by AsA and it determines the extent of stress to plants.

As stated above, the formation of leaf visible symptoms is one of the unique reactions that ozone triggers in plants. It is also of high importance in agriculture, since the leaf visible symptoms can cause detrimental effects on the quality and production of leafy vegetables, forage crops, and ornamental plants (Middleton, 1956). Leaf visible symptoms under ozone stress in plants usually occur in the form of unevenly distributed small spot-like lesions, which often appear along veins (Wohlgemuth *et al.*, 2002), while some plant species show chlorotic leaf symptoms and bleaching (Langebartels *et al.*, 2002). The former type of symptoms resembles the ones developed during incompatible pathogen infection (Wohlgemuth *et al.*, 2002), which induces hypersensitive response (HR). HR is a reaction induced upon attack of incompatible pathogen and is characterized by programmed cell death in the infected leaves. In addition to the above-mentioned cell death, the similarity between ozone

stress and pathogen infection can be also portrayed from other perspectives, such as the induction of pathogenesis-related genes (PR genes) and production of ROS (Heath, 2000; Rao *et al.*, 2000). Schraudner *et al.* (1992) found that two of the PR genes, namely  $\beta$ -1,3-glucanase and chitinase, were induced under ozone stress in tobacco plants. Rao *et al.* (2000) noted that ROS formation, especially in the apoplast, is a specific characteristic common to both ozone stress (which directly induces apoplastic ROS) and pathogen infection. As a consequence of these similarities, enhanced pathogen tolerance was observed in ozone-treated plants (Yalpani *et al.*, 1994). However, these efforts linking ozone stress and pathogen infection have not completely elucidated specific mechanisms for ozone stress tolerance or the target genes for future crop breeding.

In more recent years, the mechanisms of cell death under ozone stress have been elucidated through intensive research by Kangasjärvi *et al.* (2005) in the model plant *Arabidopsis*. Plant hormones are major factors participating in the response to ozone and formation of visible symptoms. Especially, ethylene (ET), salicylic acid (SA), and jasmonic acid (JA) play crucial roles in the signal transduction and cell death formation under ozone stress. The involvement of these plant hormones has been shown by using hormone-insensitive or hormone-overproducer mutant lines (Overmyer *et al.*, 2000; Rao and Davis, 2001; Kangasjärvi *et al.*, 2005). It is generally agreed that SA and ET stimulate the propagation of cell death, while JA contains cell death (Rao and Davis, 2001; Kangasjärvi *et al.*, 2005). These regulation systems involve gene expression reprogramming. Since ozone first attacks the apoplastic space of the plant cells, it has to be transmitted to the nuclei and cellular organelles to facilitate proper acclimation/resistance such as changes of gene expression and photosynthetic properties. Several possible modes of action have been proposed to date: (i) direct transport of ROS, especially hydrogen peroxide, which has long life (approximately 1 ms) and small molecule size (Petrov and Van Breusegem, 2012), into the cytosol from the apoplast through aquaporins (Bienert and Chaumont, 2014); (ii) recognition of the overall redox status of antioxidants (*e.g.* AsA) in the apoplast (Munné-Bosch *et al.*, 2012); (iii) involvement of receptor-like protein kinases on the plasma membrane, which transmits the external environmental status towards inside via phosphorylation (Wrzaczek *et al.*, 2010); (iv) oxidative damage of membranes (Mueller and Berger, 2009); and (v) retrograde signalling from the plastids to the

nuclei (Baier and Dietz, 2005). To date, the involvement of these components are not clarified yet and no consensus has been claimed yet, although they are not mutually exclusive.

Contrary to the intensive exploration on the mechanisms of leaf visible symptoms, the physiological mechanisms of reduced biomass and grain yield under ozone stress have not been well described to date. Although some cultivars are more tolerant than others under ozone stress in terms of biomass production (*i.e.* the biomass production of some cultivars is less vulnerable to ozone stress; Frei *et al.*, 2008; Sawada and Kohno, 2009), few candidate genes for this trait have been proposed to date. In rice, Tsukahara *et al.* (2013) conducted a QTL mapping study and suggested an *ABERRANT PANICLE ORGANIZATION 1 (APO1)* as the candidate gene for total grain yield loss under chronic ozone stress. *APO1*, which codes an F-box protein, was implied to affect the grain yield by controlling the primary rachis branch formation, and it showed contrasting expression patterns between the tolerant and the susceptible cultivars (Tsukahara *et al.*, 2013). Notably, the total grain yield was decreased although the total biomass production and photosynthesis rate were not substantially affected by ozone treatment in the study by Tsukahara *et al.* In another study, Shi *et al.* (2009) observed that the reduced rice grain yield under ozone stress was ascribed to decreased spikelets number per panicle, rather than the number of panicle or single grain mass. These studies imply that different resource allocation, rather than source limitation, determines the grain yield under ozone stress in rice. Some studies with the model plant *Arabidopsis* showed that the resource distribution under adverse conditions is responsible for determining biomass production, since the total available energy is limited (Lozano-Durán and Zipfel, 2015). A study by Todesco *et al.* (2010) identified an *ACCELERATED CELL DEATH 6 (ACD6)* gene, which confers broad-range biotic stress tolerance at the cost of retarded growth. The study by Todesco *et al.* illustrated plants' adaptive mechanism between vigorous growth and protection against pathogens. Recently, Lozano-Durán *et al.* (2013) proposed that a transcription factor BZR1 orchestrates the resource allocation to these two trade-off factors (*i.e.* growth and defence) under biotic stress and hence determines the biomass production in *Arabidopsis*. These studies point to the possibility that a key modulator, such as a transcription factor, determines the impact of ozone on the biomass production by affecting the resource allocation to growth and defence response under ozone stress.

Another explanation for reduced biomass production is that the lowered productivity under ozone stress is ascribed to significantly decreased leaf area and impaired photosynthetic activity (Ainsworth *et al.*, 2012). Ozone causes impairment of photosynthesis and photosynthetic apparatus at multiple levels. Closure of stomata is one of the fastest physiological responses to elevated ozone, occurring within less than 10 min from the onset of ozone exposure (Vahisalu *et al.*, 2008). Several mechanisms have been suggested for the stomatal closure (*i.e.* decreased stomatal conductance) under ozone stress. Paoletti and Grulke (2005) proposed that elevated CO<sub>2</sub> concentration in the stomatal pore due to impaired carbon assimilation rate (discussed later) is responsible for stomatal closure under ozone stress. On the other hand, Vahisalu *et al.* (2008) identified a protein SLOW ANION CHANNEL-ASSOCIATED 1 (SLAC1) from an ozone-susceptible *Arabidopsis* mutant, which regulates anion effluxes in guard cells and therefore controls stomatal aperture under ozone (ROS) stress. The closure of stomata is considered as an adaptive mechanism for elevated ozone, since the stomatal aperture determines ozone flux and damage to the plants (Fiscus *et al.*, 2005; Brosché *et al.*, 2010; Hoshika *et al.*, 2014). However, the closure of stomata succeedingly leads to lower CO<sub>2</sub> uptake, directly limiting the carbon availability for the photosynthetic apparatus. Ozone also damages photosystem II (PSII) reaction centre and decreases the efficiency of PSII (Fiscus *et al.*, 2005; Kobayakawa and Imai, 2011), which catalyzes the first step of the light reaction of photosynthesis. Most notably, ozone lowers ribulose 1,5-bisphosphate carboxylase/oxygenase (Rubisco) activity, which is the primary cause of decreased carbon assimilation (Fiscus *et al.*, 2005). The transcript level of Rubisco small subunit, as well as protein content decreases under ozone stress (Fiscus *et al.*, 2005; Ueda *et al.*, unpublished data). These negative effects lead to lower production of carbohydrate and consequently, lower biomass production.

## 4. Genetic mapping of ozone stress tolerance

One major strategy to dissect quantitative genetic factors and get insight into unknown mechanisms underlying a certain trait is genetic mapping (Yano and Sasaki, 1997; Salvi and Tuberosa, 2005). In general, two parental cultivars showing contrasting phenotypes are crossed at the first step, and the mapping population is subsequently developed by various methods (reviewed in McCouch and Doerge, 1995; Collard *et al.*, 2005). By obtaining genotypic and phenotypic data, chromosomal regions which carry genetic factors contributing to a certain phenotype (quantitative trait locus; QTL) can be identified. This mapping strategy is called QTL mapping. Probably due to the lack of proper mapping population and awareness of the threat of ozone, QTL studies under ozone stress in plant species were first conducted only after the year 2000. Several studies have successfully identified QTLs related to ozone stress in several plant species such as wheat (Quarrie *et al.*, 2006), poplar (Street *et al.*, 2011), and *Arabidopsis* (Brosché *et al.*, 2010). The identification of QTLs clearly showed that ozone stress tolerance is genetically regulated. Rice is the first plant species in which QTL study was reported for ozone tolerance. Lee *et al.* (2000) used a tolerant cultivar Milyang 23 and a susceptible cultivar Gihobyeyo as parental lines, and the resultant 164 recombinant inbred lines were used for mapping for leaf visible damage under acute ozone stress (300 ppb, 3 h). This study identified three QTLs on chromosomes 1, 7 and 11, which were responsible for the formation of leaf visible symptoms. Subsequent analysis revealed significant association between three DNA markers and the formation of leaf visible symptoms (Kim *et al.*, 2004). However, as Chen *et al.* (2009) mentioned, acute and short-term (usually more than 150 ppb, for several hours) ozone exposure, and mild and long-term (usually less than 150 ppb, for more than a week) exposure result in different responses in plants in terms of distribution of damage and changes in photosynthetic parameters. This implies that the effect of extreme ozone stress cannot be directly applied to the mapping of long-term related traits such as biomass production and yield. As discussed above, the current ozone concentration in the troposphere is stably high (monthly average exceeding 70 ppb in some areas in Asia; Yamaji *et al.*, 2008), and the high ozone levels may persist for extended periods of time. Therefore taking into account the future application of mapping for the agriculture, a mapping under mild and long-term exposure of ozone would have been needed.

In a detailed QTL mapping study in rice by Frei *et al.* (2008), a *temperate japonica* rice cultivar Nipponbare (sensitive to ozone) and an *aus* rice cultivar Kasalath (tolerant to ozone) served as parental lines. A QTL mapping was conducted targeting leaf visible injury, biomass production and stomatal conductance under long-term ozone stress. A total of six loci were identified through the mapping. Among them, three QTLs (*OzT3*, *OzT8* and *OzT9*) were verified using chromosomal segment substitution lines (CSSLs) containing each QTL. As a result, it was shown that a CSSL line SL41 harbouring the QTL on the chromosome 9 (*OzT9*) from Kasalath allele in the genetic background of Nipponbare showed attenuated leaf visible symptoms under ozone stress. Another CSSL line SL15 harbouring the QTL on the chromosome 3 (*OzT3*) from the tolerant cultivar Kasalath showed accelerated formation of leaf visible symptoms (Fig. 1-4). The other QTL on chromosome 8 (*OzT8*) derived from Kasalath was responsible for maintaining high biomass production under ozone stress. A detailed physiological study on *OzT8* (Chen *et al.*, 2011) showed that the photosynthetic capacity of SL46, which contains Kasalath allele at *OzT8*, was maintained high under ozone stress compared with Nipponbare. Another study focusing on leaf visible symptoms (Frei *et al.*, 2010) revealed differential gene regulations and biochemical properties among Nipponbare and two CSSL lines, SL41 and SL15, which harbour *OzT9* and *OzT3* from Kasalath, respectively. In the latter study, a comparative transcriptome analysis, supplemented by the information of previous QTL mapping study, identified a potential candidate gene near the QTL *OzT9*, which might be involved in the formation of leaf visible symptoms under ozone stress (discussed later).



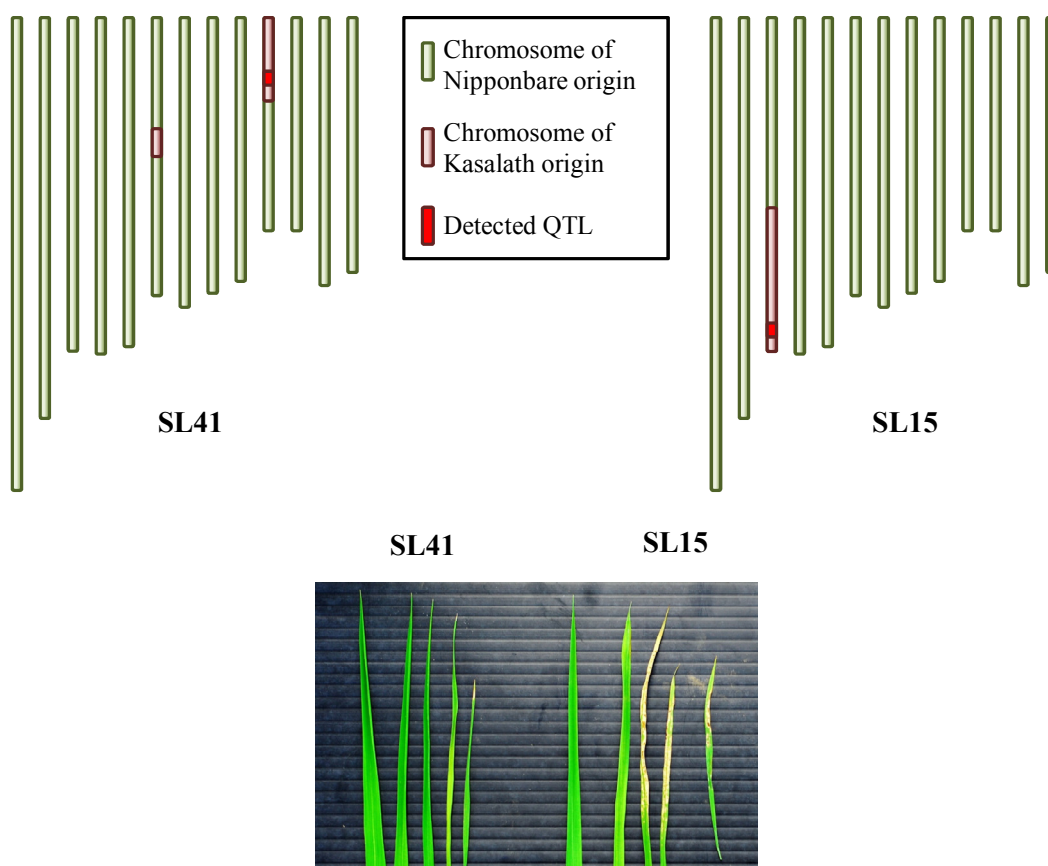


Figure 1-4: Two QTLs affecting leaf symptom formation under ozone stress and their effect in rice. SL41 and SL15 are chromosome segment substitution lines with Nipponbare genetic background with chromosome segment(s) from tolerant cultivar Kasalath. The 12 chromosomes of Nipponbare origin are shown in green colour, and the introgressions from Kasalath are shown in pale red colour. The detected QTLs, namely *OzT3* and *OzT9*, are shown in bright red colour. The below picture shows the extent of leaf visible symptoms after ozone stress in the two lines.

In addition to the mitigated leaf visible symptom formation in SL41 carrying *OzT9* locus from Kasalath allele, it was also associated with another favourable trait *i.e.* attenuated lignin formation under ozone stress. Lignin is one of the cell wall components, which gives rigidity to plant cells. Its formation is accelerated by ozone, probably by enhancing the radical formation of lignin precursors in the apoplast (Frei, 2013). SL41 showed significantly lower increase of lignin under elevated ozone concentration compared with the parent line Nipponbare (Frei *et al.*, 2011). Higher lignin content decreases the digestible fraction of rice straw, leading to lower feed value of the straw for the ruminant animals. Therefore lower lignin content under ozone stress in SL41 is an agronomically favourable trait.

## 5. Aims of this study

### *(I) Optimization of high-throughput apoplastic AsA analysis method*

As mentioned above, the apoplastic AsA is considered to be a determinant for ozone stress tolerance. Therefore it is indispensable to measure the AsA content from the apoplast to assess and shed light on ozone stress tolerance in plant species. However, several factors have been making it difficult to analyse the apoplastic AsA levels in rice plants: (i) the extremely low content of AsA in the apoplast; (ii) the time and effort needed to obtain the apoplastic AsA from rice leaves; and (iii) the long time needed to analyse AsA in biological samples. In most cases, the apoplastic AsA is measured by first obtaining intercellular washing fluid (IWF), which is a mixture of apoplastic solution and infiltrated buffer. In detail, a buffer is first infiltrated into the apoplastic space of a leaf by vacuum and, if necessary, pressurization, and later the IWF is obtained by centrifugation, which is conducted at a gentle speed to avoid damage of cell membranes. This ‘infiltration-centrifugation method’ is preferable to other ones such as direct centrifugation method (Meinzer and Moore, 1988), perfusion method (Bernstein, 1971) and the chamber pressurization method (Jachetta *et al.*, 1986) in terms of lower contamination by cytosolic compounds (Mühling and Sattelmacher, 1995). Considering the high AsA concentration in the cytosol, a slight contamination of cytosolic fluid in the IWF might distort the results and therefore should be avoided. The first step to obtain IWF by the infiltration-centrifugation method is to infiltrate a buffer solution into the apoplastic space from the stomata. Therefore, the effort needed for the infiltration step highly depends on the stomatal pore size. Rice has extremely small stomatal pore size (Nouchi *et al.*, 2012), and it makes the infiltration difficult. This difficulty was overcome by repetition of vacuum and pressurization only recently (Nouchi *et al.*, 2012). However, the extremely low amount of IWF obtained from the rice leaf samples and the time-consuming AsA measurement process still remained the hurdle for the analysis of apoplastic AsA from many samples. Moreover, AsA extract should be quickly assayed because extended storage leads to oxidation or degradation of AsA (Weissberger *et al.*, 1943; Koshiishi and Imanari, 1997). High-throughput metabolite analysis is crucial for the phenotyping of large population, which is indispensable for a breeding process targeting certain trait or stress tolerance. In Chapter 2, two previously reported AsA analysis methods, namely the dipyriddy-based method and the AO-based method, were compared in

terms of sensitivity, accuracy and the effect of interfering substances in high-throughput protocols. This chapter provides a strong basis for the reliable, highly sensitive and high-throughput AsA measurements, which enabled the in-depth analysis of apoplastic AsA in rice.

*(II) Characterization of a previously suggested candidate gene*

Previous mapping and microarray studies by Frei *et al.* (2008, 2010) suggested a candidate gene underlying tolerance in SL41 compared with Nipponbare cultivar. This is a putative AO gene. Several lines of evidence support the plausibility of this gene as the genetic factor explaining the effect of the QTL *OzT9* from Kasalath: (i) the gene expression level is highly induced (up to 100-fold) under ozone stress, and the expression patterns under ozone stress show differences among lines, being low in the tolerant line (SL41) while the susceptible lines (Nipponbare and SL15) showed higher expression than SL41; (ii) the selected putative AO is likely to control the oxidation of reduced AsA to the oxidized form, which relates to the previously established modes of action of ozone stress in the plant tissues; and (iii) the genetic locus of this gene is in the proximity of the identified *OzT9* chromosomal region. To date, several studies have attempted to elucidate the physiological significance of AO family proteins in several plant species (reviewed in De Tullio *et al.*, 2004, 2013). Conclusively, these studies have revealed higher stress tolerance in the AO knock-out lines and lower tolerance in the AO over-expression lines to abiotic stresses such as salinity stress, herbicide (methyl viologen), and oxidative stresses (hydrogen peroxide and ozone) (Sanmartin *et al.*, 2003; Yamamoto *et al.*, 2005). These pieces of evidence demonstrated the high cost of possessing AO, which have led to the notion that AO is a ‘mysterious enzyme’ (Dowdle *et al.*, 2007). Although each plant species possesses multiple AO homologues (Hoegger *et al.*, 2006; De Tullio *et al.*, 2013), only five AO genes have been thus far experimentally shown to code enzymes with AO activity, through enzyme fractioning or genetic engineering: the ones from cucumber (*Cucumis sativus*) (Ohkawa *et al.*, 1989), pumpkin (*Cucurbita maxima*) (Esaka *et al.*, 1990), tobacco (*Nicotiana tabacum*) (Kato and Esaka, 1996; Pignocchi *et al.*, 2003), tomato (*Solanum lycopersicum*) (Garchery *et al.*, 2013) and *Arabidopsis* (Yamamoto *et al.*, 2005). Many other ‘AO proteins’ were deduced based on the sequence similarity with previously known AO proteins, based on homology search or DNA hybridization

experiments using probe sequences originating from partial AO sequences. Therefore it remains still questionable if other homologues also possess AO activity. In Chapter 3, these questions were tackled by using reverse-genetics in rice. One knock-out and over-expression line of the rice putative AO gene, which was named *OZONE-RESPONSIVE APOPLASTIC PROTEIN1* (*OsORAPI*), were obtained and physiological and functional investigations were conducted. A novel physiological mechanism of cell death under ozone stress will be also discussed.

### *(III) Genome-wide association study under ozone stress*

While previous studies successfully shed light on genetic factors contributing to the ozone stress tolerance in rice, the following three questions had not been addressed: (i) Are there some other novel genetic factors and genes involved in and determining the ozone stress tolerance in rice?; (ii) Are other traits besides leaf visible symptom formation and biomass production also controlled by genetic factors under ozone stress?; and (iii) What are these factors? One pitfall of the classical QTL mapping is that the mapping populations are derived from only two parental cultivars. The resolution of the mapping (*i.e.* the size of chromosomal segment identified by mapping) is limited by the genetic recombination events between the two parental cultivars. Furthermore, it neglects all the genetic factors which do not show sequence variation between the two cultivars. A new technique called ‘genome-wide association study (GWAS)’ has been developed in plant species in the last decade to overcome this limitation. In GWAS, dozens or hundreds of independent cultivars are used for the mapping, based on, in most cases in recent years, single-nucleotide polymorphism (SNP) markers across the genome of the species. In plant species, since the development of the first genome-wide SNP markers in *Arabidopsis* by Schmid *et al.* (2003), the power and usefulness of GWAS have been shown to date. Among many studies, the one by Atwell *et al.* (2010) is quite noteworthy in terms of the number of markers and phenotypic traits assessed. In the study by Atwell *et al.*, a total of 216,130 SNP markers were used for the mapping of 107 traits from 199 *Arabidopsis* accessions. In rice, several large-scale GWASs including SNP genotyping have been conducted until now (Huang *et al.*, 2010; Zhao *et al.*, 2011; Huang *et al.*, 2012; Chen *et al.*, 2014). Among them, Zhao *et al.* (2011) used 413 different rice accessions from 82 countries, and genotyped them by 44,100 SNP markers (Fig. 1-5). Their study provided a strong

basis for the use of the population and the SNP markers to reveal hitherto unknown genetic factors underlying phenotypic traits in rice. The advantage of conducting GWAS in plant species is that the genotyping data can be used again if the same population is used for the mapping of other traits ('genotype or sequence once and phenotype many times over' strategy; Zhao *et al.*, 2011). Indeed, the same mapping population and genotyping data was utilized for mapping of aluminium stress tolerance (Famoso *et al.*, 2011), demonstrating the appropriateness of the population and SNP markers for abiotic stress tolerance. In Chapter 4, the first attempt to use GWAS for ozone stress in rice will be reported. This is the first GWAS under ozone stress in any crop species and provides evidence for the applicability of GWAS for environmental stresses. Based on the result of mapping and the sequence analyses, local linkage disequilibrium analysis was subsequently conducted. Potential candidate genes and their involvement in ozone stress tolerance will be also discussed.

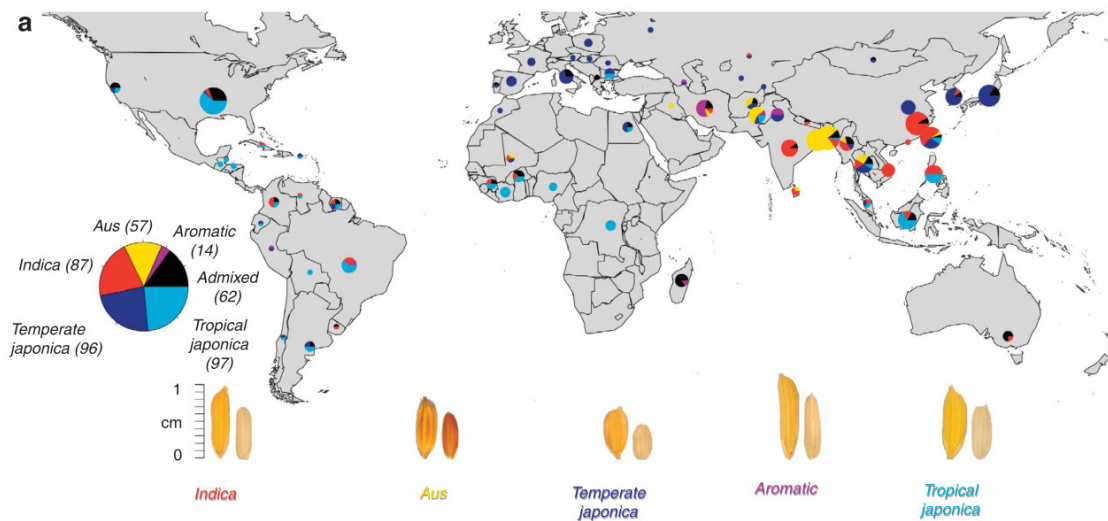


Figure 1-5: Rice population used for the mapping in Zhao *et al.* (2011). The country of origin, the number of accessions deriving from the country, and subpopulation classification are shown. Representative grains from each subpopulation are shown below with and without hull.

In summary, this thesis investigated the following three main questions:

- (I) How can AsA analysis be improved, especially for the analysis of apoplastic AsA?  
What is the most appropriate analysis method?;

(II) How does the putative AO gene (*OsORAPI*) affect ozone stress tolerance in rice? Can this gene explain the effect of *OzT9* from the tolerant Kasalath cultivar mitigating ozone stress tolerance in rice?;

and

(III) Are other ozone-related traits besides leaf visible symptom and biomass production (shoot weight and total grain yield) also genetically regulated? Are there potential novel genetic loci affecting ozone stress tolerance in rice?

## References

- Ainsworth EA, Yendrek CR, Sitch S, Collins WJ, Emberson LD.** 2012. The effects of tropospheric ozone on net primary productivity and implications for climate change. *Annual review of plant biology* **63**, 637–661.
- Akimoto H.** 2003. Global air quality and pollution. *Science* **302**, 1716–1720.
- Asada K.** 1999. The water-water cycle in chloroplasts: Scavenging of active oxygens and dissipation of excess photons. *Annual review of plant physiology and plant molecular biology* **50**, 601–639.
- Atwell S, Huang YS, Vilhjálmsson BJ, et al.** 2010. Genome-wide association study of 107 phenotypes in *Arabidopsis thaliana* inbred lines. *Nature* **465**, 627–631.
- Baier M, Dietz K-J.** 2005 Chloroplasts as source and target of cellular redox regulation: a discussion on chloroplast redox signals in the context of plant physiology. *Journal of Experimental Botany* **56**, 1449–1462.
- Bernstein L.** 1971. Method for determining solutes in the cell walls of leaves. *Plant Physiology* **47**, 361–365.
- Bienert GP, Chaumont F.** 2014. Aquaporin-facilitated transmembrane diffusion of hydrogen peroxide. *Biochimica et Biophysica Acta* **1840**, 1596–1604.
- Brosché M, Merilo E, Mayer F, et al.** 2010. Natural variation in ozone sensitivity among *Arabidopsis thaliana* accessions and its relation to stomatal conductance. *Plant, Cell and Environment* **33**, 914–925.
- Chen CP, Frank TD, Long SP.** 2009. Is a short, sharp shock equivalent to long-term punishment? Contrasting the spatial pattern of acute and chronic ozone damage to soybean leaves via chlorophyll fluorescence imaging. *Plant, Cell and Environment* **32**, 327–335.
- Chen CP, Frei M, Wissuwa M.** 2011. The *OzT8* locus in rice protects leaf carbon assimilation rate and photosynthetic capacity under ozone stress. *Plant, Cell and Environment* **34**, 1141–1149.
- Chen W, Gao Y, Xie W, et al.** 2014. Genome-wide association analyses provide genetic and biochemical insights into natural variation in rice metabolism. *Nature genetics* **46**, 714–721.
- Collard BCY, Jahufer MZZ, Brouwer JB, Pang ECK.** 2005. An introduction to markers, quantitative trait loci (QTL) mapping and marker-assisted selection for crop improvement: The basic concepts. *Euphytica* **142**, 169–196.
- Conklin PL, Pallanca JE, Last RL, Smirnov N.** 1997. L-ascorbic acid metabolism in the ascorbate-deficient *Arabidopsis* mutant *vtc1*. *Plant Physiology* **115**, 1277–1285.
- Conklin PL, Saracco SA, Norris SR, Last RL.** 2000. Identification of ascorbic acid-deficient *Arabidopsis thaliana* mutants. *Genetics* **154**, 847–856.

- Conklin PL, Williams EH, Last RL.** 1996. Environmental stress sensitivity of an ascorbic acid-deficient *Arabidopsis* mutant. *Proceedings of the National Academy of Sciences of the United States of America* **93**, 9970–9974.
- Dentener F, Stevenson D, Ellingsen K, et al.** 2006. The global atmospheric environment for the next generation. *Environmental Science & Technology* **40**, 3586–3594.
- Devendra C, Sevilla CC.** 2002. Availability and use of feed resources in crop–animal systems in Asia. *Agricultural Systems* **71**, 59–73.
- Van Dingenen R, Dentener FJ, Raes F, Krol MC, Emberson L, Cofala J.** 2009. The global impact of ozone on agricultural crop yields under current and future air quality legislation. *Atmospheric Environment* **43**, 604–618.
- Donahue NM.** 2011. Atmospheric chemistry: The reaction that wouldn't quit. *Nature chemistry* **3**, 98–99.
- Dowdle J, Ishikawa T, Gatzek S, Rolinski S, Smirnoff N.** 2007. Two genes in *Arabidopsis thaliana* encoding GDP-L-galactose phosphorylase are required for ascorbate biosynthesis and seedling viability. *The Plant Journal* **52**, 673–689.
- Esaka M, Hattori T, Fujisawa K, Sakajo S, Asahi T.** 1990. Molecular cloning and nucleotide sequence of full-length cDNA for ascorbate oxidase from cultured pumpkin cells. *European Journal of Biochemistry* **191**, 537–541.
- Famoso AN, Zhao K, Clark RT, et al.** 2011. Genetic architecture of aluminum tolerance in rice (*Oryza sativa*) determined through genome-wide association analysis and QTL mapping. *PLoS genetics* **7**, e1002221.
- Feng Z, Pang J, Nouchi I, Kobayashi K, Yamakawa T, Zhu J.** 2010. Apoplastic ascorbate contributes to the differential ozone sensitivity in two varieties of winter wheat under fully open-air field conditions. *Environmental Pollution* **158**, 3539–3545.
- Feng Z, Sun J, Wan W, Hu E, Calatayud V.** 2014. Evidence of widespread ozone-induced visible injury on plants in Beijing, China. *Environmental Pollution* **193**, 206–301.
- Feuillet C, Leach JE, Rogers J, Schnable PS, Eversole K.** 2011. Crop genome sequencing: lessons and rationales. *Trends in plant science* **16**, 77–88.
- Fiscus EL, Booker FL, Burkey KO.** 2005. Crop responses to ozone: uptake, modes of action, carbon assimilation and partitioning. *Plant, Cell and Environment* **28**, 997–1011.
- Foley JA, DeFries R, Asner GP, et al.** 2005. Global consequences of land use. *Science* **309**, 570–574.
- Foyer CH, Halliwell B.** 1976. The presence of glutathione and glutathione reductase in chloroplasts: A proposed role in ascorbic acid metabolism. *Planta* **133**, 21–25.
- Freebairn HT.** 1960. The prevention of air pollution damage to plants by the use of vitamin C sprays. *Journal of the Air Pollution Control Association* **10**, 314–317.
- Frei M.** 2013. Lignin : Characterization of a multifaceted crop component. *The Scientific World Journal* **2013**, 436517.



- Frei M, Kohno Y, Wissuwa M, Makkar HPS, Becker K.** 2011. Negative effects of tropospheric ozone on the feed value of rice straw are mitigated by an ozone tolerance QTL. *Global Change Biology* **17**, 2319–2329.
- Frei M, Tanaka JP, Chen CP, Wissuwa M.** 2010. Mechanisms of ozone tolerance in rice: characterization of two QTLs affecting leaf bronzing by gene expression profiling and biochemical analyses. *Journal of Experimental Botany* **61**, 1405–1417.
- Frei M, Tanaka JP, Wissuwa M.** 2008. Genotypic variation in tolerance to elevated ozone in rice: dissection of distinct genetic factors linked to tolerance mechanisms. *Journal of Experimental Botany* **59**, 3741–3752.
- Frei M, Wissuwa M, Pariasca-Tanaka J, Chen CP, Südekum K-H, Kohno Y.** 2012. Leaf ascorbic acid level—Is it really important for ozone tolerance in rice? *Plant Physiology and Biochemistry* **59**, 63–70.
- Garchery C, Gest N, Do PT, et al.** 2013. A diminution in ascorbate oxidase activity affects carbon allocation and improves yield in tomato under water deficit. *Plant, Cell and Environment* **36**, 159–175.
- Garris AJ, Tai TH, Coburn J, Kresovich S, McCouch S.** 2005. Genetic structure and diversity in *Oryza sativa* L. *Genetics* **169**, 1631–1638.
- Heath MC.** 2000. Hypersensitive response-related death. *Plant molecular biology* **44**, 321–334.
- Hoegger PJ, Kilaru S, James TY, Thacker JR, Kües U.** 2006. Phylogenetic comparison and classification of laccase and related multicopper oxidase protein sequences. *The FEBS Journal* **273**, 2308–2326.
- Horemans N, Foyer CH, Potters G, Asard H.** 2000. Ascorbate function and associated transport systems in plants. *Plant Physiology and Biochemistry* **38**, 531–540.
- Hoshika Y, Carriero G, Feng Z, Zhang Y, Paoletti E.** 2014. Determinants of stomatal sluggishness in ozone-exposed deciduous tree species. *Science of the Total Environment* **481**, 453–458.
- Huang X, Kurata N, Wei X, et al.** 2012. A map of rice genome variation reveals the origin of cultivated rice. *Nature* **490**, 497–501.
- Huang X, Wei X, Sang T, et al.** 2010. Genome-wide association studies of 14 agronomic traits in rice landraces. *Nature genetics* **42**, 961–967.
- International Rice Genome Sequencing Project.** 2005. The map-based sequence of the rice genome. *Nature* **436**, 793–800.
- Jachetta JJ, Appleby AP, Boersma L.** 1986. Use of the pressure vessel to measure concentrations of solutes in apoplastic and membrane-filtered symplastic sap in sunflower leaves. *Plant Physiology* **82**, 995–999.
- Jiang L, Liu L.** 2006. New evidence for the origins of sedentism and rice domestication in the Lower Yangzi River, China. *Antiquity* **80**, 355–361.

- Juliano BO.** 1993. *Rice in human nutrition*. Rome: FAO.
- Kangasjärvi J, Jaspers P, Kollist H.** 2005. Signalling and cell death in ozone-exposed plants. *Plant, Cell and Environment* **28**, 1021–1036.
- Kato N, Esaka M.** 1996. cDNA cloning and gene expression of ascorbate oxidase in tobacco. *Plant molecular biology* **30**, 833–837.
- Kim K-M, Kwon Y-S, Lee J-J, Eun M-Y, Sohn J-K.** 2004. QTL mapping and molecular marker analysis for the resistance of rice to ozone. *Molecules and cells* **17**, 151–155.
- Kobayakawa H, Imai K.** 2011. Effects of the interaction between ozone and carbon dioxide on gas exchange, photosystem II and antioxidants in rice leaves. *Photosynthetica* **49**, 227–238.
- Koshiishi I, Imanari T.** 1997. Measurement of ascorbate and dehydroascorbate contents in biological fluids. *Analytical Chemistry* **69**, 216–220.
- Kovach MJ, Sweeney MT, McCouch SR.** 2007. New insights into the history of rice domestication. *Trends in genetics* **23**, 578–587.
- Laisk A, Kull O, Moldau H.** 1989. Ozone concentration in leaf intercellular air spaces is close to zero. *Plant Physiology* **90**, 1163–1167.
- Langebartels C, Wohlgemuth H, Kschieschan S, Grün S, Sandermann H.** 2002. Oxidative burst and cell death in ozone-exposed plants. *Plant Physiology and Biochemistry* **40**, 567–575.
- Lea MC.** 1864. On the influence of ozone and some other chemical agents on germination and vegetation. *American Journal of Science* **37**, 373–376.
- Lee JJ, Kwon YS, Sohn JK.** 2000. Identification of RFLP marker associated with ozone resistance in rice. *Korean Journal of Breeding* **32**, 279–284.
- Lei H, Wuebbles DJ, Liang X-Z, Olsen S.** 2013. Domestic versus international contributions on 2050 ozone air quality: How much is convertible by regional control? *Atmospheric Environment* **68**, 315–325.
- Li Z-K, Zhang F.** 2013. Rice breeding in the post-genomics era: from concept to practice. *Current opinion in plant biology* **16**, 261–269.
- Linares OF.** 2002. African rice (*Oryza glaberrima*): History and future potential. *Proceedings of the National Academy of Sciences of the United States of America* **99**, 16360–16365.
- Loya WM, Pregitzer KS, Karberg NJ, King JS, Giardina CP.** 2003. Reduction of soil carbon formation by tropospheric ozone under increased carbon dioxide levels. *Nature* **425**, 705–707.
- Lozano-Durán R, Macho AP, Boutrot F, Segonzac C, Somssich IE, Zipfel C.** 2013. The transcriptional regulator BZR1 mediates trade-off between plant innate immunity and growth. *eLIFE* **2**, e00983.

- Lozano-Durán R, Zipfel C.** 2015. Trade-off between growth and immunity: role of brassinosteroids. *Trends in plant science* **20**, 12–19.
- Luwe MWF, Takahama U, Heber U.** 1993. Role of ascorbate in detoxifying ozone in the apoplast of spinach (*Spinacia oleracea* L.) leaves. *Plant Physiology* **101**, 969–976.
- Maclean JL, Dawe DC, Hardy B, Hettel GP.** 2002. *Rice almanac*. 3rd Edition. Wallingford: CABI publishing.
- Matsuzaki A, Matsushima S, Tomita T.** 1973. Analysis of yield-determining process and its application to yield-prediction and culture improvement of lowland rice: CXIII. Effects of the nitrogen top-dressing at the full heading stage on kernel qualities. *Japanese Journal of Crop Science* **42**, 54–62.
- McCouch SR, Doerge RW.** 1995. QTL mapping in rice. *Trends in genetics* **11**, 482–487.
- Meinzer FC, Moore PH.** 1988. Effect of apoplastic solutes on water potential in elongating sugarcane leaves. *Plant Physiology* **86**, 873–879.
- Menser HA.** 1964. Response of plants to air pollutants. III. A relation between ascorbic acid levels and ozone susceptibility of light-preconditioned tobacco plants. *Plant Physiology* **39**, 564–567.
- Middleton JT.** 1956. Response of plants to air pollution. *Journal of the Air Pollution Control Association* **6**, 7–9, 50.
- Middleton JT, Darley EF, Brewer RF.** 1958. Damage to vegetation from polluted atmospheres. *Journal of the Air Pollution Control Association* **8**, 9–15.
- Mills G, Buse A, Gimeno B, Bermejo V, Holland M, Emberson L, Pleijel H.** 2007. A synthesis of AOT40-based response functions and critical levels of ozone for agricultural and horticultural crops. *Atmospheric Environment* **41**, 2630–2643.
- Mueller MJ, Berger S.** 2009. Reactive electrophilic oxylipins: Pattern recognition and signalling. *Phytochemistry* **70**, 1511–1521.
- Mueller ND, Gerber JS, Johnston M, Ray DK, Ramankutty N, Foley JA.** 2012. Closing yield gaps through nutrient and water management. *Nature* **490**, 254–257.
- Mühling KH, Sattelmacher B.** 1995. Apoplastic ion concentration of intact leaves of field bean (*Vicia faba*) as influenced by ammonium and nitrate nutrition. *Journal of plant physiology* **147**, 81–86.
- Munné-Bosch S, Queval G, Foyer CH.** 2012. The impact of global change factors on redox signaling underpinning stress tolerance. *Plant Physiology* **161**, 5–19.
- Nouchi I.** 2002. Responses of whole plants to air pollutants. In: Omasa K, Saji H, Youssefian S, Kondo N, eds. *Air Pollution and Plant Biotechnology*. Tokyo: Springer, 3–39.
- Nouchi I, Hayashi K, Hiradate S, Ishikawa S, Fukuoka M, Chen CP, Kobayashi K.** 2012. Overcoming the difficulties in collecting apoplastic fluid from rice leaves by the infiltration-centrifugation method. *Plant and cell physiology* **53**, 1659–1668.

- Ohkawa J, Okada N, Shinmyo A, Takano M.** 1989. Primary structure of cucumber (*Cucumis sativus*) ascorbate oxidase deduced from cDNA sequence: Homology with blue copper proteins and tissue-specific expression. *Proceedings of the National Academy of Sciences of the United States of America* **86**, 1239–1243.
- Omasa K, Tobe K, Kondo T.** 2002. Absorption of organic and inorganic air pollutants by plants. In: Omasa K, Saji H, Youssefian S, Kondo N, eds. *Air Pollution and Plant Biotechnology*. Tokyo: Springer, 155–178.
- Orru H, Andersson C, Ebi KL, Langner J, Åström C, Forsberg B.** 2013. Impact of climate change on ozone-related mortality and morbidity in Europe. *The European Respiratory Journal* **41**, 285–294.
- Overmyer K, Tuominen H, Kettunen R, Betz C, Langebartels C, Sandermann H, Kangasjärvi J.** 2000. Ozone-sensitive *Arabidopsis rcd1* mutant reveals opposite roles for ethylene and jasmonate signaling pathways in regulating superoxide-dependent cell death. *The Plant Cell* **12**, 1849–1862.
- Paoletti E, Grulke NE.** 2005. Does living in elevated CO<sub>2</sub> ameliorate tree response to ozone? A review on stomatal responses. *Environmental Pollution* **137**, 483–493.
- Petrov VD, Van Breusegem F.** 2012. Hydrogen peroxide—a central hub for information flow in plant cells. *AoB plants* **2012**, pls014.
- Pignocchi C, Foyer CH.** 2003. Apoplastic ascorbate metabolism and its role in the regulation of cell signalling. *Current opinion in plant biology* **6**, 379–389.
- Quarrie SA, Quarrie SP, Radosevic R, et al.** 2006. Dissecting a wheat QTL for yield present in a range of environments: from the QTL to candidate genes. *Journal of Experimental Botany* **57**, 2627–2637.
- Rao MV, Davis KR.** 2001. The physiology of ozone induced cell death. *Planta* **213**, 682–690.
- Rao MV, Koch JR, Davis KR.** 2000. Ozone: a tool for probing programmed cell death in plants. *Plant molecular biology* **44**, 345–358.
- Salvi S, Tuberosa R.** 2005. To clone or not to clone plant QTLs: present and future challenges. *Trends in plant science* **10**, 297–304.
- Sanmartin M, Drogoudi PD, Lyons T, Pateraki I, Barnes J, Kanellis AK.** 2003. Over-expression of ascorbate oxidase in the apoplast of transgenic tobacco results in altered ascorbate and glutathione redox states and increased sensitivity to ozone. *Planta* **216**, 918–928.
- Sawada H, Kohno Y.** 2009. Differential ozone sensitivity of rice cultivars as indicated by visible injury and grain yield. *Plant Biology* **11**, 70–75.
- Schmid KJ, Sørensen TR, Stracke R, Törjék O, Altmann T, Mitchell-Olds T, Weisshaar B.** 2003. Large-scale identification and analysis of genome-wide single-nucleotide polymorphisms for mapping in *Arabidopsis thaliana*. *Genome research* **13**, 1250–1257.

- Schraudner M, Ernst D, Langebartels C, Sandermann H.** 1992. Biochemical plant responses to ozone. III. Activation of the defense-related proteins  $\beta$ -1, 3-glucanase and chitinase in tobacco leaves. *Plant Physiology* **99**, 1321–1328.
- Sheffield PE, Knowlton K, Carr JL, Kinney PL.** 2011. Modeling of regional climate change effects on ground-level ozone and childhood asthma. *American journal of preventive medicine* **41**, 251–257.
- Shi G, Yang L, Wang Y, et al.** 2009. Impact of elevated ozone concentration on yield of four Chinese rice cultivars under fully open-air field conditions. *Agriculture, Ecosystems and Environment* **131**, 178–184.
- Shiraiwa M, Sosedova Y, Rouvière A, et al.** 2011. The role of long-lived reactive oxygen intermediates in the reaction of ozone with aerosol particles. *Nature chemistry* **3**, 291–295.
- Street NR, Tallis MJ, Tucker J, Brosché M, Kangasjärvi J, Broadmeadow M, Taylor G.** 2011. The physiological, transcriptional and genetic responses of an ozone-sensitive and an ozone tolerant poplar and selected extremes of their F<sub>2</sub> progeny. *Environmental Pollution* **159**, 45–54.
- Streets DG, Waldhoff ST.** 2000. Present and future emissions of air pollutants in China: SO<sub>2</sub>, NO<sub>x</sub>, and CO. *Atmospheric Environment* **34**, 363–374.
- Teixeira E, Fischer G, van Velthuizen H, et al.** 2011. Limited potential of crop management for mitigating surface ozone impacts on global food supply. *Atmospheric Environment* **45**, 2569–2576.
- The 3,000 rice genomes project.** 2014. The 3,000 rice genomes project. *GigaScience* **3**, 7.
- Thompson JE, Legge RL, Barber RF.** 1987. The role of free radicals in senescence and wounding. *New Phytologist* **105**, 317–344.
- Tilman D, Balzer C, Hill J, Belfort BL.** 2011. Global food demand and the sustainable intensification of agriculture. *Proceedings of the National Academy of Sciences of the United States of America* **108**, 20260–20264.
- Todesco M, Balasubramanian S, Hu TT, et al.** 2010. Natural allelic variation underlying a major fitness trade-off in *Arabidopsis thaliana*. *Nature* **465**, 632–636.
- Tsukahara K, Sawada H, Matsumura H, Kohno Y, Tamaoki M.** 2013. Quantitative trait locus analyses of ozone-induced grain yield reduction in rice. *Environmental and Experimental Botany* **88**, 100–106.
- De Tullio MC, Guether M, Balestrini R.** 2013. Ascorbate oxidase is the potential conductor of a symphony of signaling pathways. *Plant Signaling and Behavior* **8**, e23213.
- De Tullio MC, Liso R, Arrigoni O.** 2004. Ascorbic acid oxidase: an enzyme in search of a role. *Biologia Plantarum* **48**, 161–166.
- Turcsányi E, Lyons T, Plöchl M, Barnes J.** 2000. Does ascorbate in the mesophyll cell walls form the first line of defence against ozone? Testing the concept using broad bean (*Vicia faba* L.). *Journal of Experimental Botany* **51**, 901–910.

- Ueda Y, Uehara N, Sasaki H, Kobayashi K, Yamakawa T.** 2013. Impacts of acute ozone stress on superoxide dismutase (SOD) expression and reactive oxygen species (ROS) formation in rice leaves. *Plant Physiology and Biochemistry* **70**, 396–402.
- Urbach W, Schmidt W, Rümmele S, et al.** 1990. Wirkungen von Umweltschadstoffen (SO<sub>2</sub>, O<sub>3</sub> und NO<sub>x</sub>) auf Photosynthese und Membran intakter Blätter und Pflanzen. In: Urbach W, ed. *Waldschadenforschung und Wirkungen von Umweltschadstoffen*. Würzburg: Projektgruppe Bayern zur Erforschung der Wirkung von Umweltschadstoffen (PBWU).
- Vahisalu T, Kollist H, Wang Y-F, et al.** 2008. SLAC1 is required for plant guard cell S-type anion channel function in stomatal signalling. *Nature* **452**, 487–491.
- Vanacker H, Carver TLW, Foyer CH.** 1998. Pathogen-induced changes in the antioxidant status of the apoplast in barley leaves. *Plant Physiology* **117**, 1103–1114.
- Vingarzan R.** 2004. A review of surface ozone background levels and trends. *Atmospheric Environment* **38**, 3431–3442.
- Wang Y, Frei M.** 2011. Stressed food – The impact of abiotic environmental stresses on crop quality. *Agriculture, Ecosystems and Environment* **141**, 271–286.
- Wang F, Yuan Q-H, Shi L, et al.** 2006. A large-scale field study of transgene flow from cultivated rice (*Oryza sativa*) to common wild rice (*O. rufipogon*) and barnyard grass (*Echinochloa crusgalli*). *Plant Biotechnology Journal* **4**, 667–676.
- Weissberger A, LuValle JE, Thomas DS.** 1943. Oxidation processes. XVI. The autoxidation of ascorbic acid. *Journal of the American chemical society* **65**, 1934–1939.
- Wohlgenuth H, Mittelstrass K, Kschieschan S, et al.** 2002. Activation of an oxidative burst is a general feature of sensitive plants exposed to the air pollutant ozone. *Plant, Cell and Environment* **25**, 717–726.
- Wrzaczek M, Brosché M, Salojärvi J, et al.** 2010. Transcriptional regulation of the CRK/DUF26 group of receptor-like protein kinases by ozone and plant hormones in Arabidopsis. *BMC plant biology* **10**, 95.
- Yalpani N, Enyedi AJ, León J, Raskin I.** 1994. Ultraviolet light and ozone stimulate accumulation of salicylic acid, pathogenesis-related proteins and virus resistance in tobacco. *Planta* **193**, 372–376.
- Yamaji K, Ohara T, Uno I, Kurokawa J, Pochanart P, Akimoto H.** 2008. Future prediction of surface ozone over east Asia using Models-3 Community Multiscale Air Quality Modeling System and Regional Emission Inventory in Asia. *Journal of Geophysical Research* **113**, D08306.
- Yamaji K, Ohara T, Uno I, Tanimoto H, Kurokawa J, Akimoto H.** 2006. Analysis of the seasonal variation of ozone in the boundary layer in East Asia using the Community Multi-scale Air Quality model: What controls surface ozone levels over Japan? *Atmospheric Environment* **40**, 1856–1868.
- Yamamoto A, Bhuiyan MNH, Waditee R, et al.** 2005. Suppressed expression of the apoplastic ascorbate oxidase gene increases salt tolerance in tobacco and *Arabidopsis* plants. *Journal of Experimental Botany* **56**, 1785–1796.

**Yano M, Sasaki T.** 1997. Genetic and molecular dissection of quantitative traits in rice. *Plant molecular biology* **35**, 145–153.

**Zhao K, Tung C-W, Eizenga GC, et al.** 2011. Genome-wide association mapping reveals a rich genetic architecture of complex traits in *Oryza sativa*. *Nature communications* **2**, 467.

## Chapter 2

# Comparison of two high-throughput ascorbate measurements

(Ueda Y, Wu L, Frei M. 2013. A critical comparison of two high-throughput ascorbate analyses methods for plant samples. *Plant Physiology and Biochemistry* **70**, 418–423.)

### Abstract

Ascorbate (AsA) is an important metabolite involved in stress response and development of plants. Therefore it is necessary to quantify the AsA content in many fields of plant science, including high-throughput and critical applications. In this study we compared two different microplate-based AsA assays, which are suitable for high-throughput applications: an ascorbate oxidase (AO)-based assay and a dipyridyl (DPD)-based assay. These methods were compared in critical applications, *i.e.* (i) when AsA concentrations were very low such as in apoplastic extracts, (ii) when plants contained pigments interfering with the spectrometric measurements, and (iii) when plants contained high iron concentration interfering with the colour reactions. The precision of measurements was higher with the DPD method, as illustrated by higher recovery rates of internal AsA standards. On the other hand, the AO method was more sensitive to low levels of AsA. This was an advantage in determining apoplastic AsA concentration in rice, which was substantially lower than that of whole tissues. The AO method also had the advantage that plant pigments and high iron concentrations in plants tissues did not interfere with the analysis, as opposed to the DPD assay. In conclusion, both assays had advantages, and the choice of a suitable method depends on the specific application.



## 1. Introduction

Ascorbate (AsA) is one of the most important antioxidants determining abiotic and biotic stress tolerance in plants, as well as plant growth (Gallie, 2013). AsA is involved in the detoxification of reactive oxygen species (ROS) due to its capacity to donate electrons to ROS without becoming a toxic radical itself (Asada, 1999). AsA occurs both in the symplast and the apoplast, but the concentrations in the apoplast are much lower and usually account for only around 5 to 10% of the total AsA pool (Horemans *et al.*, 2000). Apoplastic ascorbate plays an important role in determining the redox status of the apoplast and transducing signals to cytosol (Pignocchi and Foyer, 2003). Due to its outstanding function as presumably the most important antioxidant in plants, ascorbate has been suggested as a potential breeding target to develop crops resistant to abiotic and biotic stresses (Frei *et al.*, 2008, 2010; Lisko *et al.*, 2013). Breeding applications typically require the screening of a large number of plant samples; however, ascorbate degrades easily (Koshiishi and Imanari, 1997), which makes it difficult to analyse large numbers of samples, as a time lag in the measurement may lead to distorted results. Therefore, high-throughput methods are required that allow for the processing of a large number of samples quickly.

Many methods have been used in determining the AsA concentration in biological samples, including spectrometric and chromatographic methods (Washko *et al.*, 1992; Koshiishi and Imanari, 1997; Badrakhan *et al.*, 2004). However, some of these methods require special equipment or are not suitable for high-throughput applications in plants. Microplate-based spectrometric methods may overcome these difficulties. An ascorbate oxidase (AO) based method (hereafter referred to as the AO method; Queval and Noctor, 2007) relies on spectrometric measurements at a wavelength of 265 nm, which represents the absorbance maximum of reduced AsA. Changes in absorbance are measured after adding AO (EC 1.10.3.3) to the samples to determine reduced AsA, while dehydroascorbate (DHA) is measured by monitoring DHA reduction after adding the reducing agent dithiothreitol (DTT). An alternative method (Stevens *et al.*, 2006; Gillespie and Ainsworth, 2007) is based on the reduction of ferric to ferrous iron by reduced AsA, and a subsequent colour reaction between ferrous iron and 2, 2'-dipyridyl (DPD), which is measured at 525 nm (hereafter referred to as the DPD method). To our knowledge, no direct comparison between these two methods has been reported, and these methods have not been evaluated

under critical applications. In our work with plants exposed to environmental stresses, we encountered problems with AsA analyses under the following conditions: (i) when sample concentrations were very low; (ii) when plants contained pigments interfering with spectrometric measurements; and (iii) when plants contained high levels of iron. The latter problem is particularly relevant in rice research, because excessive iron concentrations in rice tissue are a very widespread phenomenon limiting rice productivity (Becker and Asch, 2005). Therefore, the aim of this study was to directly compare two microplate-based assays for AsA analysis regarding their suitability for critical applications.

## 2. Materials and Methods

### 2.1. Plant material

Rice (*Oryza sativa* L., cultivars Nipponbare and Dongjin) was grown in a greenhouse in 60-L hydroponic tanks with Yoshida solution (Yoshida *et al.*, 1976). Rice shoots of around eight week old plants were harvested around noontime, flash-frozen in liquid nitrogen and stored at -80 °C until analysis. In the iron stress experiment, rice plants were grown hydroponically in Yoshida solution for 7 weeks, and were exposed to an excess ferrous iron stress at 300 ppm of FeSO<sub>4</sub> for 10 days as described (Engel *et al.*, 2012). Red cabbage was obtained from a local market, ground with liquid nitrogen soon after the purchase and stored at -80 °C until analysis.

### 2.2. Extraction of AsA

Sample materials were ground with a mortar and pestle in liquid nitrogen, and AsA was extracted with 1 mL extraction solvent from around 70 mg of flash-frozen sample. The extract was cleared by centrifugation for 20 min at 4 °C and 15,000 g and kept on ice for further analysis.

### 2.3. AsA measurement (dipyridyl method)

The method was similar to that used by Gillespie and Ainsworth (2007), but it was adjusted to 200 µL micro tube scale. All the following procedures except for DTT and *N*-ethylmaleimide (NEM) treatment were conducted with samples stored on ice. Four 20 µL aliquots of each sample or AsA standard (Thermo Fisher Scientific, Waltham, MA) were pipetted into PCR tubes and were mixed with 10 µL of 75 mM potassium phosphate buffer (pH 7.0). Two sub-samples for the total AsA assay were mixed with 10 µL of 10 mM DTT and incubated at room temperature for 10 min, followed by addition of 10 µL of 0.5% (w/v) NEM to remove the remaining DTT. In the two sub-samples used for reduced AsA analyses, 20 µL of water was added to account for the amount of DTT and NEM. Finally, 50 µL of 10% (w/v) TCA, 40 µL of 43% (w/v) H<sub>3</sub>PO<sub>4</sub>, 40 µL of 4% (w/v) 2, 2'-dipyridyl (in 70% (v/v) ethanol), and 20 µL of 3% (w/v) FeCl<sub>3</sub> were added to all the tubes. The FeCl<sub>3</sub> solution was filtrated before use. Samples were immediately mixed vigorously and incubated at 37 °C for 60 min. Subsequently, 100 µL of the resultant sample was transferred to a 96-well microplate

(Brand, Wertheim, Germany), and the absorbance was read at 525 nm using a Powerwave XS2 microplate reader (BioTek, Bad Friedrichshall, Germany). AsA concentrations were estimated from a standard curve ranging from 0.1 to 8 mM. All analyses were conducted at least in duplicate.

#### 2.4. AsA measurement (ascorbate oxidase method)

This method is based on direct spectrometric measurement as described by Luwe *et al.* (1993) and Queval and Noctor (2007) with some modifications. First, lyophilized AO (Wako Pure Chemical Industries, Osaka, Japan) was dissolved in a 1:1 mixture of glycerol and 50 mM potassium phosphate buffer (pH 6.0) to obtain a 0.1 U/ $\mu$ L solution. For the measurement of reduced AsA, the reaction mixture consisted of 10  $\mu$ L of extract, 80  $\mu$ L of 0.1 M potassium phosphate buffer (pH 7.0) and 10  $\mu$ L of 0.01 U/ $\mu$ L AO (AO stock solution diluted 10-fold with 0.1 M potassium phosphate buffer, pH 7.0). In blank wells, which did not contain the enzyme, AO solution was substituted with 0.1 M potassium phosphate buffer (pH 7.0). For the measurement of DHA, the reaction mixture consisted of 10  $\mu$ L of extract, 80  $\mu$ L of 0.1 M potassium phosphate buffer (pH 7.8) and 4 mM DTT contained in the same buffer. In blank wells, DTT was substituted with potassium phosphate buffer (pH 7.8). Both measurements were started by shaking the plate for 5 sec, followed by continuous absorbance reading at 265 nm using UV-transparent microplates. Absorbance was monitored until the reactions were completed, which was after 2 min in the AO reaction and after 7 to 8 min in the DTT reaction. The absorption of AO and DTT at the final concentration was  $< 0.003 \text{ OD}_{265}$ , respectively, and was neglected. Concentrations were calculated as follows:

$$\text{Reduced AsA (mM in the extract)} = \frac{(\text{Mean OD}_{\text{withoutAO}} - \text{MinOD}_{\text{withAO}})}{14.3 \times 0.29} \times 10$$

$$\text{DHA (mM in the extract)} = \frac{(\text{MaxOD}_{\text{withDTT}} - \text{MeanOD}_{\text{withoutDTT}})}{14.3 \times 0.29} \times 10$$

where 14.3 ( $\text{mM}^{-1} \text{ cm}^{-1}$ ) is extinction coefficient of reduced AsA (Luwe *et al.*, 1993), and 0.29 represents the path length of 100  $\mu$ L solution in a 96-well flat-bottom UV

plate (Corning Inc., Corning, MA). Total AsA was calculated as the sum of reduced and oxidized AsA. All analyses were conducted at least in duplicate.

### **2.5. Preparation of IWF from rice**

Intercellular washing fluid (IWF) was obtained from rice leaves according to the method of Nouchi *et al.* (2012) with slight modifications. The 1st and 2nd fully-expanded rice leaves were detached and immediately used for the analysis. The leaves were weighed and washed with 0.05% (v/v) Triton X-100 to remove the hydrophobic layer from the leaf surface, followed by rinsing with distilled water. As infiltration buffer, 10 mM citrate buffer (pH 3.0) containing 0.2 mM EDTA was used (Frei *et al.*, 2010). The buffer was infiltrated into the apoplastic space by repeated vacuum-pressure cycles using a 60-mL syringe (DIK-8392-12, Daiki Rika Kogyo, Saitama, Japan). After the infiltration, the leaves were dried with paper towels, weighed, inserted into a 1 mL pipette tip, and placed inside a 1.5 mL tube containing 50  $\mu$ L of 6% (w/v) metaphosphoric acid (MPA). After centrifugation (4 °C and 5,000 g for 5 min), the leaves were weighed again to determine the volume of IWF, and the mixture of 6% MPA and IWF (hereafter referred to as IWF preparation) was used for AsA measurement. Possible cytosolic contamination of the IWF was tested in each sample by measuring glucose-6-phosphate content, which is specific to the cytosol (Nouchi *et al.*, 2012). Briefly, 10  $\mu$ L of IWF preparation was mixed with 80  $\mu$ L of 50 mM Tris-HCl (pH 8.1) and 10  $\mu$ L of 5 mM NADP in a microplate well. The plate was shaken for 4 sec, and the kinetics was read at 340 nm for 1 min to obtain a baseline. After adding 5  $\mu$ L of 0.01 U/ $\mu$ L glucose-6-phosphate dehydrogenase, the plate was shaken again for 4 sec, the absorbance at 340 nm was continuously monitored for 5 min, and samples were omitted if any increase in absorbance was observed. These analyses were conducted in duplicate.

### **2.6. Dilution and spiking assays**

AsA extracts were diluted with 6% MPA to 0.5 and 0.25 fold concentrations. Spiking samples were prepared by mixing the original samples with the same volume of 2 mM, 1 mM, 0.2 mM or 0 mM reduced AsA in 6% MPA (corresponding to 1 mM, 0.5 mM, 0.1 mM and 0 mM spikes). Recovery rates were determined as follows:

Recovery rate (%)

$$= \frac{(\text{concentration}_{\text{spiked samples}}) - (\text{concentration}_{0 \text{ mM spiked samples}})}{(\text{spiked concentration})} \times 100$$

### **2.7. AO inhibition assay**

The AO assay was conducted according to Pignocchi *et al.* (2003) with addition of iron. AO was dissolved in 0.1 M sodium phosphate buffer (pH 5.6) at 0.001 U/ $\mu$ L. The reaction mixture consisted of 70  $\mu$ L of 0.1 M sodium phosphate buffer (pH 5.6), 10  $\mu$ L of either 1 mM FeSO<sub>4</sub>, 1 mM FeCl<sub>3</sub> or water, 10  $\mu$ L of 0.001 U/ $\mu$ L AO and 10  $\mu$ L of 2 mM reduced AsA. The reaction mixture was mixed in 96-well microplate by pipetting, the kinetics was monitored at the wavelength of 265 nm for 1 min and the average AsA oxidation rate was calculated. Non-enzymatic AsA oxidation occurring in blank wells lacking the enzyme was deducted.

### 3. Results and Discussion

#### 3.1. Extraction Solvents

Several extraction solvents were tested regarding their suitability for the two assays. Acidic solvents are usually employed because low pH inhibits the enzymatic oxidation of reduced AsA (Nakamura *et al.*, 1968), as well as the autoxidation (Weissberger *et al.*, 1943). We tested 6% trichloroacetic acid (TCA; Gillespie and Ainsworth, 2007), 6% MPA (Lee *et al.*, 1984), and 0.2 N HCl (Queval and Noctor, 2007), and compared these acidic solvents with distilled water. AsA was extracted from 16 different rice shoot samples using each solvent, and the extracts were analysed using both the AO and the DPD method to determine the consistency between the two methods. To further test the effect of solvents on AsA degradation, the samples were stored on ice for 4 h and assayed again. Slopes and *R*-square values were calculated for the linear regressions between the values obtained from the DPD and the AO method, and for the values obtained before and after the storage of samples for 4 h (Table 2-1). Distilled water retained almost no reduced AsA even soon after the extraction, leading to reduced AsA values almost below the detection limit (data not shown). There was high consistency between the two methods as illustrated by slope values close to one and relatively high *R*-square values in all of the acidic solvents. Somewhat lower *R*-square values in total AsA might be due to relatively lower recovery rate of DHA, as previously suggested (Queval and Noctor, 2007). When values obtained after 0 and 4 h of storage were correlated, the slopes of the linear regression were close to one in the 6% MPA treatment. This indicates that total and reduced AsA were not degraded. In contrast, some degradation or oxidation occurred after 4 h of storage in 6% TCA and 0.2 N HCl, as indicated by lower slope values in these treatments (Table 2-1). Thus, MPA was more effective than other organic acids in preventing non-enzymatic AsA oxidation, which may occur due to the presence of catalytic metals (Lyman *et al.*, 1937). Therefore, we used 6% MPA as extraction solvent in all further analyses.

Table 2-1: Effects of different extraction solvents on the consistency between two ascorbate analysis methods and the stability of ascorbate during storage on ice.

Extraction Solvent		AO-DPD		AO (0 h)-AO (4 h)		DPD (0 h)-DPD (4 h)	
		Reduced	Total	Reduced	Total	Reduced	Total
		AsA	AsA	AsA	AsA	AsA	AsA
6% TCA	Slope	1.02	1.02	0.88	0.93	0.96	0.82
	<i>R</i> -square	0.95	0.62	0.97	0.85	0.85	0.75
6% MPA	Slope	1.05	1.17	1.02	1.09	0.96	0.91
	<i>R</i> -square	0.94	0.78	0.97	0.84	0.87	0.89
0.2 N HCl	Slope	1.21	1.06	0.86	0.79	0.83	0.55
	<i>R</i> -square	0.84	0.61	0.86	0.67	0.90	0.50
Distilled water	Slope	-0.23	0.63	0.14	0.70	1.19	0.87
	<i>R</i> -square	0.13	0.44	0.14	0.61	0.41	0.69

AsA was extracted from 16 rice shoot samples and the extracts were assayed with both the AO and the DPD method soon after the extraction (0 h), or after storage on ice for 4 h (4 h). AO-DPD, linear regression coefficients of values obtained from the DPD method vs values obtained from the AO method; AO (0 h)-AO (4 h) and DPD (0 h)-DPD (4 h), linear regression coefficients of values obtained after 4 h of storage vs values obtained without storage using the respective methods.

### 3.2. Validation of the analyses using ascorbate standards

To test the validity and detection limit of the analysis, multiple concentrations of AsA standards (0 to 10 mM) were prepared in 6% MPA and analysed with the two methods. In the AO method, the quantification of AsA is based on an extinction coefficient value of  $\epsilon = 14.3 \text{ (mM}^{-1} \text{ cm}^{-1}\text{)}$ . The standard AsA concentration and the calculated concentration showed high correlation between 0.02 mM and 8 mM of the standard series, showing an *R*-square value of 0.99 (Fig. 2-1). However, the slope value was 0.87 (average of two independent experiments), implying a more than 10% difference between the measured and actual concentration. Using a standard curve to quantify AsA concentration instead of an extinction coefficient might solve this problem. Outside the range of 0.02 to 8 mM, the relationship between AsA concentration and extinction at 265 nm was not strictly linear, making measurements unreliable.



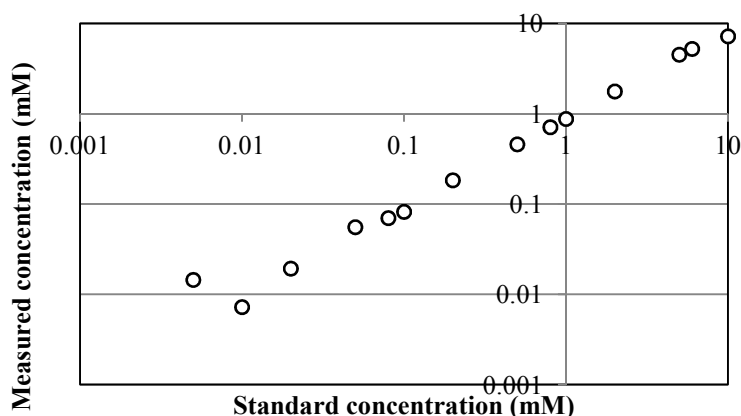


Figure 2-1: Correlation between standard AsA concentration and measured AsA concentration based on an extinction coefficient of  $\epsilon = 14.3 \text{ mM}^{-1} \text{ cm}^{-1}$  using the AO method. Measurements were conducted in duplicate.

In the DPD method, the calculation of AsA concentration is based on a standard curve. The absorption values of different standard concentrations were deducted from blanks and denoted as  $\Delta A_{525}$  values, and the correlation between the standard AsA concentration and  $\Delta A_{525}$  was tested (Fig. 2-2). The linear range of the standard series ( $R^2 = 0.99$ ) was limited to only 0.1 to 8 mM, which implies that the method is less sensitive than the AO method.

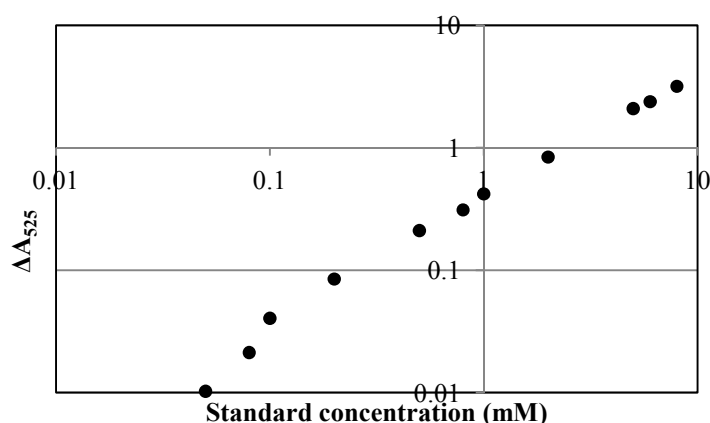


Figure 2-2: Standard curve generated by the DPD method. AsA standards were prepared in 6% MPA.  $\Delta A_{525}$  shows the difference of absorption at 525 nm between standards and blanks after the reaction. Measurements were conducted in quadruplicate.

To further confirm the reliability of the assays, extracts were spiked with internal AsA standards and the recovery rate was determined. AsA was extracted from three rice shoot samples and additional 1, 0.5 and 0.1 mM of reduced AsA were added to the samples. The original and spiked samples were assayed using both methods and the recovery rates were determined. Both methods showed recovery rates similar to those observed in other biochemical assays (Polle *et al.*, 1990; Hodges *et al.*, 1999; Queval and Noctor, 2007), but the DPD method showed higher values than the AO method (Table 2-2), implying that AsA concentration was more precisely determined in the DPD method than the AO method.

Table 2-2: Recovery rates (%) of reduced and total AsA in samples spiked with internal standards.

Method	1 mM spike		0.5 mM spike		0.1 mM spike	
	Reduced	Total	Reduced	Total	Reduced	Total
DPD method	93.1±2.9	95.8±2.2	90.9±0.5	92.1±2.1	77.3±8.1	113.7±36.2
AO method	83.8±1.8	88.5±6.1	78.5±3.4	81.8±6.2	91.6±15.8	82.8±23.8

AsA was extracted from rice shoots with 6% MPA and spiked with additional 1, 0.5 and 0.1 mM of reduced AsA. Values are means ± standard deviation (n = 3).

### 3.3. Apoplastic AsA analysis in rice

As discussed above, the AO method was more sensitive to low concentrations of AsA than the DPD method. The detection limit is usually not critical in measurements of whole plant tissues, where AsA concentration ranges from 5 to 138  $\mu\text{mol/g}$  fresh weight (FW) (Gest *et al.*, 2013). With such samples, a suitable ratio of sample weight and solvent volume can be devised to ensure concentrations  $> 0.1$  mM in the extract. However, the AsA concentration of the apoplast is quite low compared with that of whole tissue. Burkey *et al.* (2003) reported that apoplastic total AsA ranges from 15 to 600 nmol/g FW, depending on the plant species and conditions. We also conducted apoplastic AsA measurement in rice leaves using both the AO and the DPD method (Table 2-3). Unlike the AO method, the DPD method failed to detect any reduced AsA in rice apoplastic extracts, which was below 0.1 mM. Usually the amount of IWF obtained is quite low in all plant species. An additional difficulty encountered with rice leaves is their comparatively smaller stomatal pore size and a strong hydrophobic layer on the leaf surface, thus making it difficult to obtain apoplastic extracts (Nouchi

*et al.*, 2012). In our case the average yield of IFW from rice leaves was  $244 \pm 47 \mu\text{g/g}$  FW ( $n = 22$ ) and we were able to measure both the reduced and oxidized AsA concentration in the apoplast from less than 500 mg of leaf samples with at least two analytical replicates, in addition to analyses of cytosolic contaminants. The AO method thus has advantages in detecting both reduced and total AsA when the amount of sample material is limited and the concentration is low as in apoplastic extracts from rice.

Table 2-3: Apoplastic AsA concentration in rice leaves measured using two different analysis methods.

<b>Method</b>	<b>Reduced AsA (nmol/g FW)</b>	<b>Total AsA (nmol/g FW)</b>
DPD method	N.D.	$20.6 \pm 5.9$
AO method	$5.2 \pm 3.5$	$20.8 \pm 5.4$

N.D., not detected; and FW, fresh weight. Values refer to whole leaf fresh weight and represent means  $\pm$  standard deviation ( $n = 4$ ).

### ***3.4. Possible effect of interfering plant pigments***

Pigments contained in plant extracts may affect spectrometric measurements if their absorbance spectrum is similar to that of measured compounds. This may particularly affect the DPD method, which is based on a colourimetric reaction measured at 525 nm corresponding to red colour. We tested red cabbage (*Brassica oleracea*) as an example for a plant containing red pigments. The extract showing red colour was assayed with both methods. Substantial differences were seen in the values obtained from two methods if the red colour arising from plant pigments was ignored (Table 2-4). Therefore we tried to eliminate the overestimation of AsA concentration in the DPD method by subtracting the absorption caused by pigments. In additional blank samples, the DPD solution was substituted with 70% ethanol in an otherwise identical reaction mix. Alternatively, blank samples could be obtained by AO treatment to remove reduced AsA prior to the assay, as suggested previously (Garchery *et al.*, 2013). The absorption peak of the blank solution (without DPD) was about 530 nm, which greatly affected the quantification of AsA in the DPD method (Fig. 2-3). Subtraction of blank values led to very similar results as those obtained from the AO

method (Table 2-4). Therefore, unknown plant samples should always be checked for the presence of interfering pigments when the DPD method is employed. The AO method is less susceptible to artefacts produced by plant pigments, as it is based on changes in absorbance (after the addition of AO or DTT), instead of a single absorbance value. It may be considered as an advantage of the AO method that testing for the presence of pigments, and if applicable, the subtraction of blank values is not required.

Table 2-4: Effect of interfering pigments on ascorbate analysis in red cabbage samples using two different analysis methods.

Sample number	Total AsA concentration in the extract (mM)		
	AO method	DPD method without background subtraction	DPD method with background subtraction
1	0.40	1.62	0.40
2	0.45	1.70	0.44
3	0.43	1.44	0.41
4	0.68	2.42	0.69

AsA was extracted from four red cabbage leaf samples with 6% MPA and subsequently assayed with both methods. In the DPD method, additional blanks containing 70% ethanol instead of DPD solution were measured, and the absorbance of the blanks was subtracted from the sample absorbance.

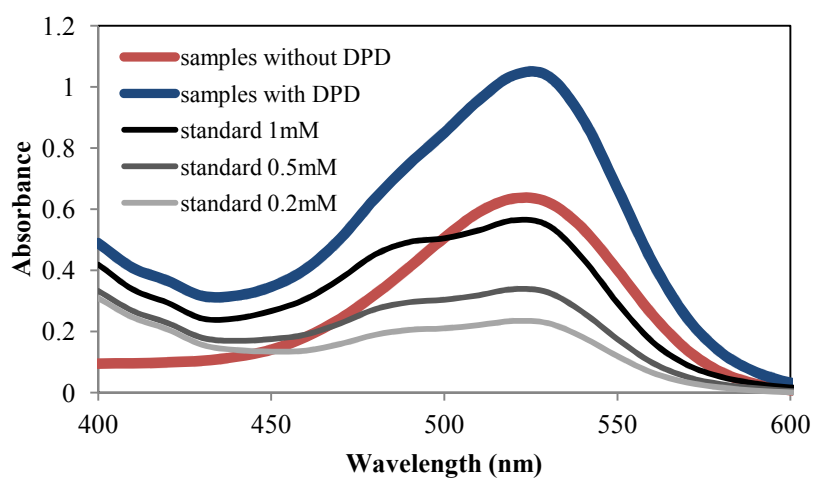


Figure 2-3: Absorbance spectrum of a red cabbage sample and three AsA standards subjected to the DPD assay compared with blank samples lacking DPD in the reaction mix.

### 3.5. Samples containing high levels of iron

The DPD method is based on the reduction of ferric iron ( $\text{Fe}^{3+}$ ) into ferrous iron ( $\text{Fe}^{2+}$ ) by reduced AsA, which then reacts with DPD. Therefore it is conceivable that high levels of iron already present in samples affect the result. To test this hypothesis we sampled leaves from rice plants which had been grown hydroponically in nutrient solutions containing excess iron (300 ppm  $\text{FeSO}_4$ ). Similar iron concentrations are frequently observed in soil solution of rice paddies, where iron toxicity constitutes one of the most important nutrient imbalances worldwide (Becker and Asch, 2005). The average iron concentration of rice shoots obtained from this experiment was 8.2 g/kg DW ( $n = 4$ ). These samples were used for AsA assays using both methods, along with control samples grown without excess iron. The correlations between the AO method and the DPD method were very poor (Fig. 2-4). Especially reduced AsA was overestimated in samples from the iron stress treatment using the DPD method, which was presumable due to the excessive uptake of ferrous iron into the leaves, which reacted with DPD. The AO method may thus be considered as more suitable to analyse samples from iron stress treatments. However, ferric iron ( $\text{Fe}^{3+}$ ) is also known as an inhibitor of AO (Itoh *et al.*, 1995), which may thus lead to an underestimation of reduced AsA using the AO method. Based on the measured shoot iron concentration, we estimated that the iron concentration in the extracted solution would be around 1 mM (final concentration 0.1 mM in the assay mixture) when 70 mg of fresh sample was extracted with 1 mL of solvent. We tested if this iron concentration affected AO activity by measuring the activity of purified AO enzyme with the addition of the above-mentioned iron concentration. AO activity was quantified by monitoring the enzyme kinetics at 265 nm in a buffer containing AsA with or without addition of iron as either  $\text{FeSO}_4$  ( $\text{Fe}^{2+}$ ) or  $\text{FeCl}_3$  ( $\text{Fe}^{3+}$ ). Almost no inhibition was observed, as AO activity with both 0.1 mM  $\text{FeSO}_4$  or 0.1 mM  $\text{FeCl}_3$  was 98% compared with a control without iron. Therefore we concluded that the AO method is suitable for analysis of samples containing high amounts of iron. AO is reported to be inhibited also by hydrogen peroxide (White and Krupka, 1965), sodium azide (Itoh *et al.*, 1995), and phenolic compounds (Gaspard *et al.*, 1997), but inhibition occurs at relatively high concentrations of these compounds, which are unlikely to be reached in plant extracts. To our present knowledge, AO activity should therefore not be significantly inhibited in plant extracts.

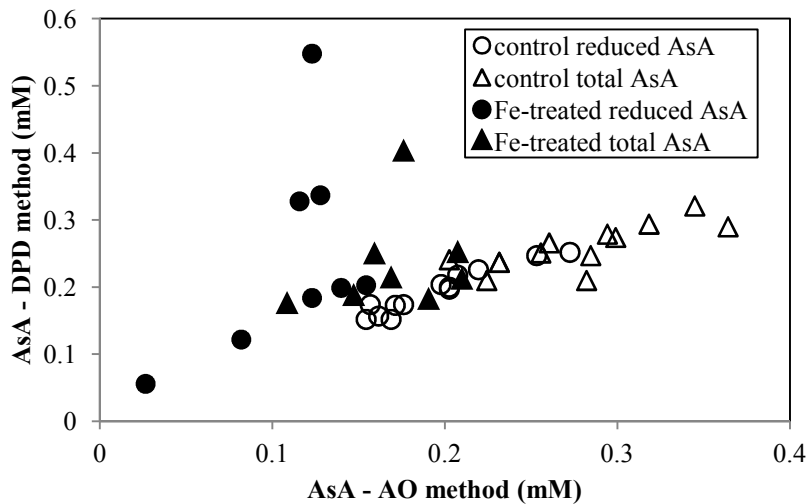


Figure 2-4: Correlation of reduced and total AsA values of rice samples obtained from an iron stress experiment using two analysis methods. Concentrations in plant extracts are plotted.

We conducted dilution and spiking experiments with samples from iron stress and control treatments to further confirm that inhibitory effects did not occur (Tables 2-5 and 2-6). Samples from the iron stress treatment showed similar recovery rates as those from the control. The ratio of AsA concentration measured in diluted/undiluted samples was similar to the dilution factor even in samples from the iron treatment (Table 2-5). As for the spiking experiment, the recovery rates of iron-stressed samples were somewhat lower and more variable compared with non-stressed samples but were still above 80%. We therefore concluded that the AO method was more suitable to determine AsA content in plant samples containing high levels of iron. Excessive iron uptake is typically associated with plants growing on anaerobic soils with low redox potential, where iron occurs in its soluble form  $\text{Fe}^{2+}$ . Apart from rice, this may affect other plant species such as *Eugenia uniflora* (Jucoski *et al.*, 2013) or tea (Hemalatha and Venkatesan, 2011).

Table 2-5: Effects of iron on the consistency of ascorbate measurements in dilution experiments.

<b>Samples</b>	<b>x0.5 dilution factor</b>		<b>x0.25 dilution factor</b>	
	<b>Reduced</b>	<b>Total</b>	<b>Reduced</b>	<b>Total</b>
Control	0.51±0.05	0.51±0.03	0.24±0.04	0.24±0.04
Fe-treated	0.57±0.16	0.51±0.13	0.26±0.08	0.25±0.04

Ratios of the concentrations measured in diluted/undiluted samples are shown, which should ideally be identical to the dilution factor. AsA was extracted from non-stressed and Fe-stressed rice shoots with 6% MPA. The extract was assayed with the AO method. Values are means ± standard deviation (n = 4).

Table 2-6: Recovery rates (%) in spiking experiments using AsA extracts obtained from rice plants exposed to iron stress and control plants.

<b>Samples</b>	<b>0.5 mM spike</b>		<b>0.1 mM spike</b>	
	<b>Reduced</b>	<b>Total</b>	<b>Reduced</b>	<b>Total</b>
Control	89.9±4.8	86.4±5.1	96.5±9.0	97.7±4.2
Fe-treated	86.6±3.6	82.7±2.0	85.6±9.3	85.6±17.0

AsA was extracted from non-stressed and Fe-stressed rice shoots with 6% MPA and spiked with additional 0.5 and 0.1 mM of reduced AsA. Samples were assayed with the AO method and recovery rate was determined as indicated in Materials and Methods. Values are means ± standard deviations (n = 4).

## **4. Conclusions**

In conclusion both the DPD and the AO method have advantages and disadvantages. The AO method is more straightforward and thus more suitable for high-throughput applications. Moreover it has the advantages of being more sensitive to low levels of AsA, and that plant pigments or iron do not affect the analytical results. However the AO method showed slightly lower recovery rate of internal standards than the DPD method, and there were slight differences between standard concentrations and measured concentrations determined by an extinction coefficients. These results should help researchers choose a suitable AsA analysis method for particular applications.

### ***Funding***

This study was funded by the Deutsche Forschungsgemeinschaft (FR2952/1-1).



## References

- Asada K.** 1999. The water-water cycle in chloroplasts: Scavenging of active oxygens and dissipation of excess photons. *Annual review of plant physiology and plant molecular biology* **50**, 601–639.
- Badrakhhan C-D, Petrat F, Holzhauser M, Fuchs A, Lomonosova EE, de Groot H, Kirsch M.** 2004. The methanol method for the quantification of ascorbic acid and dehydroascorbic acid in biological samples. *Journal of Biochemical and Biophysical Methods* **58**, 207–218.
- Becker M, Asch F.** 2005. Iron toxicity in rice—conditions and management concepts. *Journal of Plant Nutrition and Soil Science* **168**, 558–573.
- Burkey KO, Eason G, Fiscus EL.** 2003. Factors that affect leaf extracellular ascorbic acid content and redox status. *Physiologia Plantarum* **117**, 51–57.
- Engel K, Asch F, Becker M.** 2012. Classification of rice genotypes based on their mechanisms of adaptation to iron toxicity. *Journal of Plant Nutrition and Soil Science* **175**, 871–881.
- Frei M, Tanaka JP, Chen CP, Wissuwa M.** 2010. Mechanisms of ozone tolerance in rice: characterization of two QTLs affecting leaf bronzing by gene expression profiling and biochemical analyses. *Journal of Experimental Botany* **61**, 1405–1417.
- Frei M, Tanaka JP, Wissuwa M.** 2008. Genotypic variation in tolerance to elevated ozone in rice: dissection of distinct genetic factors linked to tolerance mechanisms. *Journal of Experimental Botany* **59**, 3741–3752.
- Gallie DR.** 2013. The role of L-ascorbic acid recycling in responding to environmental stress and in promoting plant growth. *Journal of Experimental Botany* **64**, 433–443.
- Garchery C, Gest N, Do PT, et al.** 2013. A diminution in ascorbate oxidase activity affects carbon allocation and improves yield in tomato under water deficit. *Plant, Cell and Environment* **36**, 159–175.
- Gaspard S, Monzani E, Casella L, Gullotti M, Maritano S, Marchesini A.** 1997. Inhibition of ascorbate oxidase by phenolic compounds. Enzymatic and spectroscopic studies. *Biochemistry* **36**, 4852–4859.
- Gest N, Gautier H, Stevens R.** 2013. Ascorbate as seen through plant evolution: the rise of a successful molecule? *Journal of Experimental Botany* **64**, 33–53.
- Gillespie KM, Ainsworth EA.** 2007. Measurement of reduced, oxidized and total ascorbate content in plants. *Nature protocols* **2**, 871–874.
- Hemalatha K, Venkatesan J.** 2011 Impact of iron toxicity on certain enzymes and biochemical parameters of tea. *Asian Journal of Biochemistry* **6**, 384–394.
- Hodges DM, DeLong JM, Forney CF, Prange RK.** 1999. Improving the thiobarbituric acid-reactive-substances assay for estimating lipid peroxidation in plant tissues containing anthocyanin and other interfering compounds. *Planta* **207**, 604–611.

- Horemans N, Foyer CH, Asard H.** 2000. Transport and action of ascorbate at the plant plasma membrane. *Trends in plant science* **5**, 263–267.
- Itoh H, Hirota A, Hirayama K, Shin T, Murao S.** 1995. Properties of ascorbate oxidase produced by *Acremonium* sp. HI-25. *Bioscience, Biotechnology, and Biochemistry* **59**, 1052–1056.
- Jucoski GD, Cambraia J, Ribeiro C, de Oliveira JA, de Paula SO, Olivia MA.** 2013. Impact of iron toxicity on oxidative metabolism in young *Eugenia uniflora* L. plants. *Acta Physiologiae Plantarum* **35**, 1645–1657.
- Koshiishi I, Imanari T.** 1997. Measurement of ascorbate and dehydroascorbate contents in biological fluids. *Analytical Chemistry* **69**, 216–220.
- Lee EH, Jersey JA, Gifford C, Bennett J.** 1984. Differential ozone tolerance in soybean and snapbeans: Analysis of ascorbic acid in O<sub>3</sub>-susceptible and O<sub>3</sub>-resistant cultivars by high-performance liquid chromatography. *Environmental and Experimental Botany* **24**, 331–341.
- Lisko KA, Hubstenberger JF, Phillips GC, Belefant-Miller H, McClung A, Lorence A.** 2013. Ontogenetic changes in vitamin C in selected rice varieties. *Plant Physiology and Biochemistry* **66**, 41–46.
- Luwe MWF, Takahama U, Heber U.** 1993. Role of ascorbate in detoxifying ozone in the apoplast of spinach (*Spinacia oleracea* L.) leaves. *Plant Physiology* **101**, 969–976.
- Lyman CM, Schultze MO, King CG.** 1937. The effect of metaphosphoric acid and some other inorganic acids on the catalytic oxidation of ascorbic acid. *Journal of Biological Chemistry* **118**, 757–764.
- Nakamura T, Makino N, Ogura Y.** 1968. Purification and properties of ascorbate oxidase from cucumber. *The Journal of Biochemistry.* **64**, 189–195.
- Nouchi I, Hayashi K, Hiradate S, Ishikawa S, Fukuoka M, Chen CP, Kobayashi K.** 2012. Overcoming the difficulties in collecting apoplastic fluid from rice leaves by the infiltration-centrifugation method. *Plant and cell physiology* **53**, 1659–1668.
- Pignocchi C, Fletcher JM, Wilkinson JE, Barnes JD, Foyer CH.** 2003. The function of ascorbate oxidase in tobacco. *Plant Physiology* **132**, 1631–1641.
- Pignocchi C, Foyer CH.** 2003. Apoplastic ascorbate metabolism and its role in the regulation of cell signalling. *Current opinion in plant biology* **6**, 379–389.
- Polle A, Chakrabarti K, Schürmann W, Rennenberg H.** 1990. Composition and properties of hydrogen peroxide decomposing systems in extracellular and total extracts from needles of Norway spruce (*Picea abies* L., Karst.). *Plant Physiology* **94**, 312–319.
- Queval G, Noctor G.** 2007. A plate reader method for the measurement of NAD, NADP, glutathione, and ascorbate in tissue extracts: Application to redox profiling during *Arabidopsis* rosette development. *Analytical Biochemistry* **363**, 58–69.

- Stevens R, Buret M, Garchery C, Carretero Y, Causse M.** 2006. Technique for rapid, small-scale analysis of vitamin C levels in fruit and application to a tomato mutant collection. *Journal of agricultural and food chemistry* **54**, 6159–6165.
- Washko PW, Welch RW, Dhariwal KR, Wang Y, Levine M.** 1992. Ascorbic acid and dehydroascorbic acid analyses in biological samples. *Analytical Biochemistry* **204**, 1–14.
- Weissberger A, LuValle JE, Thomas DS.** 1943. Oxidation processes. XVI. The autoxidation of ascorbic acid. *Journal of the American chemical society* **65**, 1934–1939.
- White GA, Krupka RM.** 1965. Ascorbic acid oxidase and ascorbic acid oxygenase of *Myrothecium verrucaria*. *Archives of Biochemistry and Biophysics* **110**, 448–461.
- Yoshida S, Forno DA, Cock JH, Gomez KA.** 1976. *Laboratory Manual for Physiological Studies of Rice*. The International Rice Research Institute. Manila, The Philippines.

## Chapter 3

# A novel gene *OsORAP1* enhances cell death in ozone stress in rice

(Ueda Y, Siddique S, Frei M. 2015. A novel gene, *OZONE-RESPONSIVE APOPLASTIC PROTEIN1*, enhances cell death in ozone stress in rice. *Plant Physiology* [in press].)

### Abstract

A novel protein, OZONE-RESPONSIVE APOPLASTIC PROTEIN1 (OsORAP1) was characterized, which was previously suggested as a candidate gene underlying *OzT9*, a QTL for ozone stress tolerance in rice (*Oryza sativa* L.). The sequence of OsORAP1 was similar to that of ascorbate oxidase (AO) proteins. It was localized in the apoplast, as shown by transient expression of an OsORAP1/GFP fusion construct in *Nicotiana benthamiana* leaf epidermal and mesophyll cells, but did not possess AO activity as shown by heterologous expression of OsORAP1 in *Arabidopsis* mutants with reduced background AO activity. A knock-out (KO) rice line of *OsORAP1* showed enhanced tolerance to ozone stress (120 ppb average daytime concentration, 20 days) as demonstrated by less formation of leaf visible symptoms (*i.e.* cell death), less lipid peroxidation, and lower NADPH oxidase activity, indicating reduced active production of reactive oxygen species. In contrast, the effect of ozone on chlorophyll content was not significantly different among the lines. These observations suggested that OsORAP1 specifically induced cell death in ozone stress. Significantly enhanced expression of jasmonic acid (JA)-responsive genes in the KO line implied the involvement of the JA pathway in symptom mitigation. Sequence analysis revealed extensive polymorphisms in the promoter region of *OsORAP1* between the ozone susceptible Nipponbare and ozone-tolerant Kasalath, the *OzT9* donor variety, which could be responsible for the differential regulation of *OsORAP1* reported earlier. These pieces of evidence suggested that OsORAP1 enhanced cell death in ozone stress, and its expression levels could explain the effect of a previously reported QTL.

## 1. Introduction

Tropospheric ozone is one of the most important environmental pollutants adversely affecting agriculture (Ainsworth *et al.*, 2012). Ozone is formed through photochemical reactions of precursor gases such as nitrogen oxides (NO<sub>x</sub>), carbon monoxide, and volatile organic compounds, which largely originate from anthropogenic gas emissions (Yamaji *et al.*, 2006). Recent economic development and industrialization have led to drastic increases of tropospheric ozone concentrations in East Asian countries. In some regions, the monthly average concentration currently exceeds 70 ppb (Yamaji *et al.*, 2006), temporarily reaching nearly 200 ppb (Wang *et al.*, 2007). Furthermore, the average level is expected to increase by up to 10 ppb by 2020 in these areas (compared with 2000) due to increasing anthropogenic gas emissions (Yamaji *et al.*, 2008). At these concentrations, ozone negatively affects both the crop yields (Ainsworth, 2008) and quality (Wang and Frei, 2011), and induces leaf visible symptoms such as chlorosis and bronzing (Feng *et al.*, 2014).

Rice (*Oryza sativa* L.) is the major staple crop throughout Asia, and it is strongly affected by tropospheric ozone because its cropping season overlaps with peak ozone concentrations especially in South and East Asia (Frei, 2015). Previous studies estimated around 3.7% of global rice yield loss and regionally more than 10% of rice yield loss due to elevated tropospheric ozone, and this trend will exacerbate in the future with increasing concentrations (Ainsworth, 2008; Van Dingenen *et al.*, 2009). Considering that the global food demand will double by the year 2050 (Tilman *et al.*, 2011), it is of paramount importance to get insight into ozone tolerance mechanisms in rice and breed ozone-tolerant rice varieties to ensure the global food supply.

A number of previous studies have determined genetic factors associated with ozone tolerance in rice, suggesting that this trait is controlled by multiple medium effect loci rather than a single large effect locus (Frei, 2015; Ueda *et al.*, 2015). In a study by Frei *et al.* (2008), several ozone-related quantitative trait loci (QTLs) were identified using a mapping population derived from the contrasting cultivars Nipponbare (susceptible) and Kasalath (tolerant). One of the identified QTLs, *OzT9*, was related to leaf visible symptom formation in ozone stress, where the allele from the tolerant Kasalath cultivar conferred tolerance. Underpinning the effect of *OzT9*, a chromosomal segment substitution line SL41 carrying a chromosomal introgression from Kasalath at the *OzT9* locus in Nipponbare background, produced less visible symptoms than

Nipponbare (Frei *et al.*, 2008). A subsequent transcriptomic analysis revealed a differential gene expression profile between Nipponbare and SL41 (Frei *et al.*, 2010). A proposed candidate gene, which was annotated as an ascorbate oxidase (AO; RAP ID: *Os09g0365900*), was located near the *OzT9* locus, and was one of the most highly induced genes in ozone stress in the whole array. The induction of gene expression in ozone stress was significantly lower in the tolerant SL41 than in Nipponbare (Frei *et al.*, 2010). From a physiological point of view, apoplastic ascorbate (AsA) has been shown to form the first line of defence against the ozone entering the plants through the stomata (Luwe *et al.*, 1993; Plöchl *et al.*, 2000; Feng *et al.*, 2010), which supports the link between the annotation of the candidate gene and ozone stress tolerance. In line with this concept, a previous study demonstrated that an AO over-expressing tobacco (*Nicotiana tabacum*) negatively affected tolerance to ozone due to altered apoplastic reduced AsA content and AsA redox status (Sanmartin *et al.*, 2003). These converging pieces of evidence suggested that the expression of this putative AO gene was associated with ozone stress tolerance in rice in terms of visible symptom formation.

AO is classified as a multicopper oxidase family protein and can be found in plant and bacterial genomes (Hoegger *et al.*, 2006). In plants, AO family proteins are localized in the apoplast, the vacuole, the tonoplast and the Golgi apparatus (Liso *et al.*, 2004; Balestrini *et al.*, 2012). AO is supposedly involved in AsA metabolism in the apoplast, thereby controlling its redox status (Pignocchi and Foyer, 2003). Although several studies have been conducted on AO proteins in different plant species, its diverse roles in plant metabolism remain to be fully understood. Yamamoto *et al.* (2005) observed that knock-down of AO led to higher tolerance to salinity and oxidative stresses in *Arabidopsis* (*Arabidopsis thaliana*). Garchery *et al.* (2013) reported an increase in the early fruit diameter and alteration in hexose and sucrose content in leaves in AO knock-down lines in tomato (*Solanum lycopersicum*). These examples raise questions regarding the physiological role of AO genes in plants, since absence or lower expression of AO genes often appears to be favourable. In contrast, AO was also suggested to enhance cell expansion and growth (Kato and Esaka, 2000; Pignocchi *et al.*, 2003). Due to its apparently contradictory roles, AO has been named a mysterious enzyme (Dowdle *et al.*, 2007), of which the diverse biological functions remain to be fully elucidated.

In this study, we aimed at characterizing the previously identified putative AO gene *Os09g0365900*, which we named *OZONE-RESPONSIVE APOPLASTIC PROTEIN1* (*OsORAP1*), by specifically testing three hypotheses:

(I) *OsORAP1* has AO activity and is localized in the apoplast;

(II) *OsORAP1* affects leaf visible symptom formation in rice under chronic ozone stress;

and

(III) Because *OsORAP1* may be the gene underlying the ozone tolerance QTL *OzT9*, it shows sequence polymorphisms between tolerant and susceptible rice cultivars.

## 2. Materials and Methods

### 2.1. Sequence analysis

Rice putative AO and laccase amino acid sequences were obtained from the RAP-DB website (<http://rapdb.dna.affrc.go.jp/>, as of December 2013; Sakai *et al.*, 2013). Putative *Arabidopsis* AO and laccase amino acid sequences were obtained from the National Center for Biotechnology Information database (<http://www.ncbi.nlm.nih.gov/>, as of December 2013). MEGA5 software (Tamura *et al.*, 2011) was used to create a phylogenetic tree using the Neighbour-Joining method (Saitou and Nei, 1987). Protein motifs were searched through the InterPro database (<http://www.ebi.ac.uk/interpro/>, as of December 2013).

### 2.2. Construction of vectors and plant transformation

The vectors for transformation were constructed using the gateway cloning system (Curtis and Grossniklaus, 2003) as detailed in the Supplementary Protocol S1. Transient expression was conducted by using *Nicotiana benthamiana* leaves. These were infiltrated with *Agrobacterium tumefaciens* strain GV3101 carrying the vector pMDC83-OsORAP1, together with *A. tumefaciens* carrying pBIN61-P19 (a gift of Dr. H. Bohlmann, University of Natural Resources and Life Sciences Vienna). P19 is an RNA-silencing inhibitor, which enhances the expression of transgenes (Shah *et al.*, 2013). Each bacterium was infiltrated at an optical density of  $OD_{600} = 2.0$  in a buffer consisting of 10 mM MES (pH 5.6), 10 mM  $MgCl_2$  and 100  $\mu$ M acetosyringone, and the signal was observed after 5 days using LSM 710 confocal microscope (Carl Zeiss, Jena, Germany). The wavelength was 488 nm for excitation and 514 to 550 nm for emission. Plasmolysis was induced by incubating the leaf segment with 1 M NaCl (Libault *et al.*, 2010) for 30 min. Mesophyll cells were directly observed by removing the epidermal cell layer using a razor blade and tweezers from the abaxial side.

Stable transformation of *Arabidopsis* was conducted by the floral-dip method (Clough and Bent, 1998). Young flowers and buds of *Arabidopsis* plants (a homozygous knock-out line: SALK\_108854 for *At5g21100*, background ecotype Columbia-0) were dipped into *A. tumefaciens* (carrying pMDC32-OsORAP1 vector) solution ( $OD_{600} = 0.8$ ) contained in 5% (w/v) sucrose solution added with 0.05% (v/v) of silwet L77. Selection of transformants was conducted on 1/2 MS medium containing 50  $\mu$ g/mL hygromycin. Homozygous T3 seeds were used for the experiments.



### 2.3. Plant material and stress treatment

T1 seeds of two rice T-DNA insertion lines, 4A-00477 and 1B-00611, were obtained from the Crop Biotech Institute at Kyung Hee University (South Korea) (Jeon *et al.*, 2000; Jeong *et al.*, 2006). These T-DNA lines had been transformed using the *japonica* cultivar Dongjin as the wildtype (WT) and the transformation vector pGA2715, which transfers an 8.3-kb T-DNA insertion containing four tandem sequence repeats of a transcriptional enhancer element from the cauliflower mosaic virus (CaMV) 35S promoter. Line 4A-00477 (hereafter referred to as over-expression line: OE) contained the T-DNA insertion in 462 bp upstream of *OsORAP1*, while line 1B-00611 (hereafter referred to as knock-out: KO) contained the insertion in the intron of *OsORAP1* (Figure S1A). The presence of the insertion near the gene should lead to over-expression via activation tagging, while an insertion in the intron should lead to suppressed expression (Jeong *et al.*, 2002). The presence and orientation of the insertion were confirmed by PCR using genomic DNA as a template and the T-DNA right border primer 5'-AAC GCT GAT CAA TTC CAC AG-3' in combination with one of the following gene-specific primers: 5'-TGC AGG TTT CGT TGT CTC TG-3' (left) or 5'-GGA CGC GGT GCT ATC TTT AC-3' (right) for line 4A-00477 and 5'-TCG CAC CAA TAT CGA GAC AG-3' (left) and 5'-AGC GAG ATG CAT GTC AAC TG-3' (right) for line 1B-00611. Homozygous plants were selected in the T2 generation and used for the experiments. The seeds were sterilized with 5% (w/v) sodium hypochlorite solution for 5 min, and were rinsed five times with deionized water before imbibition. The seeds were germinated at 28 °C in the dark, and the seedlings were then transferred to a mesh floating on deionized water placed under natural light in a greenhouse. After growing for 2 weeks, the seedlings were transplanted into 60-L plastic containers filled with one-half-strength Yoshida solution (Yoshida *et al.*, 1976). One container accommodated a total of 40 plants of the three lines (KO, OE and WT) in a random distribution. The solution was changed to full strength 3 days before the onset of ozone fumigation, and the solution was renewed every 10 days. Supplementary lighting was provided in the greenhouse from 7 AM till 8 PM every day to ensure a minimum photosynthetic photon flux density of 250  $\mu\text{mol s}^{-1} \text{m}^{-2}$ . The minimum temperature of the greenhouse was set to 30/25 °C (day/night). The temperature was controlled by an inner heating system and ventilation through opening roofs. Therefore, plants were exposed to ambient ozone concentration.

*Arabidopsis* was grown in a closed greenhouse, and the ozone concentration in the greenhouse was close to zero.

Ozone fumigation was conducted in open-top chambers (1.3-m width x 1.0-m length x 1.3-m height) surrounded by transparent plastic sheets. Ozone was generated using custom-made ozone generators (UB01; Gemke Technik, Ennepetal, Germany) after drying the air with silica gel. The generated ozone was first percolated through water to remove NO<sub>x</sub>, and then blown into perforated plastic tubes with a fan to achieve even distribution of ozone in the chambers. The ozone concentration was permanently monitored by ozone sensors (GE 703 O3; Dr. A. Kuntze, Meerbusch, Germany) for realtime regulation of the generators. In addition, the ozone concentration was independently monitored with a handheld ozone monitor (Series 500, Aeroqual, Auckland, New Zealand) placed within the canopy. Two independent chambers were used for elevated ozone treatment (E-O<sub>3</sub>), and control plants exposed to ambient concentration of ozone (A-O<sub>3</sub>) were placed in identical chambers without ozone fumigation to ensure the same microclimate in both treatments. Each chamber contained two of the hydroponic containers described above.

### Experiment 1

This experiment was conducted from June to August 2012. The target ozone concentration was set to 150 ppb because of relatively high ambient ozone concentration in the experimental area. The actually recorded average daytime ozone concentration of the E-O<sub>3</sub> treatment was 159 ± 64 ppb (average ± standard deviation, same below; 9 AM to 4 PM), while the average concentration of A-O<sub>3</sub> chambers was 40 ± 14 ppb. Gene expression analysis except for tissue-specific expression, biochemical analyses except for apoplastic AsA, and AO and NADPH oxidase activity analyses were conducted in this experiment. Plant materials were harvested on the indicated days, flash-frozen in liquid nitrogen, and stored at -80 °C until analysis. Young shoots and leaves (top half of the shoot) were used for the analyses. The plants were 7 weeks old (counting from germination) after 20 days of fumigation.

### Experiment 2

This experiment was conducted from July to October 2014. The target concentration was set to 90 ppb. The actually measured average concentration of the E-O<sub>3</sub> treatment was 86 ± 32 ppb (9 AM to 4 PM), while that of A-O<sub>3</sub> chambers was 12 ± 8 ppb.

Visible symptoms on the leaves were determined as ‘leaf bronzing score (LBS)’ (Wissuwa *et al.*, 2006). The four youngest fully expanded leaves of each plant were assigned an LBS ranging from 0 (completely healthy) to 10 (dead) and averaged for each plant. Growth parameters, LBS, apoplastic AsA, stomatal conductance, tissue-specific expression levels of *OsORAP1*, and polyphenol oxidase activity were measured in this experiment (Supplementary Protocol 2). Stomatal conductance was measured using a LI-1600 Steady State Porometer (LI-COR, Lincoln, NE). The measurement was conducted on DAY 14 on the youngest fully expanded leaves. At least nine plants were taken for the measurement from each treatment and genotype, and the highest and lowest values were excluded. The measurements were conducted within 3 h around noontime on a cloudless day. The plants were 7 weeks old after 20 days of fumigation. Although different concentrations were adopted in these two experiments, the physiological responses of the plants were similar between these two experiments, as judged by the expression of *OsORAP1* and the content of lipid peroxidation (Figure S2), probably due to the climate conditions and the extent of ozone stress that the plants suffered before the onset of fumigation.

#### **2.4. RNA extraction and gene expression analysis**

The samples were ground in liquid nitrogen to a fine powder, and RNA was extracted with a PeqGOLD Plant RNA extraction kit (Peqlab, Erlangen, Germany) according to the manufacturer’s protocol, including DNase digestion using RQ1 DNase (Promega, Mannheim, Germany). The extracted RNA was precipitated with ethanol for further purification, and the pellet was dissolved in TE buffer (10 mM Tris-HCl and 1 mM EDTA, pH 8.0). The RNA concentration was measured with a Nanodrop 2000C instrument (Thermo Fisher Scientific, Waltham, MA) and the integrity was checked using a 2100 Bioanalyzer (Agilent Technologies, Santa Clara, CA). Reverse transcription was performed with a GoScript Reverse Transcription System (Promega) using both oligo dT primers and random hexamer primers according to the manufacturer’s protocol using 300 ng of RNA (except for microRNA analysis).

MicroRNA was quantified according to Lima *et al.* (2011). Total RNA was reverse transcribed using M-MLV Reverse Transcriptase (Promega). The reaction mixture contained 500 ng of total RNA, 6  $\mu$ L of 5x reaction buffer, 1.5  $\mu$ L of 1  $\mu$ M stem-loop primer (5'-GTC GTA TCC AGT GCA GGG TCC GAG GTA TTC GCA CTG GAT

ACG CAN NNN NN-3'), 1  $\mu\text{L}$  of 10 mM dNTP mix, 25 U of RNase inhibitor, and 0.5  $\mu\text{L}$  of reverse transcriptase in a 30  $\mu\text{L}$  scale. The reaction was performed using the following conditions: 30 min at 16  $^{\circ}\text{C}$ , 30 min at 42  $^{\circ}\text{C}$ , and 5 min at 85  $^{\circ}\text{C}$ .

Quantitative PCR was performed with the StepOnePlus real-time PCR system (Applied Biosystems, Foster City, CA). The reaction mixture consisted of 5  $\mu\text{L}$  of GoTaq qPCR Master Mix (Promega), 0.2  $\mu\text{L}$  of each gene-specific primer (10  $\mu\text{M}$ ) (Table S1), 3.6  $\mu\text{L}$  of nuclease-free water, and 1  $\mu\text{L}$  of cDNA sample. The reaction mixture was denatured at 95  $^{\circ}\text{C}$  for 10 min, followed by 40 cycles of 15 sec of denaturation at 95  $^{\circ}\text{C}$  and 1 min of annealing and extension at 60  $^{\circ}\text{C}$ . Melting curves were analysed after each reaction to check primer specificity. A house-keeping gene *Os05g0564200* was used as an internal control (Höller *et al.*, 2014a). The quantification of target genes was performed using  $\Delta\Delta\text{C}_T$  method as in Frei *et al.* (2010). The efficiency of amplification was checked for all primer pairs using cDNA dilution series, and the values between 80% and 112% were obtained. All gene expression analyses were conducted in analytical duplicates.

## 2.5. Enzyme assays

### *Ascorbate oxidase activity*

AO activity was measured according to Pignocchi *et al.* (2003). Briefly, the enzyme was extracted with 1 mL of 0.1 M sodium phosphate buffer (pH 6.5) from around 80 mg of sample ground in liquid nitrogen. The ion concentration was high enough to extract the AO from the cell wall since another extract using the same buffer including 1 M NaCl after the first extraction step retrieved only negligible AO activity in rice and *Arabidopsis*. The assay mixture consisted of 10  $\mu\text{L}$  of the enzyme extract, 80  $\mu\text{L}$  of sodium phosphate buffer (pH 5.6), and 10  $\mu\text{L}$  of 2 mM reduced AsA. The solution was mixed by pipetting, and the kinetics were read at 265 nm ( $\epsilon = 14.3 \text{ mM}^{-1} \text{ cm}^{-1}$ ) with a microplate reader (Powerwave XS2 microplate reader, BioTek, Bad Friedrichshall, Germany). The protein concentration was measured according to the method of Bradford (1976).

### *NADPH oxidase activity*

NADPH oxidase activity was measured according to Ishibashi *et al.* (2010). First, the enzyme was extracted from around 60 mg of frozen sample with 1 mL of 10 mM

sodium phosphate buffer (pH 6.0) and two times of 15-sec sonication. The supernatant was obtained by centrifugation at 16,000 g, at 4 °C for 15 min. An aliquot of 200 µL of the extract was mixed with 1.8 mL of 100% (v/v) acetone and placed at -20 °C for more than 15 min. The protein was recovered by centrifugation at 12,500 rpm, at 4 °C for 10 min. The pellet was dissolved in 50 mM Tris-HCl (pH 8.0) containing 0.1 mM MgCl<sub>2</sub>, 0.25 M sucrose, and 0.1% (v/v) Triton X-100. The assay mixture consisted of 10 µL of the protein extract, 10 µL of 5 mM nitroblue tetrazolium, 10 µL of 1 mM NADPH, and 70 µL of the above-mentioned Tris buffer containing MgCl<sub>2</sub>, sucrose, and Triton X-100. The kinetics were read at 530 nm ( $\epsilon = 12.8 \text{ mM}^{-1} \text{ cm}^{-1}$ ) and the activity was calculated based on the protein concentration.

## 2.6. Biochemical assays

### *AsA assay*

Extraction and quantification of AsA from the apoplast and the whole tissue were based on Ueda *et al.* (2013b). The reduced AsA content was measured from the absorption decrease at 265 nm after the addition of 10 µL of 0.01 U/µL AO to a mixture of 10 µL of extracted AsA and 80 µL of 0.1 M potassium phosphate buffer (pH 7.0). The oxidized AsA content was measured from the absorption increase at 265 nm after addition of 10 µL of 4 mM dithiothreitol to a mixture of 10 µL of extracted AsA and 80 µL of 0.1 M potassium phosphate buffer (pH 7.8). The calculation of the AsA content was based on the extinction coefficient of  $\epsilon = 14.3 \text{ mM}^{-1} \text{ cm}^{-1}$ .

### *Chlorophyll measurements*

Chlorophyll content was measured according to Porra *et al.* (1989) using dimethyl formamide (DMF) as a solvent. Approximately 10 mg of fresh sample was taken from the middle part of the second fully expanded leaf, put into a 1.5-mL tube together with 1 mL DMF without grinding, and stored at 4 °C for 24 h. The absorption of the resultant solution was read at 647, 664, and 750 nm (background) using a microplate reader. The concentrations of chlorophylls *a* and *b* were calculated by the following formulae:

$$\text{Chl } a = \frac{12.00 \times (A_{664} - A_{750}) - 3.11 \times (A_{647} - A_{750})}{0.29}$$

$$\text{Chl } b = \frac{20.78 \times (A_{647} - A_{750}) - 4.88(A_{664} - A_{750})}{0.29}$$

Here, 0.29 denotes the path length (cm) of the solution when 100  $\mu\text{L}$  was put onto a 96-well plate (No. 3635, Corning, Corning, NY).

#### *MDA quantification*

The amount of malondialdehyde (MDA) was determined as described previously (Hodges *et al.* 1999; Höller *et al.*, 2014b). Extraction was performed from approximately 100 mg of ground tissues with 2 mL of 0.1% (w/v) trichloroacetic acid (TCA). The supernatant was obtained after centrifugation at 4 °C and 15,000 g for 15 min. An aliquot of 250  $\mu\text{L}$  of the supernatant was mixed with 250  $\mu\text{L}$  of 20% (w/v) TCA, 0.01% (w/v) 2,6-di-tert-butyl-4-methylphenol and 0.65% (w/v) thiobarbituric acid (TBA). The mixture was heated to 95 °C for 30 min, and the absorbance of the supernatant was measured at 440, 532 and 600 nm. The absorption of blank samples, which did not contain TBA, was subtracted for each sample.

#### **2.7. Statistical analyses**

Statistical analyses were performed using the SAS programme (SAS Institute, Cary, NC) applying a PROC MIXED model. Genotype, treatment, and genotype and treatment interaction were set as fixed effects, and chambers and chamber x container were set as random effects as described by Frei *et al.* (2011). Tukey's test was conducted as a post-hoc test. *P* values below 0.05 were considered to be significant.

### 3. Results

#### 3.1. Hypothesis 1: *OsORAP1 is an ascorbate oxidase localized in the apoplast*

The amino acid sequence of AO (EC. 1.10.3.3) is highly similar to that of laccases (EC. 1.10.3.2), which are also classified as multicopper oxidases and have a large number of family proteins (Hoegger *et al.*, 2006). To analyse phylogenetic relationships of the rice *OsORAP1* gene (*Os09g0365900*) with other similar genes, we first compared the sequence of OsORAP1 with other *Arabidopsis* and rice AO and laccase proteins. OsORAP1 was in the same clade as other *Arabidopsis* AO proteins (At5g21100, At5g21105 and At4g39830; Yamamoto *et al.*, 2005; Fig. 3-1A, clade III), being closest to At4g39830 with 59% identity at the amino acid level. Three other rice proteins (Os06g0567200, Os06g0567900 and Os09g0507300) were in the same clade as the *Arabidopsis* AO proteins. This clade was further categorized into III-A and III-B, each including rice and *Arabidopsis* proteins. Analysis with other plant species also revealed clear diversification of clades III-A and III-B (Figure S3). All the known *Arabidopsis* laccase proteins were classified into clade I; therefore, we concluded that it represented the large laccase family. Another small family (clade II) was not classified as clade I or III, and was termed as AO-like. The AO-like subfamily did not contain the multicopper oxidase protein domain and copper-binding site (InterPro ID: IPR002355), while all the sequences in clade III did, including OsORAP1 (Figure S4). The proteins in clade III also contained a protein signature L-ascorbate oxidase, plants (InterPro ID: IPR017760).

Analysis with the SignalP 4.1 programme (Petersen *et al.*, 2011) predicted a signal peptide in the first 24 amino acids and a cleavage site between amino acids 24 and 25, thereby providing evidence that OsORAP1 is a secreted protein. To experimentally confirm the subcellular localization of OsORAP1, we produced a vector construct, in which the OsORAP1 protein was fused with GFP at the C-terminus, and expressed them in *N. benthamiana* leaves with the constitutive CaMV 35S promoter. Heterologous expression in *N. benthamiana* epidermal cells showed GFP signals clearly localized in the cell periphery (Fig. 3-1B-D). Signals were observed in the periphery of the cells in mesophyll cells as well (Fig. 3-1E). Upon plasmolysis (*i.e.* dissociation of the plasma membrane from the cell wall) in epidermal cells, the signals were observed in the apoplastic space (Fig. 3-1F, arrowheads), thereby confirming the apoplastic localization of OsORAP1.

Complementation analysis was conducted to examine whether OsORAP1 had AO activity. We obtained a homozygous knock-out line for an *Arabidopsis* gene in clade III-B (*At5g21100*, SALK\_108854 line) and performed an enzymatic assay of AO. Indeed, AO activity was severely reduced in this knock-out line as compared with the wildtype as reported previously (Fig. 3-1G; Yamamoto *et al.*, 2005). To assess whether OsORAP1 exhibits AO activity, we generated transgenic *Arabidopsis* plants expressing CaMV 35S::*OsORAP1* in a mutant (*At5g21100*) background. If OsORAP1 encoded a functional AO, increased AO activity would be expected in the complementation lines as compared with non-complemented mutants. However, the decreased AO activity in the knock-out line was not recovered by the introduction of *OsORAP1* despite evidence for its constitutive expression (Fig. 3-1G, H). Expression data from previous transcriptomic studies suggested that another *Arabidopsis* AO homologue (*At4g39830*, clade III-A) was specifically induced by ozone and biotic stresses (Table S2). Therefore, AO activity of a homozygous knock-out line of *At4g39830* (SALK\_046824 line) was tested in chronic and acute ozone stress along with control conditions (Fig. 3-1I). *At4g39830* was strongly induced under acute ozone stress (Fig. 3-1J). However, AO activity level did not show marked differences between the wildtype and a knock-out line, despite the expression of *At4g39830* in acute ozone stress (Fig. 3-1I, J), suggesting that *At4g39830* did not dominate AO activity in *Arabidopsis*. Transient expression of native OsORAP1 protein under the regulation of the CaMV 35S promoter in *N. benthamiana* leaf also did not lead to increased AO activity despite the expression of *OsORAP1* (Figure S5). Based on these observations, we confirmed that OsORAP1 was an apoplastic protein, but it had no detectable AO activity under the conditions tested in this study.



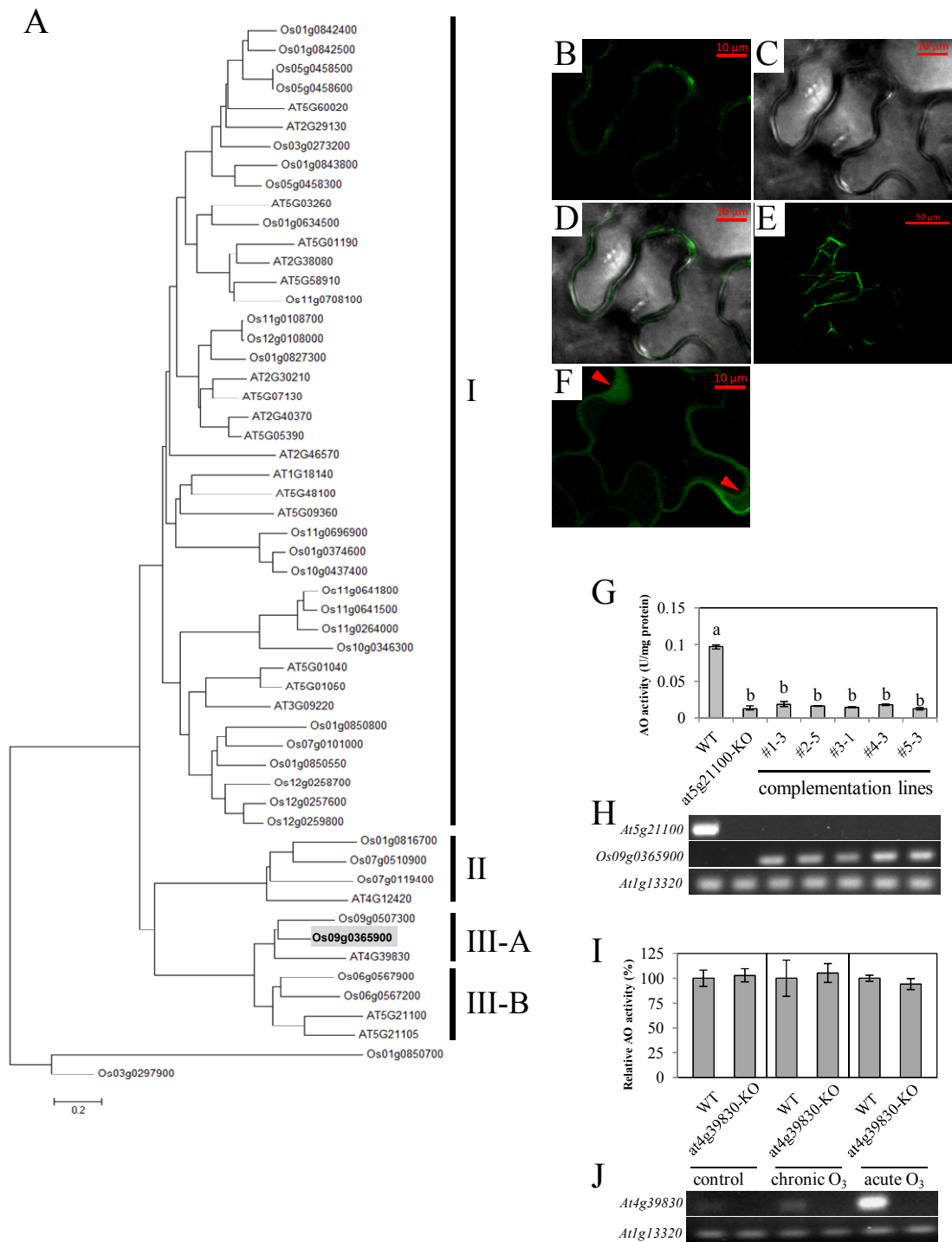


Figure 3-1: Bioinformatic and physiological analysis of *OsORAP1*. (A) Phylogenetic analysis of laccase- and ascorbate oxidase (AO)-related proteins from rice and *Arabidopsis*. The neighbour-joining method was used to generate the tree. The branch length represents the evolutionary distance calculated by the Poisson correction method. *OsORAP1* (Os09g0365900) is shown in boldface and highlighted. (B-F) Subcellular localization of the *OsORAP1* protein in *Nicotiana benthamiana* epidermal cells (B-D and F) and mesophyll cells (E). *OsORAP1* was transiently expressed under the control of the cauliflower mosaic virus 35S promoter. The signal of GFP (B, E and F), bright field (C) and merged images (D) are shown. In F, plasmolysis was induced by incubating the leaf segment with 1 M NaCl for 30 min prior to observation. Arrowheads indicate the dissociation of cell membrane from the cell wall and resultant signals in the apoplast. Bars = 10 mm (B-D and F) and 50 mm (E). (G) AO activity of wildtype *Arabidopsis* plants (WT), a homozygous knock-out line of *At5g21100* (*at5g21100*-KO), and

five individual homozygous complementation lines. Values are means of four biological replicates. (H) Expression of *At5g21100* (*Arabidopsis* AO homologue; top), *Os09g0365900* (rice *OsORAP1*; middle) and *At1g13320* (*Arabidopsis* reference gene; bottom). (I) AO activity of WT and a homozygous knock-out line of *At4g39830* (*at4g39830*-KO). The activity of WT was considered as 100% in each treatment, and the activity of *at4g39830*-KO is shown in relative values. Chronic ozone treatment was conducted at the average concentration of  $110 \pm 44$  ppb (7 h and 17 days), and acute ozone treatment was conducted at the average concentration of  $230 \pm 80$  ppb (6 h and 4 days). In all cases, rosette leaves of 4- to 6-week-old plants were used for the analysis. Values are means of four to six biological replicates. (J) Expression of *At4g39830* (*Arabidopsis* AO homologue; top) and *At1g13320* (bottom). In G and I, error bars indicate standard errors.

### 3.2. Hypothesis 2: *OsORAP1* is involved in ozone-induced cell death in rice

#### *Gene expression analysis*

To get insight into the expression patterns of *OsORAP1* in ozone stress, 4-week-old wildtype (WT) rice plants were treated either with ambient concentration of ozone (A-O<sub>3</sub>), corresponding to the naturally occurring ozone in the greenhouse atmosphere, or with elevated ozone (E-O<sub>3</sub>) for 20 days. First, gene expression levels were analysed in different tissues in both conditions. Strong induction of the expression was observed only in young leaf blades ( $P < 0.001$ ), while other tissues did not show significantly increased level of expression (Fig. 3-2A). The constitutive expression level of *OsORAP1* was high in old leaves and root tissues (Fig. 3-2A). To investigate the function and physiological importance of *OsORAP1* with respect to ozone tolerance in rice, a homozygous rice knock-out line (KO) and a homozygous over-expression line (OE) were obtained (Figure S1A). Four-week-old plants were treated with ozone for 20 days along with WT. Two independent experiments were conducted, through which similar results were obtained (stated below). KO did not produce any functional full-length *OsORAP1* transcript due to a T-DNA insertion (Figure S1B). *OsORAP1* was highly induced by elevated ozone, reaching more than 30-fold expression levels compared with A-O<sub>3</sub> in WT on DAY 10 (Fig. 3-2B). In all cases, significantly higher expression was observed in OE than in WT (Fig. 3-2B). Similar *OsORAP1* expression levels were obtained from the second ozone fumigation experiment (Figure S2A).

The gene expression levels of the aforementioned three putative rice AO homologues were also analysed. The closest homologue, *Os09g0507300*, showed no expression in any of the conditions tested in our study (data not shown). The other two homologues, *Os06g0567200* and *Os06g0567900*, showed constitutive expression in A-O<sub>3</sub> condition

(Fig. 3-2C, D). KO of *OsORAP1* showed a higher expression level of *Os06g0567200* than the other two lines ( $P < 0.05$ ; Fig. 3-2C).

*OsORAP1* is predicted to interact with a microRNA, *Osmir528*, in rice (de Lima *et al.*, 2012). Therefore, we analysed the expression of *Osmir528* in all three lines (KO, WT and OE) in A-O<sub>3</sub> and E-O<sub>3</sub> conditions. We found that transcript abundance for *Osmir528* decreased significantly in all three lines in ozone stress ( $P < 0.05$ ; Fig. 3-2E). Moreover we also observed a significant interaction between genotype and treatment (GxT) ( $P < 0.05$ ). These observations strongly suggest that *Osmir528* is involved in the ozone-induced transcriptional regulation of *OsORAP1*.

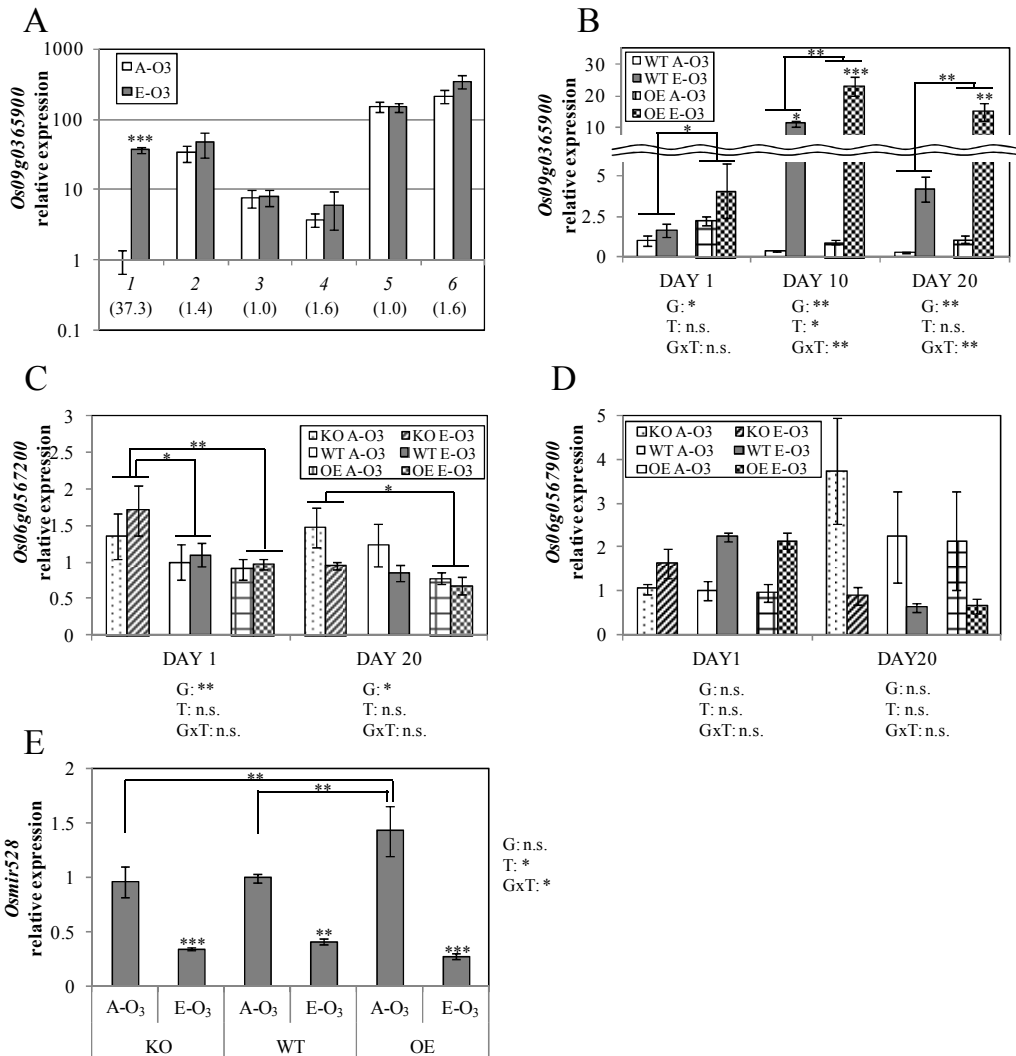


Figure 3-2: Expression analysis of *OsORAP1*, two other ascorbate oxidase (AO) genes, and a microRNA, *Osmir528*. (A) Expression levels of *OsORAP1* in different tissues in the ambient condition (A-O<sub>3</sub>, 40 ppb) and the elevated ozone condition (E-O<sub>3</sub>, 159 ppb) on DAY 20. Different tissues used in the experiment are as follows: 1, two youngest leaf blades; 2, two oldest leaf blades; 3, outer leaf sheaths; 4, inner leaf sheaths (containing newly emerging leaves); 5, half basal part of roots; and 6, half apical part of roots. The value in the parentheses is the fold increase in the E-O<sub>3</sub> condition in each tissue

as compared with the A-O<sub>3</sub> condition. Pair-wise Student's *t*-tests were conducted for each tissue between two treatments. Asterisks indicate a significant difference ( $P < 0.001$ ). The y axis is shown in logarithmic scale. The expression level in the two youngest leaf blades in A-O<sub>3</sub> was determined as 1. (B-E) Gene expression analysis in young shoot and leaves in the A-O<sub>3</sub> condition (40 ppb) and the E-O<sub>3</sub> condition (159 ppb). (B) Expression levels of *OsORAP1* in A-O<sub>3</sub> and E-O<sub>3</sub> at three different time points in two different genotypes. (C) Expression levels of a rice AO homologue (*Os06g0567200*) in A-O<sub>3</sub> and E-O<sub>3</sub> at two different time points in three different genotypes. (D) Expression levels of a rice AO homologue (*Os06g0567900*) in A-O<sub>3</sub> and E-O<sub>3</sub> at two different time points in three different genotypes. (E) Expression of the microRNA *Osmir528* on DAY 20. In all cases, E-O<sub>3</sub> treatment was started (DAY 1) at the 4-week-old stage. KO, knock-out line; WT, wildtype; and OE, over-expression line. Values are means of four biological replicates (except for the WT A-O<sub>3</sub> sample on DAY 10 due to the loss of one sample). Error bars indicate standard errors. In B-E, ANOVA was conducted for each day, and the significance is denoted as follows: G, genotype; T, treatment; GxT, genotype and treatment interaction; n.s., not significant; \*,  $P < 0.05$ ; \*\*,  $P < 0.01$ ; and \*\*\*,  $P < 0.001$ .

### *OsORAP1 knock-out mitigates cell death formation in ozone stress*

Growth parameters and LBS were measured in WT, KO, and OE plants to assess the effect of *OsORAP1* expression in ozone stress. KO showed significantly lower LBS compared with WT and OE, demonstrating enhanced tolerance to ozone stress (Fig. 3-3A, B). The difference in LBS was not due to differences in morphology since the plant height, which might affect ozone uptake due to canopy resistance, was similar in all three lines (Figures S6 and S7A). We also did not observe significant genotypic differences in chlorophyll content or chlorophyll *a/b* ratio (Fig. 3-3C).

Stomatal conductance was measured, as ozone is mainly taken up through the stomata and the uptake is proportional to the stomatal aperture (Omasa *et al.*, 2002). We observed a clear treatment effect ( $P < 0.001$ ), but no significant genotype or GxT effect (Fig. 3-4A). Growth parameters were determined on DAY 20. KO showed constitutively lower shoot fresh weight (FW) and tiller number compared with WT and OE (Fig. 3-4B). A significant correlation was seen between FW and tiller number ( $r^2 = 0.81$ ,  $P < 10^{-7}$ ), suggesting that large part of reduced FW in KO is ascribed to reduced tiller number. However, when grown in soil, KO showed significantly shorter flag leaf blade length, while the shape (ratio of leaf length and width) was not affected (Figure S7C, D). We further investigated the leaf weight per area to estimate the cell density, since it plays an important role for ozone stress tolerance in *Arabidopsis* (Barth and Conklin, 2003). The analysis revealed no significant genotypic differences in the cell density among genotypes (Figure S8). Taken together, KO specifically mitigated foliar cell death induced by ozone stress, while other leaf properties, such as cell density and chlorophyll content, were not affected, except for leaf length.

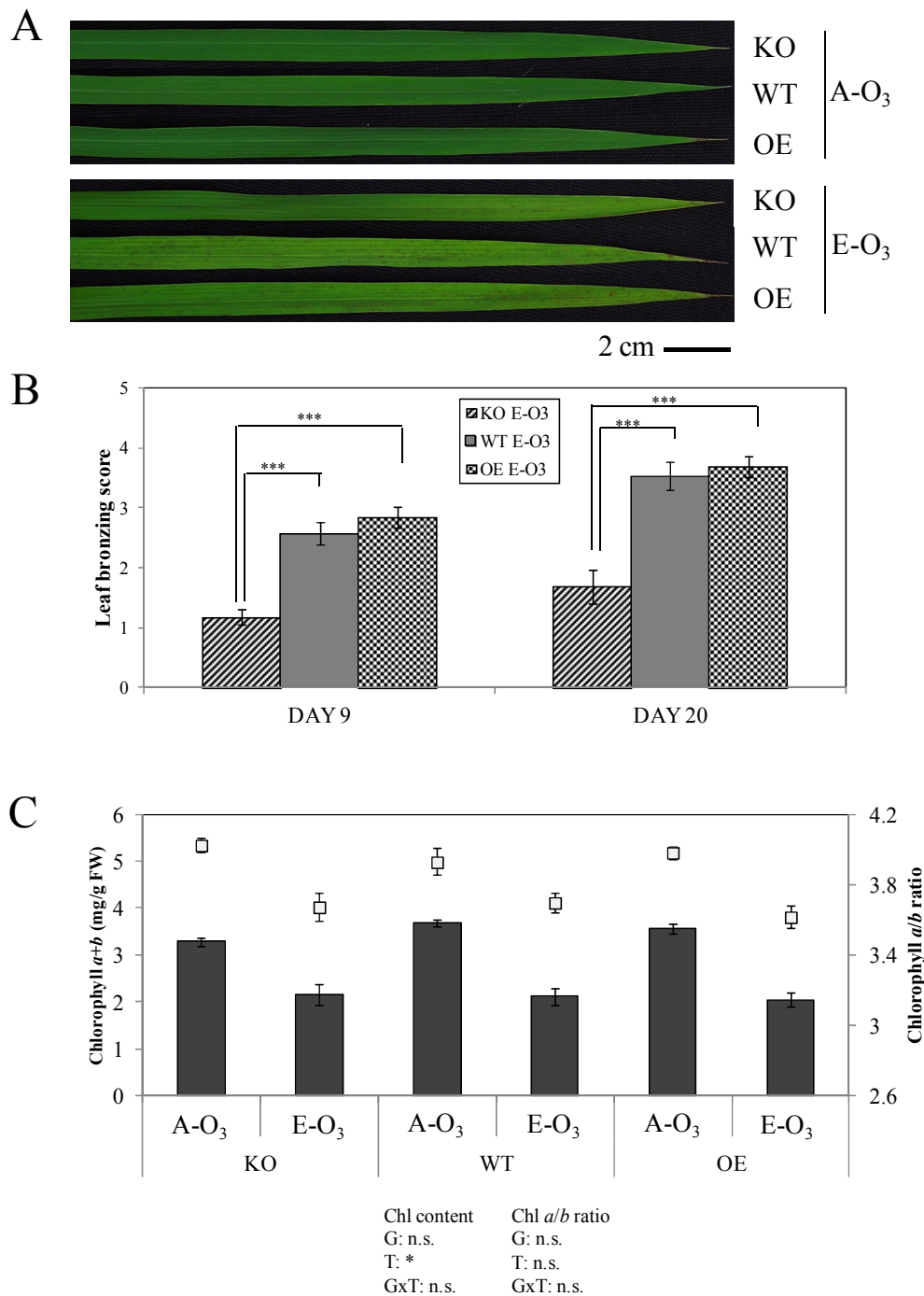


Figure 3-3: Formation of leaf visible symptoms and biochemical parameters in three rice lines. (A) Leaf images exposed to the ambient ozone concentration (A-O<sub>3</sub>, 12 ppb) or the elevated ozone treatment (E-O<sub>3</sub>, 86 ppb) after 15 days from the onset of the experiment. Representative second fully expanded leaves were photographed. (B) Leaf bronzing score from three lines on DAY 9 and DAY 20 in the E-O<sub>3</sub> condition (86 ppb). The values are means of 20 to 22 biological replicates on DAY 9, and eight biological replicates on DAY 20. (C) Chlorophyll content (bars, left axis) and chlorophyll *a/b* ratio (squares, right axis) in A-O<sub>3</sub> (40 ppb) and E-O<sub>3</sub> (159 ppb). The measurement was conducted on DAY 8. Elevated ozone treatment was started at the 4-week-old stage. Values are means of four biological replicates. KO, knock-out line; WT, wildtype; and OE, over-expression line. FW, fresh weight. All error bars indicate standard errors. In B and C, ANOVA was conducted, and the significance is denoted as follows: G, genotype; T, treatment; GxT, genotype and treatment interaction; n.s., not significant; \*,  $P < 0.05$ ; and \*\*\*,  $P < 0.001$ .

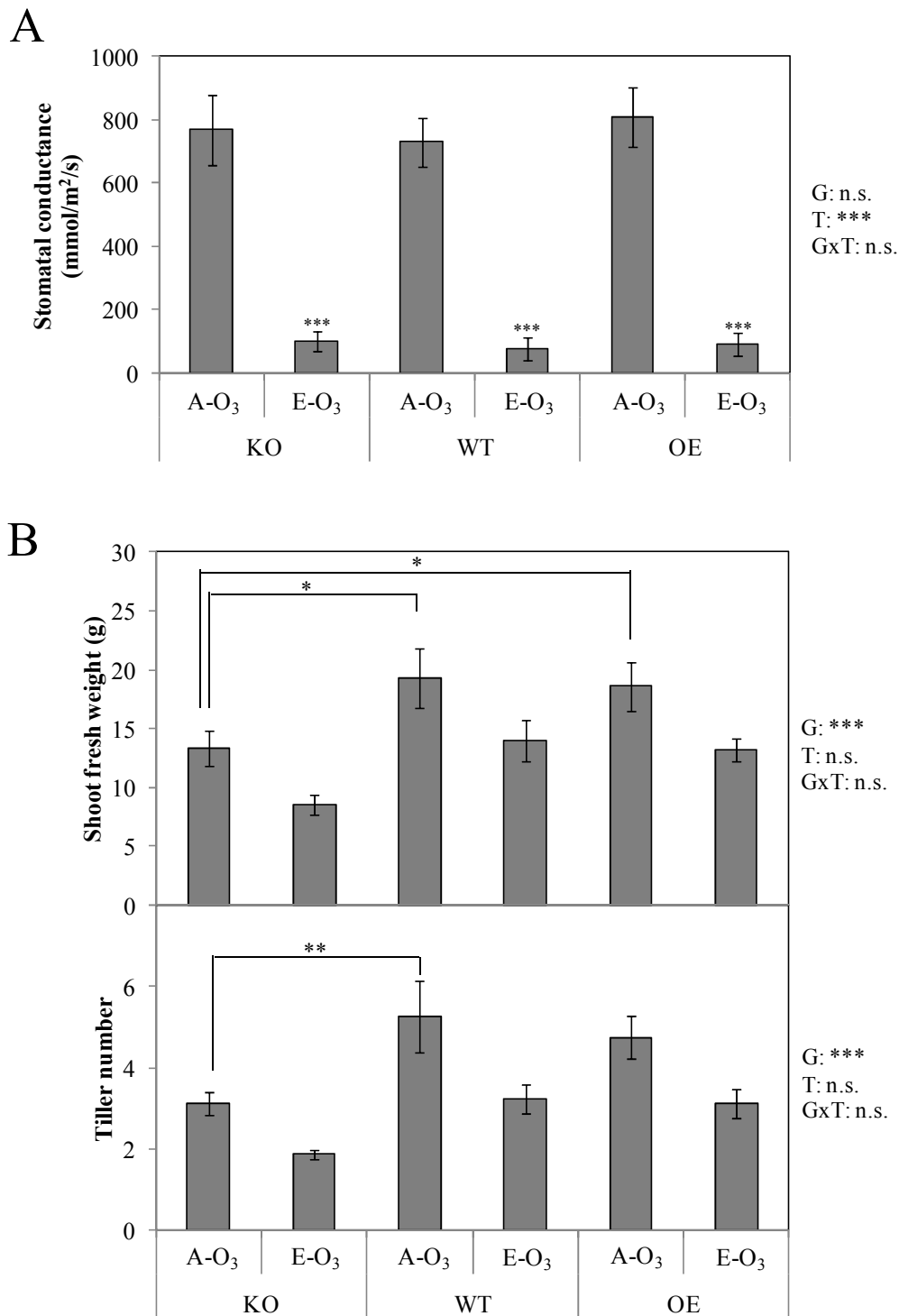


Figure 3-4: Effects of ozone on stomatal conductance and growth characteristics. (A) Stomatal conductance of the three lines in the ambient ozone concentration (A-O<sub>3</sub>, 12 ppb) and the elevated ozone concentration (E-O<sub>3</sub>, 86 ppb). The measurement was conducted on DAY 14. The values are means of seven to eleven samples. Error bars indicate standard errors. (B) Growth characteristics of the three lines in A-O<sub>3</sub> (12 ppb) and E-O<sub>3</sub> (86 ppb) on DAY 20. Values are means of eight biological replicates. Error bars indicate standard errors. E-O<sub>3</sub> treatment was started at the 4-week-old stage. KO, knock-out line; WT, wildtype; and OE, over-expression line. ANOVA was conducted, and the significance is denoted as follows: G, genotype; T, treatment; GxT, genotype and treatment interaction; n.s., not significant; \*,  $P < 0.05$ ; \*\*,  $P < 0.01$ ; and \*\*\*,  $P < 0.001$ .

*Knock-out line induces less oxidative damage*

Lipid peroxidation (assessed as MDA equivalents) occurs even before the initiation of leaf visible symptoms and, thus, represents an indicator of oxidative stress preceding symptom formation (Ueda *et al.*, 2013a; Höller *et al.*, 2014b). Elevated ozone treatment increased the MDA content even on DAY 3 ( $P < 0.01$ ; Fig. 3-5A), when the leaf symptoms had hardly emerged (data not shown). On DAY 3, MDA content was significantly lower in KO than in WT and OE. We observed a significant GxT effect on DAY 20 ( $P < 0.01$ ), where MDA increased significantly in WT and OE ( $P < 0.01$ ), while KO did not respond significantly to ozone. We obtained similar results from the second fumigation experiment, where a significant GxT effect was observed (Figure S2B). Next, we investigated active reactive oxygen species (ROS) production in the apoplast, since secondary ROS formation by NADPH oxidases contributes substantially to ozone damage (Overmyer *et al.*, 2000; Wohlgenuth *et al.*, 2002). Ozone stress significantly lowered the NADPH oxidase activity on DAY 20. On both days, KO showed constitutively less  $O_2^{\cdot-}$  producing activity compared with WT (Fig. 3-5B).

*AO activity and apoplastic AsA content*

As we expected based on the results obtained from the complementation assay, the knock-out and over-expression of *OsORAP1*, which was classified into clade III-A (Fig. 3-1A), did not affect AO activity (Fig. 3-6A). The AO activity in the whole tissue extract was also similar to that of the apoplastic washing fluid (Figure S9,  $r^2 = 0.96$ ,  $P < 0.001$ ), showing that the localization of the enzyme did not differ among lines or between the treatments. The expression level of one AO homologue (*Os06g0567900*, clade III-B) showed a highly significant correlation with measured AO activity (Fig. 3-6B), demonstrating that this homologue was the dominant AO gene in rice shoots under the conditions used for the study.

Apoplastic AsA did not show any significant differences between the lines (Fig. 3-7), which was consistent with the lack of difference in AO activity. Likewise, AsA level or redox status in the whole shoot tissue did not show genotypic differences (Figure S10). We investigated the activity of closely related laccase and other polyphenol oxidases which are also classified as copper-containing enzymes, namely catechol oxidase and tyrosine oxidase (McGuirl and Dooley, 1999). However, different

polyphenol oxidase activities, including laccase activity, also did not show genotypic differences (Figure S11).

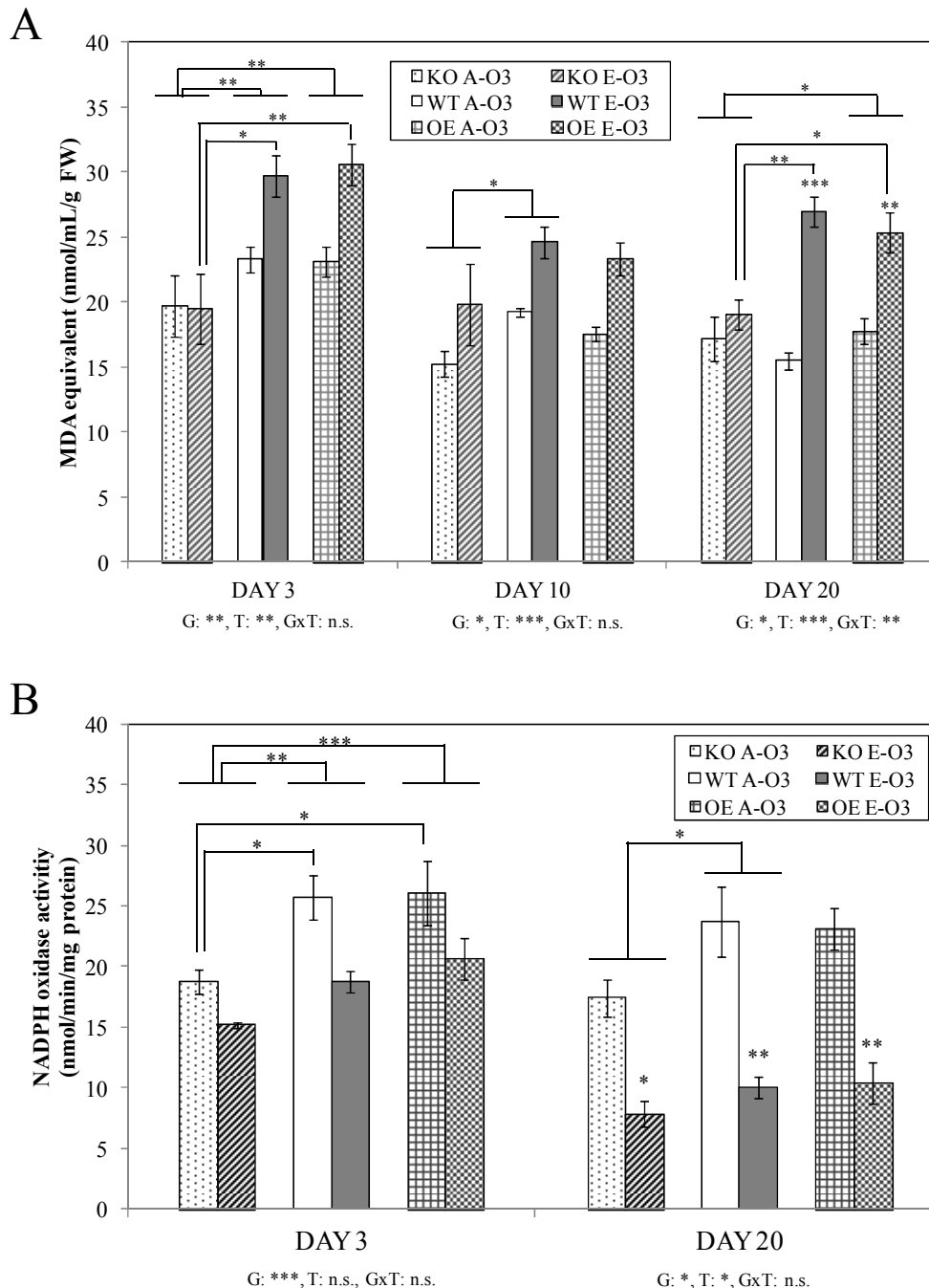


Figure 3-5: Measures of oxidative stress in three rice lines in the ambient ozone concentration (A-O<sub>3</sub>, 40 ppb) and the elevated ozone concentration (E-O<sub>3</sub>, 159 ppb). (A) Lipid peroxidation as represented by malondialdehyde (MDA) equivalents. FW, fresh weight. (B) NADPH oxidase activity. Elevated ozone treatment was started at the 4-week-old stage. KO, knock-out line; WT, wildtype; and OE, over-expression line. Values are means of four biological replicates (except for the WT A-O<sub>3</sub> sample on DAY 10, due to the loss of one sample). Error bars indicate standard errors. Asterisks on E-O<sub>3</sub> bars show that the values were significantly affected by treatment. ANOVA was conducted, and the significance is denoted as follows: G, genotype; T, treatment; GxT, genotype and treatment interaction; n.s., not significant; \*,  $P < 0.05$ ; \*\*,  $P < 0.01$ ; and \*\*\*,  $P < 0.001$ .



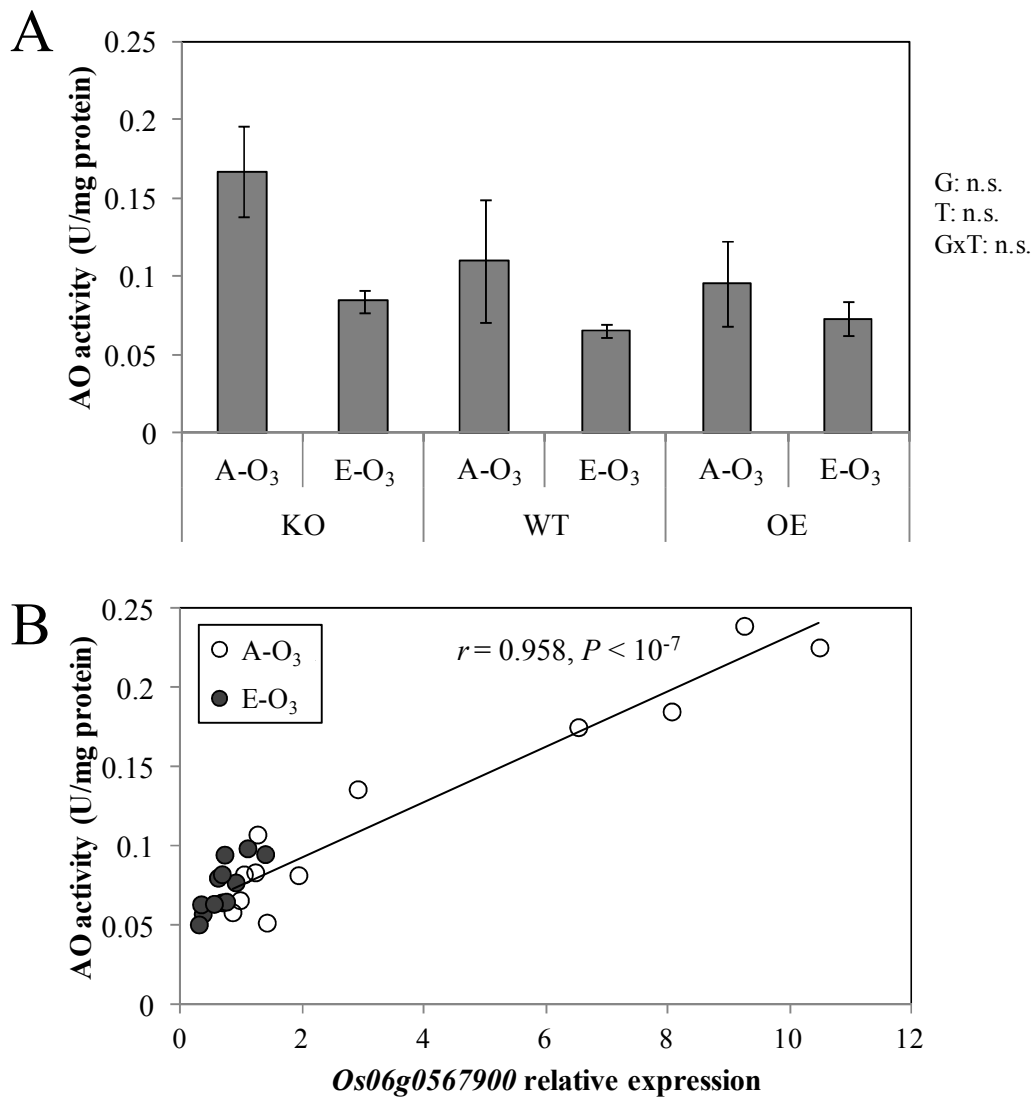


Figure 3-6: Ascorbate oxidase (AO) activity in the ambient ozone concentration (A-O<sub>3</sub>, 40 ppb) and the elevated ozone concentration (E-O<sub>3</sub>, 159 ppb). (A) AO activity in the three lines. The samples were taken on DAY 20 of E-O<sub>3</sub> treatment. KO, knock-out line; WT, wildtype; and OE, over-expression line. Values are means of four biological replicates. Error bars indicate standard errors. ANOVA was conducted, and the result is shown as follows: G, genotype; T, treatment; GxT, genotype and treatment interaction; and n.s., not significant. (B) Correlation between the expression level of an AO homologue (*Os06g0567900*) and AO activity on DAY 20 in A-O<sub>3</sub> and E-O<sub>3</sub> conditions. Pearson's correlation coefficient and the corresponding *P* value are shown. Elevated ozone treatment was started at the 4-week-old stage.

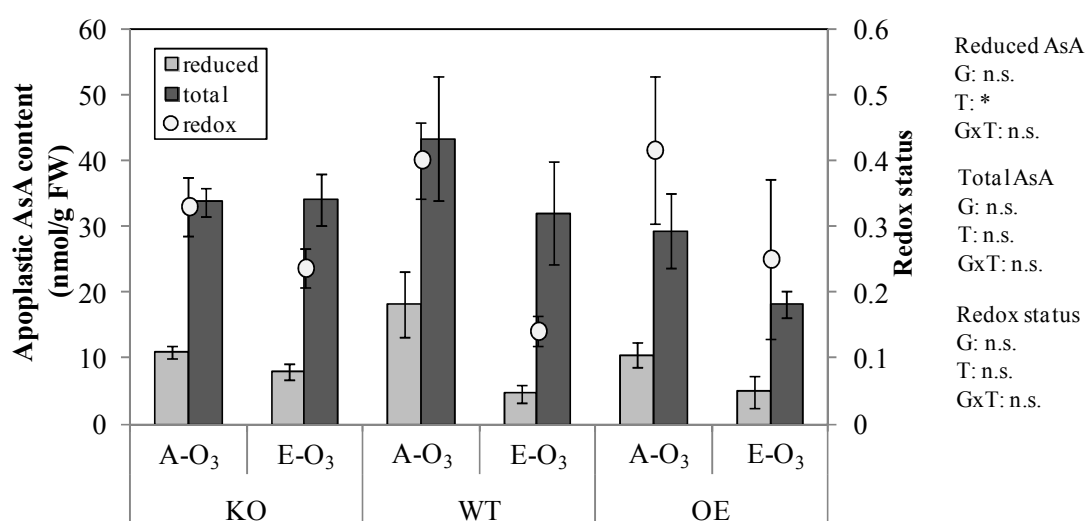


Figure 3-7: Apoplastic ascorbate characteristics in the ambient ozone concentration (A-O<sub>3</sub>, 12 ppb) and the elevated ozone concentration (E-O<sub>3</sub>, 86 ppb). Samples were taken on DAY 15 of E-O<sub>3</sub> treatment. Redox status was defined as (reduced AsA)/(total AsA). Elevated ozone treatment was started at the 4-week-old stage. KO, knock-out line; WT, wildtype; and OE, over-expression line. FW, fresh weight. Values are means of four biological replicates. Error bars indicate standard errors. ANOVA was conducted, and the result is shown as follows: G, genotype; T, treatment; GxT, genotype and treatment interaction; n.s., not significant; and \*,  $P < 0.05$ .

#### *Involvement of plant hormones*

We investigated the involvement of plant hormones related to the formation and propagation of leaf visible symptoms in ozone stress, such as ethylene (ET), salicylic acid (SA) and jasmonic acid (JA) (Rao and Davis, 2001; Kangasjärvi *et al.*, 2005). Through an analysis of public microarray data, it was found that *OsORAP1* is induced by exogenous SA application, which was also experimentally confirmed (Fig. 3-8A). To further investigate the interaction of *OsORAP1* with SA, we investigated in public microarray data sources the expression levels of *OsORAP1* in mutant lines for the transcription factor *OsWRKY45*, which is a regulator of SA response in rice (Shimono *et al.*, 2007). In the first dataset (NCBI Gene Expression Omnibus [GEO] ID: GSE23733), *OsORAP1* was induced by benzothiadiazole (BTH; a functional analogue of SA), and the expression was significantly lower in a knock-down line of *OsWRKY45* compared with the wildtype (Fig. 3-8B). Consistently, the expression of *OsORAP1* was significantly higher in the *OsWRKY45* over-expression line in the second dataset (NCBI GEO ID: GSE48202; Fig. 3-8C).

We further analysed the expression levels of genes which are involved in either biosynthetic or signalling pathways of the above-mentioned hormones on DAY 1 and

DAY 20 in our mutant lines (Fig. 3-8D-H, Figure S12). The expression of *OsWRKY45* was higher in KO and OE than in WT on both days (Fig. 3-8D). On the other hand, the expression level of *Nonexpressor of Pathogenesis-Related Genes1 (OsNPR1)*, another transcription factor controlling SA response (Shimono *et al.*, 2007), was lower in KO than WT on DAY 1 (Fig. 3-8E). Differential regulation of genes was also observed in JA-related genes. The enzyme 12-oxophytodienoate reductase7 (*OsOPR7*) is involved in JA biosynthesis in rice, and its expression level correlates with JA level (Tani *et al.*, 2008). *OsJAZ8* is involved in JA signalling and its expression level is induced by JA application (Yamada *et al.*, 2012). *OsJAmyb* is a transcription factor which is induced by JA (Lee *et al.*, 2001). On DAY 20, *OsOPR7* showed significantly higher expression in KO (Fig. 3-8F), and the expression of *OsJAZ8* and *OsJAmyb* was significantly higher on DAY 1 in KO (Fig. 3-8G, H). The expression level of *OsJAmyb* was higher in KO even in the A-O<sub>3</sub> condition on DAY 1 (Fig. 3-8H).

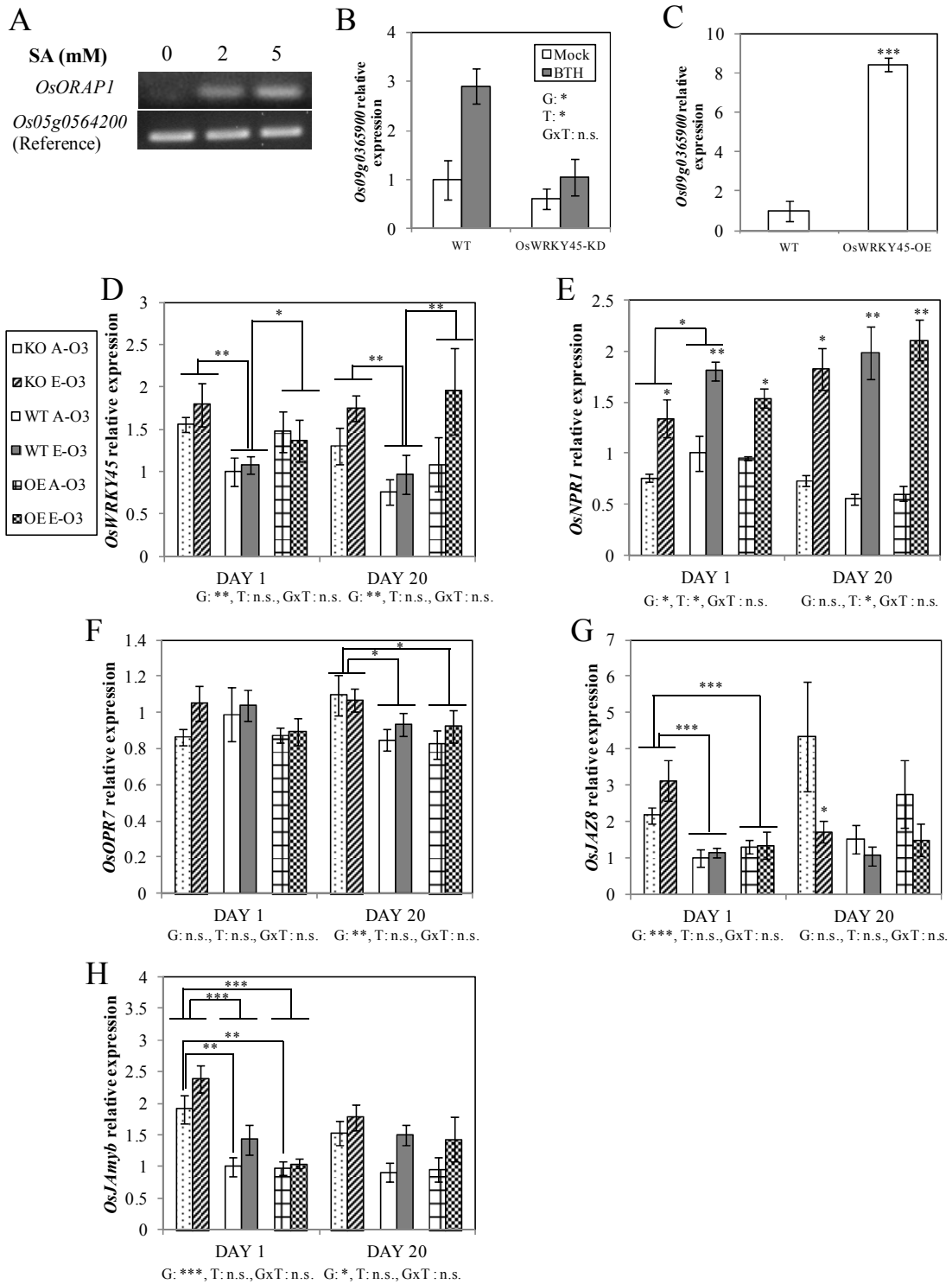


Figure 3-8: Involvement of OsORAP1 in phytohormone signalling. (A) Induction of *OsORAP1* by salicylic acid (SA) treatment. Six-week-old plants were sprayed with the indicated concentrations of SA in 0.1% (v/v) Tween 20, and the two youngest leaves were harvested after 48 h. The expression levels of *OsORAP1* (using primers OsORAP1-F2/R2) and an internal control (*Os05g0564200*) are shown. (B) Expression levels of *OsORAP1* in the wildtype (WT) and an *OsWRKY45* knock-down line (OsWRKY45-KD) after mock treatment (0.05% (v/v) acetone and 0.05% (v/v) Tween 20) or benzothiadiazole (BTH) treatment (0.5 mM BTH in 0.5% (v/v) acetone and 0.05% (v/v) Tween 20). The samples were taken after 12 h of treatment. The data were retrieved from an open microarray data source (NCBI GEO ID: GSE 23733). Original log<sub>2</sub>-converted values were processed and expressed as linear values. The expression level of WT sample with mock treatment was set to 1. (C) Expression

levels of OsORAP1 in the wildtype (WT) and an *OsWRKY45* over-expression line (OsWRKY45-OE). The data were retrieved from an open microarray data source (NCBI GEO ID: GSE48202). Original  $\log_2$ -converted values were processed and expressed as linear values. The expression level of WT sample was set to 1. Student's *t*-test was conducted, and the asterisks indicate a significant difference ( $P < 0.001$ ). (D-H) Expression levels of phytohormone-related genes in the ambient ozone concentration (A-O<sub>3</sub>, 40 ppb) and the elevated ozone concentration (E-O<sub>3</sub>, 159 ppb). The gene IDs are as follows: *OsWRKY45*, *Os05g0322900*; *OsNPR1*, *Os01g0194300*; *OsOPR7*, *Os08g0459600*; *OsJAZ8*, *Os09g0439200*; and *OsJAmyb*, *Os11g0684000*. Elevated ozone treatment was started at the 4-week-old stage. Values are means of four biological replicates. Error bars indicate standard errors. KO, knock-out line; WT, wildtype; and OE, over-expression line. In B and D-H, ANOVA was conducted, and the significance is denoted as follows: G, genotype; T, treatment; GxT, genotype and treatment interaction; n.s., not significant; \*,  $P < 0.05$ ; \*\*,  $P < 0.01$ ; and \*\*\*,  $P < 0.001$ .

### ***3.3. Hypothesis 3: Sequence variation at the OsORAP1 locus explains the effect of the QTL OzT9***

Since *OsORAP1* had been proposed as a candidate gene underlying the ozone tolerance QTL *OzT9*, we compared the genomic sequences of *OsORAP1* in the ozone-susceptible Nipponbare, and the tolerant *OzT9* donor variety Kasalath (Frei *et al.*, 2008). Our analysis revealed a number of polymorphic sites between the two cultivars in the upstream promoter region, while the coding sequence was largely conserved (Fig. 3-9, Figure S13). The deduced amino acid sequence revealed slight modifications in the signal peptide and three amino acid substitutions in the rest of the sequence (Figure S14). These polymorphic amino acid positions were not located at conserved amino acids, and the copper binding sites were conserved in both cultivars. The first 30 amino acids in Kasalath were also predicted to be transit peptides (by SignalP 4.1); therefore, the amino acid polymorphisms in the signal peptides probably did not affect the localization of the protein. The amino acid sequence of OsORAP1 in Dongjin, which was the background cultivar for the mutant lines in this study, was identical to that of Nipponbare (Figure S14). We searched possible regulatory sequences in the promoter region (upstream 1,000 bp) of both Nipponbare and Kasalath to get insight into the differential expression patterns of *OsORAP1* in these two cultivars (Tables S3-S5). In both cultivars, a W-box sequence (TTGAC) was found, which is crucial for WRKY transcription factors to bind and activate the transcription of downstream genes (Yu *et al.*, 2001). The Nipponbare-specific *cis*-elements contained ethylene responsive elements, A(A/T)TTCAAA (Itzhaki *et al.*, 1994), GCCGCC (Hao *et al.*, 1998), and AGCCGCC (Sato *et al.*, 1996; Kitajima *et al.*, 1998), which are supposedly binding sites of ethylene-responsive element binding proteins.

We also analysed the *OsORAP1* sequences in a previously reported ozone-tolerant chromosome segment substitution line, SL41, which was genetically identical to Nipponbare except for a 13-Mb introgression including the *OzT9* region and another introgression on chromosome 6 from the tolerant Kasalath cultivar (Frei *et al.*, 2010). Our analysis showed that the sequence of SL41 at the *OsORAP1* locus was identical to that of Kasalath (Figure S14).

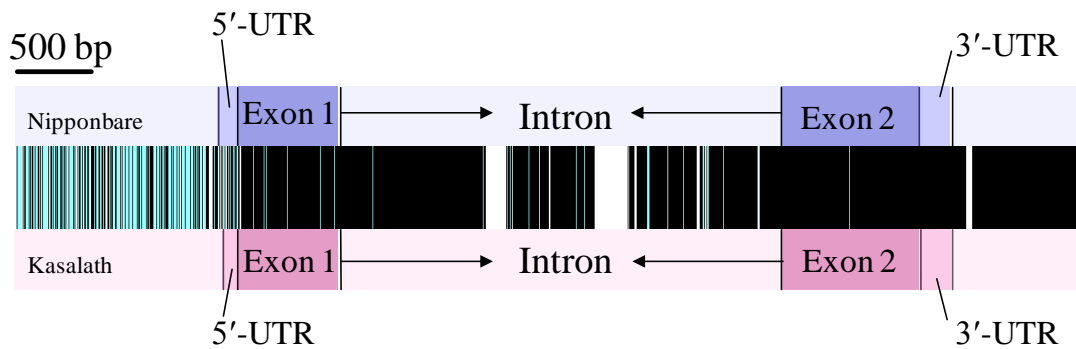


Figure 3-9: Sequence comparison of *OsORAP1* of Nipponbare (top) and Kasalath (bottom) rice cultivars. First, multiple alignment was conducted using MEGA5 software. Matched nucleotides are shown in black, mismatched nucleotides are shown in light blue, and gaps are shown in white. Upstream 1,500 bp, *OsORAP1* region, and downstream 1,000 bp sequences are shown. The 5'- and 3'-untranslated regions (UTR), exons, and intron are also shown for each cultivar. Bar = 500 bp.

## 4. Discussion

Cell death due to ozone stress leads to losses of photosynthetically active leaf area, which is suggested to be one of the factors limiting the total productivity of plants (Fiscus *et al.*, 2005). Therefore, identification of the genetic factors underlying the formation of visible symptoms would potentially have a large effect on crop production in the future. Although no or only weak correlations between symptom formation and yield were seen when rice cultivars with very heterogeneous genetic backgrounds were tested (Sawada and Kohno, 2009; Ueda *et al.*, 2015), the implications for yield became more apparent when genetically similar lines differing in symptom formation were compared (Frei *et al.*, 2012; Wang *et al.*, 2014). In this study, we characterized *OsORAP1*, which emerged as a candidate gene for ozone stress tolerance (*i.e.* the formation of cell death) in a previous study (Frei *et al.*, 2010). To elucidate the physiological function of OsORAP1 in ozone stress, three hypotheses were tested.

### ***Hypothesis 1: OsORAP1 is an ascorbate oxidase localized in the apoplast***

Apoplastic AsA has been considered important in the context of ozone stress tolerance, as it detoxifies incoming ozone (Luwe *et al.*, 1993; Turcsányi *et al.*, 2000). In support of this hypothesis, altered apoplastic AsA status through the introduction of an AO gene led to differential ozone stress tolerance in tobacco plants (Sanmartin *et al.*, 2003). In agreement with the current rice gene annotation for *OsORAP1* ('L-ascorbate oxidase precursor' in RAP-DB, <http://rapdb.dna.affrc.go.jp/index.html>, as of January 2015), phylogenetic analysis indeed showed close relatedness of OsORAP1 to *Arabidopsis* AO proteins. Observation of the OsORAP1-GFP fusion protein (Fig. 3-1B-F) indeed determined the apoplastic localization of OsORAP1, which is in accordance with bioinformatic analysis (*i.e.* the existence of signal peptide) and the observed localization of AO family proteins (Liso *et al.*, 2004; Balestrini *et al.*, 2012). Next, we tested whether the protein had AO activity. *Arabidopsis* At5g21100 (clade III-B) is an AO homologue of which AO activity was previously confirmed (Yamamoto *et al.*, 2005). Supporting these previous results, a drastic decline of AO activity was observed in a knock-out line of *At5g21100* (Fig. 3-1G). This clearly showed that At5g21100 is responsible for a large part of the AO activity in *Arabidopsis*. In consequence, the lack of increased AO activity in the complemented

lines (Fig. 3-1G) demonstrated the absence of AO activity in OsORAP1. In rice, the AO homologue Os06g0567900 dominated the AO activity in shoots (Fig. 3-6B). Interestingly, the dominant At5g21100 and Os06g0567900 were in the same clade III-B, while OsORAP1 and At4g39830, of which homozygous knock-out lines did not show decreased AO activity, were in clade III-A (Fig. 3-1A, Figure S3). Previous transcriptomic studies and our own experiment showed that both *OsORAP1* and *At4g39830* (clade III-A) were specifically induced under oxidative and biotic stresses, while *Os06g0567900* and *At5g21100* (clade III-B) were suppressed or less affected by these treatments with the exception of methyl viologen (MV) treatment (Tables S2 and S6). These data suggest that different subclades might represent different molecular functions. Taken together, the apoplastic localization, but not the AO activity of OsORAP1, was confirmed in this study.

A constitutively high expression level of *OsORAP1* was observed in root tissues, especially in the half apical side of the root (Fig. 3-2A). According to a previous microarray study (Sato *et al.*, 2011), high expression was observed in the root cap (Figure S15). Moreover, our further investigations into the possible molecular functions revealed that *OsORAP1* was highly induced during seed imbibition (Figure S16). Supporting this, a homozygous knock-out line of *OsORAP1* (ID: M0083940-8-A) in the genetic background of Tainung 67 (a *japonica* rice cultivar) was lethal (Table S7). Therefore, OsORAP1 might be related to embryogenesis or cell elongation. It also seems that OsORAP1 is involved in leaf expansion and tiller formation (Fig. 3-4 and Figure S7). This observation is similar to previous findings that AO family proteins enhanced cell elongation and growth rate in tobacco (Kato and Esaka, 2000; Pignocchi *et al.*, 2003). The molecular function of OsORAP1 warrants further detailed investigations.

### ***Hypothesis 2: OsORAP1 is involved in ozone-induced cell death in rice***

KO was more tolerant to ozone stress in terms of leaf visible symptom formation and lipid peroxidation (Figs. 3-3A, B and 3-5A), and the lower  $O_2^{\bullet-}$  production rate further supported that KO experienced less oxidative damage (Fig. 3-5B). The AO activity and apoplastic AsA content did not show any significant differences between the lines (Figs. 3-6A and 3-7), implying that tolerance in KO was not the consequence of higher ozone-detoxifying capacity through AsA in the apoplast. Apart from apoplastic AsA, mutant screening experiments in *Arabidopsis* have revealed several tolerance



mechanisms to ozone stress to date. These include AsA content, stomatal conductance, and leaf parenchyma cell density (Conklin *et al.*, 1996; Barth and Conklin, 2003; Overmyer *et al.*, 2008; Vahisalu *et al.*, 2008). In this study, none of these traits was significantly affected in *OsORAP1* mutant lines compared with WT (Fig. 3-4A, Figures S8 and S10), indicating that KO shows tolerance due to a novel mechanism. Chlorophyll content, which decreases during senescence (Miller *et al.*, 1999), thus reflecting the overall stress levels of leaves, also did not show any genotypic differences (Fig. 3-3C). Together, these data suggest that KO of *OsORAP1* specifically mitigated cell death by a novel mechanism, but not antioxidant capacity or the general status of leaves as affected by ozone.

Induction of *OsORAP1* in ozone stress was specific to young leaf blades, which had very low expression in the A-O<sub>3</sub> condition (Fig. 3-2B). In other words, gene expression was induced in photosynthetically active tissues with high intake of ozone, since older rice leaves have reduced stomatal aperture resulting in reduced ozone influx (Maggs and Ashmore, 1998). Besides ozone stress, *OsORAP1* was also induced by pathogen infection and MV stress (Table S6). Both ozone and pathogen infection induce apoplastic oxidative stress and, consequently, programmed cell death (PCD) if ROS formation exceeds a certain threshold (Heath, 2000; Kangasjärvi *et al.*, 2005). Cell death under MV stress also shares similar characteristics with PCD (Chen and Dickman, 2004; Chen *et al.*, 2009). In addition, PCD plays an important role during embryogenesis (Helmersson *et al.*, 2008) and in the root cap (Pennell and Lamb, 1997), where *OsORAP1* is highly expressed (Figures S15 and S16). These facts imply that *OsORAP1* is closely related to PCD, possibly via ROS, while it is not induced under many other abiotic stresses such as zinc deficiency (Table S6), where the foliar symptoms are assumed to occur via traumatic oxidative damage, not via PCD (Cakmak, 2000).

SA was another factor inducing *OsORAP1*, although SA itself does not induce PCD. This induction could occur either due to SA itself or apoplastic ROS accumulation caused by SA application (Kawano and Muto, 2000; Khokon *et al.*, 2011). The expression pattern of *OsORAP1* in *OsWRKY45* mutant lines strongly suggested that its expression is highly *OsWRKY45*-dependent. The presence of a W-box (Eulgem *et al.*, 2000) in the promoter region of *OsORAP1* supports this concept. Although no induction of *OsWRKY45* was observed in our study, *OsWRKY45* might be post-translationally processed and affect the expression level of downstream genes

(Matsushita *et al.*, 2013). Gene expression levels of JA-related genes (*OsOPR7*, *OsJAZ8*, and *OsJAmyb*) suggested that JA production is enhanced in KO. Higher expression of OsWRKY45 in KO might be due to the fact that it is also induced by JA as well as SA (De Vleeschauwer *et al.*, 2013). JA counteracts ROS production and the effect of SA and ET, which promote cell death, thus containing the spread of cell death caused by ozone (Overmyer *et al.*, 2000, 2003; Kangasjärvi *et al.*, 2005). Therefore the mitigation of cell death in KO is probably associated with the JA signalling pathway.

***Hypothesis 3: Sequence variation at the OsORAP1 locus explains the effect of the QTL OzT9***

The sequence analysis of different rice cultivars revealed highly conserved amino acid sequences and highly divergent promoter regions (Fig. 3-9, Figure S13). The lower *OsORAP1* expression in ozone stress in the tolerant line SL41 as compared with Nipponbare (Frei *et al.*, 2010) might be explained by *cis*-elements such as ethylene responsive element binding sites specific to the Nipponbare promoter sequence. Moreover, retarded growth during the vegetative growth stage seen in KO was also observed in SL41 in a previous study (Frei *et al.*, 2008), further supporting the possibility that *OsORAP1* is the causative gene underlying the effect of *OzT9*. However, we did not observe differences in AsA content of the whole tissue and apoplast between the lines, as seen previously between Nipponbare and SL41 (Fig. 3-7, Figure S10; Frei *et al.*, 2010), suggesting that other genes might add to the effect of *OzT9* in SL41. Nucleotide polymorphisms in the promoter or regulatory sequence of a gene have been suggested to underlie several QTLs in rice, such as blast resistance (Davidson *et al.*, 2010) and flowering time (Kojima *et al.*, 2002; Takahashi *et al.*, 2009). Similarly, in this study, the expression level of *OsORAP1*, rather than functional alteration, could be the causal polymorphism for *OzT9*. Fine-mapping of *OzT9*, further transgenic approaches (*e.g.* swapping the gene and promoter of *OsORAP1* between contrasting cultivars), and analysis of naturally occurring polymorphisms in the *OsORAP1* promoter region and their correlation with ozone tolerance are warranted to confirm this conclusion.

## 5. Conclusions and Outlook

Regarding the hypotheses tested in this study it can be concluded that (I) OsORAP1 is an apoplastic protein similar to an AO, but it has no measurable AO activity, (II) OsORAP1 enhances leaf visible symptoms and lipid peroxidation in ozone stress and interacts with plant hormones, and (III) sequence polymorphisms in the promoter region of *OsORAP1* supported the idea that it may underlie the effect of the QTL *OzT9*. Based on the results obtained in this study, we hypothesize that OsORAP1 is an apoplastic protein acting as a hub for signal transduction in ozone stress in rice (Fig. 3-10). As a future perspective, the molecular function of OsORAP1 needs to be further elucidated. Considering the localization of OsORAP1, a metabolomics analysis of apoplastic fluid (Floerl *et al.*, 2012) would presumably be helpful in identifying its substrate (Fridman and Pichersky, 2005; Pourcel *et al.*, 2005). It is also quite tempting to examine the pathogen resistance of the lines used in the study. This has implications beyond the breeding of ozone resistance, because PCD plays an important role in pathogen resistance by confining pathogens in dead cells, thereby preventing their spread to the other tissues (Apel and Hirt, 2004). OsORAP1 may be representative of the conflicting roles of intentional PCD due to pathogen attack and unintentional PCD due to ozone influx and, therefore, warrants further investigation.

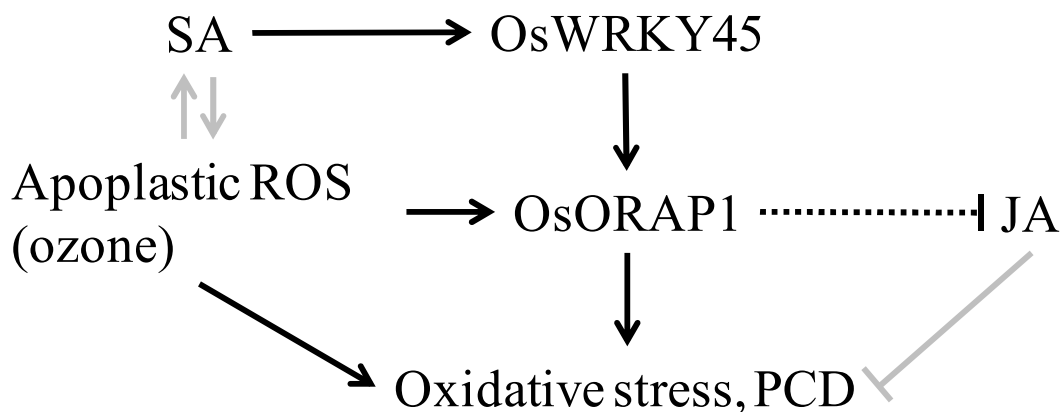


Figure 3-10: Hypothetical mode of action of OsORAP1 in rice. Apoplastic ROS (ozone) leads to oxidative stress and, consequently, programmed cell death (PCD), directly or via OsORAP1. Salicylic acid (SA) induces *OsWRKY45* expression (Shimono *et al.*, 2007), and *OsWRKY45* induces OsORAP1. OsORAP1 might possibly interact with the jasmonic acid (JA) pathway (shown in the dotted line). The enhanced production of SA by ROS, production of ROS by SA, and preventive role of JA in cell death in ozone stress are established in other plant species (Rao *et al.*, 2000, 2002; Khokon *et al.*, 2011) but not yet in rice; therefore, these are shown with gray lines.

**Supplementary material**

- Protocol S1 Method for vector construction.
- Protocol S2 Method for polyphenol oxidase activity measurement.
- Figure S1 Gene model of *OsORAP1*.
- Figure S2 Expression of *OsORAP1* and MDA content from Experiment 2.
- Figure S3 Phylogenetic analysis of clade III from 14 different plant species.
- Figure S4 Multiple alignment of the proteins in clades II and III.
- Figure S5 Transient expression of OsORAP1 in *Nicotiana benthamiana* leaves.
- Figure S6 Plant shape in ambient ozone and elevated ozone stress conditions.
- Figure S7 Growth parameters of three lines.
- Figure S8 Leaf dry weight per area in three lines.
- Figure S9 Ascorbate oxidase activity in the apoplast.
- Figure S10 Ascorbate content and redox status of whole-tissue extract.
- Figure S11 Polyphenol oxidase activity.
- Figure S12 Expression levels of phytohormone-related genes.
- Figure S13 Sequence alignment of the *OsORAP1* locus from four different rice lines.
- Figure S14 Sequence alignment of the OsORAP1 proteins from four different rice lines.
- Figure S15 Expression pattern of *OsORAP1* in rice root.
- Figure S16 Expression of *OsORAP1* during seed imbibition.
- Table S1 Primers used for this study.
- Table S2 Expression profile of *Arabidopsis* AO homologues under several conditions.
- Table S3 *Cis*-elements found only in Nipponbare.
- Table S4 *Cis*-elements found in both Nipponbare and Kasalath.
- Table S5 *Cis*-elements found only in Kasalath.
- Table S6 Expression profile of *OsORAP1* and *Os06g067900* under several conditions.
- Table S7 Seed germination test of an *OsORAP1* knock-out line in Tainung 67 genetic background.

### ***Sequence data***

Sequence data from this article can be found in the GenBank/EMBL data libraries under accession numbers: *OsORAP1* genomic sequence of Kasalath (KT369009) and Dongjin (KT369010).

### ***Funding***

This work was supported by Deutsche Forschungsgemeinschaft (FR-2952/1-1).

### ***Acknowledgments***

The authors thank Prof. Dr. Holger Bohlmann, (University of Natural Resources and Life Sciences Vienna) for providing pBIN61-P19 vector. The authors also wish to thank Prof. Dr. Rogerio Margis (Federal University of Rio Grande do Sul) for useful advice on microRNA analysis and Prof. Dr. Florian M. W. Grundler and Philipp Gutbrod (University of Bonn) for sharing experimental facilities and technical support on vector construction.

## References

- Ainsworth EA.** 2008. Rice production in a changing climate: a meta-analysis of responses to elevated carbon dioxide and elevated ozone concentration. *Global Change Biology* **14**, 1642–1650.
- Ainsworth EA, Yendrek CR, Sitch S, Collins WJ, Emberson LD.** 2012. The effects of tropospheric ozone on net primary productivity and implications for climate change. *Annual review of plant biology* **63**, 637–661.
- Apel K, Hirt H.** 2004. Reactive oxygen species: metabolism, oxidative stress, and signal transduction. *Annual review of plant biology* **55**, 373–399.
- Balestrini R, Ott T, Güther M, Bonfante P, Udvardi MK, De Tullio MC.** 2012. Ascorbate oxidase: The unexpected involvement of a 'wasteful enzyme' in the symbioses with nitrogen-fixing bacteria and arbuscular mycorrhizal fungi. *Plant Physiology and Biochemistry* **59**, 71–79.
- Barth C, Conklin PL.** 2003. The lower cell density of leaf parenchyma in the *Arabidopsis thaliana* mutant *lcd1-1* is associated with increased sensitivity to ozone and virulent *Pseudomonas syringae*. *The Plant Journal* **35**, 206–218.
- Bradford MM.** 1976. A rapid and sensitive method for the quantitation of microgram quantities of protein utilizing the principle of protein-dye binding. *Analytical Biochemistry* **72**, 248–254.
- Cakmak I.** 2000. Possible roles of zinc in protecting plant cells from damage by reactive oxygen species. *New Phytologist* **146**, 185–205.
- Chen S, Dickman MB.** 2004 Bcl-2 family members localize to tobacco chloroplasts and inhibit programmed cell death induced by chloroplast-targeted herbicides. *Journal of Experimental Botany* **55**, 2617–2623.
- Chen R, Sun S, Wang C, et al.** 2009. The *Arabidopsis* *PARAQUAT RESISTANT2* gene encodes an S-nitrosoglutathione reductase that is a key regulator of cell death. *Cell Research* **19**, 1377–1387.
- Clough SJ, Bent AF.** 1998. Floral dip: a simplified method for *Agrobacterium*-mediated transformation of *Arabidopsis thaliana*. *The Plant Journal* **16**, 735–743.
- Conklin PL, Williams EH, Last LR.** 1996. Environmental stress sensitivity of an ascorbic acid-deficient *Arabidopsis* mutant. *Proceedings of the National Academy of Sciences of the United States of America* **93**, 9970–9974.
- Curtis MD, Grossniklaus U.** 2003. A gateway cloning vector set for high-throughput functional analysis of gene in planta. *Plant Physiology* **133**, 462–469.
- Davidson RM, Manosalva PM, Snelling J, Bruce M, Leung H, Leach JE.** 2010. Rice germin-like proteins: Allelic diversity and relationships to early stress responses. *Rice* **3**, 43–55.

- Van Dingenen R, Dentener FJ, Raes F, Krol MC, Emberson L, Cofala J.** 2009. The global impact of ozone on agricultural crop yields under current and future air quality legislation. *Atmospheric Environment* **43**, 604–618.
- Dowdle J, Ishikawa T, Gatzek S, Rolinski S, Smirnov N.** 2007. Two genes in *Arabidopsis thaliana* encoding GDP-L-galactose phosphorylase are required for ascorbate biosynthesis and seedling viability. *The Plant Journal* **52**, 673–689.
- Eulgem T, Rushton PJ, Robatzek S, Somssich IE.** 2000. The WRKY superfamily of plant transcription factors. *Trends in plant science* **5**, 199-206.
- Feng Z, Pang J, Nouchi I, Kobayashi K, Yamakawa T, Zhu J.** 2010. Apoplastic ascorbate contributes to the differential ozone sensitivity in two varieties of winter wheat under fully open-air field conditions. *Environmental Pollution* **158**, 3539–3545.
- Feng Z, Sun J, Wan W, Hu E, Calatayud V.** 2014. Evidence of widespread ozone-induced visible injury on plants in Beijing, China. *Environmental Pollution* **193**, 296–301.
- Fiscus EL, Booker FL, Burkey KO.** 2005. Crop responses to ozone: uptake, modes of action, carbon assimilation and partitioning. *Plant, Cell and Environment* **28**, 997–1011.
- Floerl S, Majcherczyk A, Possienke M, et al.** 2012. *Verticillium longisporum* infection affects the leaf apoplastic proteome, metabolome, and cell wall properties in *Arabidopsis thaliana*. *PLoS One* **7**; e31435.
- Frei M.** 2015. Breeding of ozone resistant rice: Relevance, approaches and challenges. *Environmental Pollution* **197**, 144–155.
- Frei M, Kohno Y, Wissuwa M, Makkar HPS, Becker K.** 2011. Negative effects of tropospheric ozone on the feed value of rice straw are mitigated by an ozone tolerance QTL. *Global Change Biology* **17**, 2319–2329.
- Frei M, Tanaka JP, Chen CP, Wissuwa M.** 2010. Mechanisms of ozone tolerance in rice: characterization of two QTLs affecting leaf bronzing by gene expression profiling and biochemical analyses. *Journal of Experimental Botany* **61**, 1405–1417.
- Frei M, Tanaka JP, Wissuwa M.** 2008. Genotypic variation in tolerance to elevated ozone in rice: dissection of distinct genetic factors linked to tolerance mechanisms. *Journal of Experimental Botany* **59**, 3741–3752.
- Frei M, Wissuwa M, Pariasca-Tanaka J, Chen CP, Südekum K-H, Kohno Y.** 2012. Leaf ascorbic acid level—Is it really important for ozone tolerance in rice? *Plant Physiology and Biochemistry* **59**, 63–70.
- Fridman E, Pichersky E.** 2005. Metabolomics, genomics, proteomics, and the identification of enzymes and their substrates and products. *Curr Opin Plant Biol* **8**; 242-248.
- Garchery C, Gest N, Do PT, et al.** 2013. A diminution in ascorbate oxidase activity affects carbon allocation and improves yield in tomato under water deficit. *Plant, Cell and Environment* **36**, 159–175.

- Hao D, Ohme-Takagi M, Sarai A.** 1998. Unique mode of GCC box recognition by the DNA-binding domain of ethylene-responsive element-binding factor (ERF domain) in plant. *Journal of Biological Chemistry* **273**, 26857-26861.
- Heath M.** 2000. Hypersensitive response-related death. *Plant molecular biology* **44**, 321–334.
- Helmersson A, von Arnold S, Bozhkov PV.** 2008. The level of free intracellular zinc mediates programmed cell death/cell survival decisions in plant embryos. *Plant Physiology* **147**, 1158-1167.
- Hodges DM, DeLong JM, Forney CF, Prange RK.** 1999. Improving the thiobarbituric acid-reactive-substances assay for estimating lipid peroxidation in plant tissues containing anthocyanin and other interfering compounds. *Planta* **207**, 604–611.
- Hoegger PJ, Kilaru S, James TY, Thacker JR, Kües U.** 2006. Phylogenetic comparison and classification of laccase and related multicopper oxidase protein sequences. *The FEBS Journal* **273**, 2308–2326.
- Höller S, Hajirezaei M-R, von Wirén N, Frei M.** 2014a. Ascorbate metabolism in rice genotypes differing in zinc efficiency. *Planta* **239**, 367–379.
- Höller S, Meyer A, Frei M.** 2014b. Zinc deficiency differentially affects redox homeostasis of rice genotypes contrasting in ascorbate level. *Journal of plant physiology* **171**, 1748–1756.
- Ishibashi Y, Tawaratsumida T, Zheng S-H, Yuasa T, Iwaya-Inoue M.** 2010. NADPH oxidases act as key enzyme on germination and seedling growth in barley (*Hordeum vulgare* L.). *Plant Production Science* **13**, 45–52.
- Itzhaki H, Maxson JM, Woodson WR.** 1994. An ethylene-responsive enhancer element is involved in the senescence-related expression of the carnation glutathione-S-transferase (*GST1*) gene. *Proceedings of the National Academy of Sciences of the United States of America* **91**, 8925-8929.
- Jeon J-S, Lee S, Jung K-H, et al.** 2000. T-DNA insertional mutagenesis for functional genomics in rice. *The Plant Journal* **22**, 561–570.
- Jeong D-H, An S, Kang H-G, et al.** 2002. T-DNA insertional mutagenesis for activation tagging in rice. *Plant Physiology* **130**, 1636-1644.
- Jeong D-H, An S, Park S, et al.** 2006. Generation of a flanking sequence-tag database for activation-tagging lines in japonica rice. *The Plant Journal* **45**, 123–132.
- Kangasjärvi J, Jaspers P, Kollist H.** 2005. Signalling and cell death in ozone-exposed plants. *Plant, Cell and Environment* **28**, 1021–1036.
- Kato N, Esaka M.** 2000. Expansion of transgenic tobacco protoplasts expressing pumpkin ascorbate oxidase is more rapid than that of wild-type protoplasts. *Planta* **210**, 1018–1022.
- Kawano T, Muto S.** 2000. Mechanism of peroxidase actions for salicylic acid-induced generation of active oxygen species and an increase in cytosolic calcium in tobacco cell suspension culture. *Journal of Experimental Botany* **51**, 685-693.



- Khokon MAR, Okuma E, Hossain MA, et al.** 2011. Involvement of extracellular oxidative burst in salicylic acid-induced stomatal closure in *Arabidopsis*. *Plant, Cell and Environment* **34**, 434-443.
- Kitajima S, Koyama T, Yamada Y, Sato F.** 1998. Constitutive expression of the neutral PR-5 (OLP, PR-5d) gene in roots and cultured cells of tobacco is mediated by ethylene-responsive *cis*-element AGCCGCC sequences. *Plant Cell Reports* **18**, 173-179.
- Kojima S, Takahashi Y, Kobayashi Y, Monna L, Sasaki T, Araki T, Yano M.** 2002. *Hd3a*, a rice ortholog of the *Arabidopsis FT* gene, promotes transition to flowering downstream of *Hd1* under short-day conditions. *Plant and cell physiology* **43**, 1096-1105.
- Lee M-W, Qi M, Yang Y.** 2001. A novel jasmonic acid-inducible rice *myb* gene associates with fungal infection and host cell death. *Molecular Plant-Microbe Interactions* **14**, 527-535.
- Libault M, Zhang X-C, Govindarajulu M, et al.** 2010. A member of the highly conserved *FWL* (tomato *FW2.2-like*) gene family is essential for soybean nodule organogenesis. *The Plant Journal* **62**, 852-864.
- Lima JC, Arenhart RA, Margis-Pinheiro M, Margis R.** 2011. Aluminum triggers broad changes in microRNA expression in rice roots. *Genetics and Molecular Research* **10**, 2817-2832.
- De Lima JC, Loss-Morais G, Margis R.** 2012. MicroRNAs play critical roles during plant development and in response to abiotic stresses. *Genetics and Molecular Biology* **35**, 1069-1077.
- Liso R, De Tullio MC, Ciraci S, et al.** 2004. Localization of ascorbic acid, ascorbic acid oxidase, and glutathione in roots of *Cucurbita maxima* L. *Journal of Experimental Botany* **55**, 2589-2597.
- Luwe MWF, Takahama U, Heber U.** 1993. Role of ascorbate in detoxifying ozone in the apoplast of spinach (*Spinacia oleracea* L.) leaves. *Plant Physiology* **101**, 969-976.
- Maggs R, Ashmore MR.** 1998. Growth and yield responses of Pakistan rice (*Oryza sativa* L.) cultivars to O<sub>3</sub> and NO<sub>2</sub>. *Environmental Pollution* **103**, 159-170.
- Matsushita A, Inoue H, Goto S, Nakayama A, Sugano S, Hayashi N, Takatsuji H.** 2013. The nuclear ubiquitin proteasome degradation affects WRKY45 function in the rice defense program. *The Plant Journal* **73**, 302-313.
- McGuirl MA, Dooley DM.** 1999. Copper-containing oxidases. *Current opinion in chemical biology* **3**, 138-144.
- Miller JD, Arteca RN, Pell EJ.** 1999. Senescence-associated gene expression during ozone-induced leaf senescence in *Arabidopsis*. *Plant Physiology* **120**, 1015-1023.
- Omasa K, Tobe K, Kondo T.** 2002. Absorption of organic and inorganic air pollutants by plants. In: Omasa K, Saji H, Youssefian S, Kondo N, eds. *Air Pollution and Plant Biotechnology*. Tokyo: Springer, 155-178.

- Overmyer K, Brosché M, Kangasjärvi J.** 2003. Reactive oxygen species and hormonal control of cell death. *Trends in plant science* **8**, 335-342.
- Overmyer K, Kollist H, Tuominen H, et al.** 2008. Complex phenotypic profiles leading to ozone sensitivity in *Arabidopsis thaliana* mutants. *Plant, Cell and Environment* **31**, 1237-1249.
- Overmyer K, Tuominen H, Kettunen R, Betz C, Langebartels C, Sandermann H, Kangasjärvi J.** 2000. Ozone-sensitive *Arabidopsis rcd1* mutant reveals opposite roles for ethylene and jasmonate signaling pathways in regulating superoxide-dependent cell death. *The Plant Cell* **12**, 1849–1862.
- Pennel RI, Lamb C.** 1997. Programmed cell death in plants. *The Plant Cell* **9**, 1157-1168.
- Petersen TN, Brunak S, von Heijne G, Nielsen H.** 2011. SignalP 4.0: discriminating signal peptides from transmembrane regions. *Nature methods* **8**, 785–786.
- Pignocchi C, Fletcher JM, Wilkinson JE, Barnes JD, Foyer CH.** 2003. The function of ascorbate oxidase in tobacco. *Plant Physiology* **132**, 1631–1641.
- Pignocchi C, Foyer CH.** 2003. Apoplastic ascorbate metabolism and its role in the regulation of cell signalling. *Current opinion in plant biology* **6**, 379–389.
- Plöchl M, Lyons T, Ollerenshaw J, Barnes J.** 2000. Simulating ozone detoxification in the leaf apoplast through the direct reaction with ascorbate. *Planta* **210**, 454–467.
- Porra RJ, Thompson WA, Kriedemann PE.** 1989. Determination of accurate extinction coefficients and simultaneous equations for assaying chlorophylls *a* and *b* extracted with four different solvents: verification of the concentration of chlorophyll standards by atomic absorption spectroscopy. *Biochimica et Biophysica Acta* **975**, 384–394.
- Pourcel L, Routaboul J-M, Kerhoas L, Caboche M, Lepiniec L, Debeaujon I.** 2005. *TRANSPARENT TESTA10* encodes a laccase-like enzyme involved in oxidative polymerization of flavonoids in *Arabidopsis* seed coat. *Plant Cell* **17**; 2966-2980.
- Rao MV, Davis KR.** 2001. The physiology of ozone induced cell death. *Planta* **213**, 682–690.
- Rao MV, Lee H, Creelman RA, Mullet JE, Davis KR.** 2000. Jasmonic acid signaling modulates ozone-induced hypersensitive cell death. *The Plant Cell* **12**, 1633-1646.
- Rao MV, Lee H, Davis KR.** 2002. Ozone-induced ethylene production is dependent on salicylic acid, and both salicylic acid and ethylene act in concert to regulate ozone-induced cell death. *The Plant Journal* **32**, 447-456.
- Saitou N, Nei M.** 1987. The neighbor-joining method: a new method for reconstructing phylogenetic trees. *Molecular Biology and Evolution* **4**, 406–425.
- Sakai H, Lee SS, Tanaka T, et al.** 2013. Rice Annotation Project Database (RAP-DB): An integrative and interactive database for rice genomics. *Plant and cell physiology* **54**, e6.
- Sanmartin M, Drogoudi PD, Lyons T, Pateraki I, Barnes J, Kanellis AK.** 2003 Over-expression of ascorbate oxidase in the apoplast of transgenic tobacco results in altered

- ascorbate and glutathione redox states and increased sensitivity to ozone. *Planta* **216**, 918–928.
- Sato Y, Antonio BA, Namiki N, et al.** 2011. RiceXPro: a platform for monitoring gene expression in *japonica* rice grown under natural field conditions. *Nucleic acids research* **39**, D1141–D1148.
- Sato F, Kitajima S, Koyama T, Yamada Y.** 1996. Ethylene-induced gene expression of osmotin-like protein, a neutral isoform of tobacco PR-5, is mediated by the AGCCGCC *cis*-sequence. *Plant and cell physiology* **37**, 249–255.
- Sawada H, Kohno Y.** 2009. Differential ozone sensitivity of rice cultivars as indicated by visible injury and grain yield. *Plant Biology* **11**, 70–75.
- Shah KH, Almaghrabi B, Bohlmann H.** 2013. Comparison of expression vectors for transient expression of recombinant proteins in plants. *Plant Molecular Biology Reporter* **31**, 1529–1538.
- Shimono M, Sugano S, Nakayama A, Jiang C-J, Ono K, Toki S, Takatsuji H.** 2007. Rice WRKY45 plays a crucial role in benzothiadiazole-inducible blast resistance. *The Plant Cell* **19**, 2064–2076.
- Takahashi Y, Teshima KM, Yokoi S, Innan H, Shimamoto K.** 2009. Variations in *Hd1* proteins, *Hd3a* promoters, and *Ehd1* expression levels contribute to diversity of flowering time in cultivated rice. *Proceedings of the National Academy of Sciences of the United States of America* **106**, 4555–4560.
- Tamura K, Peterson D, Peterson N, Stecher G, Nei M, Kumar S.** 2011. MEGA5: Molecular evolutionary genetics analysis using maximum likelihood, evolutionary distance, and maximum parsimony methods. *Molecular Biology and Evolution* **28**, 2731–2739.
- Tani T, Sobajima H, Okada K, et al.** 2008. Identification of the *OsOPR7* gene encoding 12-oxophytodienoate reductase involved in the biosynthesis of jasmonic acid in rice. *Planta* **227**, 517–526.
- Tilman D, Balzer C, Hill J, Befort BL.** 2011. Global food demand and the sustainable intensification of agriculture. *Proceedings of the National Academy of Sciences of the United States of America* **108**, 20260–20264.
- Turcsányi E, Lyons T, Plöchl M, Barnes J.** 2000. Does ascorbate in the mesophyll cell walls form the first line of defence against ozone? Testing the concept using broad bean (*Vicia faba* L.). *Journal of Experimental Botany* **51**, 901–910.
- Ueda Y, Frimpong F, Qi Y, et al.** 2015. Genetic dissection of ozone tolerance in rice (*Oryza sativa* L.) by a genome-wide association study. *Journal of Experimental Botany* **66**, 293–306.
- Ueda Y, Uehara N, Sasaki H, Kobayashi K, Yamakawa T.** 2013a. Impacts of acute ozone stress on superoxide dismutase (SOD) expression and reactive oxygen species (ROS) formation in rice leaves. *Plant Physiology and Biochemistry* **70**, 396–402.

- Ueda Y, Wu L, Frei M.** 2013b. A critical comparison of two high-throughput ascorbate analyses methods for plant samples. *Plant Physiology and Biochemistry* **70**, 418–423.
- Vahisalu T, Kollist H, Wang Y-F, et al.** 2008. SLAC1 is required for plant guard cell S-type anion channel function in stomatal signalling. *Nature* **452**, 487-491.
- De Vleeschauwer D, Gheysen G, Höfte M.** 2013. Hormone defense networking in rice: tales from a different world. *Trends in plant science* **18**, 555–565.
- Wang Y, Frei M.** 2011. Stressed food – The impact of abiotic environmental stresses on crop quality. *Agriculture, Ecosystem and Environment* **141**, 271–286.
- Wang X, Manning W, Feng Z, Zhu Y.** 2007. Ground-level ozone in China: Distribution and effects on crop yields. *Environmental Pollution* **147**, 394–400.
- Wang Y, Yang L, Höller M, Zaisheng S, Pariasca-Tanaka J, Wissuwa M, Frei M.** 2014. Pyramiding of ozone tolerance QTLs *OzT8* and *OzT9* confers improved tolerance to season-long ozone exposure in rice. *Environmental and Experimental Botany* **104**, 26–33.
- Wissuwa M, Ismail AM, Yanagihara S.** 2006. Effects of zinc deficiency on rice growth and genetic factors contributing to tolerance. *Plant Physiology* **142**, 731–741.
- Wohlgemuth H, Mittelstrass K, Kschieschan S, et al.** 2002. Activation of an oxidative burst is a general feature of sensitive plants exposed to the air pollutant ozone. *Plant, Cell and Environment* **25**, 717–726.
- Yamada S, Kano A, Tamaoki D, et al.** 2012. Involvement of OsJAZ8 in jasmonate-induced resistance to bacterial blight in rice. *Plant and cell physiology* **53**, 2060–2072.
- Yamaji K, Ohara T, Uno I, Kurokawa J, Pochanart P, Akimoto H.** 2008. Future prediction of surface ozone over east Asia using Models-3 Community Multiscale Air Quality Modeling System and Regional Emission Inventory in Asia. *Journal of Geophysical Research* **113**, D08306.
- Yamaji K, Ohara T, Uno I, Tanimoto H, Kurokawa J, Akimoto H.** 2006. Analysis of the seasonal variation of ozone in the boundary layer in East Asia using the Community Multi-scale Air Quality model: What controls surface ozone levels over Japan? *Atmospheric Environment* **40**, 1856–1868.
- Yamamoto A, Bhuiyan MNH, Waditee R, et al.** 2005. Suppressed expression of the apoplastic ascorbate oxidase gene increases salt tolerance in tobacco and *Arabidopsis* plants. *Journal of Experimental Botany* **56**, 1785–1796.
- Yoshida S, Forno DA, Cock JH, Gomez KA.** 1976. *Laboratory Manual for Physiological Studies of Rice*. The International Rice Research Institute. Manila, The Philippines.
- Yu D, Chen C, Chen Z.** 2001. Evidence for an important role of WRKY DNA binding proteins in the regulation of *NPR1* gene expression. *The Plant Cell* **13**, 1527-1539.

## Chapter 4

# Identification of novel loci involved in ozone stress tolerance in rice

(Ueda Y, Frimpong F, Qi Y, Matthus E, Wu L, Höller S, Kraska T, Frei M. 2015. Genetic dissection of ozone tolerance in rice (*Oryza sativa* L.) by genome-wide association study. *Journal of Experimental Botany* **66**, 293–306.)

### Abstract

Tropospheric ozone causes various negative effects on plants and affects the yield and quality of agricultural crops. Here, we report a genome-wide association study (GWAS) in rice (*Oryza sativa* L.) to determine candidate loci associated with ozone tolerance. A diversity panel consisting of 328 accessions representing all subpopulations of *O. sativa* was exposed to ozone stress at 60 ppb for 7 h every day throughout the growth season, or to control conditions. Averaged over all genotypes, ozone significantly affected biomass-related traits (plant height -1.0%, shoot dry weight -15.9%, tiller number -8.3%, grain weight -9.3%, total panicle weight -19.7%, single panicle weight -5.5%) and biochemical/physiological traits (symptom formation, SPAD value -4.4%, foliar lignin content +3.4%). A wide range of genotypic variance in response to ozone stress were observed in all phenotypes. Association mapping based on more than 30,000 single-nucleotide polymorphism (SNP) markers yielded 16 significant markers throughout the genome by applying a significance threshold of  $P < 0.0001$ . Furthermore, by determining linkage disequilibrium blocks associated with significant SNPs, we gained a total of 195 candidate genes for these traits. The following sequence analysis revealed a number of novel polymorphisms in two candidate genes for the formation of leaf visible symptoms, a *RING* and an *EREBP* gene, both of which are involved in cell death and stress defence reactions. This study demonstrated substantial natural variation of responses to ozone in rice and the possibility of using GWAS in elucidating the genetic factors underlying ozone tolerance.

## 1. Introduction

Due to anthropogenic gas emissions, the tropospheric ozone concentration is increasing and negatively affects natural vegetation and crop production (Ainsworth *et al.*, 2012). Ozone is known to reduce photosynthetic rates (Chen *et al.*, 2011), induce cell death (Kangasjärvi *et al.*, 2005) and affects numerous metabolic pathways (Frei *et al.*, 2010), thus decreasing crop yields (Feng and Kobayashi, 2009) and changing crop quality (Wang and Frei, 2011). A steep increase in tropospheric ozone has been observed mainly in Asian countries (Lei *et al.*, 2013), where rice is the staple food. It is estimated that rice grain yields are already being affected in Asian countries at present ozone levels. Teixeira *et al.* (2011) estimated yield losses of 18 million and 11 million t of rice per year in India and China, respectively, which corresponds to more than 5% of relative loss due to increased tropospheric ozone.

Some typical symptoms of ozone stress in plants are directly related to crop quality and yield: (i) chlorosis and pale colour of leaves; (ii) necrotic dark brown spots or dead regions on leaves; and (iii) reduced growth rate and a stunted phenotype, leading to reduced yield. Among those traits, necrotic dark brown spots are closely related to acute ozone stress and are caused either by direct oxidative damage or by programmed cell death (PCD), which involves plant hormonal pathways (Kangasjärvi *et al.*, 2005). Generally, the correlation between the above-mentioned traits is not very pronounced, suggesting that they are under independent genetic control. For example, little correlation was observed between the extent of leaf damage and growth reduction (Frei *et al.*, 2008) or grain yield (Sawada and Kohno, 2009) in screening experiments with rice.

Genotypic variation in adaptation to ozone has been reported for a number of crop species such as rice, snap bean and wheat (Flowers *et al.*, 2007; Frei *et al.*, 2008; Feng *et al.*, 2011). However, only a few studies have attempted to dissect and use this genetic variability in ozone tolerance for molecular breeding of ozone tolerant crop genotypes. A number of genetic mapping studies have employed bi-parental mapping populations to identify quantitative trait loci (QTLs) for ozone tolerance (Frei *et al.*, 2008; Brosché *et al.*, 2010; Street *et al.*, 2011; Tsukahara *et al.*, 2013). In our previous study, such a QTL-based approach was successfully employed in developing rice genotypes with superior quality traits (Frei *et al.*, 2011) and biomass production (Wang *et al.*, 2014) under ozone stress. The shortcoming of such classical QTL studies

is that they use bi-parental mapping populations, thus covering only a narrow genetic variability. Moreover, the resolution of mapping is limited by the number of genetic recombination events occurring in the mapping populations (Flint-Garcia *et al.*, 2003). More recently, genome-wide association study (GWAS) has been emerging as a powerful tool to dissect a much broader genetic variability for important traits in crops (Brachi *et al.*, 2011). This method employs populations of unrelated individuals representing a broad genetic variability, and abundant single-nucleotide polymorphisms (SNPs) are usually used as genetic markers. Since such populations reflect the diverse evolutionary recombination events of a species, high-resolution mapping is possible depending on the extent of linkage disequilibrium (LD) in the population. In the case of rice, which was developed into a domesticated crop by self-pollination plus forced pollination by humans, GWAS has been successfully conducted with a limited number of markers due to relatively slow LD decay (half decay is achieved in around 100 to 200 kb, compared with 0.5 to 7 kb in an outcrossing crop maize; Gupta *et al.*, 2005), while achieving high resolution. Another advantage of using rice as a model plant is that it has a relatively small genome size, which reduces the number of necessary markers. Zhao *et al.* (2011) conducted a GWAS using 413 rice genotypes from most of the rice growing areas in the world, based on a 44,000-SNP genotyping array, followed by mapping for 34 agronomically relevant phenotypic traits. They provided evidence for the suitability of their population for GWAS by identifying significant marker associations near known genes affecting certain traits such as plant height. The population known as the ‘diversity panel’, can thus be used for the mapping of hitherto unknown genes.

Here, we report the first GWAS for ozone tolerance in any agricultural crop using a panel covering a broad genetic diversity and representing all subpopulations of rice. Our aims were: (i) to gain insight into the extent of genetic variability of ozone tolerance in rice; (ii) to dissect this genetic variability into distinct loci; and (iii) identify possible candidate genes underlying these loci.

## 2. Materials and Methods

### 2.1. Plant materials and growth condition

The experiment was conducted in a greenhouse at the University of Bonn, Germany, from May to November 2013. A mapping population consisting of 328 rice cultivars was obtained from the International Rice Research Institute (IRRI, Los Baños, The Philippines). The seeds were germinated in the dark for 3 days at 28 °C, and then transferred to a greenhouse under natural light. Three-week-old seedlings were transplanted into 2 x 6 m ponds filled with soil (a local luvisol: 16% clay, 77% silt, 7% sand, 1.2% organic carbon, pH 6.3; Schneider, 2005) at 16.5 x 19 cm spacing. A constant water level of at least 3 cm was maintained from 10 days after transplanting throughout the growth season. Each of the six plots contained one replicate of all 328 cultivars in a completely randomized distribution. The plots were randomly assigned to ozone and control treatments, and open-top chambers (height 1.3 m) were built around all plots to ensure an identical microclimate. To avoid nutrient limitations, 107 g of K<sub>2</sub>SO<sub>4</sub> and 98 g of Ca(H<sub>2</sub>PO<sub>4</sub>)<sub>2</sub> were applied to each plot as basal fertilizer at the beginning of the season, and 155 g of urea was applied in three splits during the season. Temperature, air humidity and CO<sub>2</sub> concentration were constantly monitored at 12 min intervals using sensors installed at 2-m height in the greenhouse. The average temperature was 25/19 °C (day/night), the average humidity was 60/80% (day/night), and the average CO<sub>2</sub> concentration was 460/600 ppm (day/night). Supplementary lighting was installed above the plots to ensure a minimum light intensity of 12.5 klux even on cloudy days. Water was removed from the ponds in week 19, and the plants were harvested in week 21. Panicles were separated from the shoots and dried at 50 °C for at least 72 h to complete dryness. The shoot samples were dried for 10 weeks in the greenhouse until they reached a constant moisture content of around 11% and then weighed.

### 2.2. Ozone treatment

Five weeks after transplanting, ozone fumigation was initiated to induce chronic stress at a target level of 60 ppb for 7 h every day. Comparable concentrations are already being observed in some areas and are expected to be reached in many countries in the future (Lelieveld and Dentener, 2000; Yamaji *et al.*, 2006). Ozone was produced using custom-made ozone generators (UB 01; Gemke Technik GmbH, Ennepetal, Germany)



with dried air passing through silica gels as input. Ozone output was regulated by an ozone monitor (K 100 W; Dr. A. Kuntze GmbH, Meerbusch, Germany) with an ozone sensor (GE 760 O3; Dr. A. Kuntze GmbH) placed inside the chambers. The generated ozone was blown into a central pipe running above the plant canopy, from which three parallel perforated side pipes for ozone distribution branched off at a distance of 40 cm from each other. The pipes were calibrated for even ozone distribution prior to transplanting of rice seedlings using a handheld ozone monitor (series 500; Aeroqual, Auckland, New Zealand). The fumigation lasted from 9 AM until 4 PM each day for 15 weeks until the end of the growth season. During the growth season, acute ozone stress was applied three times in weeks 8, 10 and 14 after transplanting. The average concentration of acute stress was 150 ppb and it lasted for 7 h (9 AM to 4 PM). The ozone concentration was constantly monitored by the handheld ozone monitor placed within the canopy during the fumigation. The average ozone concentration recorded was 63 ppb in the ozone treatment (excluding the episodes of acute stress), while in the control the concentration was 12 ppb on average.

### ***2.3. Plant phenotyping***

Leaf visible symptom and SPAD values were measured in week 12 after transplanting (*i.e.* after two applications of acute ozone stress). Tiller number and plant height were measured during the harvesting. Shoot dry weight (DW), grain yield components and lignin content were measured after the end of the season.

A modified leaf bronzing score (LBS; Wissuwa *et al.*, 2006) was assigned to each plant to evaluate leaf symptoms. It ranged from 0 to 10 according to the following criteria after evaluating all the leaves: 0, no ozone-induced symptoms in any of the leaves; 2, some symptoms on a few leaves; 4, easily visible symptoms on a few leaves; 6, moderate to severe symptoms on many leaves; 8, severe symptoms on many leaves; and 10, whole plant severely damaged. Most of the symptoms began to emerge after the episodes of acute ozone exposure.

SPAD values were measured using a SPAD 502 instrument (Konica Minolta, Osaka, Japan). Three points were measured at 20 cm distance from the tip of the second youngest fully expanded leaf of each plant, and the average of the three points was determined.

Thousand kernel weight (TKW), total panicle weight (TPW) and single panicle weight (SPW) were measured after completely drying the panicles. Twenty randomly chosen

grains were weighed from the dried panicles and the value was multiplied by 50 to obtain the TKW. Next, TPW and panicle number were measured, and SPW was obtained by dividing TPW by the number of panicles. Some accessions did not reach grain maturity or showed constitutively high spikelet sterility under the climatic conditions of this study and thus showed very high variability in the data. Therefore, 63 accessions (ten *admix*, four *aromatic*, three *aus*, 26 *indica*, four *temperate japonica* and 16 *tropical japonica*) with less than 10 g of TKW were removed from the analysis for grain-related traits (TKW, TPW and SPW) to only analyse filled grains. A further eight accessions (one *admix*, six *aus* and one *indica*) were removed for TPW and SPW because of high grain shattering.

Lignin content was measured in the third youngest fully expanded leaves from the main culm. The leaf samples were dried and pulverized, and the lignin content was determined spectrophotometrically according to Suzuki *et al.* (2009) based on the thioglycolic acid method. The pulverized samples were dried at 60 °C and extracted with water and methanol to obtain cell wall fractions. Then the samples were digested with thioglycolic acid to obtain the thioglycolic acid lignin (TGAL) complex. Finally the TGAL was dissolved in 1 N NaOH and the concentration was determined based on a standard curve using standard lignin (Sigma, St. Louis, MO) dissolved into 1 N NaOH. The final lignin content was expressed as a percentage on a DW basis.

#### **2.4. Data analysis**

A mean value of three biological replicates was used for the analysis (Table S8). To remove extreme values in each trait, data points which did not fall into the range of (mean of all accessions)  $\pm$  (3 times the standard deviation) were removed from the dataset prior to the mapping. This procedure eliminated 32 of 3075 total data points. A square-root transformation was conducted for LBS prior to the mapping, which showed skewed distribution in the original dataset. One-way ANOVA for subpopulation comparison was conducted with IBM SPSS version 21 (IBM Corp., Armonk, NY), applying a general linear model (GLM) and Tukey's HSD for the post-hoc test. Two-way ANOVA was applied to analyse the effects of treatment, genotype, and the interaction of both on the phenotypic traits using a GLM. Association mapping was conducted using TASSEL 3.0 (Bradbury *et al.*, 2007) based on the SNP marker data, kinship matrix, and principal component analysis (PCA) matrix described by Zhao *et al.* (2011). This SNP array provides approximately one SNP every 10 kb,

covering all twelve chromosomes of rice. SNPs which showed a minor allele frequency (MAF) < 10% in our population were removed to decrease overestimation of the effect of SNPs with a low MAF (Brachi *et al.*, 2011). The resultant number of SNPs was 32,175. A mixed linear model (MLM) was used to calculate the association in all analyses, incorporating both PCA and kinship data. MLM was applied using the default settings (P3D for variance component analysis, compression level set to optimum level). The threshold for significantly associated markers was set to  $P < 0.0001$  (*i.e.*  $-\log_{10}P > 4.0$ ). LD analysis was conducted using Haploview 4.2 (Barrett *et al.*, 2005). An LD block was created when the upper 95% confidence bounds of  $D'$  value exceeded 0.98 and the lower bounds exceeded 0.70 (Gabriel *et al.*, 2002). LD blocks harbouring significant SNPs were then defined as the candidate loci. The genes located in these loci were collected. The gene annotation, closest *Arabidopsis* (*Arabidopsis thaliana*) homologue and gene ontology (GO) were obtained from the MSU rice genome database (<http://rice.plantbiology.msu.edu/>, as of March 2014).

### ***2.5. Candidate gene sequencing and analysis***

DNA sequencing of candidate genes was conducted as follows. First, genomic DNA from selected lines was extracted from seeds using a PeqGOLD plant DNA extraction kit (Peqlab, Erlangen, Germany). The region of interest was amplified by PCR with the following setup: 15  $\mu\text{L}$  of GoTaq Green Master Mix (Promega, Mannheim, Germany), 0.6  $\mu\text{L}$  of each primer (10  $\mu\text{M}$ ), 1.5  $\mu\text{L}$  of dimethyl sulfoxide, 10.3  $\mu\text{L}$  of water and 2  $\mu\text{L}$  of extracted DNA. The following conditions were used for amplification of *EREBP/RING* respectively: 95 °C for 2 min, 32 cycles of 95 °C for 30 sec, 57/55 °C for 30 sec, and 72 °C for 2/1.5 min, followed by an additional 72 °C extension for 5 min. The primer sequences were 5'-AGC CAG CGA CTG TGC CAA TGT AC-3' (forward) and 5'-TAA TGT CTT CAG CAG TTC AGC CGG AG-3' (reverse) for *EREBP*, and 5'-CCA AAA CCC CCA AAA GCC AAT G-3' (forward) and 5'-ACC ACA CAT CCC TTA GCA ATA CAC-3' (reverse) for *RING*. The amplified DNA was purified after gel electrophoresis using a FastGene Gel/PCR Extraction kit (Nippon Genetics, Tokyo, Japan). The purified DNA was subjected to cycle sequencing using one of the primers used for the PCR. Sequences were compared and analysed using MEGA5 software (Tamura *et al.*, 2011). The protein motifs were searched using the InterPro database (<https://www.ebi.ac.uk/interpro/>, as

of March 2014). Additional genomic sequences of *EREBP* and *RING* were obtained from the TASUKE rice genome browser (<http://rice50.dna.affrc.go.jp/>, as of September 2014), where the genomic sequences of 26 accessions from our mapping population were available (Kumagai *et al.*, 2013).

### 3. Results

#### 3.1. Ozone effect and genotypic variation in phenotypic traits

We tested the effect of ozone on nine traits, including leaf cell death as represented by LBS; growth parameters such as plant height, shoot DW, and tiller number; grain yield component parameters such as TKW, TPW, and SPW; and biochemical parameters such as chlorophyll content (SPAD value) and foliar lignin content. We analysed foliar lignin content as an agronomically important parameter, which may represent apoplastic stress, since the coupling of monolignol molecules requires the oxidation of hydroxyl group and therefore is highly dependent on the apoplastic redox status (Frei, 2013). ANOVA (Table 4-1) demonstrated that all of these traits were significantly affected by the ozone concentration employed, *i.e.* 60 ppb for 7 h daily plus three additional episodes of 150 ppb for one day. In plant height, shoot DW, SPW, and SPAD value, we also observed a significant interaction between genotype and treatment (GxT). On average, plant height decreased by 1.0%, DW decreased by 15.9%, tiller number decreased by 8.3%, TKW decreased by 9.3%, TPW decreased by 19.7%, SPW decreased by 5.5%, SPAD decreased by 4.4%, and lignin content increased by 3.4% in ozone-treated plants as compared to control plants. Box plots for relative phenotypic values (*e.g.* [Relative plant height] =  $\frac{\text{Plant height (ozone)}}{\text{Plant height (control)}} \times 100$ ) indicated substantial genotypic variation in ozone responses, which was particularly pronounced in the case of relative DW, relative TPW, and relative SPW (Fig. 4-1). Growth parameters and grain yield components mostly correlated significantly with each other, and LBS showed a significant correlation with relative tiller number (Table 4-2). We also compared the ozone response among the five subpopulations (*aromatic*, *aus*, *indica*, *temperate japonica* and *tropical japonica*) plus the admixed group, which cannot be clearly assigned to any of these subpopulations (Zhao *et al.*, 2010; Figure S17, Table S9). Subpopulations *indica* and *temperate japonica* showed a significantly lower LBS than the other subpopulations. Constitutive lignin content and relative lignin content also showed significant differences among the subpopulations.

Table 4-1: Effect of ozone stress on phenotypic values.

Phenotype	control	ozone	Treatment	Genotype	GxT
LBS	0	1.72	***	***	N.A. <sup>a</sup>
Plant height (cm)	181.3	179.4	***	***	*
Shoot DW (g)	43.15	36.27	***	***	***
Tiller number	8.08	7.41	***	***	n.s.
TKW (g)	20.39	18.5	***	***	n.s.
TPW (g)	19.83	15.92	***	***	n.s.
SPW(g)	2.18	2.06	**	***	**
SPAD value	39.21	37.5	***	***	**
Lignin content (%)	1.74	1.8	**	***	N.A. <sup>b</sup>

The phenotypic values under control and ozone are shown. The phenotypic value is the mean of all accessions. ANOVA was performed with treatment, genotype and genotype x treatment (GxT) as fixed values. \*,  $P < 0.05$ ; \*\*,  $P < 0.01$ ; \*\*\*,  $P < 0.001$ ; n.s., not significant; and N.A., not analysed.

<sup>a</sup>GxT effect in LBS was not analysed since none of the control plants showed any symptoms.

<sup>b</sup>GxT effect in lignin content was not analysed since there were no biological replicates.

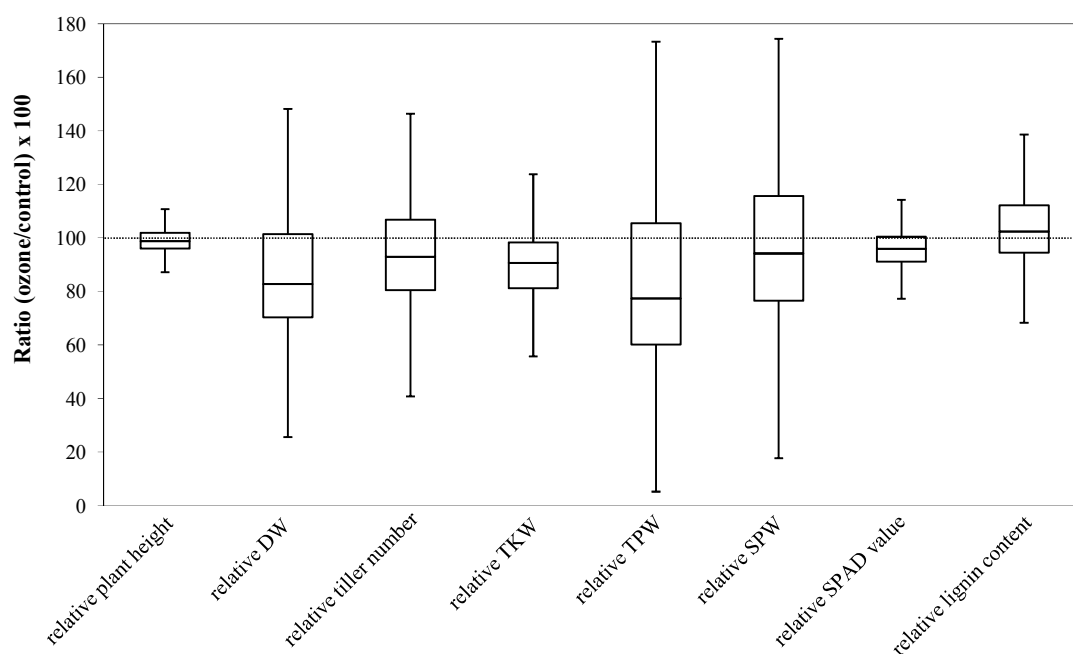


Figure 4-1: Box plots for relative phenotypic values. The median of each trait is shown as the horizontal bar in the box, and the upper and lower sides of a box represent the first and third quartile values of the distribution, respectively. Whiskers extended to 1.5 times the interquartile range (box size) or to the maximum/minimum values.

Table 4-2: Correlation coefficient and  $P$  value of pair-wise comparison of each phenotype.

	LBS	Relative plant height	Relative shoot DW	Relative tiller number	Relative TKW	Relative TPW	Relative SPW	Relative SPAD value	Lignin content	Relative lignin content	Flowering time in Arkansas
LBS	1	0.114	0.189	<0.001	0.279	0.545	0.437	0.067	0.182	0.113	0.008
Relative plant height	-0.09	1	<0.001	0.056	0.054	0.008	<0.001	0.890	0.095	0.705	0.242
Relative shoot DW	-0.07	0.23	1	<0.001	<0.001	<0.001	<0.001	0.970	0.484	0.058	0.300
Relative tiller number	-0.18	0.11	0.68	1	0.007	<0.001	<0.001	0.866	0.270	0.189	0.028
Relative TKW	0.07	0.12	0.21	0.16	1	<0.001	<0.001	0.334	0.883	0.825	0.353
Relative TPW	-0.04	0.17	0.62	0.56	0.33	1	<0.001	0.751	0.608	0.329	0.026
Relative SPW	-0.05	0.25	0.30	0.23	0.42	0.75	1	0.582	0.504	0.669	0.461
Relative SPAD value	-0.10	-0.01	0.00	-0.01	-0.06	-0.02	0.03	1	0.654	0.197	0.122
Lignin content	0.07	-0.09	-0.04	-0.06	-0.01	-0.03	-0.04	-0.02	1	<0.001	0.489
Relative lignin content	0.09	0.02	-0.10	-0.07	-0.01	-0.06	-0.03	-0.07	-0.52	1	0.960
Flowering time in Arkansas	0.15	-0.07	-0.06	-0.13	-0.06	-0.14	-0.05	0.09	0.04	0.00	1

The lower triangle shows the Pearson's correlation coefficient of each pair-wise phenotype comparison. The upper triangle shows the  $P$  value of the correlation.  $P$  values were determined by a two-tailed Student's  $t$ -test. Data for flowering time in Arkansas (in 305 accessions) were adopted from Zhao *et al.* (2011), where the same mapping population was used.

### 3.2. Association mapping

We conducted association mapping to identify loci underlying the genetic regulation of the traits mentioned above. We applied an MLM on all datasets, which takes into account the population structure and therefore renders fewer false positives compared with a GLM (Larsson *et al.*, 2013). We set a threshold of  $-\log_{10}P > 4.0$  as a significant association, as adopted in other studies using the same mapping population (Famoso *et al.*, 2011; Zhao *et al.*, 2011). The threshold of  $-\log_{10}P > 4.0$  was also derived from the quantile-quantile (QQ) plots, since most of the upward deviation from the linear line occurred at around  $-\log_{10}P = 4.0$ , which presumably indicates true positives. For all traits analysed, we identified 16 SNP markers which satisfied this threshold, being distributed throughout the rice genome (Table S10). As an alternative approach, we also compiled the top 50 SNPs in each trait (*i.e.* SNPs showing the 50 highest  $-\log_{10}P$  values in each trait) to identify SNPs forming potentially important clusters even

though the individual  $P$  values might be less significant (Table S11) as suggested by Verslues *et al.* (2014). We further determined LD blocks harbouring significant SNPs (*i.e.*  $-\log_{10}P > 4.0$ ) as regions containing putative candidate genes, which led to a total of 195 genes (Table S12). For several traits,  $-\log_{10}P$  values and QQ plots suggested relatively weak genetic association (Figures S18-S24). In the following, we focused on LBS, relative DW, and relative SPW, for which MLM analysis yielded more robust genetic associations taking into account heritability (Table S13),  $-\log_{10}P$  values, and the QQ plots, where the deviation from the expected values occurred only in the most significant  $P$  value range.

#### *Leaf bronzing score*

The square-root transformed LBS (t-LBS) ranged from 0.0 to 2.4 (Fig. 4-2A). The corresponding QQ plot indicated deviation from the expected  $P$  values only in the most significantly associated markers, thus limiting the possibility of declaring false positives (Fig. 4-2B). Two distinct peaks were observed on the Manhattan plot when setting the threshold of  $-\log_{10}P > 4.0$  (Fig. 4-2C). Determining LD blocks on the chromosomal regions where significant SNPs were observed narrowed down the region in which to look for the candidate genes (Fig. 4-2D, E). On chromosome 1, only one gene was found in the LD blocks. Although not located in the LD blocks, many  $\beta$ -1,3-glucanase genes were identified in the neighbouring region (12 homologues in the surrounding 285 kb). One significant SNP marker was located between two  $\beta$ -1,3-glucanase genes: *LOC\_Os01g71670* (188 bp distance) and *LOC\_Os01g71680* (1.8 kb distance). On chromosome 5, the peak was quite sharp and the flanking LD blocks showed very low  $-\log_{10}P$  values (Fig. 4-2E). This region contained candidate genes encoding an *EREBP* and a *RING* which were further characterized by sequencing of contrasting haplotypes as detailed below. Several other potentially interesting genes were found by analysing LD blocks containing the top 50 SNPs although most of them did not exceed the threshold of  $-\log_{10}P > 4.0$ . One locus on chromosome 2 (associated with id2009675,  $-\log_{10}P = 3.52$ ) contained a chitinase gene (*LOC\_Os02g39330*) along with four other genes, and a locus on chromosome 3 (associated with 8 SNPs, maximum  $-\log_{10}P = 3.74$ ) contained a mitogen-activated protein kinase gene (*LOC\_Os03g17700*).



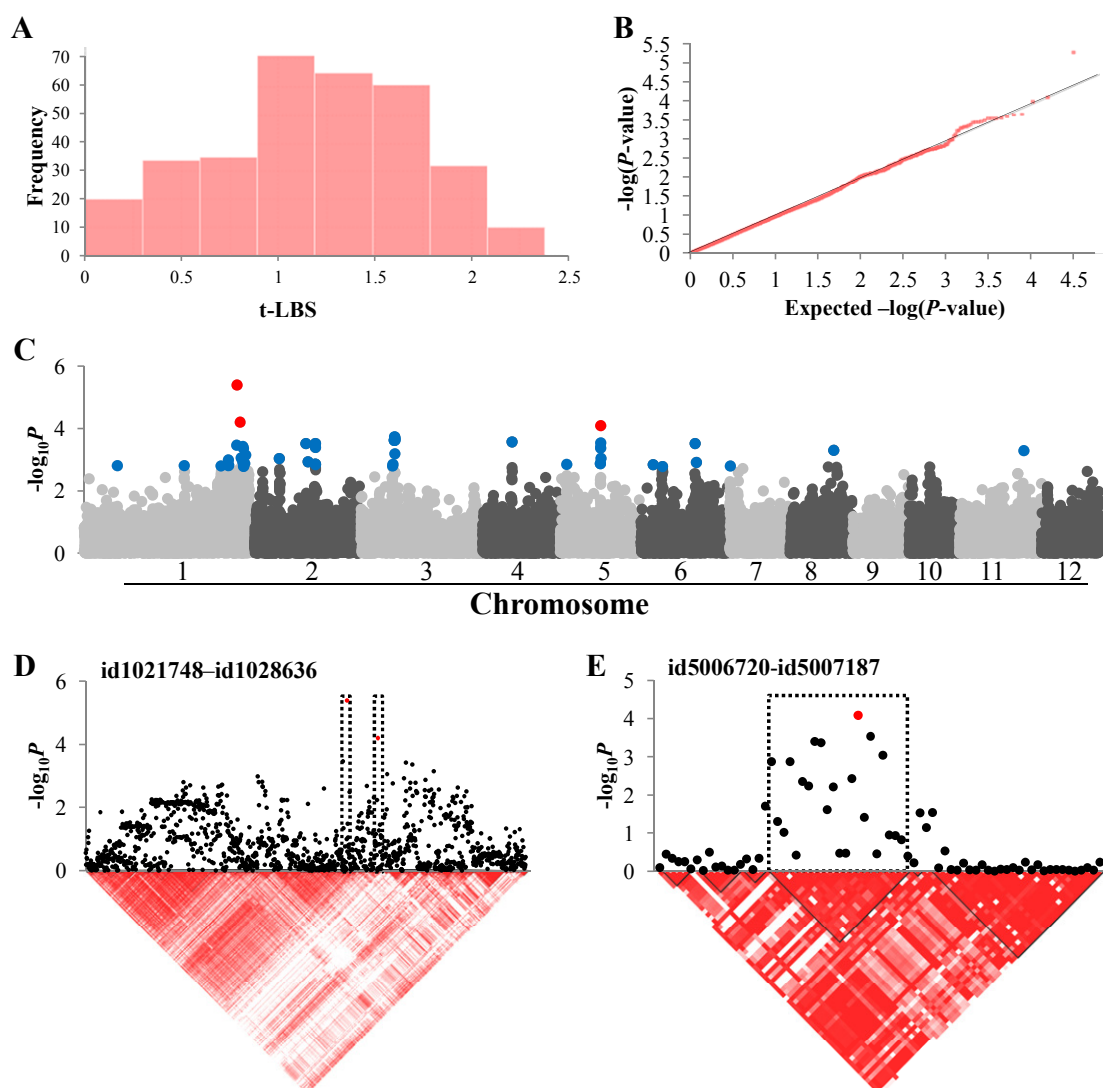


Figure 4-2: Association mapping result for square-root transformed leaf bronzing score (t-LBS). (A) Frequency distribution of observed t-LBS. (B) QQ plot of expected and observed  $P$  values. (C) Manhattan plots from association mapping using the Mixed Linear Model. The top 50 SNPs are shown in blue and the SNPs exceeding the significance threshold of  $P < 0.0001$  are shown in red. (D) The peak region on chromosome 1. (E) The peak region on chromosome 5. In D and E, pair-wise linkage disequilibrium between SNP markers is indicated as  $D'$  values: dark red indicates a value of 1 and white indicates 0. The dotted squares in D and E denote the linkage disequilibrium blocks which contain significant SNPs.

### Relative DW

Relative DW showed a normal distribution (Fig. 4-3A) and the QQ plot showed deviation from the linear line in the most significant  $P$  value range (Fig. 4-3B). Three significant SNPs were located on chromosomes 6, 8 and 12 (Fig. 4-3C). However, we were unable to identify interesting genes among the ones located within these LD

blocks (Fig. 4-3D, E and Table S12). We also searched for genes from the LD blocks determined from the top 50 SNPs. A small but sharp peak was observed on chromosome 2. The corresponding LD block (associated with id2016513,  $-\log_{10}P = 3.85$ ) contained genes such as a putative hexose transporter (*LOC\_Os02g58530*) and a putative sucrose synthase (*LOC\_Os02g58480*), which could be related to carbon metabolism and translocation. Another LD block on chromosome 5 (associated with four SNPs, maximum  $-\log_{10}P = 2.59$ ) contained several sugar transporters (*LOC\_Os05g36414*, *LOC\_Os05g36440*, *LOC\_Os05g36450* and *LOC\_Os05g36700*).

#### *Relative SPW*

Relative SPW was distributed approximately normally (Fig. 4-4A). The  $-\log_{10}P$  values showed deviation from the expected values only in the most significantly associated markers (Fig. 4-4B), suggesting reliable performance of the MLM for this trait. By applying the threshold of  $-\log_{10}P > 4.0$ , we identified three significant SNPs on chromosomes 2 and 10 (Fig. 4-4C). On both chromosomes, the LD blocks consisted of a relatively small number of SNPs (Fig. 4-4D, E) and a total of 38 genes were located in the LD blocks containing these three SNPs (Table S12). The LD block on chromosome 10 contained 20 genes (excluding retrotransposons and a non-expressed gene), among which six genes had leucine-rich repeat regions including five with a GO annotation of ‘signal transduction’, which could be involved in ozone sensing and triggering downstream reactions.

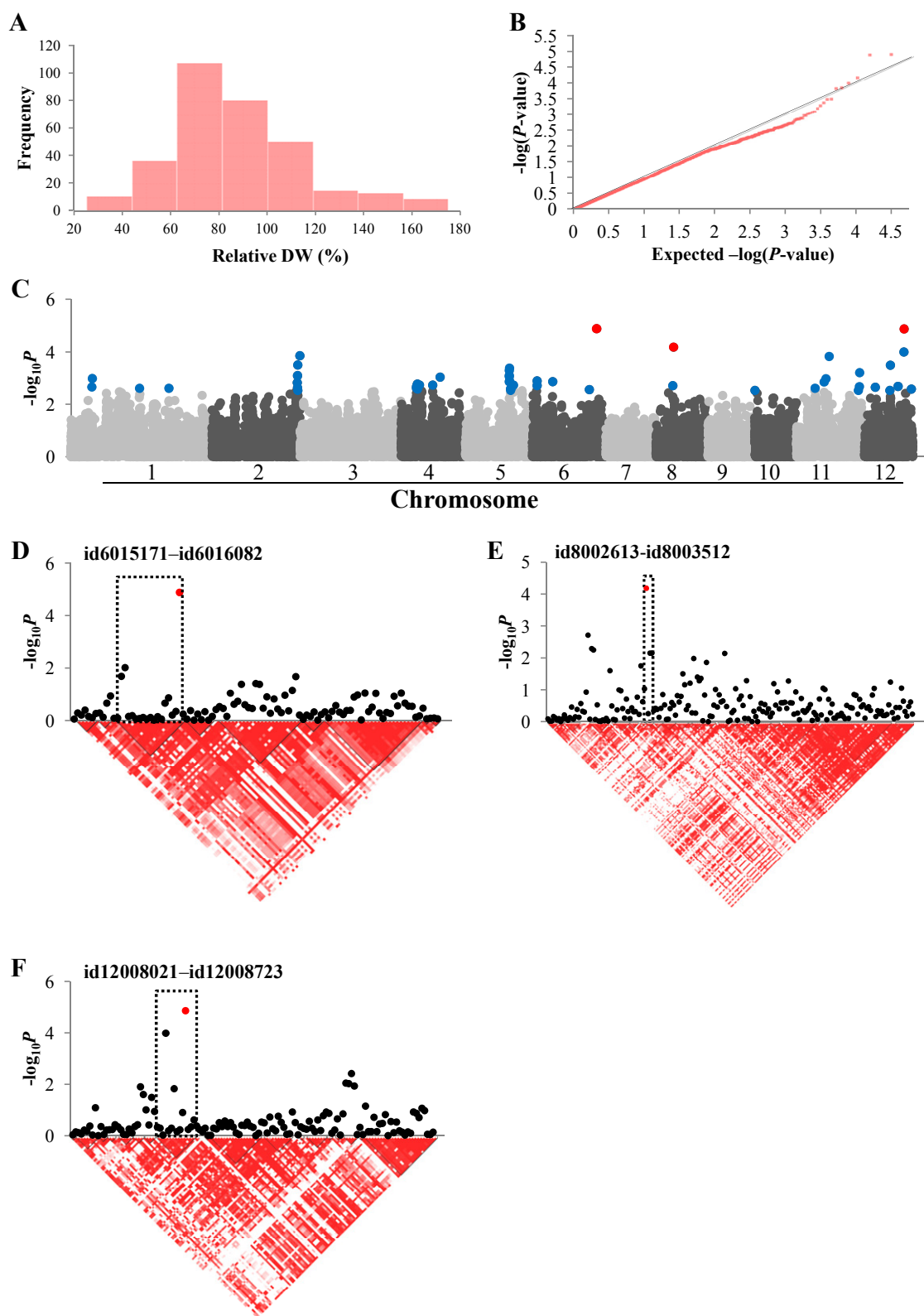


Figure 4-3: Association mapping result for relative dry weight (DW). (A) Frequency distribution of observed relative DW. (B) QQ plot of expected and observed  $P$  values. (C) Manhattan plots from association mapping using the Mixed Linear Model. The top 50 SNPs are shown in blue and the SNPs exceeding the significance threshold of  $P < 0.0001$  are shown in red. (D) The peak region on chromosome 6. (E) The peak region on chromosome 8. (F) The peak region on chromosome 12. In D-F, pair-wise linkage disequilibrium between SNP markers is indicated as  $D'$  values: dark red indicates a value of 1 and white indicates 0. The dotted squares in D-F denote the linkage disequilibrium blocks which contain significant SNPs.

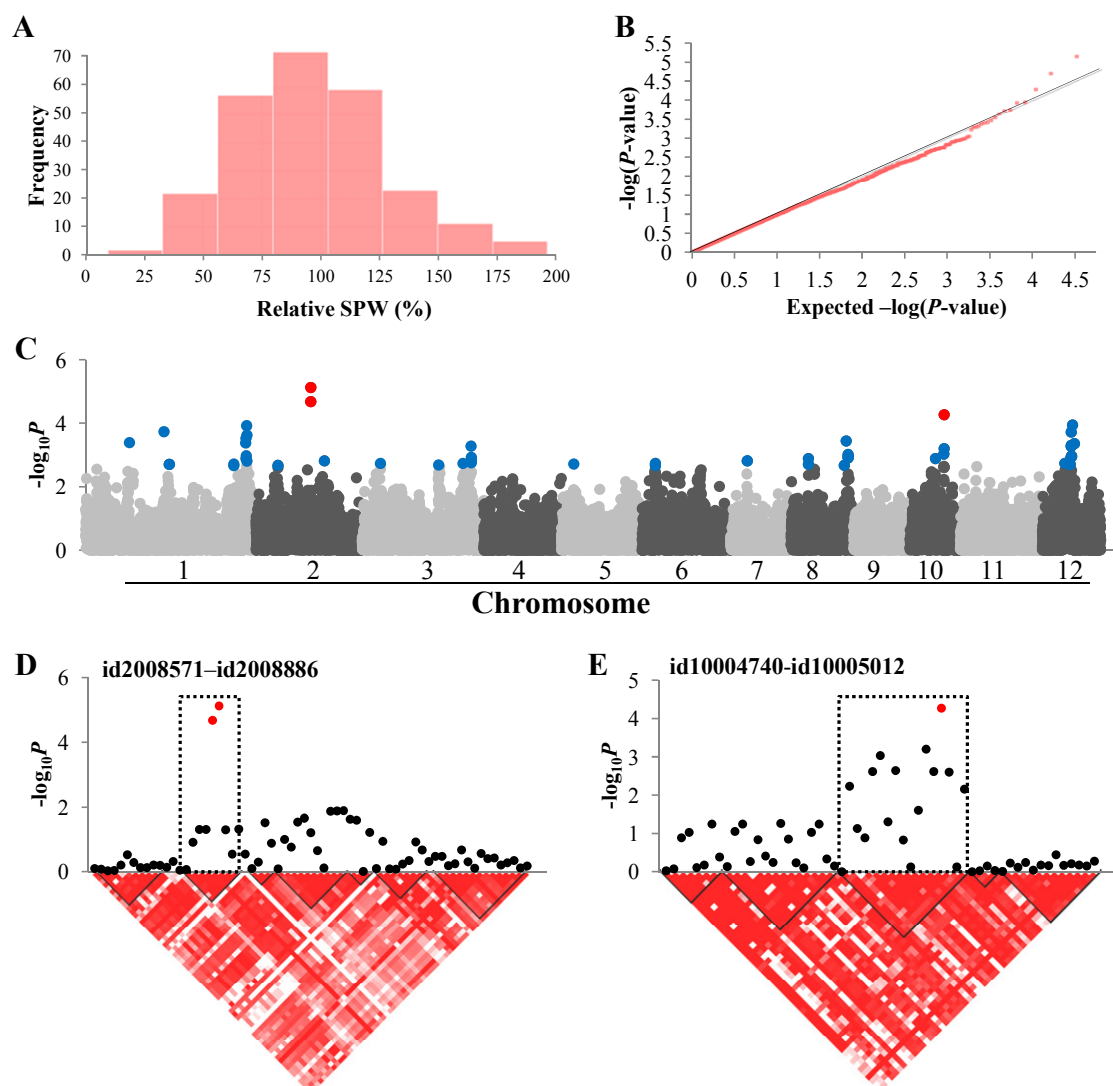


Figure 4-4: Association mapping results for relative single panicle weight (SPW). (A) Frequency distribution of observed relative SPW. (B) QQ plot of expected and observed  $P$  values. (C) Manhattan plot from association mapping using the Mixed Linear Model. The top 50 SNPs are shown in blue and the SNPs exceeding the significance threshold of  $P < 0.0001$  are shown in red. (D) The peak region on chromosome 2. (E) The peak region on chromosome 10. In D and E, pair-wise linkage disequilibrium between SNP markers is indicated as  $D'$  values: dark red indicates a value of 1 and white indicates 0. The dotted squares in D and E denote the linkage blocks which contain significant SNPs.

### 3.3. Co-localization of candidate loci

We analysed whether some loci were common to more than one trait. By curating the top 50 SNPs from all traits, we found that a total of 28 SNPs were shared in multiple traits (Table S11), which suggests pleiotropy of the SNPs or the existence of a closely linked gene (Zhao *et al.*, 2011). One of the SNPs (id1027640) affected four traits (relative plant height, relative tiller number, relative TPW, and relative SPW), although no convincing candidate gene was found within the LD block. Some SNPs

affected multiple categories of traits, such as leaf cell death and biochemical components (id1026656 and id5000980), leaf cell death and growth parameter (id1027571), and growth parameter and biochemical components (id12005469). These traits sharing common candidate loci were not necessarily correlated with each other (Table 4-2).

### 3.4. Candidate gene identification and sequence analysis

To test the plausibility of candidate genes, we determined sequence variations in contrasting haplotypes, which could be related to functional alterations. We chose the aforementioned locus on chromosome 5, which was identified for LBS, as a target region for the sequencing for the following reasons: (i) leaf cell death is one of the most conspicuous symptoms induced by ozone and is therefore of high importance and physiological interest; (ii) it gave a significant  $-\log_{10}P$  value in the peak region; (iii) LBS had a higher genetic heritability ( $h^2_{t-LBS} = 0.33$ ) than the average heritability from all traits ( $h^2_{all} = 0.27$ ), showing that a larger portion of phenotypic variance for LBS is ascribed to genetic variance (Table S13); (iv) the LD block contained a relatively small number of candidate genes; and (v) evidence from other studies strongly supports the role of candidate genes under ozone stress (discussed later). Among the 41 genes contained in this locus (Table S12), we selected genes which had informative annotation. Thus 17 retro- or transposon genes and a further two non-expressed genes were eliminated (Table S12). From the remaining 22 genes, we chose genes which were involved in either cell death pathways or were related to ethylene, which plays a crucial role in inducing cell death (Kangasjärvi *et al.*, 2005), for further characterization by sequencing: an *EREBP* (*ethylene-responsive element binding protein*, *LOC\_Os05g29810*) and a *RING* (*‘really interesting new gene’*, *LOC\_Os05g29710*). The EREBP was a transcription factor which contains an ethylene-responsive binding domain. Its closest *Arabidopsis* homologue (At1g53910) is known to regulate oxygen sensing and trigger downstream response (Licausi *et al.*, 2011). The RING protein contained a transmembrane domain and a RING motif. The closest *Arabidopsis* homologue (At5g10380) is related to the induction of pathogen resistance and cell death (Lin *et al.*, 2008). First, we chose contrasting haplotypes for markers surrounding the genes and sequenced the genes. Genome sequences of additional accessions from a public rice genome database were also included in the analysis (Figure S25). Analysing these 34 accessions revealed eight nucleotide

polymorphisms in the *EREBP* gene (Fig. 4-5). We assessed the  $r^2$  values between the observed polymorphic sites and those SNPs in the LD block, which were in the top 50 SNPs for LBS. Here, we used  $r^2$  value rather than  $D'$  value for the assessment of association, since our objective was to get insight into the functional relationship rather than determining LD blocks. The highest  $r^2$  value was observed at a polymorphic site in the intron (position 204 and id5006957,  $r^2 = 0.53$ ,  $P < 0.0001$  by a two-tailed Fisher's exact test). The polymorphic sites causing amino acid substitutions generally had low  $r^2$  values (average  $r^2 = 0.17$ , highest  $r^2 = 0.37$ ,  $P = 0.0017$ ). In other words, the observed amino acid substitutions were not closely associated with the significant SNPs detected through GWAS.

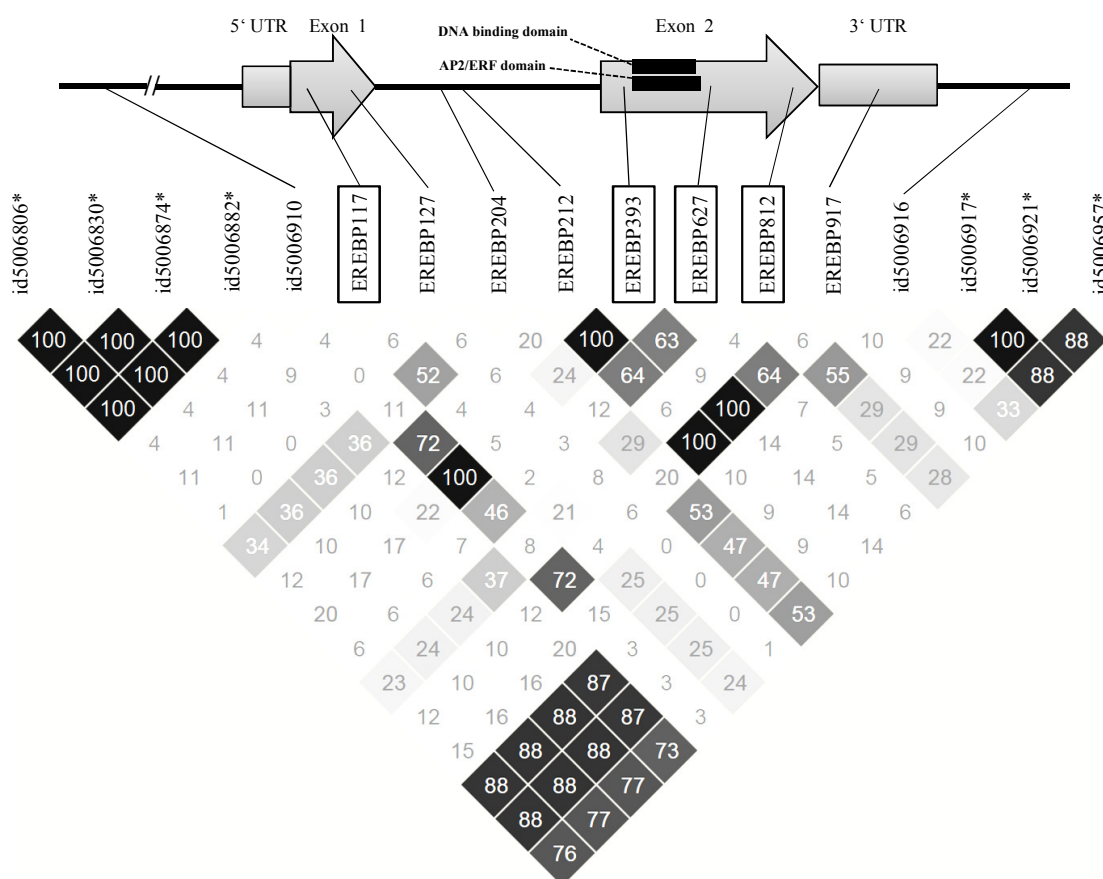


Figure 4-5: Sequence variation of *EREBP* (*LOC\_Os05g29810*). The polymorphic sites of *EREBP* in 34 accessions are shown together with two adjacent SNP markers and those among the top 50 SNP markers for leaf bronzing score, which are located within the linkage disequilibrium block (shown with asterisks). In the observed polymorphic sites, the number after *EREBP* indicates the position from the transcription initiation site. The sites within black frames (*EREBP*117, *EREBP*393, *EREBP*627 and *EREBP*812) cause amino acid substitution/insertion. The matrix shows the  $r^2$  values of each pair-wise comparison of markers and polymorphic sites. Higher values are shown in a darker colour. The number in the square shows the 100-fold value of  $r^2$ , which ranged from 0 to 100. The amino acid sequence 53 to 111 is a DNA-binding domain, and 53 to 116 is an AP2/ERF domain.

The *RING* was located near a SNP marker with a high  $-\log_{10}P$  value (id5006874,  $-\log_{10}P = 3.40$ ; Fig. 4-6A). Allele A at the position id5006874 occurred mainly in *aromatic* and *temperate japonica*, and allele G occurred mainly in *aus* and *indica* subpopulations, while *tropical japonica* subpopulation contained both alleles at a relatively high ratio (Fig. 4-6B). When conducting association mapping separately for each subpopulation, the same peak at this locus occurred only in the *tropical japonica* subpopulation (Figure S26). Therefore, we chose two to five lines from each subpopulation, plus randomly selected additional lines from *tropical japonica* subpopulation carrying each allele, and sequenced the genomic region of the *RING*. We also added rice genome sequences from a public database into the analysis (Figure S27). In a total of 50 accessions, nucleotide sequence variation was observed at 12 positions (Fig. 4-6A). Four of them caused an amino acid substitution or insertion. We determined the correlation between the observed polymorphisms and those among the 50 SNPs, which were located within the LD block. Two of the amino acid substitutions (positions 635 and 652) were highly associated with significant SNPs (average  $r^2 = 0.70$  and  $0.65$ , highest  $r^2 = 0.89$  and  $0.80$  respectively,  $P < 0.0001$  for both positions). Moreover, these two amino acid substitution sites were located in the *RING* motif, which is crucial for the activity of this protein (Fig. 4-6A). We classified the accessions according to the allele at id5006874, which showed the strongest association with the amino acid substitutions in the *RING* motif (Fig. 4-6B). Type 1 contained allele A at id5006874 and was highly significantly associated with arginine at the amino acid positions 141 and 147. In contrast, type 2 had allele G at id5006874 and was associated with histidine at the amino acid position 141 and serine at the amino acid position 147 (Figure S27). We compared the t-LBS of genotypes carrying the alleles A and G at this position in the *tropical japonica* subpopulation. The allele G was associated with a higher t-LBS than allele A ( $P < 0.01$ ; Fig. 4-6C). We then obtained the amino acid sequences of previously characterized *RING* proteins from other plant species and compared the *RING* motif sequence with the *RING* protein in our study. Comparison of the motif showed that a conserved amino acid arginine was substituted by serine in type 2 (Fig. 4-6D).

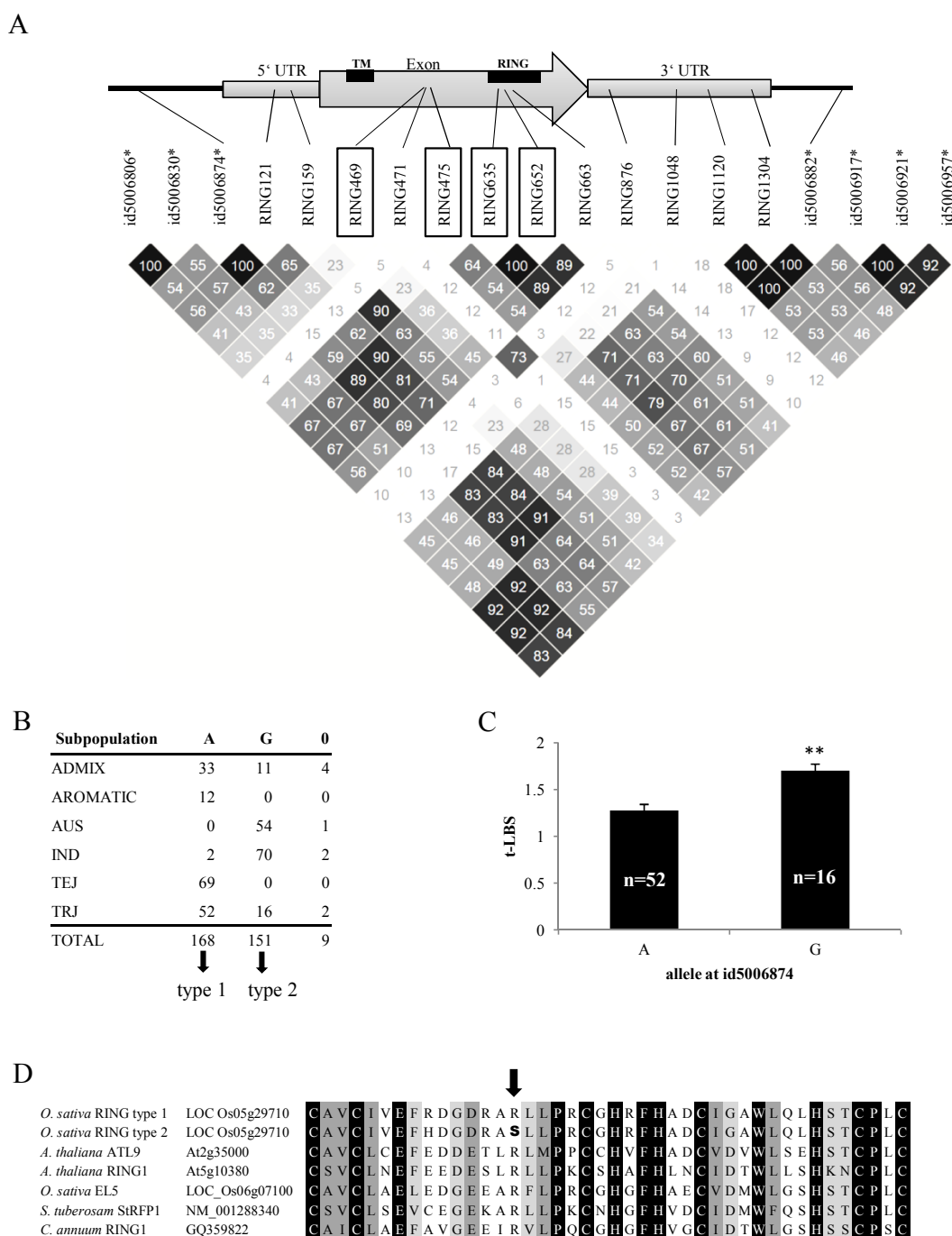


Figure 4-6: Analysis of *RING* (*LOC\_Os05g29710*) as a candidate gene underlying the peak for square-root transformed leaf bronzing score (t-LBS) on chromosome 5. (A) The polymorphic sites of the *RING* gene. The genomic sequences of the *RING* gene from 50 accessions are shown together with two adjacent SNP markers and those among the top 50 SNP markers for t-LBS, which were located within the linkage disequilibrium block (shown with asterisks). In the observed polymorphic sites, the number after RING shows the position from the transcription initiation site. The sites with black frames (RING469, RING475, RING635 and RING652) cause amino acid substitution/insertion. The matrix shows the  $r^2$  values of each pair-wise comparison of markers and polymorphic sites. Higher values are shown in a darker colour. The number in the square shows the 100-fold value of  $r^2$ , which ranged from 0 to 100. The amino acid sequence 29 to 50 is a transmembrane domain (TM), and 133 to 175 is a zinc-finger motif (RING). (B) Allele frequency of each subpopulation at id5006874. '0' stands for missing data in the original genotyping. Accessions containing A at this position are termed as 'type 1' and those containing G are termed as 'type 2'. IND, *indica*; TEJ, *temperate japonica*; and TRJ, *tropical japonica*.



*japonica*. (C) t-LBS in the *tropical japonica* subpopulation. The asterisks indicate that the allele G at id5006874 is associated with a significantly higher t-LBS by Student's *t*-test ( $P < 0.01$ ). (D) Amino acid sequence comparison of the 42 amino acid RING motif between the rice RING protein and other previously reported cell death or defence reaction-related RING proteins: *Arabidopsis* ATL9 (Berrocal-Lobo *et al.*, 2010), *Arabidopsis* RING1 (Lin *et al.*, 2008), rice EL5 (Takai *et al.*, 2001), potato StRFP1 (Ni *et al.*, 2010), and pepper RING1 (Lee *et al.*, 2011). Completely conserved amino acids are shown against a black background. Strong groups (as defined by Pam250 score of  $> 0.5$ ) are shown against a dark gray background, and weak groups (as defined by Pam250 score of  $\leq 0.5$ ) are shown against a light gray background (Gonnet *et al.*, 1992). An amino acid substitution between type 1 and type 2 (R  $\rightarrow$  S) is shown in boldface in the arrowed position.

## 4. Discussion

We studied the natural variation of rice in response to ozone and identified candidate loci regulating important phenotypes under ozone stress. To the best of our knowledge, this is the first large scale tolerance screening and GWAS focusing on ozone stress in any crop species. We adopted a target concentration of 60 ppb for the whole season and obtained an average concentration of 63 ppb during the season. This corresponds to an increase around 25 to 75% compared with the current average tropospheric ozone concentration (Ainsworth *et al.*, 2012) and is known to cause rice yield reduction by around 14% (Ainsworth, 2008). Additionally, three episodes of acute ozone stress (150 ppb) were applied, which is frequently observed in the early summer season in Asia (Tang *et al.*, 2012). On average, all the growth parameters and SPAD value decreased under ozone stress, while lignin content increased, which is in accordance with previous studies (Shi *et al.*, 2009; Frei *et al.*, 2011; Ainsworth *et al.*, 2014). A slightly higher yield reduction as assessed by TPW in the current study (Table 4-1) compared with the previous reports might be ascribed to the three episodes of acute ozone stress applied during the season. The substantial genotypic differences observed in ozone response in all phenotypic traits highlight the rich genetic diversity which can be exploited through GWAS. Thus, our fumigation scheme proved optimal to induce a wide range of phenotypic variation, and therefore we concluded that this mapping population and the observed phenotypes constitute a powerful resource for association mapping.

The significant positive correlation between growth parameters and yield components suggests source limitations for the grain yield under ozone stress. In other words, carbon assimilation or sugar loading is limiting grain yield, rather than sink limitations such as storage and phloem unloading. Another factor highly affecting the yield could be flowering time. Although we did not measure the flowering time for the whole population, we found a significant negative correlation between relative TPW and the flowering time (*i.e.* the number of days from transplanting until flowering) recorded in Arkansas (data adopted from Zhao *et al.* 2011, where the same population was used;  $r = -0.14$ ,  $P = 0.026$ ). This negative correlation could suggest that the longer the plants were exposed to ozone before flowering, the more the grain yield was affected. We also found that five SNPs (id1013335, id1013354, id1013362, id1013402 and id1013422) appeared in the top 50 SNPs for both relative TPW and the flowering time

recorded in Arkansas, which further implies an effect of flowering time on the grain yield under ozone stress. However, one should be cautious in applying the flowering time recorded elsewhere to our dataset, since this trait is highly affected by day length and temperature sum.

We applied an MLM incorporating both a kinship and PCA matrix to all the phenotypes to avoid false positives, which are likely to result from naïve GLM (Larsson *et al.*, 2013). The QQ plots for t-LBS, relative DW and relative SPW (Figs. 4-2B, 4-3B and 4-4B) indicated good applicability of the model for these traits (Zhang *et al.*, 2010). For several traits, the MLM might have been too conservative and rendered false negatives, as QQ plots indicated  $-\log_{10}P$  values even below the expected distribution, although Manhattan plots exhibited clearly defined peaks (Figures S18-S24). Employing LD blocks to define the genomic regions in which to search for candidate genes has advantages over the fixed window approach, in which a certain distance from a significant SNP is considered as the region containing candidate genes (Courtois *et al.*, 2013), in terms of elimination of falsely included or excluded genes (Chen *et al.*, 2012). In our study, the candidate regions ranged from < 1 kb to > 1 Mb depending on the chromosomal position. This suggests that the resolution of the association mapping depends highly on the LD of the neighbouring regions of the significant SNPs. Since some of the LD blocks harbouring significant SNPs did not contain any annotated gene, this method might have produced some false negatives, or the identified region contained important DNA binding or gene regulation sites, in which case the causal gene is not directly detected in the LD block (Sur *et al.*, 2013).

Some of the putative candidate genes were involved in pathogen resistance and response. Ozone stress differs from many other abiotic stresses in the sense that the apoplast is the first cell component encountering oxidative stress. Ozone enters the plants through the stomata and produces reactive oxygen species in the apoplast, which induces responses and downstream signals similar to those observed under pathogen attack (Conklin and Barth, 2004), and ultimately lead to PCD (Kangasjärvi *et al.*, 2005), coinciding with the expression of pathogenesis-related (PR) genes (Rao *et al.*, 2000). Thus, the identification of several candidate genes for LBS, which have been characterized in connection with pathogen resistance, appears highly plausible. For example,  $\beta$ -1,3-glucanase and chitinase belong to the glycosyl hydrolase families

19 and 17, and are classified as PR-2 and PR-3 protein, respectively (Brederode *et al.*, 1991). Both have catalytic activity causing degradation of fungal cell walls (Mauch *et al.*, 1988), thereby enhancing the resistance to pathogens (Zhu *et al.*, 1994). Both genes have been recognized as ozone-inducible genes and are proposed to determine ozone sensitivity (Ernst *et al.*, 1992; Street *et al.*, 2011). Since two of the PR proteins were detected near the significantly associated loci based on leaf cell death, our study supports the concept of similarities in pathogen and ozone response.

Another candidate gene possibly associated with leaf visible symptoms is an *EREBP* gene (*LOC\_Os05g29810*), which was found in the LD block containing the significant SNPs on chromosome 5 (Fig. 4-2E). A low correlation between amino acid substitution/insertion and the significant SNPs (Fig. 4-5) suggests that the polymorphisms in this gene were not directly associated with the significant GWAS signal. Also, since polymorphisms were not in the functional domain of EREBP, its effect on leaf visible symptoms, if any, would presumably be through post-transcriptional modification or expression level rather than functional alteration of the protein. An even more plausible candidate identified in the peak on chromosome 5 was a *RING* gene (*LOC\_Os05g29710*), encoding an E3 ubiquitin ligase, and is classified as C3-H2-C3 RING protein due to the amino acid sequence of the zinc ion binding site. This RING protein is part of a large protein family which is emerging as an important factor during pathogen infection and induction of defence reactions (Trujillo and Shirasu, 2010). Amino acid sequence comparison with the homologues showed that one of the amino acid substitutions in the type 2 (which is associated with allele G at position id5006917) is located in the conserved region of the RING motif (Fig. 4-6D). In many previous studies, amino acid changes leading to functional variance or phenotypic difference occurred in conserved protein motifs (Yamanouchi *et al.*, 2002; Kobayashi *et al.*, 2008). In the case of the RING protein, we assume that this conserved region is crucial for the activity or determines the selectivity of the substrate protein.

In summary, our study demonstrated substantial genotypic variation in ozone tolerance in rice, which provides a rich basis for adaptive breeding. GWAS identified convincing candidate loci based on significant peaks, heritability, LD analysis, and candidate gene identification for LBS. We found a number of novel polymorphisms in an *EREBP* and a *RING* gene, which could be candidate genes controlling leaf visible damage due to their locations in an identified LD block and their annotated functions.

These indirect lines of evidence warrant further investigation of these genes and their involvement in ozone tolerance using reverse genetic approaches.

### ***Supplementary material***

Figure S17 Subpopulation comparison of all phenotypes.

Figures S18-S24

Distribution and association mapping results for all phenotypic traits.

Figure S25 Sequence variation of *EREBP* gene.

Figure S26 Association mapping for square-root transformed leaf bronzing score (t-LBS) in each subpopulation.

Figure S27 Sequence variation of *RING* gene.

Table S8 List of all the phenotypic values.

Table S9 Correlation coefficient and *P* value of pair-wise comparison of each phenotype in each subpopulation.

Table S10 List of significant SNPs identified through association mapping.

Table S11 List of the top 50 SNPs from each phenotype.

Table S12 List of genes located within the identified candidate loci for all phenotypes.

Table S13 Heritability of each trait.

### ***Funding***

This work was supported by Deutsche Forschungsgemeinschaft (FR-2952/1-1) and Stiftung Fiat Panis.

### ***Acknowledgments***

The authors thank Dr. Matthias Wissuwa (JIRCAS, Tsukuba, Japan) and all members of the GRiSP Global Rice Phenotyping Network for sharing experiences in GWAS and the International Rice Research Institute (IRRI), especially Dr. Kenneth McNally, for providing seeds. The authors also thank the technical assistants in the experimental facility of the University of Bonn.

## References

- Ainsworth EA.** 2008. Rice production in a changing climate: a meta-analysis of responses to elevated carbon dioxide and elevated ozone concentration. *Global Change Biology* **14**, 1642–1650.
- Ainsworth EA, Serbin SP, Skoneczka JA, Townsend PA.** 2014. Using leaf optical properties to detect ozone effects on foliar biochemistry. *Photosynthesis research* **119**, 65–76.
- Ainsworth EA, Yendrek CR, Sitch S, Collins WJ, Emberson LD.** 2012. The effects of tropospheric ozone on net primary productivity and implications for climate change. *Annual review of plant biology* **63**, 637–661.
- Barrett JC, Fry B, Maller J, Daly MJ.** 2005. Haploview: analysis and visualization of LD and haplotype maps. *Bioinformatics* **21**, 263–265.
- Berrocal-Lobo M, Stone S, Yang X, Antico J, Callis J, Ramonell KM, Somerville S.** 2010. ATL9, a RING zinc finger protein with E3 ubiquitin ligase activity implicated in chitin- and NADPH oxidase-mediated defense responses. *PLoS one* **5**, e14426.
- Brachi B, Morris GP, Borevitz JO.** 2011. Genome-wide association studies in plants: the missing heritability is in the field. *Genome biology* **12**, 232.
- Bradbury PJ, Zhang Z, Kroon DE, Casstevens TM, Ramdoss Y, Buckler ES.** 2007. TASSEL: software for association mapping of complex traits in diverse samples. *Bioinformatics* **23**, 2633–2635.
- Brederode FT, Linthorst HJ, Bol JF.** 1991. Differential induction of acquired resistance and PR gene expression in tobacco by virus infection, ethephon treatment, UV light and wounding. *Plant molecular biology* **17**, 1117–1125.
- Brosché M, Merilo E, Mayer F, et al.** 2010. Natural variation in ozone sensitivity among *Arabidopsis thaliana* accessions and its relation to stomatal conductance. *Plant, Cell and Environment* **33**, 914–925.
- Chen C, DeClerck G, Tian F, Spooner W, McCouch S, Buckler E.** 2012. PICARA, an analytical pipeline providing probabilistic inference about *a priori* candidate genes underlying genome-wide association QTL in plants. *PLoS one* **7**, e46596.
- Chen CP, Frei M, Wissuwa M.** 2011. The *OzT8* locus in rice protects leaf carbon assimilation rate and photosynthetic capacity under ozone stress. *Plant, Cell and Environment* **34**, 1141–1149.
- Conklin PL, Barth C.** 2004. Ascorbic acid, a familiar small molecule intertwined in the response of plants to ozone, pathogens, and the onset of senescence. *Plant, Cell and Environment* **27**, 959–970.
- Courtois B, Audebert A, Dardou A, et al.** 2013. Genome-wide association mapping of root traits in a japonica rice panel. *PLoS one* **8**, e78037.

- Ernst D, Schraudner M, Langebartels C, Sandermann H.** 1992. Ozone-induced changes of mRNA levels of beta-1,3-glucanase, chitinase and 'pathogenesis-related' protein 1b in tobacco plants. *Plant molecular biology* **20**, 673–682.
- Famoso AN, Zhao K, Clark RT, et al.** 2011. Genetic architecture of aluminum tolerance in rice (*Oryza sativa*) determined through genome-wide association analysis and QTL mapping. *PLoS genetics* **7**, e1002221.
- Feng Z, Kobayashi K.** 2009. Assessing the impacts of current and future concentrations of surface ozone on crop yield with meta-analysis. *Atmospheric Environment* **43**, 1510–1519.
- Feng Z, Pang J, Kobayashi K, Zhu J, Ort DR.** 2011. Differential responses in two varieties of winter wheat to elevated ozone concentration under fully open-air field conditions. *Global Change Biology* **17**, 580–591.
- Flint-Garcia SA, Thornsberry JM, Buckler ES.** 2003. Structure of linkage disequilibrium in plants. *Annual review of plant biology* **54**, 357–374.
- Flowers MD, Fiscus EL, Burkey KO, Booker FL, Dubois J-JB.** 2007. Photosynthesis, chlorophyll fluorescence, and yield of snap bean (*Phaseolus vulgaris* L.) genotypes differing in sensitivity to ozone. *Environmental and Experimental Botany* **61**, 190–198.
- Frei M.** 2013. Lignin : Characterization of a multifaceted crop component. *The Scientific World Journal* **2013**, 436517.
- Frei M, Kohno Y, Wissuwa M, Makkar HPS, Becker K.** 2011. Negative effects of tropospheric ozone on the feed value of rice straw are mitigated by an ozone tolerance QTL. *Global Change Biology* **17**, 2319–2329.
- Frei M, Tanaka JP, Chen CP, Wissuwa M.** 2010. Mechanisms of ozone tolerance in rice: characterization of two QTLs affecting leaf bronzing by gene expression profiling and biochemical analyses. *Journal of Experimental Botany* **61**, 1405–1417.
- Frei M, Tanaka JP, Wissuwa M.** 2008. Genotypic variation in tolerance to elevated ozone in rice: dissection of distinct genetic factors linked to tolerance mechanisms. *Journal of Experimental Botany* **59**, 3741–3752.
- Gabriel SB, Schaffner SF, Nguyen H, et al.** 2002. The structure of haplotype blocks in the human genome. *Science* **296**, 2225–2229.
- Gonnet GH, Cohen MA, Benner SA.** 1992. Exhaustive matching of the entire protein sequence database. *Science* **256**, 1443–1445.
- Gupta PK, Rustgi S, Kulwal PL.** 2005. Linkage disequilibrium and association studies in higher plants: Present status and future prospects. *Plant molecular biology* **57**, 461–485.
- Kangasjärvi J, Jaspers P, Kollist H.** 2005. Signalling and cell death in ozone-exposed plants. *Plant, Cell and Environment* **28**, 1021–1036.
- Kobayashi Y, Kuroda K, Kimura K, et al.** 2008. Amino acid polymorphisms in strictly conserved domains of a P-type ATPase HMA5 are involved in the mechanism of copper tolerance variation in Arabidopsis. *Plant Physiology* **148**, 969–980.



- Kumagai M, Kim J, Itoh R, Itoh T.** 2013. TASUKE: a web-based visualization program for large-scale resequencing data. *Bioinformatics* **29**, 1806–1808.
- Larsson SJ, Lipka AE, Buckler ES.** 2013. Lessons from *Dwarf8* on the strengths and weaknesses of structured association mapping. *PLoS genetics* **9**, e1003246.
- Lee DH, Choi HW, Hwang BK.** 2011. The pepper E3 ubiquitin ligase RING1 gene, *CaRING1*, is required for cell death and the salicylic acid-dependent defense response. *Plant Physiology* **156**, 2011–2025.
- Lei H, Wuebbles DJ, Liang X-Z, Olsen S.** 2013. Domestic versus international contributions on 2050 ozone air quality: How much is convertible by regional control? *Atmospheric Environment* **68**, 315–325.
- Lelieveld J, Dentener FJ.** 2000. What controls tropospheric ozone? *Journal of Geophysical Research* **105**, 3531–3551.
- Licausi F, Kosmacz M, Weits DA, et al.** 2011. Oxygen sensing in plants is mediated by an N-end rule pathway for protein destabilization. *Nature* **479**, 419–422.
- Lin S-S, Martin R, Mongrand S, Vandenabeele S, Chen K-C, Jang I-C, Chua N-H.** 2008. RING1 E3 ligase localizes to plasma membrane lipid rafts to trigger FB1-induced programmed cell death in Arabidopsis. *The Plant Journal* **56**, 550–561.
- Mauch F, Mauch-Mani B, Boller T.** 1988. Antifungal hydrolases in pea tissue. II. Inhibition of fungal growth by combinations of chitinase and  $\beta$ -1,3-glucanase. *Plant Physiology* **88**, 936–942.
- Ni X, Tian Z, Liu J, Song B, Xie C.** 2010. Cloning and molecular characterization of the potato RING finger protein gene *StRFP1* and its function in potato broad-spectrum resistance against *Phytophthora infestans*. *Journal of plant physiology* **167**, 488–496.
- Rao M, Koch J, Davis K.** 2000. Ozone: a tool for probing programmed cell death in plants. *Plant molecular biology* **44**, 345–358.
- Sawada H, Kohno Y.** 2009. Differential ozone sensitivity of rice cultivars as indicated by visible injury and grain yield. *Plant Biology* **11**, 70–75.
- Schneider RJ.** 2005. Pharmaka im Urin : Abbau und Versickerung vs . Pflanzenaufnahme. In: Bastian A, Bornemann C, Hachenberg M, Oldenburg M, Schmelzer M, eds. *Nährstofftrennung und -verwertung in der Abwassertechnik am Beispiel der „Lambertsmühle“*. Bonn, Germany, 54–81.
- Shi G, Yang L, Wang Y, et al.** 2009. Impact of elevated ozone concentration on yield of four Chinese rice cultivars under fully open-air field conditions. *Agriculture, Ecosystems and Environment* **131**, 178–184.
- Street NR, Tallis MJ, Tucker J, Brosché M, Kangasjärvi J, Broadmeadow M, Taylor G.** 2011. The physiological, transcriptional and genetic responses of an ozone-sensitive and an ozone tolerant poplar and selected extremes of their F<sub>2</sub> progeny. *Environmental Pollution* **159**, 45–54.

- Sur I, Tuupanen S, Whittington T, Aaltonen LA, Taipale J.** 2013. Lessons from functional analysis of genome-wide association studies. *Cancer research* **73**, 4180–4184.
- Suzuki S, Suzuki Y, Yamamoto N, Hattori T, Sakamoto M, Umezawa T.** 2009. High-throughput determination of thioglycolic acid lignin from rice. *Plant Biotechnology* **26**, 337–340.
- Takai R, Hasegawa K, Kaku H, Shibuya N, Minami E.** 2001. Isolation and analysis of expression mechanisms of a rice gene, EL5, which shows structural similarity to ATL family from *Arabidopsis*, in response to *N*-acetylchitooligosaccharide elicitor. *Plant Science* **160**, 577–583.
- Tamura K, Peterson D, Peterson N, Stecher G, Nei M, Kumar S.** 2011. MEGA5: molecular evolutionary genetics analysis using maximum likelihood, evolutionary distance, and maximum parsimony methods. *Molecular biology and evolution* **28**, 2731–2739.
- Tang H, Liu G, Zhu J, Han Y, Kobayashi K.** 2012. Seasonal variations in surface ozone as influenced by Asian summer monsoon and biomass burning in agricultural fields of the northern Yangtze River Delta. *Atmospheric Research* **122**, 67–76.
- Teixeira E, Fischer G, van Velthuisen H, et al.** 2011. Limited potential of crop management for mitigating surface ozone impacts on global food supply. *Atmospheric Environment* **45**, 2569–2576.
- Trujillo M, Shirasu K.** 2010. Ubiquitination in plant immunity. *Current opinion in plant biology* **13**, 402–408.
- Tsukahara K, Sawada H, Matsumura H, Kohno Y, Tamaoki M.** 2013. Quantitative trait locus analyses of ozone-induced grain yield reduction in rice. *Environmental and Experimental Botany* **88**, 100–106.
- Verslues PE, Lasky JR, Juenger TE, Liu T-W, Kumar MN.** 2014 Genome-wide association mapping combined with reverse genetics identifies new effectors of low water potential-induced proline accumulation in *Arabidopsis*. *Plant Physiology* **164**, 144–159.
- Wang Y, Frei M.** 2011. Stressed food – The impact of abiotic environmental stresses on crop quality. *Agriculture, Ecosystems and Environment* **141**, 271–286.
- Wang Y, Yang L, Höller M, Zaisheng S, Pariasca-Tanaka J, Wissuwa M, Frei M.** 2014. Pyramiding of ozone tolerance QTLs *OzT8* and *OzT9* confers improved tolerance to season-long ozone exposure in rice. *Environmental and Experimental Botany* **104**, 26–33.
- Wissuwa M, Ismail AM, Yanagihara S.** 2006. Effects of zinc deficiency on rice growth and genetic factors contributing to tolerance. *Plant Physiology* **142**, 731–741.
- Yamaji K, Ohara T, Uno I, Tanimoto H, Kurokawa J, Akimoto H.** 2006. Analysis of the seasonal variation of ozone in the boundary layer in East Asia using the Community Multi-scale Air Quality model: What controls surface ozone levels over Japan? *Atmospheric Environment* **40**, 1856–1868.

- Yamanouchi U, Yano M, Lin H, Ashikari M, Yamada K.** 2002. A rice spotted leaf gene, *Spl7*, encodes a heat stress transcription factor protein. *Proceedings of the National Academy of Sciences of the United States of America* **99**, 7530–7535.
- Zhang Z, Ersoz E, Lai C-Q, et al.** 2010. Mixed linear model approach adapted for genome-wide association studies. *Nature genetics* **42**, 355–360.
- Zhao K, Tung C-W, Eizenga GC, et al.** 2011. Genome-wide association mapping reveals a rich genetic architecture of complex traits in *Oryza sativa*. *Nature communications* **2**, 467.
- Zhao K, Wright M, Kimball J, et al.** 2010. Genomic diversity and introgression in *O. sativa* reveal the impact of domestication and breeding on the rice genome. *PLoS one* **5**, e10780.
- Zhu Q, Maher EA, Masoud S, Dixon RA, Lamb CJ.** 1994. Enhanced protection against fungal attack by constitutive co-expression of chitinase and glucanase genes in transgenic tobacco. *Nature biotechnology* **12**, 807–812.

# Chapter 5

## General Discussion

### **1. Novel mechanisms and genetic loci for ozone tolerance in rice**

In the current study, novel mechanisms for cell death formation under ozone stress (Chapter 3) and genetic loci involved in ozone stress tolerance (Chapter 4) were explored in rice. Elucidation of genetic factors and isolation of causative genes for a certain trait are prerequisites for marker-assisted breeding. Therefore, these novel findings will pave the way for future crop improvement and consequently contribute to the world food supply in the 21st century.

In Chapter 2, two small-scale and high-throughput ascorbate (AsA) measurement methods were compared, and an appropriate method was suggested for different situations in plant research. For the measurement of apoplastic AsA, the ascorbate oxidase (AO) method was superior to the dipyrindyl (DPD) method, which was less sensitive and could not detect reduced AsA in the apoplast. The previously reported method using spectrophotometer and a cuvette would have needed more than 10 min for each sample (deduced from previous protocols such as Luwe *et al.*, 1993). In the new microplate-based AO method, 24 samples could be simultaneously measured within 30 min (after the extraction), with two analytical replicates. Moreover, the amount of intercellular washing fluid (IWF) needed for the measurement was around 100  $\mu\text{L}$  in the previous protocol for one technical replicate, while the AO method in the current study needs only 40  $\mu\text{L}$  for one technical replicate. This is of high importance in case of AsA measurement from IWF since the amount IWF is usually very small, especially in rice due to technical constraints (Nouchi *et al.*, 2012). These

facts demonstrate good applicability of the AO method for high-throughput measurement of apoplastic AsA. As mentioned in Chapter 1, apoplastic AsA plays a pivotal role in determining ozone tolerance of plants. Therefore the measurement of apoplastic AsA would be a possible target for future crop breeding aiming at ozone tolerance. This high-throughput apoplastic AsA measurement will aid such a breeding process, as well as other situations in plant science where a large number of samples need to be processed (as in Chapter 3).

In Chapter 3, a candidate gene for ozone stress tolerance was characterized by a reverse-genetic strategy in rice. Important clues for the physiological significance of the putative AO gene (*OsORAP1*) were presented. Contrary to the hypothesis, *OsORAP1* did not show AO activity, and the enhanced tolerance in the knock-out line (KO) was not because of higher detoxification or differential uptake of ozone. It was concluded that less leaf visible symptoms in KO resulted from the absence of ‘suicide aiding effect’ that *OsORAP1* seems to possess. Therefore, *OsORAP1* does not confer ozone stress tolerance (*i.e.* less leaf visible symptom formation) through the currently-acknowledged mechanism, where apoplastic AsA detoxification determines the extent of damage to the cells. Rather it is likely that the local *OsORAP1* expression in the attacked sites propagates the signal through some unknown mechanisms, which eventually leads to enhanced cell death formation, although the expression pattern of *OsORAP1* should be investigated at sub-tissue levels to confirm this hypothesis.

Although it is generally agreed that apoplastic AsA constitutes the first line of defence against ozone as discussed in Chapter 1, Booker *et al.* (2012) argued that apoplastic AsA contributes to the detoxification of ozone only to a minor extent. Therefore it is possible that certain unknown factor besides AsA contributes to the mitigation of ozone stress in the apoplast. Moldau (1998) suggested that phenolic compounds could also serve as electron donors for ozone. Moreover, AO proteins are capable of oxidizing phenolic compounds (Dayan and Dawson, 1976). Taking into account that *OsORAP1* is predicted to possess oxidoreductase activity by I-TASSER (Zhang, 2008), *OsORAP1* might possibly have the capability to oxidize phenolic compounds, thereby participating in ozone stress tolerance. However, the concentration of phenolic compounds in the apoplast is too low to effectively remove incoming ozone (Booker *et al.*, 2012). Hence, it is not likely that the unknown substrate of *OsORAP1* directly contributes to the detoxification of ROS in the apoplast. It is more likely that

OsORAP1 is involved in the signal transduction, which triggers certain downstream pathways.

Plants possess innate systems to amplify signals from the environment, thereby facilitating the induction of defence responses. This mechanism has been unveiled in the context of plant pathology. One example is oxidative burst mediated by plasma membrane-localized NADPH oxidases, which takes place upon incompatible pathogen infection (Lamb and Dixon, 1997; Foyer and Noctor, 2003). Oxidative burst is responsible for activation of ROS production in the apoplast, which further triggers disease resistance. In another system, endogenous molecules such as ATP and oligosaccharides released from cell walls upon cell rupture and pathogen infection are sensed by nearby cells. The recognition of these molecules (termed ‘danger-associated molecular patterns’) leads to intensification of plant defence response (Schwessinger and Zipfel, 2008; Macho and Zipfel, 2014). The possible involvement of OsORAP1 in cell death under ozone stress could be interpreted as reminiscent of this intensification of signals under pathogen infection. Since plants have not experienced high ozone concentration in their evolutionary history, this signal-amplification mechanism that OsORAP1 possesses would not have been specifically developed for ozone stress tolerance. Rather plants may have developed the OsORAP1 protein to cope with invading pathogens through induction of resistance and confinement of pathogens by cell death, which has unintentionally led to decreased ozone stress tolerance. Indeed, blast fungus infection led to contrasting expression patterns of *OsORAP1* in two rice lines showing different susceptibility (Inoue *et al.*, personal communication). The tolerant line showed earlier but somewhat weaker induction of *OsORAP1* compared with the susceptible line, which strengthens the potential role of OsORAP1 in blast fungus resistance. Mittler (2002) noted that plants decrease rather than increase the antioxidant capacity during biotic stress to enable the cells to trigger the defence response. Ueda *et al.* (2013) also observed that the gene expression levels of antioxidant enzymes decreased under ozone stress, contrary to the expectation. These observations demonstrate common responses under ozone stress and pathogen infection, where plants amplify oxidative stress (feed-forward regulation), which might be advantageous for pathogen tolerance but disadvantageous for ozone stress tolerance. However, this is not the only explanation for ozone stress tolerance, since the quantitative trait loci (QTLs) detected for leaf bronzing score (LBS) under ozone stress (Chapter 4) do not co-localize with the ones for pathogen resistance in rice (Bandillo *et*

*al.*, 2013). Altogether, it would be tempting to investigate the expression pattern of *OsORAP1* on sub-tissue level and examine pathogen resistance (*e.g.* against rice blast fungus) in the lines used in the study, as well as elucidating the molecular function of *OsORAP1*.

In Chapter 4, identification of chromosomal loci responsible for major traits under ozone stress was conducted by using 32,175 single-nucleotide polymorphism (SNP) markers through a genome-wide association study (GWAS). This marker number is by far larger compared with, for example, 3,267 restriction fragment length polymorphism markers provided for Nipponbare/Kasalath bi-parental mapping population, which can be used for classical QTL studies. This number, together with the higher recombination rate in the diverse population, proved higher resolution in GWAS. The overall significance (as judged by  $-\log_{10}P$  values) was largely comparable to previous GWASs using the same population (Zhao *et al.*, 2011; Famoso *et al.*, 2011). In some previous cases GWAS peaks showed quite high  $-\log_{10}P$  values, for example, for flowering time and seed length, where a few genes dominate the phenotype (Zhao *et al.*, 2011). Multiple peaks observed in the current study, together with moderate  $-\log_{10}P$  values, therefore implied that the phenotypes under ozone stress are controlled by many genetic factors. Moreover, some loci were shown to have pleiotropic effects. For example, a locus on chromosome 1 (42.38 to 42.43 Mb) was identified for five different traits (Table S11). These results demonstrated complex genetic regulation of traits under ozone stress in rice.

The subsequent attempt to identify a candidate gene was conducted by analysing linkage disequilibrium (LD) between sequence polymorphisms within candidate genes and detected SNP markers. This ‘GWAS and local LD analysis by re-sequencing’ approach is a major strategy of GWAS in human genetics (Service *et al.*, 2014) and model plant species *Arabidopsis* (*Arabidopsis thaliana*) (Sterken *et al.*, 2012; Barboza *et al.*, 2013; Motte *et al.*, 2014), but few studies attempted this approach in rice (such as the one by Chen *et al.* (2014)). In the current study, this approach identified strong LD between the significant SNP markers and amino acid substitutions in *RING*. This local LD analysis approach, as well as GWAS, is quite effective for plant species, since the same population can be used for many mapping studies. The currently available comparative genome sequence databases (*e.g.* *Arabidopsis* 1001 genomes project and rice TASUKE genome browser; Weigel and Mott, 2009; Kumagai *et al.*, 2013) and efforts for genome sequencing in other plant species will probably reinforce

this approach and support the identification of causative polymorphisms for a certain trait after GWAS.

The subpopulations *temperate japonica* and *indica* showed significantly lower LBS, showing higher tolerance to ozone in terms of leaf visible symptom formation. *Temperate japonica* and *indica* subpopulations have different domestication history (Fig. 5-1), and these are the two subpopulations which have the lowest level of relatedness among five subpopulations ( $F_{st}^{\dagger} = 0.45$  between *temperate japonica* and *indica*, as opposed to  $F_{st} = 0.20$  between *temperate japonica* and *tropical japonica*; Garris *et al.*, 2005). This suggests that ozone tolerance (*i.e.* less leaf visible symptom formation) was not acquired during domestication or subpopulation divergence. *Temperate japonica* and *indica* subpopulations contain a large number of accessions from East and Southeast Asia (Table 5-1). Therefore it is conceivable that ozone tolerance was conferred to *temperate japonica* and *indica* subpopulations due to the selection pressure related to geography or climate. It is tempting to speculate that the formation of leaf visible symptoms is linked to a certain trait favourable in East and Southeast Asia. In natural vegetation, evidence for natural selection of ozone stress tolerance has been observed, as shown by correlation between local ozone concentration and ozone stress tolerance of *Plantago* species (Lyons *et al.*, 1997). However, in the case of the mapping population used in the current study, the possibility that local ozone concentration has affected selection cannot be confirmed. This is because the cultivars used in the study are mostly traditional cultivars, which were developed before the tropospheric ozone concentrations became problematic in East and Southeast Asian countries (since the late 20th century; Vingarzan 2004).

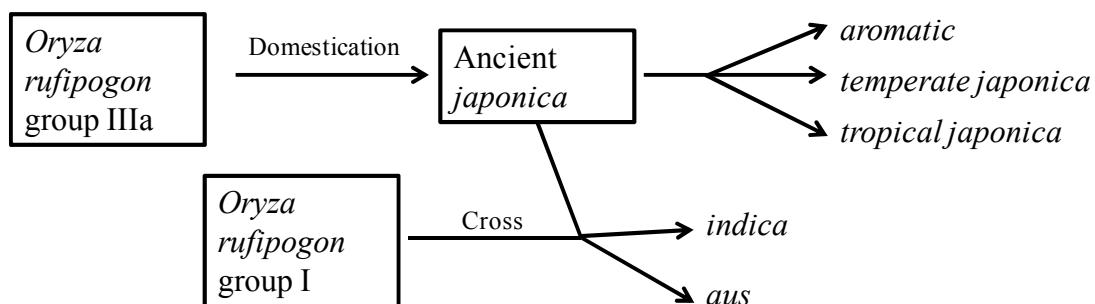


Figure 5-1: History of subpopulation divergence of rice (modified from Huang *et al.*, 2012, Figure 4).

<sup>†</sup>  $F_{st}$  is an index showing population differentiation between two groups based on genetic variability. It ranges from 0 to 1, and higher value is associated with lower relatedness (Kovach *et al.*, 2007).



Table 5-1: Origin of accessions in each subpopulation in the mapping population used in Chapter 4.

Subpopulation	Accessions	Major origin (and number of accessions)
<i>Admix</i>	48	United States (8), Madagascar (4), Bangladesh/Japan/Australia (each 3)
<i>Aromatic</i>	12	Iran (5), India (2)
<i>Aus</i>	55	Bangladesh (20), India (16), Pakistan (5)
<i>Indica</i>	74	China (including Hong Kong) (19), Taiwan (9), India (8), Philippines (5), Vietnam (4)
<i>Temperate japonica</i>	69	Japan (12), China (5), Spain/Taiwan/Korea (each 4)
<i>Tropical japonica</i>	70	United States (15), Indonesia (5), Brazil/Philippines/Cote D'Ivoire (each 4)

The mapping population consisting of 328 rice accessions was categorized into subpopulations. The number of the accessions in each subpopulation and main countries of origins are shown. The number in the parenthesis is the number of accession from the country.

The previously identified QTLs (*OzT8* for biomass production and *OzT9* for leaf visible symptoms) were not clearly detected in the current study (Fig. 5-2). A small peak was observed outside the *OzT8* region from the Manhattan plot for relative DW (Fig. 5-2A), and a very low peak value was observed within the *OzT9* region for square-root transformed LBS (Fig. 5-2B). This type of disagreement between the result of QTL study and that of GWAS has been also documented in other studies (Famoso *et al.*, 2011). Several possibilities can be considered for it. The most likely explanation is the different allele frequency in different mapping populations. In the QTL mapping by bi-parental population, all the possible sequence variations between two parental cultivars can serve as markers. On the other hand, in GWAS (Chapter 4), only SNP markers with more than 10% of minor allele frequency (MAF) were used for the subsequent mapping. Filtering out the SNPs with low MAF is necessary to prevent overestimation of the effect of SNPs with lower MAF and distorted results. Therefore, rare alleles are generally not captured by GWAS. The sequence polymorphisms (between Nipponbare and Kasalath) identified in the previous QTL study might represent rare alleles, which were not included in the mapping by GWAS. An alternative explanation is the different regulation mechanisms for ozone stress tolerance among diverse cultivars. As observed, multiple genetic loci were involved in ozone tolerance. It is conceivable that the previously identified QTLs play a role for the differential tolerance between Nipponbare and Kasalath, but these factors might not be dominant when analysing the broad large genetic variability covered by GWAS. It is possible that different rice cultivars adopt different tolerance mechanisms to ozone,

as observed in other stresses such as iron toxicity (Wu *et al.*, 2014). The last possibility originates from different environmental conditions and ozone treatment schemes that two mapping studies employed. While the mapping of *OzT8* and *OzT9* was conducted at 110 ppb ozone for 12 days using the plants grown in a hydroponic system (Frei *et al.*, 2008), the current study adopted 60 ppb ozone for the whole season using the plants grown in the soil. A QTL identified under a certain condition may not be detected under different environmental condition (QTL x environment interaction), as proposed previously (El-Soda *et al.*, 2014).

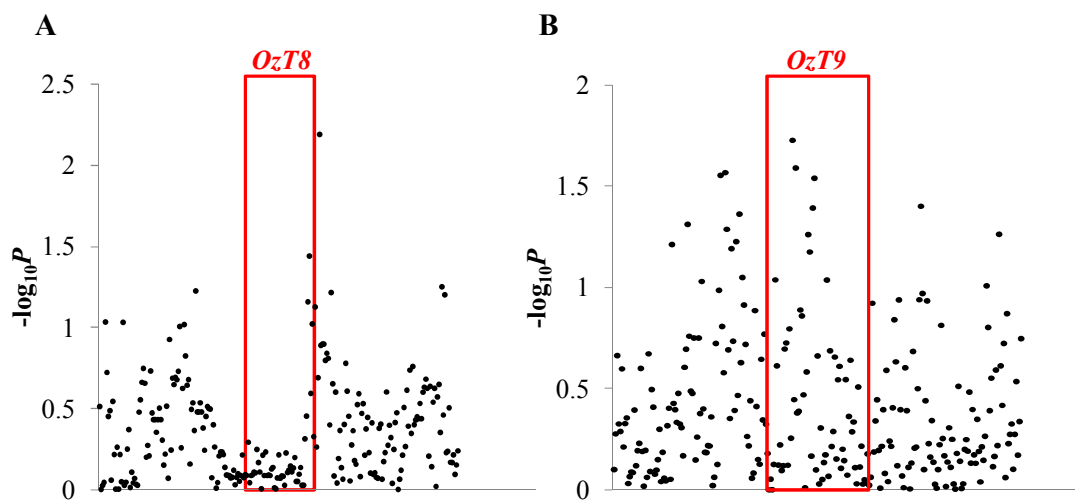


Figure 5-2: Manhattan plots in the neighbouring regions of previously identified QTLs. (A) A plot for relative DW on chromosome 8. (B) A plot for square-root transformed leaf bronzing score on chromosome 9. Previously identified QTLs (Frei *et al.*, 2008) are shown in red colour.

## 2. Future perspectives

Although the current research has partly untangled complex mechanisms and genetic regulation of ozone stress tolerance in rice, several questions remain to be answered. The first question is AsA transport across the plasma membrane. As discussed in Chapter 1, the apoplastic AsA might determine ozone stress tolerance. Since the final step of AsA biosynthesis occurs in mitochondria<sup>‡</sup> (Horemans *et al.*, 2000), it has to be transported to many compartments of the cell, including apoplast. Homologues of mammalian AsA transporter, SVCT, were found in *Arabidopsis* by Maurino *et al.* (2006). These family proteins were named NAT proteins, which has 12 members in *Arabidopsis*. However, the AsA transport activity of AtNAT family has not been confirmed to date. Moreover, several data have suggested absence of AsA transporting activity in AtNAT proteins (Hunt, 2013; Niopek-Witz *et al.*, 2014). Recently, the first AsA transporter in plant species was identified in *Arabidopsis* by Miyaji *et al.* (2015). The identified transporter, AtPHT4;4, is localized at chloroplast envelope and transports AsA from cytosol into the stroma, thereby conferring tolerance to high light stress. Further characterization of PHT family proteins in *Arabidopsis* and other plant species, as well as another independent exploration of AsA transporter (Smirnov *et al.*, 2013, presented in 11th POG conference) might identify the plasma membrane-localized AsA transporter and reveal the significance of AsA transport across the plasma membrane in ozone stress tolerance. The second question is how plant cells sense ozone. There has been a long controversy on this topic as introduced in Chapter 1. Recently Idänheimo *et al.* (2014) experimentally showed the involvement of plasma membrane-localized cysteine-rich receptor-like kinase in apoplastic oxidative stress. This supports the hypothesis that a certain substance in the apoplast is sensed by a receptor on the plasma membrane, enabling the transduction of signals from the apoplast into cytosol via phosphorylation. Indeed this observation does not exclude other mechanisms, such as direct penetration of ROS into the cytosol and involvement of redox sensors. Considering the relatively short duration of time (less than 100 years) for which the plants were exposed to elevated ozone concentrations, it is unlikely that plants possess specific receptor for ozone. It is more probable that plants have sensors which respond to general apoplastic ROS formation, probably via modification of

---

<sup>‡</sup> Alternative pathways have been also proposed. The biosynthetic pathway of ascorbate is still not completely elucidated yet and controversial, as detailed in Linster and Clarke (2008).

apoplastic proteins, and ozone also takes part in this pathway. One of the signal transduction pathways related to apoplastic ROS was recently identified through reverse-genetic screening of ozone sensitive mutants in *Arabidopsis* (Wrzaczek *et al.*, 2009, 2014), and further investigation would unveil other pathways. The last question to be answered is to validate the involvement of the identified candidate genes in ozone tolerance. One of the identified genes for leaf visible symptoms is an E3 ubiquitin ligase *RING* (Chapter 4). The author's own analysis (see the Supplementary Protocol S3) of a previously reported microarray dataset (data adopted from Frei *et al.*, 2010) implied the involvement of ubiquitin-proteasome pathway in the ozone tolerance in rice (Tables 5-2, 5-4, 5-5 and 5-6). In the ozone-tolerant SL41, which produces significantly reduced leaf visible symptoms compared with Nipponbare, the gene ontology<sup>§</sup> (GO) terms of 'protein ubiquitination', 'ubiquitin ligase complex' and 'ubiquitin-protein ligase activity' were highly over-represented among the genes down-regulated compared with Nipponbare. Similarly, the gene set which showed a significant interaction between genotype and treatment (GxT) was enriched in the terms 'protein ubiquitination', 'ubiquitin ligase complex', 'ubiquitin-protein ligase activity' and 'ubiquitin thiolesterase activity'. These results demonstrate differential regulation of ubiquitin-related genes between a tolerant and a susceptible line, supporting the possible involvement and physiological significance of this pathway. The ubiquitin-proteasome pathway plays an important role under pathogen infection and signalling (Trujillo and Shirasu, 2010). Considering the similarity between ozone stress and pathogen infection (discussed in Chapter 1), it can be speculated that the ubiquitin-proteasome pathway partially determines ozone stress tolerance. Similarly, in a comparative microarray study with Nipponbare and SL46 (Chen *et al.*, unpublished data), which maintains higher biomass under ozone stress than Nipponbare, the GO term 'sucrose synthase activity' was enriched in the gene set which showed significant GxT interactions (Tables 5-3, 5-7, 5-8 and 5-9). A sucrose synthase (*LOC\_Os02g58480*) was identified as a candidate gene through GWAS for relative dry weight (biomass production) in Chapter 4. These results strongly suggest that the sucrose metabolism is involved in the biomass production under ozone stress in rice. The elucidation of the significance of these candidate genes as well as physiological studies is to be awaited.

---

<sup>§</sup> Gene ontology shows functional categorization of proteins. It gives hierarchical annotation in each category of 'Biological process', 'Cellular component' and 'Molecular function'.

Table 5-2: Number of differentially regulated genes between Nipponbare and SL41.

Category	Number of probes
Down-regulated in SL41	6630
Up-regulated in SL41	641
GxT interaction	6549
Total	42475

The original data was adopted from Frei *et al.* (2010). Briefly, rice was treated with 120 ppb ozone for 13 days (7 h per day), and total RNA was extracted from shoots. In the original experiment, Nipponbare, SL41 (carrying *OzT9* allele from Kasalath in Nipponbare background) and SL15 (carrying *OzT3* allele from Kasalath in Nipponbare background) were used. Statistical analysis was conducted again using only Nipponbare and SL41 according to Frei *et al.* (2010) (without SL15 in the original file). Raw *P* values of 0.05 were considered significant.

Table 5-3: Number of differentially regulated genes between Nipponbare and SL46.

Category	Number of probes
Down-regulated in SL46	4481
Up-regulated in SL46	1275
GxT interaction	2629
Total	42475

The microarray data was kindly provided by Dr. Chen, Dr. Pariasca-Tanaka and Prof. Dr. Wissuwa (JIRCAS, Tsukuba, Japan). Rice was treated with 100 ppb ozone for 25 days (7 h per day), and total RNA was extracted from the second most recently expanded leaf. Nipponbare and SL46 (carrying *OzT8* allele from Kasalath in Nipponbare background) were used. Statistical analysis was conducted according to Frei *et al.* (2010). Raw *P* values of 0.05 were considered significant.

### **3. How can crop breeding contribute to future global food security?**

Since the middle of the last century, crop breeding has contributed to a huge extent to the global food supply. In case of rice, a historical epoch termed ‘green revolution’ took place in the 1960s. Through the introduction of a semidwarf gene *sd-1* (Spielmeyer *et al.*, 2002), which led to less production of straw and more grain yield, breeding programmes have drastically increased the rice yield during the green revolution (Khush, 2001). Evenson and Gollin (2003) estimated that crop production in the developing countries would be less than 80% and the price would have risen by 35 to 66% if there had been no crop breeding since 1965. This would have decreased the calorie intake per capita by more than 10% in developing countries (Evenson and Gollin, 2003). These data clearly demonstrate that crop breeding plays an outstanding role in ensuring food supply for a growing world population (Fig. 5-3). The improvement of crops is still ongoing and contributing to the rise in crop yields. Recently, a novel submergence tolerant gene (*SUB1*) was introduced into popular rice varieties (Ismail *et al.*, 2013). These submergence-tolerant rice (or ‘snorkel’ rice) cultivars are already commercially distributed, and proved to achieve 1 to 3 t/ha increase of grain yield after flooding as compared with conventional cultivars (Ismail *et al.*, 2013). Another example is the breeding for tolerance to phosphorus deficiency (-P). Phosphorus deficiency is one of the major nutrient deficiencies in soil, which leads to 50 to 70% of grain yield loss compared with well-fertilized soil (Gamuyao *et al.*, 2012). Introduction of a single gene (*PSTOL1*) that -P intolerant modern cultivars do not possess, enhanced the grain yield under -P condition by 60% compared with the background cultivar lacking the *PSTOL1* gene (Gamuyao *et al.*, 2012). This value corresponds to a mitigation of the effect of -P by around 40 to 50%. As shown by these examples, improvement of crops by breeding is still effective and much potential is left for further yield increase.

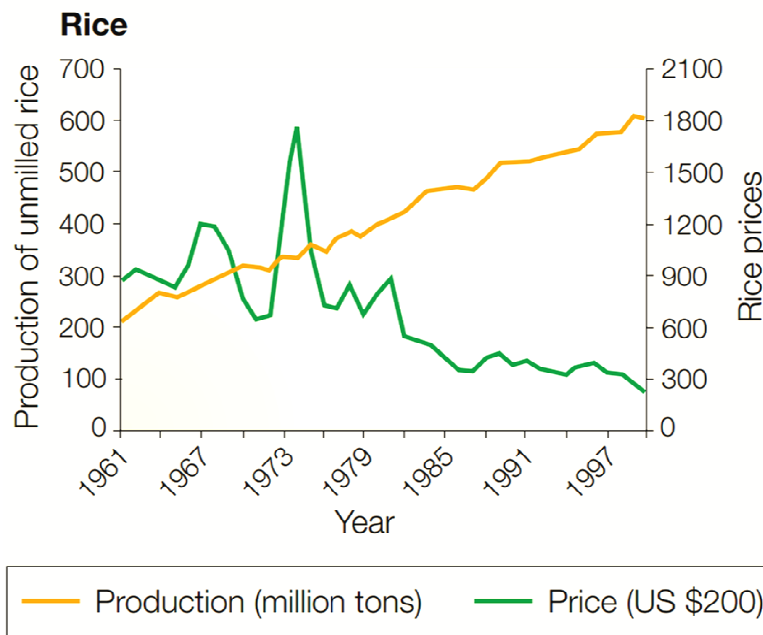


Figure 5-3: Transition of production and prices of rice since 1961 (adopted from Khush, 2001).

Isolation of the causative genes for a certain trait is desirable to break the linkage between the identified QTL and unfavourable genes (Jiang and Zeng, 1995; Alpuerto *et al.*, 2009). In other words, transferring large chromosomal fragments in the breeding process might introduce genes which cause negative effects. Besides, identifying the gene will deepen the understanding of the regulation of traits. The identification of the gene underlying a certain trait would be followed by marker-assisted breeding, which is considered faster and more precise compared with the conventional breeding (Alpuerto *et al.*, 2009). In the current study, suppressed expression of *OsORAPI* was shown to ameliorate leaf visible symptoms under ozone stress. Although the involvement of other genes cannot be ruled out, a breeding programme targeting the *ORAPI* locus in other plant species might be beneficial in the production of, for example, leafy vegetables and ornamental crops. It might also have potential roles in preventing loss of photosynthetically active leaf area, thereby contributing to the overall biomass production and crop yield (Fiscus *et al.*, 2005).

Considering the significant damage of ozone stress and effectiveness of crop breeding, a crucial question to be addressed is how beneficial the crop breeding targeting elevated tropospheric ozone is. To date, no gene has been experimentally confirmed to

affect the relative grain yield under ozone stress. Taking into account the positive correlation between the shoot dry weight and total grain yield in Chapter 4 ( $P < 0.001$ , Fig. 5-3), it seems crucial to maintain vigorous shoot growth under ozone stress to maintain the yield. Therefore, currently-ongoing efforts to isolate single gene loci responsible for biomass production under ozone stress, as well as the characterization of previously suggested candidate gene for total grain yield, *APO1* (Tsukahara *et al.*, 2013), will have a significant impact on the supply of rice in the severely affected area. The SL46 rice line, which carries the biomass-related QTL *OzT8* from the tolerant cultivar Kasalath in the genetic background of the susceptible cultivar Nipponbare, is less vulnerable to ozone stress than Nipponbare in terms of biomass production (Chen *et al.*, 2013; Wang *et al.*, 2014). In the study by Chen *et al.*, SL46 mitigated the effect of ozone by around 30% (absolute value). Moreover, pyramiding previously identified two QTLs (*OzT8* and *OzT9*) mitigated the effect of ozone by around 40% in shoot biomass production (Wang *et al.*, 2014), demonstrating a positive additive effect of genetic factors for future crop improvement. If this value is applied to the regression equation between the relative shoot dry weight ( $X$ , %) and relative total panicle weight ( $Y$ , %) from Chapter 4 (Fig. 5-4):  $Y = 0.858 X + 9.864$  ( $R^2 = 0.35$ ), an increase of 40% of shoot DW production would lead to around 34% more total panicle weight production. Taking into account the average rice yield loss estimation of 3.7% (in the year 2000) by elevated tropospheric ozone concentration (Van Dingenen *et al.*, 2009), breeding would suppress the world rice yield loss by 1.3%. This corresponds to the increase of around 7.8 million t of rice production considering the world rice yield in 2000 (600 million t; FAO STAT). Moreover, breeding of other crops such as wheat and maize for ozone tolerance would entail further yield gains. With the increase of ozone concentration and the urgent need to increase crop production in the future, the effect of crop breeding targeting ozone tolerance will be even more tremendous. This will undoubtedly contribute to the global food security in the 21st century.



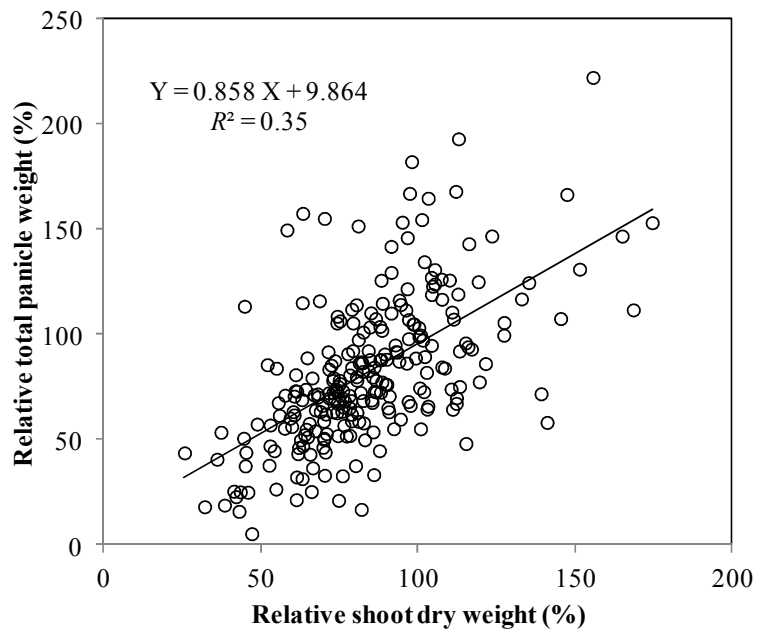


Figure 5-4: Correlation between relative shoot dry weight (x-axis) and relative total panicle weight (y-axis). The data were taken from Chapter 4. A total of 249 data points were plotted after elimination of extreme values. The regression equation and coefficient of determination are shown.

Table 5-4: Enriched gene ontology (GO) terms from the genes down-regulated in SL41.

GO ID	GO Name	Category	Hyper p value
GO:0005975	carbohydrate metabolic process	B	0.000
GO:0006096	glycolysis	B	0.000
GO:0006099	tricarboxylic acid cycle	B	0.000
GO:0006350	transcription	B	0.000
GO:0006468	protein amino acid phosphorylation	B	0.000
GO:0006810	transport	B	0.000
GO:0006886	intracellular protein transport	B	0.000
GO:0006950	response to stress	B	0.000
GO:0008152	metabolic process	B	0.000
GO:0015031	protein transport	B	0.000
GO:0016192	vesicle-mediated transport	B	0.000
GO:0045449	regulation of transcription	B	0.000
GO:0045226	extracellular polysaccharide biosynthetic process	B	0.000
GO:0055114	oxidation reduction	B	0.000
GO:0006694	steroid biosynthetic process	B	0.000
GO:0009058	biosynthetic process	B	0.000
GO:0009734	auxin mediated signaling pathway	B	0.000
GO:0044237	cellular metabolic process	B	0.000
GO:0006032	chitin catabolic process	B	0.001
GO:0006812	cation transport	B	0.001
GO:0006816	calcium ion transport	B	0.001
GO:0016567	protein ubiquitination	B	0.001
GO:0019538	protein metabolic process	B	0.001
GO:0030154	cell differentiation	B	0.001
GO:0015904	tetracycline transport	B	0.002
GO:0009873	ethylene mediated signaling pathway	B	0.002
GO:0030418	nicotianamine biosynthetic process	B	0.002
GO:0006417	regulation of translation	B	0.002
GO:0030001	metal ion transport	B	0.002
GO:0006108	malate metabolic process	B	0.003
GO:0007047	cellular cell wall organization	B	0.003
GO:0006568	tryptophan metabolic process	B	0.003
GO:0001539	ciliary or flagellar motility	B	0.003
GO:0006835	dicarboxylic acid transport	B	0.004
GO:0005737	cytoplasm	C	0.000
GO:0005794	Golgi apparatus	C	0.000
GO:0016020	membrane	C	0.000
GO:0030117	membrane coat	C	0.000
GO:0030126	COPI vesicle coat	C	0.000
GO:0031410	cytoplasmic vesicle	C	0.000
GO:0000151	ubiquitin ligase complex	C	0.000
GO:0016021	integral to membrane	C	0.000
GO:0005789	endoplasmic reticulum membrane	C	0.000
GO:0005743	mitochondrial inner membrane	C	0.000
GO:0005761	mitochondrial ribosome	C	0.001
GO:0048046	apoplast	C	0.001
GO:0009288	bacterial-type flagellum	C	0.002
GO:0009514	glyoxysome	C	0.002
GO:0005759	mitochondrial matrix	C	0.002
GO:0012511	monolayer-surrounded lipid storage body	C	0.003

Table 5-4 (continued)

GO ID	GO Name	Category	Hyper p value
GO:0000166	nucleotide binding	M	0.000
GO:0000287	magnesium ion binding	M	0.000
GO:0003700	sequence-specific DNA binding transcription factor activity	M	0.000
GO:0003824	catalytic activity	M	0.000
GO:0004672	protein kinase activity	M	0.000
GO:0004674	protein serine/threonine kinase activity	M	0.000
GO:0004713	protein tyrosine kinase activity	M	0.000
GO:0004721	phosphoprotein phosphatase activity	M	0.000
GO:0004872	receptor activity	M	0.000
GO:0005488	binding	M	0.000
GO:0005509	calcium ion binding	M	0.000
GO:0005515	protein binding	M	0.000
GO:0005524	ATP binding	M	0.000
GO:0016301	kinase activity	M	0.000
GO:0016491	oxidoreductase activity	M	0.000
GO:0016740	transferase activity	M	0.000
GO:0016757	transferase activity, transferring glycosyl groups	M	0.000
GO:0016758	transferase activity, transferring hexosyl groups	M	0.000
GO:0016787	hydrolase activity	M	0.000
GO:0030145	manganese ion binding	M	0.000
GO:0043565	sequence-specific DNA binding	M	0.000
GO:0046872	metal ion binding	M	0.000
GO:0003854	3-beta-hydroxy-delta5-steroid dehydrogenase activity	M	0.000
GO:0005215	transporter activity	M	0.000
GO:0005388	calcium-transporting ATPase activity	M	0.000
GO:0008831	dTDP-4-dehydrothiamine reductase activity	M	0.000
GO:0016616	oxidoreductase activity, acting on the CH-OH group of donors, NAD or NADP as acceptor	M	0.000
GO:0016769	transferase activity, transferring nitrogenous groups	M	0.000
GO:0016776	phosphotransferase activity, phosphate group as acceptor	M	0.000
GO:0016857	racemase and epimerase activity, acting on carbohydrates and derivatives	M	0.000
GO:0016887	ATPase activity	M	0.000
GO:0017111	nucleoside-triphosphatase activity	M	0.000
GO:0030955	potassium ion binding	M	0.000
GO:0004568	chitinase activity	M	0.000
GO:0016798	hydrolase activity, acting on glycosyl bonds	M	0.000
GO:0030528	transcription regulator activity	M	0.000
GO:0015085	calcium ion transmembrane transporter activity	M	0.000
GO:0008233	peptidase activity	M	0.000
GO:0019201	nucleotide kinase activity	M	0.001
GO:0031072	heat shock protein binding	M	0.001
GO:0004842	ubiquitin-protein ligase activity	M	0.001
GO:0004022	alcohol dehydrogenase (NAD) activity	M	0.001
GO:0008324	cation transmembrane transporter activity	M	0.001
GO:0003995	acyl-CoA dehydrogenase activity	M	0.001
GO:0015520	tetracycline:hydrogen antiporter activity	M	0.001
GO:0003743	translation initiation factor activity	M	0.001
GO:0004096	catalase activity	M	0.002
GO:0004579	dolichyl-diphosphooligosaccharide-protein glycotransferase activity	M	0.002
GO:0030410	nicotianamine synthase activity	M	0.002
GO:0004743	pyruvate kinase activity	M	0.002

Table 5-4 (continued)

GO ID	GO Name	Category	Hyper p value
GO:0005529	sugar binding	M	0.002
GO:0043169	cation binding	M	0.002
GO:0003924	GTPase activity	M	0.002
GO:0016847	1-aminocyclopropane-1-carboxylate synthase activity	M	0.003
GO:0030170	pyridoxal phosphate binding	M	0.003
GO:0015662	ATPase activity, coupled to transmembrane movement of ions, phosphorylative mechanism	M	0.003
GO:0017153	sodium:dicarboxylate symporter activity	M	0.004
GO:0008236	serine-type peptidase activity	M	0.004
GO:0004364	glutathione transferase activity	M	0.004
GO:0005506	iron ion binding	M	0.005
GO:0004553	hydrolase activity, hydrolyzing O-glycosyl compounds	M	0.005
GO:0004966	galanin receptor activity	M	0.006
GO:0019205	nucleobase, nucleoside, nucleotide kinase activity	M	0.006
GO:0015079	potassium ion transmembrane transporter activity	M	0.006
GO:0009055	electron carrier activity	M	0.007

Gene ontology (GO) enrichment analysis was conducted from a set of genes which showed significantly lower expression (according to raw  $P$  values) in SL41 compared with Nipponbare. A total of 6630 probes were subjected to GO enrichment analysis using Rice Oligonucleotide Array Database (<http://www.ricearray.org/index.shtml>, as of July 2014). The output raw Hyper  $P$  values were corrected to false discovery rate (FDR) according to Benjamini and Hochberg (1995), and  $FDR < 0.05$  was considered as significant. Only over-represented GO terms are shown together with GO ID, category and Hyper  $P$  value. The category classification is as follows: B, biological process; C, cellular component; and M, molecular function.

Table 5-5: Enriched gene ontology (GO) terms from the genes up-regulated in SL41.

GO ID	GO Name	Category	Hyper p value
GO:0006635	fatty acid beta-oxidation	B	0.000
GO:0055114	oxidation reduction	B	0.000
GO:0008152	metabolic process	B	0.000
GO:0005975	carbohydrate metabolic process	B	0.000
GO:0010152	pollen maturation	B	0.000
GO:0042128	nitrate assimilation	B	0.001
GO:0006631	fatty acid metabolic process	B	0.001
GO:0006857	oligopeptide transport	B	0.001
GO:0006810	transport	B	0.002
GO:0009737	response to abscisic acid stimulus	B	0.004
GO:0006979	response to oxidative stress	B	0.005
GO:0006281	DNA repair	B	0.006
GO:0005578	proteinaceous extracellular matrix	C	0.001
GO:0005777	peroxisome	C	0.001
GO:0016020	membrane	C	0.002
GO:0005506	iron ion binding	M	0.000
GO:0009055	electron carrier activity	M	0.000
GO:0016491	oxidoreductase activity	M	0.000
GO:0016787	hydrolase activity	M	0.000
GO:0016798	hydrolase activity, acting on glycosyl bonds	M	0.000
GO:0020037	heme binding	M	0.000
GO:0005215	transporter activity	M	0.000
GO:0046872	metal ion binding	M	0.000
GO:0004867	serine-type endopeptidase inhibitor activity	M	0.000
GO:0005509	calcium ion binding	M	0.000
GO:0003997	acyl-CoA oxidase activity	M	0.000
GO:0050660	FAD or FADH2 binding	M	0.000
GO:0043169	cation binding	M	0.001
GO:0004497	monooxygenase activity	M	0.002
GO:0051539	4 iron, 4 sulfur cluster binding	M	0.003
GO:0005201	extracellular matrix structural constituent	M	0.003
GO:0004553	hydrolase activity, hydrolyzing O-glycosyl compounds	M	0.003
GO:0030414	peptidase inhibitor activity	M	0.004

Gene ontology (GO) enrichment analysis was conducted from a set of genes which showed significantly higher expression (according to raw *P* values) in SL41 compared with Nipponbare. A total of 641 probes were subjected to GO enrichment analysis using Rice Oligonucleotide Array Database (<http://www.ricearray.org/index.shtml>, as of July 2014). The output raw Hyper *P* values were corrected to false discovery rate (FDR) according to Benjamini and Hochberg (1995), and  $FDR < 0.05$  was considered as significant. Only over-represented GO terms are shown together with GO ID, category and Hyper *P* value. The category classification is as follows: B, biological process; C, cellular component; and M, molecular function.

Table 5-6: Enriched gene ontology (GO) terms from the genes showing a significant interaction between genotype and treatment between Nipponbare and SL41.

GO ID	GO Name	Category	Hyper p value
GO:0005975	carbohydrate metabolic process	B	0.000
GO:0006099	tricarboxylic acid cycle	B	0.000
GO:0006350	transcription	B	0.000
GO:0006468	protein amino acid phosphorylation	B	0.000
GO:0006810	transport	B	0.000
GO:0006886	intracellular protein transport	B	0.000
GO:0006950	response to stress	B	0.000
GO:0008152	metabolic process	B	0.000
GO:0015031	protein transport	B	0.000
GO:0016192	vesicle-mediated transport	B	0.000
GO:0045449	regulation of transcription	B	0.000
GO:0055114	oxidation reduction	B	0.000
GO:0006096	glycolysis	B	0.000
GO:0006635	fatty acid beta-oxidation	B	0.000
GO:0019538	protein metabolic process	B	0.000
GO:0042128	nitrate assimilation	B	0.000
GO:0045226	extracellular polysaccharide biosynthetic process	B	0.001
GO:0030001	metal ion transport	B	0.001
GO:0006812	cation transport	B	0.001
GO:0015904	tetracycline transport	B	0.001
GO:0016567	protein ubiquitination	B	0.001
GO:0006835	dicarboxylic acid transport	B	0.002
GO:0006857	oligopeptide transport	B	0.002
GO:0009873	ethylene mediated signaling pathway	B	0.002
GO:0030418	nicotianamine biosynthetic process	B	0.002
GO:0006032	chitin catabolic process	B	0.002
GO:0006417	regulation of translation	B	0.002
GO:0007165	signal transduction	B	0.002
GO:0009058	biosynthetic process	B	0.002
GO:0006108	malate metabolic process	B	0.003
GO:0009734	auxin mediated signaling pathway	B	0.003
GO:0000272	polysaccharide catabolic process	B	0.003
GO:0001539	ciliary or flagellar motility	B	0.003
GO:0009239	enterobactin biosynthetic process	B	0.004
GO:0005737	cytoplasm	C	0.000
GO:0005794	Golgi apparatus	C	0.000
GO:0016020	membrane	C	0.000
GO:0030117	membrane coat	C	0.000
GO:0030126	COPI vesicle coat	C	0.000
GO:0031410	cytoplasmic vesicle	C	0.000
GO:0005789	endoplasmic reticulum membrane	C	0.000
GO:0000151	ubiquitin ligase complex	C	0.000
GO:0005743	mitochondrial inner membrane	C	0.000
GO:0005761	mitochondrial ribosome	C	0.000
GO:0016021	integral to membrane	C	0.001
GO:0009288	bacterial-type flagellum	C	0.001
GO:0005759	mitochondrial matrix	C	0.002
GO:0005777	peroxisome	C	0.006
GO:0048046	apoplast	C	0.007
GO:0000166	nucleotide binding	M	0.000

Table 5-6 (continued)

GO ID	GO Name	Category	Hyper p value
GO:0000287	magnesium ion binding	M	0.000
GO:0003700	sequence-specific DNA binding transcription factor activity	M	0.000
GO:0003824	catalytic activity	M	0.000
GO:0004672	protein kinase activity	M	0.000
GO:0004674	protein serine/threonine kinase activity	M	0.000
GO:0004713	protein tyrosine kinase activity	M	0.000
GO:0005215	transporter activity	M	0.000
GO:0005488	binding	M	0.000
GO:0005509	calcium ion binding	M	0.000
GO:0005515	protein binding	M	0.000
GO:0005524	ATP binding	M	0.000
GO:0016301	kinase activity	M	0.000
GO:0016491	oxidoreductase activity	M	0.000
GO:0016740	transferase activity	M	0.000
GO:0016757	transferase activity, transferring glycosyl groups	M	0.000
GO:0016758	transferase activity, transferring hexosyl groups	M	0.000
GO:0016787	hydrolase activity	M	0.000
GO:0016798	hydrolase activity, acting on glycosyl bonds	M	0.000
GO:0030145	manganese ion binding	M	0.000
GO:0043565	sequence-specific DNA binding	M	0.000
GO:0046872	metal ion binding	M	0.000
GO:0050660	FAD or FADH2 binding	M	0.000
GO:0004721	phosphoprotein phosphatase activity	M	0.000
GO:0004872	receptor activity	M	0.000
GO:0016616	oxidoreductase activity, acting on the CH-OH group of donors, NAD or NADP as acceptor	M	0.000
GO:0004568	chitinase activity	M	0.000
GO:0009055	electron carrier activity	M	0.000
GO:0031072	heat shock protein binding	M	0.000
GO:0016857	racemase and epimerase activity, acting on carbohydrates and derivatives	M	0.000
GO:0008233	peptidase activity	M	0.000
GO:0005506	iron ion binding	M	0.001
GO:0008831	dTDP-4-dehydrothiamine reductase activity	M	0.001
GO:0016887	ATPase activity	M	0.001
GO:0050662	coenzyme binding	M	0.001
GO:0004022	alcohol dehydrogenase (NAD) activity	M	0.001
GO:0030955	potassium ion binding	M	0.001
GO:0003924	GTPase activity	M	0.001
GO:0008324	cation transmembrane transporter activity	M	0.001
GO:0017111	nucleoside-triphosphatase activity	M	0.001
GO:0003995	acyl-CoA dehydrogenase activity	M	0.001
GO:0005388	calcium-transporting ATPase activity	M	0.001
GO:0016776	phosphotransferase activity, phosphate group as acceptor	M	0.001
GO:0030151	molybdenum ion binding	M	0.001
GO:0047800	cysteamine dioxygenase activity	M	0.001
GO:0004842	ubiquitin-protein ligase activity	M	0.001
GO:0015520	tetracycline:hydrogen antiporter activity	M	0.001
GO:0017153	sodium:dicarboxylate symporter activity	M	0.001
GO:0005525	GTP binding	M	0.001
GO:0030528	transcription regulator activity	M	0.001
GO:0043169	cation binding	M	0.001

Table 5-6 (continued)

GO ID	GO Name	Category	Hyper p value
GO:0003997	acyl-CoA oxidase activity	M	0.002
GO:0004579	dolichyl-diphosphooligosaccharide-protein glycotransferase activity	M	0.002
GO:0030410	nicotianamine synthase activity	M	0.002
GO:0046857	oxidoreductase activity, acting on other nitrogenous compounds as donors, with NAD or NADP as acceptor	M	0.002
GO:0004743	pyruvate kinase activity	M	0.002
GO:0030414	peptidase inhibitor activity	M	0.002
GO:0051082	unfolded protein binding	M	0.002
GO:0016769	transferase activity, transferring nitrogenous groups	M	0.002
GO:0015662	ATPase activity, coupled to transmembrane movement of ions, phosphorylative mechanism	M	0.002
GO:0015085	calcium ion transmembrane transporter activity	M	0.003
GO:0016829	lyase activity	M	0.003
GO:0046873	metal ion transmembrane transporter activity	M	0.003
GO:0008667	2,3-dihydro-2,3-dihydroxybenzoate dehydrogenase activity	M	0.003
GO:0008236	serine-type peptidase activity	M	0.003
GO:0004553	hydrolase activity, hydrolyzing O-glycosyl compounds	M	0.004
GO:0004364	glutathione transferase activity	M	0.004
GO:0005529	sugar binding	M	0.004
GO:0019201	nucleotide kinase activity	M	0.004
GO:0004221	ubiquitin thioesterase activity	M	0.004
GO:0020037	heme binding	M	0.004
GO:0015079	potassium ion transmembrane transporter activity	M	0.005
GO:0048037	cofactor binding	M	0.005
GO:0008061	chitin binding	M	0.006
GO:0030170	pyridoxal phosphate binding	M	0.007
GO:0003854	3-beta-hydroxy-delta5-steroid dehydrogenase activity	M	0.007
GO:0008237	metallopeptidase activity	M	0.007
GO:0016705	oxidoreductase activity, acting on paired donors, with incorporation or reduction of molecular oxygen	M	0.007
GO:0016614	oxidoreductase activity, acting on CH-OH group of donors	M	0.007
GO:0051287	NAD or NADH binding	M	0.007
GO:0008312	7S RNA binding	M	0.007
GO:0019904	protein domain specific binding	M	0.007
GO:0008565	protein transporter activity	M	0.008

Gene ontology (GO) enrichment analysis was conducted from a set of genes which showed a significant interaction between treatment (control/ozone) and genotype (Nipponbare/SL41). A total of 6549 probes were subjected to GO enrichment analysis using Rice Oligonucleotide Array Database (<http://www.ricearray.org/index.shtml>, as of July 2014). The output raw Hyper *P* values were corrected to false discovery rate (FDR) according to Benjamini and Hochberg (1995), and FDR < 0.05 was considered as significant. Only over-represented GO terms are shown together with GO ID, category and Hyper *P* value. The category classification is as follows: B, biological process; C, cellular component; and M, molecular function.



Table 5-7: Enriched gene ontology (GO) terms from the genes down-regulated in SL46.

GO ID	GO Name	Category	Hyper p value
GO:0006468	protein amino acid phosphorylation	B	0.000
GO:0006564	L-serine biosynthetic process	B	0.000
GO:0006810	transport	B	0.000
GO:0006915	apoptosis	B	0.000
GO:0006952	defense response	B	0.000
GO:0009698	phenylpropanoid metabolic process	B	0.000
GO:0055114	oxidation reduction	B	0.000
GO:0006754	ATP biosynthetic process	B	0.000
GO:0006811	ion transport	B	0.000
GO:0008152	metabolic process	B	0.000
GO:0009765	photosynthesis, light harvesting	B	0.000
GO:0006350	transcription	B	0.000
GO:0006032	chitin catabolic process	B	0.001
GO:0006355	regulation of transcription, DNA-dependent	B	0.001
GO:0008652	cellular amino acid biosynthetic process	B	0.001
GO:0006559	L-phenylalanine catabolic process	B	0.001
GO:0000160	two-component signal transduction system (phosphorelay)	B	0.001
GO:0009738	abscisic acid mediated signaling pathway	B	0.002
GO:0046854	phosphoinositide phosphorylation	B	0.002
GO:0043687	post-translational protein modification	B	0.002
GO:0051246	regulation of protein metabolic process	B	0.002
GO:0045449	regulation of transcription	B	0.002
GO:0006950	response to stress	B	0.003
GO:0008643	carbohydrate transport	B	0.003
GO:0006544	glycine metabolic process	B	0.004
GO:0006812	cation transport	B	0.004
GO:0016020	membrane	C	0.000
GO:0000166	nucleotide binding	M	0.000
GO:0003824	catalytic activity	M	0.000
GO:0004672	protein kinase activity	M	0.000
GO:0004674	protein serine/threonine kinase activity	M	0.000
GO:0004713	protein tyrosine kinase activity	M	0.000
GO:0005488	binding	M	0.000
GO:0005524	ATP binding	M	0.000
GO:0016301	kinase activity	M	0.000
GO:0016491	oxidoreductase activity	M	0.000
GO:0016740	transferase activity	M	0.000
GO:0017111	nucleoside-triphosphatase activity	M	0.000
GO:0030170	pyridoxal phosphate binding	M	0.000
GO:0046872	metal ion binding	M	0.000
GO:0005215	transporter activity	M	0.000
GO:0015662	ATPase activity, coupled to transmembrane movement of ions, phosphorylative mechanism	M	0.000
GO:0016787	hydrolase activity	M	0.000
GO:0000287	magnesium ion binding	M	0.000
GO:0005506	iron ion binding	M	0.000
GO:0003700	sequence-specific DNA binding transcription factor activity	M	0.000
GO:0004568	chitinase activity	M	0.000
GO:0030145	manganese ion binding	M	0.000
GO:0004617	phosphoglycerate dehydrogenase activity	M	0.001
GO:0016211	ammonia ligase activity	M	0.001

Table 5-7 (continued)

GO ID	GO Name	Category	Hyper p value
GO:0016841	ammonia-lyase activity	M	0.001
GO:0004693	cyclin-dependent protein kinase activity	M	0.001
GO:0008353	RNA polymerase II carboxy-terminal domain kinase activity	M	0.001
GO:0016791	phosphatase activity	M	0.001
GO:0016820	hydrolase activity, acting on acid anhydrides, catalyzing transmembrane movement of substances	M	0.001
GO:0005515	protein binding	M	0.001
GO:0043565	sequence-specific DNA binding	M	0.002
GO:0016616	oxidoreductase activity, acting on the CH-OH group of donors, NAD or NADP as acceptor	M	0.002
GO:0019787	small conjugating protein ligase activity	M	0.002
GO:0004428	inositol or phosphatidylinositol kinase activity	M	0.002
GO:0019904	protein domain specific binding	M	0.002
GO:0004872	receptor activity	M	0.002
GO:0016597	amino acid binding	M	0.003
GO:0016773	phosphotransferase activity, alcohol group as acceptor	M	0.004
GO:0005509	calcium ion binding	M	0.004
GO:0016874	ligase activity	M	0.004

Gene ontology (GO) enrichment analysis was conducted from a set of genes which showed significantly lower expression (according to raw  $P$  values) in SL46 compared with Nipponbare. A total of 4481 probes were subjected to GO enrichment analysis using Rice Oligonucleotide Array Database (<http://www.ricearray.org/index.shtml>, as of July 2014). The output raw Hyper  $P$  values were corrected to false discovery rate (FDR) according to Benjamini and Hochberg (1995), and  $FDR < 0.05$  was considered as significant. Only over-represented GO terms are shown together with GO ID, category and Hyper  $P$  value. The category classification is as follows: B, biological process; C, cellular component; and M, molecular function.

Table 5-8: Enriched gene ontology (GO) terms from the genes up-regulated in SL46.

GO ID	GO Name	Category	Hyper p value
GO:0006412	translation	B	0.000
GO:0007018	microtubule-based movement	B	0.000
GO:0045449	regulation of transcription	B	0.000
GO:0006626	protein targeting to mitochondrion	B	0.001
GO:0045039	protein import into mitochondrial inner membrane	B	0.001
GO:0019953	sexual reproduction	B	0.002
GO:0005622	intracellular	C	0.000
GO:0005840	ribosome	C	0.000
GO:0030529	ribonucleoprotein complex	C	0.000
GO:0042719	mitochondrial intermembrane space protein transporter complex	C	0.001
GO:0005794	Golgi apparatus	C	0.004
GO:0005874	microtubule	C	0.008
GO:0000166	nucleotide binding	M	0.000
GO:0003735	structural constituent of ribosome	M	0.000
GO:0005524	ATP binding	M	0.000
GO:0016787	hydrolase activity	M	0.000
GO:0030528	transcription regulator activity	M	0.000
GO:0003777	microtubule motor activity	M	0.000
GO:0016740	transferase activity	M	0.000
GO:0016757	transferase activity, transferring glycosyl groups	M	0.001
GO:0004553	hydrolase activity, hydrolyzing O-glycosyl compounds	M	0.002
GO:0003774	motor activity	M	0.002
GO:0016301	kinase activity	M	0.002
GO:0005385	zinc ion transmembrane transporter activity	M	0.002
GO:0004031	aldehyde oxidase activity	M	0.003
GO:0016491	oxidoreductase activity	M	0.003
GO:0051537	2 iron, 2 sulfur cluster binding	M	0.003
GO:0017111	nucleoside-triphosphatase activity	M	0.003
GO:0005488	binding	M	0.004
GO:0008199	ferric iron binding	M	0.004
GO:0004347	glucose-6-phosphate isomerase activity	M	0.004
GO:0043169	cation binding	M	0.004
GO:0042626	ATPase activity, coupled to transmembrane movement of substances	M	0.005
GO:0046872	metal ion binding	M	0.006
GO:0046873	metal ion transmembrane transporter activity	M	0.006
GO:0005506	iron ion binding	M	0.006
GO:0008233	peptidase activity	M	0.006

Gene ontology (GO) enrichment analysis was conducted from a set of genes which showed significantly higher expression (according to raw *P* values) in SL46 compared with Nipponbare. A total of 1275 probes were subjected to GO enrichment analysis using Rice Oligonucleotide Array Database (<http://www.ricearray.org/index.shtml>, as of July 2014). The output raw Hyper *P* values were corrected to false discovery rate (FDR) according to Benjamini and Hochberg (1995), and  $FDR < 0.05$  was considered as significant. Only over-represented GO terms are shown together with GO ID, category and Hyper *P* value. The category classification is as follows: B, biological process; C, cellular component; and M, molecular function.

Table 5-9: Enriched gene ontology (GO) terms from the genes showing a significant interaction between genotype and treatment between Nipponbare and SL46.

GO ID	GO Name	Category	Hyper p value
GO:0006468	protein amino acid phosphorylation	B	0.000
GO:0006915	apoptosis	B	0.000
GO:0006952	defense response	B	0.000
GO:0009698	phenylpropanoid metabolic process	B	0.000
GO:0006559	L-phenylalanine catabolic process	B	0.000
GO:0006887	exocytosis	B	0.000
GO:0008152	metabolic process	B	0.000
GO:0006810	transport	B	0.000
GO:0006094	gluconeogenesis	B	0.001
GO:0016998	cell wall macromolecule catabolic process	B	0.001
GO:0015746	citrate transport	B	0.001
GO:0006950	response to stress	B	0.001
GO:0055085	transmembrane transport	B	0.001
GO:0006096	glycolysis	B	0.002
GO:0050832	defense response to fungus	B	0.002
GO:0006334	nucleosome assembly	B	0.002
GO:0006829	zinc ion transport	B	0.003
GO:0009058	biosynthetic process	B	0.003
GO:0006563	L-serine metabolic process	B	0.003
GO:0016020	membrane	C	0.000
GO:0016021	integral to membrane	C	0.000
GO:0000145	exocyst	C	0.000
GO:0005874	microtubule	C	0.003
GO:0000786	nucleosome	C	0.005
GO:0000166	nucleotide binding	M	0.000
GO:0004672	protein kinase activity	M	0.000
GO:0004674	protein serine/threonine kinase activity	M	0.000
GO:0004713	protein tyrosine kinase activity	M	0.000
GO:0004872	receptor activity	M	0.000
GO:0005515	protein binding	M	0.000
GO:0005524	ATP binding	M	0.000
GO:0016301	kinase activity	M	0.000
GO:0017111	nucleoside-triphosphatase activity	M	0.000
GO:0003824	catalytic activity	M	0.000
GO:0016211	ammonia ligase activity	M	0.000
GO:0016841	ammonia-lyase activity	M	0.000
GO:0016887	ATPase activity	M	0.000
GO:0016874	ligase activity	M	0.000
GO:0046872	metal ion binding	M	0.000
GO:0015137	citrate transmembrane transporter activity	M	0.001
GO:0004347	glucose-6-phosphate isomerase activity	M	0.001
GO:0042626	ATPase activity, coupled to transmembrane movement of substances	M	0.001
GO:0030145	manganese ion binding	M	0.001
GO:0022891	substrate-specific transmembrane transporter activity	M	0.002
GO:0000287	magnesium ion binding	M	0.002
GO:0005215	transporter activity	M	0.002
GO:0016740	transferase activity	M	0.003
GO:0005385	zinc ion transmembrane transporter activity	M	0.003
GO:0005488	binding	M	0.003
GO:0016705	oxidoreductase activity, acting on paired donors, with incorporation or reduction of molecular oxygen	M	0.003

Table 5-9 (continued)

GO ID	GO Name	Category	Hyper p value
GO:0004372	glycine hydroxymethyltransferase activity	M	0.004
GO:0016157	sucrose synthase activity	M	0.004
GO:0004568	chitinase activity	M	0.004
GO:0016491	oxidoreductase activity	M	0.004

Gene ontology (GO) enrichment analysis was conducted from a set of genes which showed a significant interaction between treatment (control/ozone) and genotype (Nipponbare/SL46). A total of 2629 probes were subjected to GO enrichment analysis using Rice Oligonucleotide Array Database (<http://www.ricearray.org/index.shtml>, as of July 2014). The output raw Hyper *P* values were corrected to false discovery rate (FDR) according to Benjamini and Hochberg (1995), and  $FDR < 0.05$  was considered as significant. Only over-represented GO terms are shown together with GO ID, category and Hyper *P* value. The category classification is as follows: B, biological process; C, cellular component; and M, molecular function.

## References

- Alpuerto V-LEB, Norton GW, Alwang J, Ismail AM.** 2009. Economic impact analysis of marker-assisted breeding for tolerance to salinity and phosphorous deficiency in rice. *Review of Agricultural Economics* **31**, 779–792.
- Bandillo N, Raghavan C, Muyco PA, et al.** 2013. Multi-parent advanced generation inter-cross (MAGIC) populations in rice: progress and potential for genetics research and breeding. *Rice* **6**, 11.
- Barboza L, Effgen S, Alonso-Blanco C, Kooke R, Keurentjes JJB, Koornneef M, Alcázar R.** 2013. *Arabidopsis* semidwarfs evolved from independent mutations in *GA20ox1*, ortholog to green revolution dwarf alleles in rice and barley. *Proceedings of the National Academy of Sciences of the United States of America* **110**, 15818–15823.
- Benjamini Y, Hochberg Y.** 1995. Controlling the false discovery rate: A practical and powerful approach to multiple testing. *Journal of the Royal Statistical Society. Series B (Methodological)* **57**, 289–300.
- Booker FL, Burkey KO, Jones AM.** 2012. Re-evaluating the role of ascorbic acid and phenolic glycosides in ozone scavenging in the leaf apoplast of *Arabidopsis thaliana* L. *Plant, Cell and Environment* **35**, 1456–1466.
- Chen CP, Frei M, Wissuwa M.** 2011. The *OzT8* locus in rice protects leaf carbon assimilation rate and photosynthetic capacity under ozone stress. *Plant, Cell and Environment* **34**, 1141–1149.
- Chen W, Gao Y, Xie W, et al.** 2014. Genome-wide association analyses provide genetic and biochemical insights into natural variation in rice metabolism. *Nature genetics* **46**, 714–721.
- Dayan J, Dawson CR.** 1976. Substrate specificity of ascorbate oxidase. *Biochemical and Biophysical Research Communications* **73**, 451–458.
- Van Dingenen R, Dentener FJ, Raes F, Krol MC, Emberson L, Cofala J.** 2009. The global impact of ozone on agricultural crop yields under current and future air quality legislation. *Atmospheric Environment* **43**, 604–618.
- El-Soda M, Malosetti M, Zwaan BJ, Koornneef M, Aarts MGM.** 2014. Genotype × environment interaction QTL mapping in plants: lessons from *Arabidopsis*. *Trends in plant science* **19**, 390-398.
- Evenson RE, Gollin D.** 2003. Assessing the impact of the green revolution, 1960 to 2000. *Science* **300**, 758–762.
- Famoso AN, Zhao K, Clark RT, et al.** 2011. Genetic architecture of aluminum tolerance in rice (*Oryza sativa*) determined through genome-wide association analysis and QTL mapping. *PLoS genetics* **7**, e1002221.
- Fiscus EL, Booker FL, Burkey KO.** 2005. Crop responses to ozone: uptake, modes of action, carbon assimilation and partitioning. *Plant, Cell and Environment* **28**, 997–1011.

- Foyer CH, Noctor G.** 2003. Redox sensing and signalling associated with reactive oxygen in chloroplasts, peroxisomes and mitochondria. *Physiologia Plantarum* **119**, 355–364.
- Frei M, Tanaka JP, Chen CP, Wissuwa M.** 2010. Mechanisms of ozone tolerance in rice: characterization of two QTLs affecting leaf bronzing by gene expression profiling and biochemical analyses. *Journal of Experimental Botany* **61**, 1405–1417.
- Frei M, Tanaka JP, Wissuwa M.** 2008. Genotypic variation in tolerance to elevated ozone in rice: dissection of distinct genetic factors linked to tolerance mechanisms. *Journal of Experimental Botany* **59**, 3741–3752.
- Gamuyao R, Chin JH, Pariasca-Tanaka J, et al.** 2012. The protein kinase Pstol1 from traditional rice confers tolerance of phosphorus deficiency. *Nature* **488**, 535–539.
- Garris AJ, Tai TH, Coburn J, Kresovich S, McCouch S.** 2005. Genetic structure and diversity in *Oryza sativa* L. *Genetics* **169**, 1631–1638.
- Horemans N, Foyer CH, Potters G, Asard H.** 2000. Ascorbate function and associated transport systems in plants. *Plant Physiology and Biochemistry* **38**, 531–540.
- Huang X, Kurata N, Wei X, et al.** 2012. A map of rice genome variation reveals the origin of cultivated rice. *Nature* **490**, 497–501.
- Hunt KA.** 2013. Functional characterization of the *Arabidopsis* Nucleobase-Ascorbate Transporter family (NAT) reveals distinct transport profiles and novel substrate specificity. *2013 IPFW Student Research and Creative Endeavor Symposium*. Indiana University Purdue University Fort Wayne.
- Idänheimo N, Gauthier A, Salojärvi J, et al.** 2014. The *Arabidopsis thaliana* cysteine-rich receptor-like kinases CRK6 and CRK7 protect against apoplastic oxidative stress. *Biochemical and Biophysical Research Communications* **445**, 457–462.
- Ismail AM, Singh US, Singh S, Dar MH, Mackill DJ.** 2013. The contribution of submergence-tolerant (Sub1) rice varieties to food security in flood-prone rainfed lowland areas in Asia. *Field Crops Research* **152**, 83–93.
- Jiang C, Zeng Z-B.** 1995. Multiple trait analysis of genetic mapping for quantitative trait loci. *Genetics* **140**, 1111–1127.
- Khush GS.** 2001. Green revolution: the way forward. *Nature Reviews Genetics* **2**, 815–822.
- Kovach MJ, Sweeney MT, McCouch SR.** 2007. New insights into the history of rice domestication. *Trends in genetics* **23**, 578–587.
- Kumagai M, Kim J, Itoh R, Itoh T.** 2013. TASUKE: a web-based visualization program for large-scale resequencing data. *Bioinformatics* **29**, 1806–1808.
- Lamb C, Dixon RA.** 1997. The oxidative burst in plant disease resistance. *Annual review of plant physiology and plant molecular biology* **48**, 251–275.
- Linster CL, Clarke SG.** 2008. L-ascorbate biosynthesis in higher plants: the role of VTC2. *Trends in plant science* **13**, 567–573.

- Luwe MWF, Takahama U, Heber U.** 1993. Role of ascorbate in detoxifying ozone in the apoplast of spinach (*Spinacia oleracea* L.) leaves. *Plant Physiology* **101**, 969–976.
- Lyons TM, Barnes JD, Davison AW.** 1997. Relationships between ozone resistance and climate in European populations of *Plantago major*. *New Phytologist* **136**, 503–510.
- Macho AP, Zipfel C.** 2014. Plant PRRs and the activation of innate immune signaling. *Molecular Cell* **54**, 263–272.
- Maurino VG, Grube E, Zielinski J, Schild A, Fischer K, Flügge U-I.** 2006. Identification and expression analysis of twelve members of the nucleobase-ascorbate transporter (NAT) gene family in *Arabidopsis thaliana*. *Plant and cell physiology* **47**, 1381–1393.
- Mittler R.** 2002. Oxidative stress, antioxidants and stress tolerance. *Trends in plant science* **7**, 405–410.
- Miyaji T, Kuromori T, Takeuchi Y, et al.** 2015. AtPHP4;4 is a chloroplast-localized ascorbate transporter in *Arabidopsis*. *Nature communications* **6**, 5928.
- Moldau H.** 1998. Hierarchy of ozone scavenging reactions in the plant cell wall. *Physiologia Plantarum* **104**, 617–622.
- Motte H, Vercauteren A, Depuydt S, et al.** 2014. Combining linkage and association mapping identifies *RECEPTOR-LIKE PROTEIN KINASE1* as an essential *Arabidopsis* shoot regeneration gene. *Proceedings of the National Academy of Sciences of the United States of America* **111**, 8305–8510.
- Niopek-Witz S, Deppe J, Lemieux MJ, Möhlmann T.** 2014. Biochemical characterization and structure–function relationship of two plant NCS2 proteins, the nucleobase transporters NAT3 and NAT12 from *Arabidopsis thaliana*. *Biochimica et Biophysica Acta* **1838**, 3025–3035.
- Nouchi I, Hayashi K, Hiradate S, Ishikawa S, Fukuoka M, Chen CP, Kobayashi K.** 2012. Overcoming the difficulties in collecting apoplastic fluid from rice leaves by the infiltration-centrifugation method. *Plant and cell physiology* **53**, 1659–1668.
- Schwessinger B, Zipfel C.** 2008. News from the frontline: recent insights into PAMP-triggered immunity in plants. *Current opinion in plant biology* **11**, 389–395.
- Service SK, Teslovich TM, Fuchsberger C, et al.** 2014. Re-sequencing expands our understanding of the phenotypic impact of variants at GWAS loci. *PLoS genetics* **10**, e1004147.
- Smirnoff N, Page M, Ishikawa T.** 2013. Ascorbate and photosynthesis: how does *Arabidopsis* adjust leaf ascorbate concentration to light intensity? *11th International POG Conference (Reactive Oxygen and Nitrogen Species in Plants)*. Warsaw.
- Spielmeier W, Ellis MH, Chandler PM.** 2002. Semidwarf (*sd-1*), “green revolution” rice, contains a defective gibberellin 20-oxidase gene. *Proceedings of the National Academy of Sciences of the United States of America* **99**, 9043–9048.
- Sterken R, Kiekens R, Boruc J, et al.** 2012. Combined linkage and association mapping reveals *CYCD5;1* as a quantitative trait gene for endoreduplication in *Arabidopsis*.



- Proceedings of the National Academy of Sciences of the United States of America* **109**, 4678–4683.
- Trujillo M, Shirasu K.** 2010. Ubiquitination in plant immunity. *Current opinion in plant biology* **13**, 402–408.
- Tsukahara K, Sawada H, Matsumura H, Kohno Y, Tamaoki M.** 2013. Quantitative trait locus analyses of ozone-induced grain yield reduction in rice. *Environmental and Experimental Botany* **88**, 100–106.
- Ueda Y, Uehara N, Sasaki H, Kobayashi K, Yamakawa T.** 2013. Impacts of acute ozone stress on superoxide dismutase (SOD) expression and reactive oxygen species (ROS) formation in rice leaves. *Plant Physiology and Biochemistry* **70**, 396–402.
- Vingarzan R.** 2004. A review of surface ozone background levels and trends. *Atmospheric Environment* **38**, 3431–3442.
- Wang Y, Yang L, Höller M, Zaisheng S, Pariasca-Tanaka J, Wissuwa M, Frei M.** 2014. Pyramiding of ozone tolerance QTLs *OzT8* and *OzT9* confers improved tolerance to season-long ozone exposure in rice. *Environmental and Experimental Botany* **104**, 26–33.
- Weigel D, Mott R.** 2009. The 1001 genomes project for *Arabidopsis thaliana*. *Genome biology* **10**, 107.
- Wrzaczek M, Brosché M, Kollist H, Kangasjärvi J.** 2009. *Arabidopsis* GRI is involved in the regulation of cell death induced by extracellular ROS. *Proceedings of the National Academy of Sciences of the United States of America* **106**, 5412–5417.
- Wrzaczek M, Vainonen J, Stael S, et al.** 2014. GRIM REAPER peptide binds to receptor kinase PRK5 to trigger cell death in *Arabidopsis*. *The EMBO Journal* **34**, 55–66.
- Wu L-B, Shhadi MY, Gregorio G, Matthus E, Becker M, Frei M.** 2014. Genetic and physiological analysis of tolerance to acute iron toxicity in rice. *Rice* **7**, 8.
- Zhang Y.** 2008. I-TASSER server for protein 3D structure prediction. *BMC Bioinformatics* **9**, 40.
- Zhao K, Tung C-W, Eizenga GC, et al.** 2011. Genome-wide association mapping reveals a rich genetic architecture of complex traits in *Oryza sativa*. *Nature communications* **2**, 467.

# **‘Genetic and physiological factors of ozone tolerance in rice (*Oryza sativa* L.)’**

## **Summary of the thesis**

### ***Introduction***

Anthropogenic gas emission has led to a significant increase of tropospheric ozone. The ozone concentration in the troposphere has reached more than four times that the level of the beginning of the 20th century in some areas (Vingarzan, 2004; Yamaji *et al.*, 2006). Ozone has high reactivity and oxidation power, which cause severe damage to living organisms. It also adversely affects crop production and food supply. Global crop losses caused by elevated tropospheric ozone sums up to more than 10 billion USD annually (Van Dingenen *et al.*, 2009). The ozone concentration is predicted to increase further in the future in many parts of the world (Lei *et al.*, 2013). To cope with the food shortage caused by further growth of global population and shrinkage in the arable area, it is of paramount importance to get insight into the mechanisms of ozone tolerance and adapt crops to the elevated ozone concentration.

A very important crop contributing to the world food supply is rice (*Oryza sativa* L.). It is cultivated in more than 100 countries around the world and serves as a staple crop for more than half of the world’s population, mainly in Asian countries (Maclean *et al.*, 2002). Currently the annual production of rice is 750 million t, which is the third among cereal crops next to wheat and maize (in 2013, FAO STAT, <http://faostat3.fao.org/home/E>, as of November 2014). However, rice is largely cultivated in areas where high tropospheric ozone is expected, thus suffering from severe damage (Fig. P1). For example, current-level ozone concentration in the troposphere is estimated to cause more than 15% of rice yield losses in some areas (Ainsworth, 2008). Hence, it is urgently needed to elucidate ozone tolerance mechanisms and enhance the stress tolerance in rice. Having been cultivated for more than 10,000 years in diverse geographical and climatic conditions (Kovach *et al.*,

2007), rice has rich genetic diversity, which is shown by an extremely large number of rice germplasm accessions in public seed banks (more than 100,000 types of rice; IRRI website, <http://irri.org/our-work/research/genetic-diversity/international-rice-genebank>, as of November 2014). Moreover, it is the first crop species of which complete genome sequence was determined due to the importance as a crop and relatively small genome size compared with other crop species (International Rice Genome Sequencing Project, 2005). Since then, rice has served as an ideal model crop for functional genomics.



Figure P1: Rice plants affected by elevated tropospheric ozone concentration. Visible symptoms are observed on the leaf blades. The photo was taken in Yangzhou, China, in September 2013.

Physiological and genetic studies have been conducted to date to unravel the complex mechanisms of ozone stress tolerance. In plants, ozone causes early senescence, cell death (Fig. P2), growth retardation and altered chemical composition (Fiscus *et al.*, 2005; Wang and Frei, 2011). The toxicity of ozone to plants is ascribed to its ability to produce harmful reactive oxygen species (ROS). Upon intake of ozone to plants through the stomata, ozone is rapidly degraded in the apoplast and produces ROS such as hydrogen peroxide, superoxide anion radical and hydroxyl radical. These ROS damage cells and induce further responses in plants (Kangasjärvi *et al.*, 2005).

Therefore it is important to detoxify the harmful and highly reactive ROS from the apoplast to avoid extensive damage to plants. Plants have an innate system to remove excessive ROS generated by adverse conditions. In this system, ascorbate (AsA) plays a crucial role to accept excessive electron from ROS (Foyer and Halliwell, 1976; Asada, 1999). The apoplast also contains a relatively large amount of AsA (approximately 10% of the total content; Horemans *et al.*, 2000). The apoplastic AsA is considered to react with incoming ozone and serve as the first line of defence against ozone. Previous studies using several approaches illustrated the involvement of apoplastic AsA in ozone tolerance in crop species (Luwe *et al.*, 1993; Turcsányi *et al.*, 2000; Sanmartin *et al.*, 2003; Feng *et al.*, 2010). Through these studies, it was shown that higher apoplastic AsA content is favourable in coping with ozone stress, which is presumably due to a higher capacity to detoxify ozone in the apoplast before it leads to damage. However, in the case of rice, the technique to extract intercellular washing fluid (IWF) (containing apoplastic solutes) was developed only recently due to small stomata size and the hydrophobic layer on the leaf surface (Nouchi *et al.*, 2012). Furthermore, the AsA measurement is quite laborious and requires large amount of samples. This is specifically a hurdle for AsA measurement of IWF since the volume of samples is quite limited. Time-consuming processes of AsA measurement also hindered the measurement of AsA from large numbers of samples due to instability of AsA. Therefore, few studies have attempted to prove the significance of apoplastic AsA under ozone stress in rice.



Figure P2: Necrotic leaf symptoms on a rice leaf (left), chlorotic leaf symptoms and bleaching on a tomato leaf (middle) and a healthy tomato leaf (right).

Forward-genetic approaches have also been used to identify the mechanisms of ozone tolerance. In rice, Frei *et al.* (2008) conducted a QTL mapping under chronic ozone stress using a bi-parental population. This mapping study identified and validated three QTLs for formation of leaf visible symptoms and biomass production. In a following detailed study, Frei *et al.* (2010) suggested a candidate gene conferring ozone stress tolerance in rice, *i.e.* a putative ascorbate oxidase (AO) gene (RAP ID: *Os09g0365900*). This putative AO gene (named *OZONE-RESPONSIVE APOPLASTIC PROTEIN1*; *OsORAPI*) was located in the proximity of the identified QTL *OzT9*, which affected the visible symptoms under ozone stress. Moreover, a chromosomal segment substitution line SL41 (containing *OzT9* allele from the tolerant Kasalath cultivar in the background cultivar Nipponbare) showed significantly lower expression level of *OsORAPI*. Considering lower visible symptoms in SL41, it was hypothesized that the expression level of *OsORAPI* determined the extent of leaf visible symptom by altering apoplastic AsA content and redox status. AO is considered as a ‘mysterious enzyme’ which has puzzled researchers for a long time (Dowdle *et al.*, 2007). The reason is that it oxidizes reduced AsA in the apoplast, which is crucial to detoxify excessive ROS in the apoplast. Therefore this reaction seems ‘wasteful’, considering the physiological importance of reduced AsA as discussed above. Furthermore, the physiological significance of AO family proteins under stress conditions still remained enigmatic.

While the mapping study by Frei *et al.* (2008) successfully identified several QTLs related to ozone stress tolerance, the following questions remained: (i) Are there novel loci affecting ozone stress tolerance?; (ii) Are ozone-related traits other than symptom formation and biomass production also genetically regulated?; and (iii) What are the responsible genetic factors? A key to answer these questions is to conduct a genome-wide association mapping study (GWAS), a technique which was recently established in rice. In GWAS, independent cultivars (usually several dozens to several hundreds) serve as the mapping population. Genetic markers (usually single-nucleotide polymorphism (SNP) markers) are then combined with phenotypic value of each cultivar, through which significant markers can be identified. GWAS has several advantages over the classical bi-parental QTL studies such as exploitation of larger genetic diversity and higher resolution of mapping (Han and Huang, 2013).

In this thesis, the following questions were addressed:

(I) How can we overcome the difficulties in measuring apoplastic AsA in rice leaves? Which method is the most appropriate and enables high-throughput analysis?;

(II) How is the candidate gene, putative AO, involved in ozone stress tolerance in rice? What is the physiological function of the putative AO under ozone stress?;

and

(III) Are there novel genetic loci affecting ozone stress tolerance? How does GWAS perform under ozone stress in rice? Can we identify candidate genes?

### ***Materials and Methods***

#### *(I) Comparison of two AsA measurement methods*

Two previously reported AsA measurement methods, namely a dipyriddy (DPD)-based method (Stevens *et al.*, 2006; Gillespie and Ainsworth, 2007) and an AO-based method (Takahama and Oniki, 1992; Queval and Noctor, 2007) were adjusted to microplate-scale and compared regarding their detection limit, effect of interfering substance and accuracy. The DPD method was based on the reduction of  $\text{Fe}^{3+}$  to  $\text{Fe}^{2+}$  by reduced AsA under acidic conditions.  $\text{Fe}^{2+}$  further reacted with DPD and formed red colour deriving from  $\text{Fe}^{2+}$ -DPD chelate. The quantification was based on a standard curve made with a standard AsA series. In the AO method, direct absorption of reduced AsA (at the wavelength of 265 nm) was monitored and used for the quantification ( $\epsilon = 14.3 \text{ mM}^{-1} \text{ cm}^{-1}$ ). The absorption of sample AsA solution was read before and after addition of AO or dithiothreitol (DTT). AO led to the decrease of the absorption, while DTT increased the absorption, since only reduced AsA has absorption at 265 nm. The content of reduced AsA and dehydroascorbate (DHA) was determined from the absorption shift after the addition of AO/DTT.

Rice shoots and red cabbage (for the assessment of interfering pigments) were used as sample materials. AsA was extracted from the samples using four different extraction solvents (6% (w/v) metaphosphoric acid, 6% (w/v) trichloroacetic acid, 0.2 N HCl and deionized water) and AsA was quantified by both the DPD and the AO method. For the iron inhibition assay, rice shoots stressed with 300 ppm  $\text{FeSO}_4$  was used for the sample. For the assay of apoplastic AsA, IWF was obtained from rice leaves by the infiltration-centrifugation method (Nouchi *et al.*, 2012) and used for the assay.

*(II) Characterization of a rice putative AO gene*

The above-mentioned putative AO gene (*OsORAP1*) was characterized through a reverse-genetic approach. An over-expression line (OE) and a knock-out rice line (KO) were obtained from the Crop Biotech Institute, Kyung Hee University (South Korea). These original seeds were grown and subjected to genotyping using gene-specific primers and a vector primer. Seeds from homozygous plants were used for all the analyses. These homozygous transgenic plants were grown together with the wildtype Dongjin in standard Yoshida hydroponic culture system (Yoshida *et al.*, 1976) in a greenhouse in Bonn. Ozone fumigation was initiated around 3 weeks after the transplanting at the average concentration of 120 ppb for 7 h per day and lasted for 20 days to give chronic stress. Custom-made ozone generators and self-made open-top chambers (Fig. P3A) were used for the experiment. Ozone was blown into perforated plastic tubes with a fan, enabling even distribution of ozone in the chamber. Two independent chambers were prepared both for control and ozone treatments. Growth phenotype (shoot fresh weight and tiller number), leaf visible symptoms as represented by ‘leaf bronzing score (LBS)’ (Wissuwa *et al.*, 2006), gene expression analysis and other biochemical assays were conducted.

Agrobacterium-mediated transformation of *Arabidopsis* (*Arabidopsis thaliana*) and *Nicotiana benthamiana* plants were conducted via gateway cloning system (Curtis and Grossniklaus, 2003) as follows. The coding sequence of *OsORAP1* was cloned into pMDC83 and pMDC32, yielding a fusion protein of OsORAP1-GFP and the original OsORAP1 protein, respectively, under the regulation of cauliflower mosaic virus 35S promoter. OsORAP1-GFP was transiently expressed in *N. benthamiana* epidermal cells by the agroinfiltration method (Shah *et al.*, 2013) and subjected to confocal microscopy after 5 days. Native OsORAP1 protein was introduced into an *Arabidopsis* homozygous AO knock-out line by floral-dip transformation (Clough and Bent, 1998) for complementation analysis. Phylogenetic and sequence analyses were conducted using MEGA5 software (Tamura *et al.*, 2011).

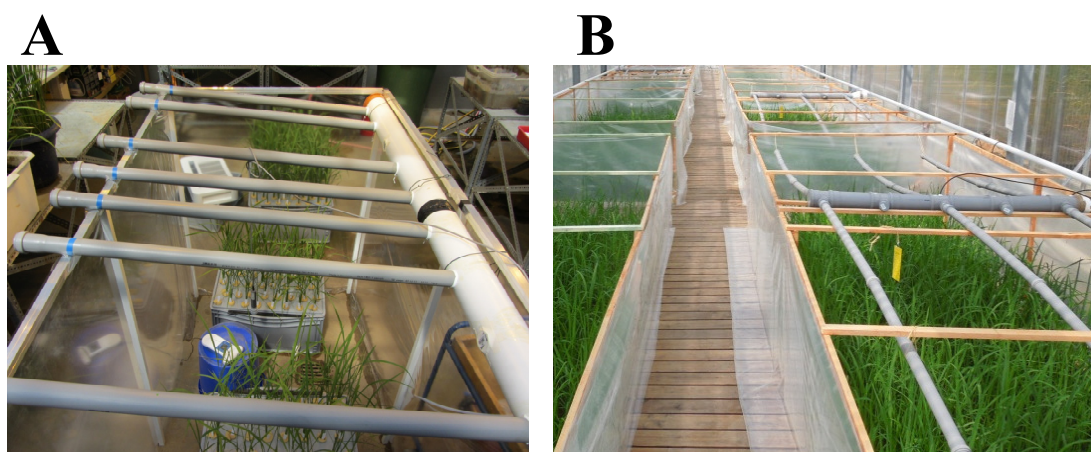


Figure P3: Two different ozone fumigation systems used in the study. (A) Small scale open-top chamber used in the greenhouse in Bonn. The size was typically 1.0 x 1.3 x 1.3 m (width, length and height). (B) Large scale open-top chamber used in the association mapping in Rheinbach. The size was 2.0 x 6.0 x 1.3 m (width, length and height).

### *(III) Genome-wide association study for ozone stress tolerance in rice*

A mapping population consisting of 328 rice accessions from 77 countries was obtained from the International Rice Research Institute (IRRI, Los Baños, The Philippines). The experiment was conducted in Campus Klein-Altendorf of University of Bonn (Rheinbach, Germany). The plants were transplanted into soil and supplied with basic fertilizers (N, P and K) in six different ponds (2 x 6 m), each containing all 328 lines. Three of them were randomly assigned to the ozone treatment, while the other three were subjected to control conditions. Open-top chambers (Fig. P3B) were constructed around each pond, including control chambers to ensure similar microclimate. Ozone was generated with custom-made ozone generators and blown into perforated plastic tubes with a fan. Ozone treatment lasted for 7 h every day (from 9 AM to 4 PM) at a target ozone concentration of 60 ppb. The actually measured ozone concentration in the treatment was 63 ppb, while that of control chambers was 12 ppb. Acute ozone stress (150 ppb, 7 h) was introduced three times during the season. LBS and chlorophyll content (SPAD value) were measured on the 12th week from the transplanting, and all growth traits and lignin content were measured during or after the harvesting in the 21st week. The panicle and shoot samples were dried and the weight was determined. Panicle number and thousand kernel weight were also measured. Lignin content was determined using the thioglycolic acid method from the third fully expanded leaves from the top (Suzuki *et al.*, 2009).



Phenotypic values were loaded into TASSEL 3.0 (Bradbury *et al.*, 2007), together with previously reported > 30,000 SNP markers for the population (Zhao *et al.*, 2011). A mixed linear model was used to eliminate confounding effects due to population structure and obtain more reliable mapping results. Linkage disequilibrium (LD) blocks were determined using Haploview 4.2 (Barret *et al.*, 2005). Genomic sequence data were obtained either from a public comparative rice genome database (TASUKE genome browser; Kumagai *et al.*, 2013) or the author's own sequencing experiment.

## ***Results and Discussion***

### *(I) Comparison of two AsA measurement methods*

Among various extraction solvents, 6% metaphosphoric acid was superior to other solvents in terms of preventing AsA oxidation during storage. When the two analysis methods were compared, the DPD method showed higher accuracy as assessed by higher recovery rate of standard AsA. However, the AO method had lower detection limit (*i.e.* higher sensitivity) than the DPD method. The AO method was more robust when interfering substances (*e.g.* excessive iron or red pigment) existed in the samples. As mentioned above, the AsA content in the apoplast is extremely low and the detection limit is often critical. In this study, reduced AsA was not detected by the DPD method, but the AO method successfully detected it. Therefore it was shown that both the DPD method and the AO method have advantages and disadvantages depending on conditions. Particularly, the AO method turned out to be more suitable for the analysis of apoplastic AsA.

### *(II) Characterization of a rice putative AO gene*

Phylogenetic analysis showed that OsORAP1 was in the same clade as previously reported *Arabidopsis* AO proteins and contained a crucial protein motif possibly determining the activity. However, OsORAP1 was classified into different subclades from proteins of which the presence of AO activity was previously demonstrated. A complementation analysis did not show the existence of AO activity in OsORAP1. A localization study using OsORAP1-GFP fusion protein and *in silico* analysis demonstrated that OsORAP1 was localized in the apoplast. Taken together, it was

concluded that OsORAP1 is an apoplastic enzyme which is classified into a novel class of AO protein with unknown function.

*OsORAP1* expression was strongly induced under ozone stress. Complete absence of the expression in KO and enhanced expression in OE were also confirmed (Fig. P4). KO showed significantly lowered leaf visible symptoms than WT and OE under ozone stress. KO accumulated significantly lower amounts of lipid peroxidation products, which is used as an oxidative stress marker. However, the content of chlorophyll, which reflects the overall stress level in the whole leaf, did not show significant differences between the lines. Moreover, the apoplastic AsA content and redox status did not significantly differ between the lines. These observations suggested that *OsORAP1* is involved in the formation of leaf visible symptoms (*i.e.* cell death formation) rather than attenuation of overall stress level to the plant. This notion was further supported by the expression levels of phytohormone-related genes. Two of jasmonic acid (JA) marker genes, *OsJAZ8* and *OsJAmyb*, showed increased expression levels in KO than WT. JA has been reported to help containment of ozone-induced lesion. Therefore it is likely that *OsORAP1* is involved in leaf visible symptoms partly in co-regulation with phytohormones.

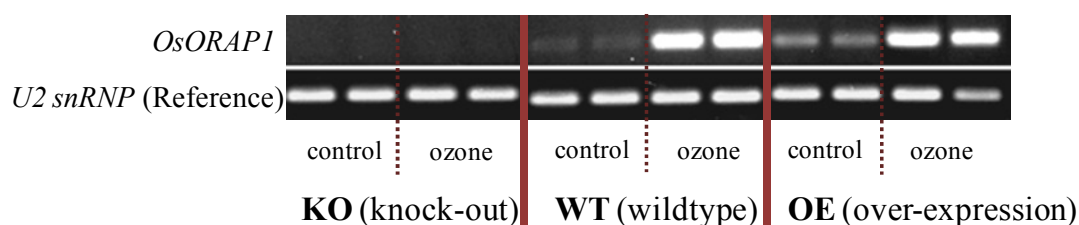


Figure P4: Expression levels of *OsORAP1* under control and ozone stress condition in three lines used in the study. Plants were treated with 150 ppb ozone for 10 days, and RT-PCR was conducted using gene-specific primers (*OsORAP1*-F1/R1). The electrophoresed band of *OsORAP1* is shown with the band of a house-keeping gene (*U2 snRNP*).

Sequence comparison of the *OsORAP1* locus between the susceptible Nipponbare and the tolerant Kasalath cultivars, which served as parental lines for the previous QTL mapping study (Frei *et al.*, 2008), revealed extensive polymorphisms in the promoter region. As discussed above, the expression levels of *OsORAP1* was associated with the extent of leaf visible symptoms. The observed polymorphisms could be responsible for the determination of transcript levels of *OsORAP1*, thus affecting the formation of

symptoms under ozone stress (Frei *et al.*, 2010). Furthermore, tolerant SL41 carried Kasalath allele of *OsORAP1*, which further implied the involvement of *OsORAP1* in the mitigation of leaf visible symptoms under ozone stress in SL41.

In conclusion, *OsORAP1* was shown to positively affect the leaf visible symptom formation. Higher ozone stress tolerance in SL41 might be partly ascribed to different promoter sequence at *OsORAP1* locus compared with Nipponbare.

### *(III) Genome-wide association study for ozone stress tolerance in rice*

Season-long ozone treatment significantly affected all growth/yield traits (plant height, tiller number, dry weight, thousand kernel weight, total panicle weight and single panicle weight). Significant decreases in chlorophyll content (SPAD value) and significant increase in lignin content were observed, which is consistent with previous reports (Shi *et al.*, 2009; Frei *et al.*, 2011; Ainsworth *et al.*, 2014). LBS ranged from 0 to 5.7. Subpopulation analysis revealed that LBS was significantly lower in *indica* and *temperate japonica*.

The subsequent association mapping yielded a total of 16 significant ( $P < 0.0001$ ) SNP markers for the above traits. An LD block containing significant SNP marker(s) was defined as a candidate locus. The candidate loci from the 16 SNP markers contained 195 genes. Among the traits analysed, a detailed sequence analysis was conducted for candidate genes for LBS due to high genetic heritability and significance. Two genes were chosen for further characterization based on their possible involvement in ethylene signalling and the cell death cycle. One of them, an *ethylene-responsive element binding protein (EREBP)* contained eight sequence polymorphisms. However, only one polymorphism in an intron showed strong LD with the detected markers. On the other hand, the other candidate gene, a *really interesting new gene (RING)*, contained 12 polymorphisms. Overall LD with the detected markers was higher in *RING*, and especially, two amino acid mutations in the RING motif (zinc binding domain) showed strong linkage with the detected markers. Therefore, it is highly plausible that *RING* could determine the formation of leaf visible formation under ozone stress in rice, although the involvement of other genes cannot be ruled out. This is supported by the function of an *Arabidopsis RING* homologue, which is involved in signal transduction upon pathogen infection (Lin *et al.*, 2008). Identification of other pathogen-related genes ( $\beta$ -1,3-glucanase and chitinase) on other loci detected for LBS

further supported the similarity between ozone stress and pathogen infection, as demonstrated previously (Ernst *et al.*, 1992; Rao *et al.*, 2000).

Curation of top 50 SNPs (*i.e.* SNPs with the 50 lowest *P* values) from all traits elucidated co-localization of the identified loci. This approach demonstrated pleiotropy of some identified loci. It was also observed that the flowering time (*i.e.* the days before flowering) and relative yield showed significant negative correlation. This raises the possibility that the longer the plant is exposed to ozone before flowering, the more yields are affected. All these results provide useful information for the improvement of crops to cope with elevated ozone concentration in the future.

## References

- Ainsworth EA.** 2008. Rice production in a changing climate: a meta-analysis of responses to elevated carbon dioxide and elevated ozone concentration. *Global Change Biology* **14**, 1642–1650.
- Ainsworth EA, Serbin SP, Skoneczka JA, Townsend PA.** 2014. Using leaf optical properties to detect ozone effects on foliar biochemistry. *Photosynthesis research* **119**, 65–76.
- Asada K.** 1999. The water-water cycle in chloroplasts: Scavenging of Active Oxygens and Dissipation of Excess Photons. *Annual review of plant physiology and plant molecular biology* **50**, 601–639.
- Barrett JC, Fry B, Maller J, Daly MJ.** 2005. Haploview: analysis and visualization of LD and haplotype maps. *Bioinformatics* **21**, 263–265.
- Bradbury PJ, Zhang Z, Kroon DE, Casstevens TM, Ramdoss Y, Buckler ES.** 2007. TASSEL: software for association mapping of complex traits in diverse samples. *Bioinformatics* **23**, 2633–2635.
- Clough SJ, Bent AF.** 1998. Floral dip: a simplified method for *Agrobacterium*-mediated transformation of *Arabidopsis thaliana*. *The Plant Journal* **16**, 735–743.
- Curtis MD, Grossniklaus U.** 2003. A gateway cloning vector set for high-throughput functional analysis of genes in planta. *Plant Physiology* **133**, 462–469.
- Van Dingenen R, Dentener FJ, Raes F, Krol MC, Emberson L, Cofala J.** 2009. The global impact of ozone on agricultural crop yields under current and future air quality legislation. *Atmospheric Environment* **43**, 604–618.
- Dowdle J, Ishikawa T, Gatzek S, Rolinski S, Smirnoff N.** 2007. Two genes in *Arabidopsis thaliana* encoding GDP-L-galactose phosphorylase are required for ascorbate biosynthesis and seedling viability. *The Plant Journal* **52**, 673–689.

- Ernst D, Schraudner M, Langebartels C, Sandermann H.** 1992. Ozone-induced changes of mRNA levels of beta-1,3-glucanase, chitinase and 'pathogenesis-related' protein 1b in tobacco plants. *Plant molecular biology* **20**, 673–682.
- Feng Z, Pang J, Nouchi I, Kobayashi K, Yamakawa T, Zhu J.** 2010. Apoplastic ascorbate contributes to the differential ozone sensitivity in two varieties of winter wheat under fully open-air field conditions. *Environmental Pollution* **158**, 3539–3545.
- Fiscus EL, Booker FL, Burkey KO.** 2005. Crop responses to ozone: uptake, modes of action, carbon assimilation and partitioning. *Plant, Cell and Environment* **28**, 997–1011.
- Foyer CH, Halliwell B.** 1976. The presence of glutathione and glutathione reductase in chloroplasts: A proposed role in ascorbic acid metabolism. *Planta* **133**, 21–25.
- Frei M, Kohno Y, Wissuwa M, Makkar HPS, Becker K.** 2011. Negative effects of tropospheric ozone on the feed value of rice straw are mitigated by an ozone tolerance QTL. *Global Change Biology* **17**, 2319–2329.
- Frei M, Tanaka JP, Chen CP, Wissuwa M.** 2010. Mechanisms of ozone tolerance in rice: characterization of two QTLs affecting leaf bronzing by gene expression profiling and biochemical analyses. *Journal of Experimental Botany* **61**, 1405–1417.
- Frei M, Tanaka JP, Wissuwa M.** 2008. Genotypic variation in tolerance to elevated ozone in rice: dissection of distinct genetic factors linked to tolerance mechanisms. *Journal of Experimental Botany* **59**, 3741–3752.
- Gillespie KM, Ainsworth EA.** 2007. Measurement of reduced, oxidized and total ascorbate content in plants. *Nature protocols* **2**, 871–874.
- Han B, Huang X.** 2013. Sequencing-based genome-wide association study in rice. *Current opinion in plant biology* **16**, 133–138.
- Horemans N, Foyer CH, Potters G, Asard H.** 2000. Ascorbate function and associated transport systems in plants. *Plant Physiology and Biochemistry* **38**, 531–540.
- International Rice Genome Sequencing Project.** 2005. The map-based sequence of the rice genome. *Nature* **436**, 793–800.
- Kangasjärvi J, Jaspers P, Kollist H.** 2005. Signalling and cell death in ozone-exposed plants. *Plant, Cell and Environment* **28**, 1021–1036.
- Kato N, Esaka M.** 1996. cDNA cloning and gene expression of ascorbate oxidase in tobacco. *Plant molecular biology* **30**, 833–837.
- Kovach MJ, Sweeney MT, McCouch SR.** 2007. New insights into the history of rice domestication. *Trends in genetics* **23**, 578–587.
- Kumagai M, Kim J, Itoh R, Itoh T.** 2013. TASUKE: a web-based visualization program for large-scale resequencing data. *Bioinformatics* **29**, 1806–1808.

- Lei H, Wuebbles DJ, Liang X-Z, Olsen S.** 2013. Domestic versus international contributions on 2050 ozone air quality: How much is convertible by regional control? *Atmospheric Environment* **68**, 315–325.
- Lin S-S, Martin R, Mongrand S, Vandenabeele S, Chen K-C, Jang I-C, Chua N-H.** 2008. RING1 E3 ligase localizes to plasma membrane lipid rafts to trigger FB1-induced programmed cell death in Arabidopsis. *The Plant Journal* **56**, 550–561.
- Luwe MWF, Takahama U, Heber U.** 1993. Role of ascorbate in detoxifying ozone in the apoplast of spinach (*Spinacia oleracea* L.) leaves. *Plant Physiology* **101**, 969–976.
- Maclean JL, Dawe DC, Hardy B, Hettel GP.** 2002. *Rice almanac*. 3rd Edition. Wallingford: CABI publishing.
- Nouchi I, Hayashi K, Hiradate S, Ishikawa S, Fukuoka M, Chen CP, Kobayashi K.** 2012. Overcoming the difficulties in collecting apoplastic fluid from rice leaves by the infiltration-centrifugation method. *Plant and cell physiology* **53**, 1659–1668.
- Queval G, Noctor G.** 2007. A plate reader method for the measurement of NAD, NADP, glutathione, and ascorbate in tissue extracts: Application to redox profiling during *Arabidopsis* rosette development. *Analytical Biochemistry* **363**, 58–69.
- Rao MV, Koch JR, Davis KR.** 2000. Ozone: a tool for probing programmed cell death in plants. *Plant molecular biology* **44**, 345–358.
- Sanmartin M, Drogoudi PD, Lyons T, Pateraki I, Barnes J, Kanellis AK.** 2003. Over-expression of ascorbate oxidase in the apoplast of transgenic tobacco results in altered ascorbate and glutathione redox states and increased sensitivity to ozone. *Planta* **216**, 918–928.
- Shah KH, Almaghrabi B, Bohlmann H.** 2013. Comparison of expression vectors for transient expression of recombinant proteins in plants. *Plant Molecular Biology Reporter* **31**, 1529–1538.
- Shi G, Yang L, Wang Y, et al.** 2009. Impact of elevated ozone concentration on yield of four Chinese rice cultivars under fully open-air field conditions. *Agriculture, Ecosystems and Environment* **131**, 178–184.
- Stevens R, Buret M, Garchery C, Carretero Y, Causse M.** 2006. Technique for rapid, small-scale analysis of vitamin C levels in fruit and application to a tomato mutant collection. *Journal of agricultural and food chemistry* **54**, 6159–6165.
- Suzuki S, Suzuki Y, Yamamoto N, Hattori T, Sakamoto M, Umezawa T.** 2009. High-throughput determination of thioglycolic acid lignin from rice. *Plant Biotechnology* **26**, 337–340.
- Takahama U, Oniki T.** 1992. Regulation of peroxidase-dependent oxidation of phenolics in the apoplast of spinach leaves by ascorbate. *Plant and cell physiology* **33**, 379–387.
- Tamura K, Peterson D, Peterson N, Stecher G, Nei M, Kumar S.** 2011. MEGA5: Molecular evolutionary genetics analysis using maximum likelihood, evolutionary

- distance, and maximum parsimony methods. *Molecular Biology and Evolution* **28**, 2731–2739.
- Turcsányi E, Lyons T, Plöchl M, Barnes J.** 2000. Does ascorbate in the mesophyll cell walls form the first line of defence against ozone? Testing the concept using broad bean (*Vicia faba* L.). *Journal of Experimental Botany* **51**, 901–910.
- Vingarzan R.** 2004. A review of surface ozone background levels and trends. *Atmospheric Environment* **38**, 3431–3442.
- Wissuwa M, Ismail AM, Yanagihara S.** 2006. Effects of zinc deficiency on rice growth and genetic factors contributing to tolerance. *Plant Physiology* **142**, 731–741.
- Yamaji K, Ohara T, Uno I, Tanimoto H, Kurokawa J, Akimoto H.** 2006. Analysis of the seasonal variation of ozone in the boundary layer in East Asia using the Community Multi-scale Air Quality model: What controls surface ozone levels over Japan? *Atmospheric Environment* **40**, 1856–1868.
- Yoshida S, Forno DA, Cock JH, Gomez KA.** 1976. *Laboratory Manual for Physiological Studies of Rice*. The International Rice Research Institute. Manila, The Philippines.
- Wang Y, Frei M.** 2011. Stressed food – The impact of abiotic environmental stresses on crop quality. *Agriculture, Ecosystems and Environment* **141**, 271–286.
- Zhao K, Tung C-W, Eizenga GC, et al.** 2011. Genome-wide association mapping reveals a rich genetic architecture of complex traits in *Oryza sativa*. *Nature communications* **2**, 467.

## Appendices

### Supplementary data

#### Chapter 3

Supplementary Protocol S1: Vector construction.....	171
Supplementary Protocol S2: Measurement of enzyme activity.....	174
Supplementary Figure S1: Gene model of <i>OsORAPI</i> .....	176
Supplementary Figure S2: Expression of <i>OsORAPI</i> and MDA content from the Experiment 2.....	177
Supplementary Figure S3: Phylogenetic analysis of clade III from 14 different plant species.....	178
Supplementary Figure S4: Multiple alignment of ascorbate oxidase (AO) and AO-like proteins from <i>Arabidopsis</i> and rice.....	180
Supplementary Figure S5: Transient expression of <i>OsORAPI</i> in <i>Nicotiana benthamiana</i> plant. ....	181
Supplementary Figure S6: Plant shape of three lines.....	182
Supplementary Figure S7: Growth parameters of three lines.....	183
Supplementary Figure S8: Leaf dry weight per area in three lines. ....	184
Supplementary Figure S9: Ascorbate oxidase (AO) activity in the apoplast. ....	185
Supplementary Figure S10: Ascorbate content and redox status of whole tissue extract. .....	186
Supplementary Figure S11: Polyphenol oxidase activity.....	187
Supplementary Figure S12: Expression levels of phytohormone-related genes. ....	188
Supplementary Figure S13: Multiple alignment of <i>OsORAPI</i> locus from four different rice lines.....	190
Supplementary Figure S14: Multiple alignment of OsORAPI protein from four different rice lines. ....	195
Supplementary Figure S15: Expression pattern of <i>OsORAPI</i> in root tissues. ....	196
Supplementary Figure S16: Expression of <i>OsORAPI</i> during seed imbibition. ....	197



Supplementary Table S1: Primers used for the study.....	198
Supplementary Table S2: Expression profile of <i>Arabidopsis</i> AO homologues under several conditions. ....	199
Supplementary Table S3: <i>Cis</i> -elements found only in Nipponbare. ....	200
Supplementary Table S4: <i>Cis</i> -elements found both in Nipponbare and Kasalath. ....	202
Supplementary Table S5: <i>Cis</i> -elements found only in Kasalath. ....	206
Supplementary Table S6: Expression profile of OsORAP1 and Os06g0567900 under several conditions. ....	208
Supplementary Table S7: Seed germination test of an OsORAP1 knock-out line in Tainung 67 genetic background.....	208

## Chapter 4

Supplementary Figure S17: Subpopulation comparison of all phenotypes.....	209
Supplementary Figure S18: Association mapping result for relative plant height. ....	211
Supplementary Figure S19: Association mapping result for relative tiller number. ...	212
Supplementary Figure S20: Association mapping result for relative thousand kernel weight (TKW).....	213
Supplementary Figure S21: Association mapping result for relative total panicle weight (TPW). ....	214
Supplementary Figure S22: Association mapping result for relative SPAD value. ...	215
Supplementary Figure S23: Association mapping result for constitutive lignin content. ....	216
Supplementary Figure S24: Association mapping result for relative lignin content. .	217
Supplementary Figure S25: Sequence variation of <i>EREBP</i> gene.....	218
Supplementary Figure S26: Association mapping result in each subpopulation for square-root transformed leaf bronzing score (t-LBS).....	219
Supplementary Figure S27: Sequence variation of <i>RING</i> gene.....	220
Supplementary Table S8: All the accessions and phenotypic data used for the mapping. ....	221
Supplementary Table S9: Correlation matrix in each subpopulation.....	230

Supplementary Table S10: List of significant SNPs identified through association mapping. ....	233
Supplementary Table S11: List of the top 50 SNPs from each trait.....	234
Supplementary Table S12: List of genes located within the identified candidate loci for all phenotypes. ....	242
Supplementary Table S13: Heritability of each trait. ....	245

## **Chapter 5**

Supplementary Protocol S3: Gene ontology (GO) enrichment analysis of microarray datasets.....	246
---	-----

---

## Supplementary data for Chapter 3

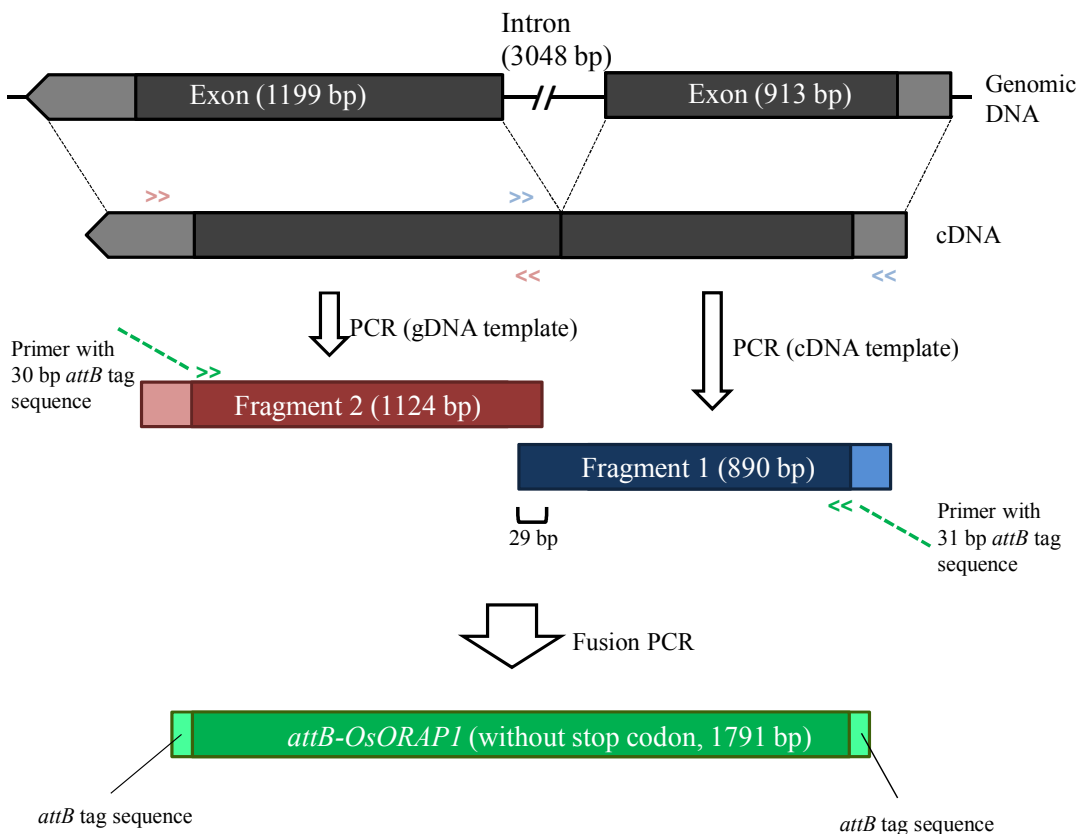
### Supplementary Protocol S1

#### *Vector construction*

The coding sequence of the putative rice AO gene (*Os09g0365900*; *OsORAPI*) was amplified through the following strategy. First, a partial fragment beginning from the start codon (fragment 1, 890 bp) of the sequence was obtained by PCR using Nipponbare (a *japonica* cultivar) cDNA as a template with the following thermal condition: 98 °C 2 min, 33 cycles of 98 °C 15 sec, 58 °C 30 sec and 72 °C 30 sec, followed by extra 3 min of 72 °C extension. The reaction mixture consisted of 4 µL of 5x Phusion HF buffer (Thermo Fisher Scientific, Waltham, MA), 0.4 µL of each primer (10 µM), 1 µL of dimethyl sulfoxide (DMSO), 0.4 µL of dNTP (10 mM), 0.2 µL of Phusion DNA polymerase (Thermo Fisher Scientific), 12 µL of nuclease-free water and 2 µL of cDNA. The other partial sequence (fragment 2, 1124 bp) was obtained using Nipponbare genomic DNA as a template for PCR since this fragment did not contain an intron region. The PCR thermal condition was the following: 95 °C 2 min, 33 cycles of 95 °C 30 sec, 55 °C 30 sec and 72 °C 75 sec, followed by extra 5 min of 72 °C extension. The reaction mixture consisted of 15 µL of 2x GoTaq Green Master Mix (Promega, Mannheim, Germany), 0.6 µL of each primer (10 µM), 1.5 µL of DMSO, 10.3 µL of nuclease-free water, and 2 µL of template DNA. In both cases, DMSO was added at a final concentration of 5% (v/v) to facilitate the amplification of high GC region contained in *OsORAPI* (71% overall GC content, 81% partial GC content in 212 bp repeat region) (Varadaraj and Skinner, 1994). The fragments were purified using a GenElute Gel Extraction Kit (Sigma, St. Louis, MO) after agarose gel electrophoresis with minimum exposure to UV light. The primers were created so that the two fragments had 29 bp overlap. The primer sequences were the following; 5'-CTA GCT ACC AAA GCA TAA CAA GCT C-3' (forward) and 5'-GTA GAT GTT GAG GTT CTT CAC CAC-3' (reverse) for the fragment 1, and 5'-CGT TCG TGG TGA AGA ACC TC-3' (forward) and 5'-GCA AAT TAC ACA CCA TAG TGT GG-3' (reverse) for the fragment 2. Next, a fusion-PCR was conducted using the two fragments obtained above using a pair of nested primers following the protocol of Szewczyk *et al.* (2006) with the following reaction setup: 0.5 µL of each eluted DNA

fragment, 5  $\mu$ L of 2x GoTaq Green Master Mix, 0.4  $\mu$ L of each primer (10  $\mu$ M), 0.5  $\mu$ L of DMSO, and 2.2  $\mu$ L of nuclease-free water. The thermal condition was the following: 95  $^{\circ}$ C 2 min, 25 cycles of 95  $^{\circ}$ C 20 sec, 70  $^{\circ}$ C 1 sec, 0.1  $^{\circ}$ C/sec down to 54  $^{\circ}$ C, 54  $^{\circ}$ C 30 sec, 0.2  $^{\circ}$ C/sec up to 72  $^{\circ}$ C, and 72  $^{\circ}$ C for extension. The extension time was 2 min constant till cycle 10, and was extended 5 sec for each cycle till cycle 25 (*i.e.* 3 min 15 sec at cycle 25) to compensate for the loss of the extension activity of *Taq* enzyme in the later phase of the PCR reaction. The primer sequences were 5'-GGG GAC AAG TTT GTA CAA AAA AGC AGG CTG CAT GAT GCG GTG TAG CGA CCG-3' (forward) and 5'-GGG GAC CAC TTT GTA CAA GAA AGC TGG GTC GTG GCC GCC CCT GGT TTT G-3' (reverse). The resultant fragment (*attB-OsORAP1*, 1791 bp) was cut out from an agarose gel after electrophoresis and purified. The underlined sequences are the *attB* tags necessary for the following BP reaction. The *attB-OsORAP1* fragment was introduced into pDONR207 by BP reaction. An aliquot of 2  $\mu$ L of the *attB-OsORAP1* fragment after gel purification was mixed with 260 ng of pDONR207 (carrying anti-gentamicin gene) and 1  $\mu$ L of BP clonase (Thermo Fisher Scientific), and TE buffer (10 mM Tris-HCl and 1 mM EDTA, pH 8.0) was added to make a final volume of 5  $\mu$ L. The reaction mixture was incubated at room temperature for 6 h yielding an entry vector pENTR207-OsORAP1, and 1  $\mu$ L of proteinase K was added to stop the reaction. The transformation of *E. coli* strain DH5 $\alpha$  was conducted according to the following procedure: an aliquot of 2  $\mu$ L of the BP reaction solution was added to 100  $\mu$ L of *E. coli* competent cells and incubated for 30 min on ice. The mixture was heat-shocked for 30 sec at 42  $^{\circ}$ C, immediately transferred on ice, and 450  $\mu$ L of SOC medium was added. The mixture was incubated for 1 h at 37  $^{\circ}$ C with gentle shaking, and the resultant culture was plated on an LB plate containing 10  $\mu$ g/mL of gentamicin. The colony was grown overnight, and a single colony was picked and used for cell culture (in LB medium containing gentamicin) and a colony PCR for insertion check. The plasmid was extracted from 5 mL of cell culture using a plasmid extraction kit (GenElute Plasmid Miniprep Kit, Sigma). LR reaction was conducted to introduce *OsORAP1* to the destination vector pMDC83 and pMDC32. pMDC83 contains C-terminal GFP fusion protein under the target protein driven by 2x 35S promoter. pMDC32 contains 2x 35S promoter and it expresses the native protein of the target gene (Curtis and Grossniklaus, 2003). The reaction mixture consisted of 170 ng of pENTR207-OsORAP1, 300 ng of destination vector (pMDC83

or pMDC32) and 1  $\mu$ L of LR clonase (Thermo Fisher Scientific), and TE buffer (pH 8.0) was added up to 5  $\mu$ L. The mixture was incubated at room temperature for 6 h yielding the vector pMDC83-OsORAP1 and pMDC32-OsORAP1, and 1  $\mu$ L of proteinase K was added to stop the reaction. The transformation of *E. coli* strain DH5 $\alpha$  was conducted as described above except for that LB plates contained 50  $\mu$ g/mL of kanamycin. The insertion was checked by a colony PCR. The two vectors were verified by sequencing, and complete match to the original *OsORAP1* sequence was confirmed. The transformation of *Agrobacterium tumefaciens* strain GV3101::pMP90 was conducted as follows. First, 900 ng of each plasmid was added to 50  $\mu$ L of competent cells of agrobacterium, and the mixture was frozen in liquid nitrogen. Then the mixture was incubated for 5 min at 37  $^{\circ}$ C and 1 mL of YEB medium was added. After 3 h of incubation at room temperature, the cells were cultured on a YEB plate containing 10  $\mu$ g/mL of gentamicin, 50  $\mu$ g/mL of rifampicin, and 50  $\mu$ g/mL of kanamycin. The transformants were checked by a colony PCR.



## Supplementary Protocol S2

### *Measurement of enzyme activity*

The activity of three enzymes was measured from the soluble fraction and the ionically-bound fraction. Enzyme was extracted from approximately 80 mg of sample ground with liquid nitrogen. The sample was mixed with 1 mL of 0.1 M sodium phosphate buffer (pH 6.5) and centrifuged for 10 min at 4 °C and 15,000 g. The supernatant was defined as soluble fraction. Another buffer consisting of 0.1 M sodium phosphate butter (pH 6.5) and 1 M NaCl was added to the pellet after the first extraction, mixed vigorously, and the supernatant was recovered by centrifugation. This fraction was defined as ionically-bound fraction. The protein concentration of each fraction was determined by the Bradford method (Bradford, 1976).

#### 1) Laccase activity

Laccase activity was determined according to Zarivi *et al.* (2013). The reaction mixture contained 10  $\mu$ L of protein extract, 80  $\mu$ L of McIlvaine buffer (0.1 M citric acid/0.2 M  $K_2HPO_4$ ; pH 4.0) and 10  $\mu$ L of 5 mM 2,2'-azino-bis(3-ethyl-benzothiazoline-6-sulphonic acid) (ABTS) as a substrate. The reaction mixture was mixed, and the kinetics was read at 420 nm at 25 °C for 40 min with the microplate reader. The slope was determined from the linear phase (between 10 to 40 min) and used for the calculation. The extinction coefficient of  $\epsilon = 36 \text{ mM}^{-1} \text{ cm}^{-1}$  (at 420 nm) was used for the calculation.

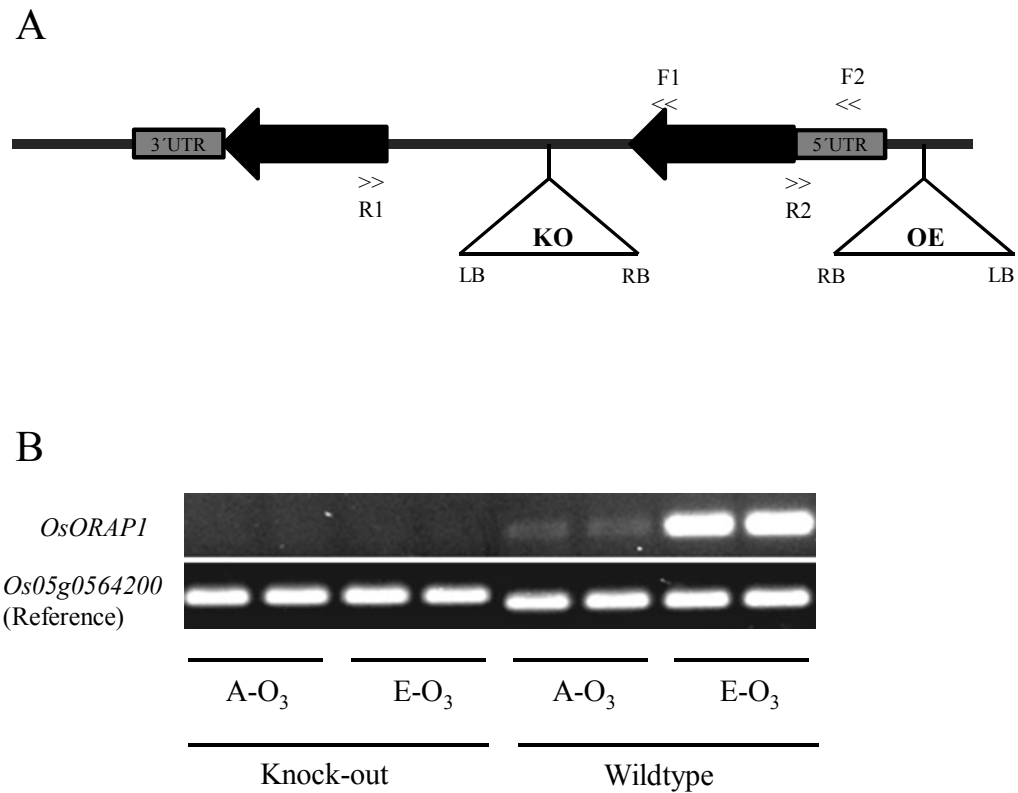
#### 2) Catechol oxidase activity

The reaction mixture contained 10  $\mu$ L of protein extract, 80  $\mu$ L of 0.1 M potassium phosphate buffer (pH 7.0) and 10  $\mu$ L of 50 mM catechol as a substrate. The mixture was mixed and the kinetics was read at 390 nm at 25 °C for 80 min with the microplate reader. The slope was determined from the linear phase (between 0 to 30 min) and used for the calculation. The extinction coefficient of  $\epsilon = 1.37 \text{ mM}^{-1} \text{ cm}^{-1}$  (at 390 nm) was used for the calculation.

#### 3) Tyrosinase activity

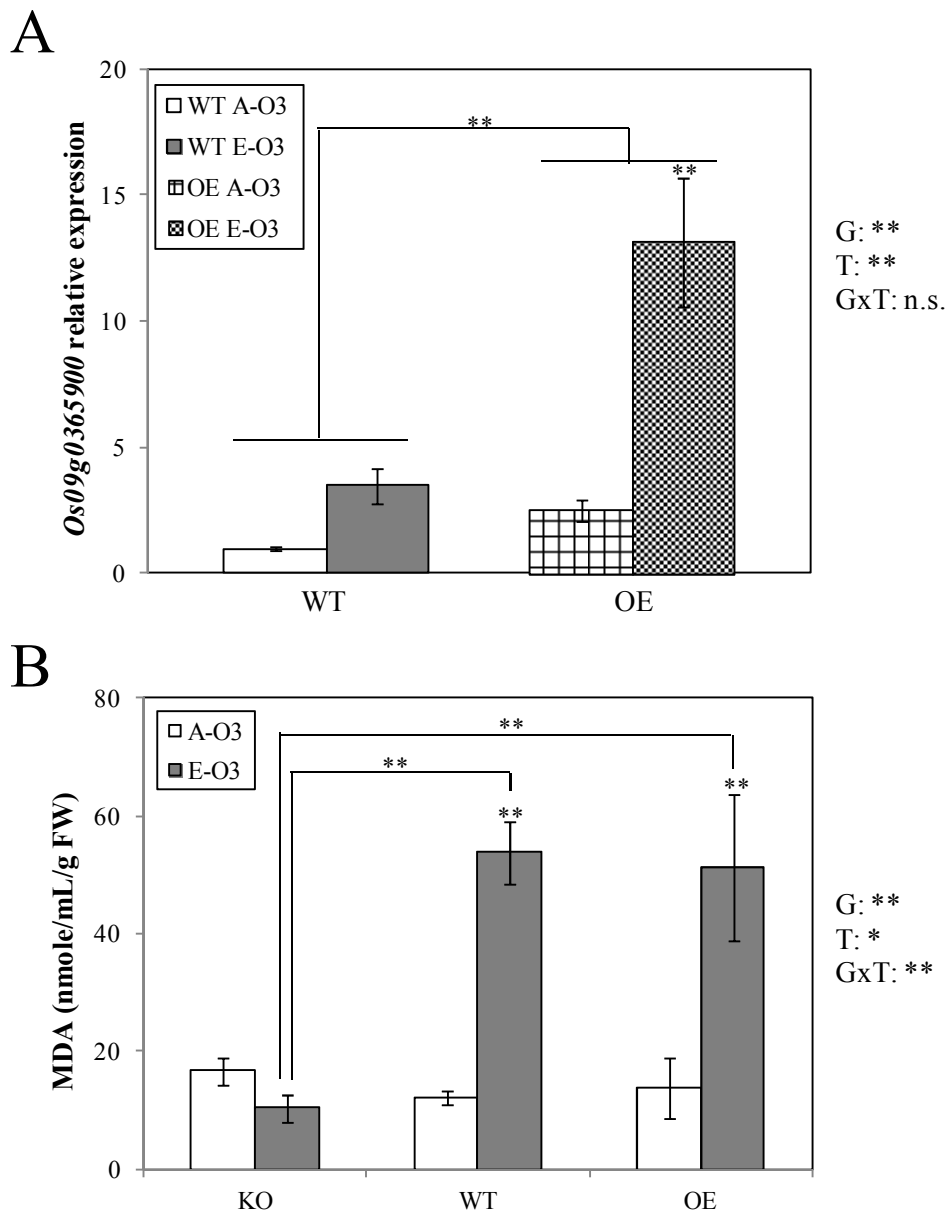
The reaction mixture contained 10  $\mu$ L of protein extract, 80  $\mu$ L of 0.1 M potassium phosphate buffer (pH 7.0) and 10  $\mu$ L of 1 mM tyrosine as a substrate. The mixture was mixed and the kinetics was read at 280 nm at 25 °C for 80 min with the microplate

reader. The slope was determined from the linear phase (between 10 to 30 min) and used for the calculation. The extinction coefficient of  $\varepsilon = 2.63 \text{ mM}^{-1} \text{ cm}^{-1}$  (at 280 nm) was used for the calculation.



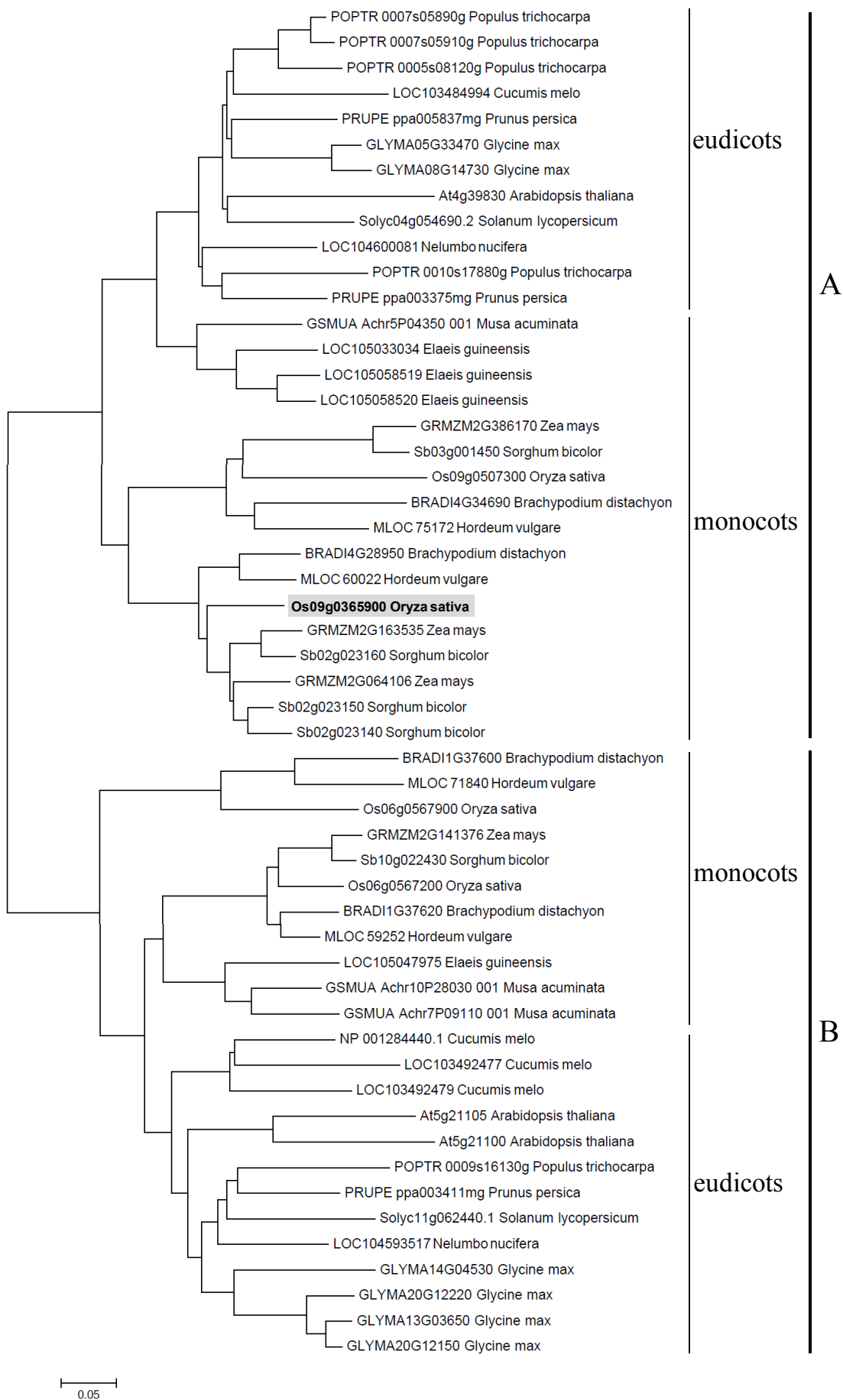
Supplementary Figure S1: (A) Gene model of *OsORAP1*. The T-DNA insertion position and direction in a knock-out line (KO) and an over-expression line (OE) are shown. LB: left border, RB: right border. The positions of primers used for RT-PCR are also shown. (B) Expression of *OsORAP1* in wildtype and knock-out line in the ambient ozone concentration (A-O<sub>3</sub>) and the elevated ozone concentration (E-O<sub>3</sub>). *OsORAP1* was amplified by PCR using *OsORAP1*-F1/R1 primers and gel electrophoresis was conducted. The electrophoresis bands of *OsORAP1* and *U2 snRNP* (an internal control) are shown.





Supplementary Figure S2: Physiological response of plants from the second fumigation experiment. (A) Expression of *OsORAP1* and (B) malondialdehyde (MDA) content from the ambient condition (A-O<sub>3</sub>, 12 ppb) and the elevated ozone condition (E-O<sub>3</sub>, 86 ppb). Plants were treated with elevated ozone for 20 days, and young shoots and leaves were used for the analysis. Values are means of four biological replicates. Error bars indicate standard errors. KO, knock-out line; WT, wildtype; and OE, over-expression line. ANOVA was conducted, and the significance is denoted as follows: G, genotype; T, treatment; GxT, genotype and treatment interaction; n.s., not significant; \*,  $P < 0.05$ ; and \*\*,  $P < 0.01$ .

Appendices



Supplementary Figure S3: Phylogenetic analysis of ascorbate oxidase family proteins from 14 different plant species with complete genome sequences (7 monocot species and 7 eudicot species). Amino acid sequence of OsORAP1 was subjected to pattern-hit initiated BLAST (PHI-BLAST; Zhang *et al.*, 1998) on NCBI BLAST tool (<http://blast.ncbi.nlm.nih.gov/Blast.cgi>) with default settings, specifying multicopper-oxidases 1 and 2 patterns (consensus sequence: GX[FYW]X[LIVMFYW]HCH{PR}{K}XH{S}X{LFH}G[LM]X(3)[LIVMFY]) from indicated plant species.  $E < 10^{-100}$  was set to the cutoff value, since this threshold eliminated similar sequences such as laccase, while including ascorbate oxidase family proteins. Redundant proteins and partial sequences were manually removed. Gene IDs were obtained from either NCBI database (<http://www.ncbi.nlm.nih.gov/>) or Ensembl Plants database (<http://plants.ensembl.org/index.html>). Phylogenetic tree was generated by MEGA 5 software (Tamura *et al.*, 2011) using the neighbour-joining method. The branch length indicates the evolutionary distances as calculated by the Poisson correction method. A and B correspond to the classification of subclades III-A and III-B as in Fig. 3-1A.

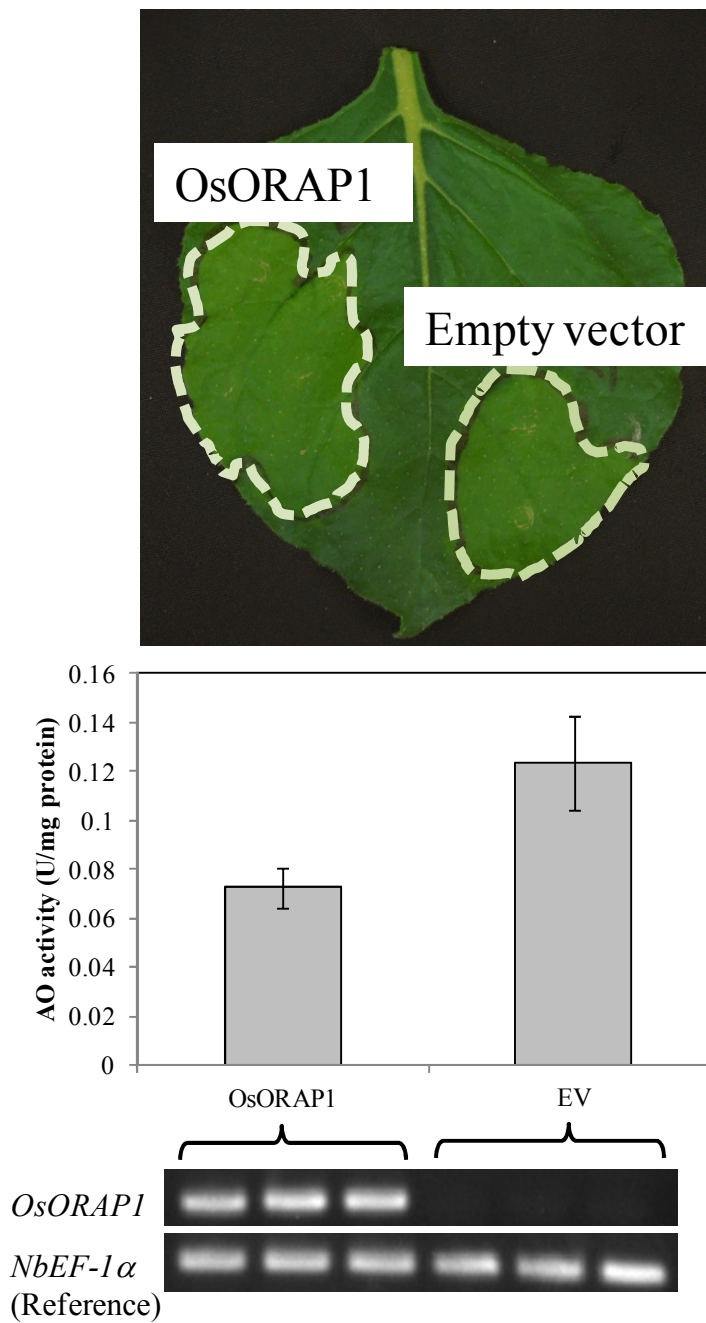
Appendices

Os01g0816700	-----MTMPASALLLVAAVLAAR-AEDPYHFFDVKWTYVGR-TRTMDVAQKVMILINDMFPGPPTICSSNNNIVVNVFN-QLDHLPLFN	83
Os07g0510900	-----D-----	2
Os07g0119400	-----MAPPPAAAAAALACILAVAAATLAGADDPYRFFTWNVTYGSINPLGSLPQQGILINGQFPGPRI DCVFNNDIIIVNVFN-NLDEPFLIT	86
AT4g12420	-----MDLFLKLLLVFVFNISFCFAADPYSFYNFVSYTASPLG-VEQQVIAINGKFPGPPTINVTNENLVNVNFRN-KLDEGLLH	80
Os09g0507300	---MR-----TWRLAVLACLCAAAAAPA-----EAKTHHHWNTITQYKSPDC-FRKLAVTINGESPGPTIRAAQGDITLVVTVHMLDENTAIH	82
Os09g0365900	---MR-----CSDRLLCSLFLAALAFGVA---AAATRHRDWDISYQFTSPDC-VRKLAVTINGHGPPTIRAVQGDITVNVNKNLLTENVAH	83
AT4g39830	---MMRKRSSDTHVFNMLVLCFIALFFSSVLC---QSKIRRFKWEVYEFKSPDC-FEKLVTITNGKFPGPPTIKAQQGDITVVELKNSFMENVAH	92
Os06g0567200	-----MRLSLLFLVCFFTVAMSQCAA---AAARAHFRWEVSMFWSDC-EKVVVINGIQFPGPPTIRAKAGDITVHLKNGLHTEGVH	83
Os06g0567900	-----MAAAVQLLVAAAAAAMAAACAGMAAAATVEVTDVVEYLVWAPDC-QQRVMIINGRFPGPPTIRARAGDITVSMNNKMHTEGVH	87
AT5g21100	-----MAVIWVLLTVVVVAFHSAS---AAVVESTWEVYKWWPDC-REGIVMAINGQFPGPPTIDAVAGDITVIVHVNKLSLTEGVH	80
AT5g21105	MSYDEHTSSSFTYISQMGVWVIVLVAVLHTAS---AAVREYHWEVYKWSDC-REGAVMTVNGEFPGPPTIRAFAGDITVIVNLNKLITTEGLVH	94
Os01g0816700	WGTRCRKNSMDGMPG-INCFI-EGTNWYKWPQDQICFFVFPFSGMGRRAAGGCGIITVHSRLL-----I FVPFDEPAGDYP-----VLVGDWYTKDH	173
Os07g0510900	RNGTRCRNNSHEDGAG-ITCFIHPGGNITVILQVKDQICGFVFPFSLAFHRAAGGCGAIRVLSRPM-----I FVPFPPPAADYP-----LLHGQWYKANH	92
Os07g0119400	WNGTRCRKNSMDGVLG-INCFIHPGANWYKQAKDQICGFVFPFSAVHRAAGGCGALNVVQRPA-----I FVPVYPPAGDFT-----LLHGQWYKAGH	176
AT4g12420	WNGTRCRRVSDGVLG-INCFIHPKWNWYEFQVKDQICGFVFPFSLHFQASGCGESFVWNPRAI-----I FVPFSTPDGDT-----VTHGQWYLRNH	170
Os09g0507300	WNGTRCIGSPWADGAGVWCCFHPGSETTYRFFVVD-RGCLYVHSHYGMGRSAGCGEMIVVVEVAPGAGDGEREPFRDYGEHT-----VLNDWYHRST	177
Os09g0365900	WNGTRCIGTSPWADGEGVWCCFHPGSEVTVQFVVD-RGCLYVHSHYGMGRSAGCGEMIVVVEVAPGAGDGEREPFRDYGEHT-----VLNDWYHRST	177
AT4g39830	WNGTRCIGTSPWADGEGVWCCFHPGSEVTVQFVVD-RGCLYVHSHYGMGRSAGCGEMIVVVEVAPGAGDGEREPFRDYGEHT-----VLNDWYHRST	181
Os06g0567200	WNGTRCIGTSPWADGEGVWCCFHPGSEVTVQFVVD-RGCLYVHSHYGMGRSAGCGEMIVVVEVAPGAGDGEREPFRDYGEHT-----VLNDWYHRST	172
Os06g0567900	WNGTRCIGTSPWADGEGVWCCFHPGSEVTVQFVVD-RGCLYVHSHYGMGRSAGCGEMIVVVEVAPGAGDGEREPFRDYGEHT-----VLNDWYHRST	181
AT5g21100	WNGTRCIGTSPWADGEGVWCCFHPGSEVTVQFVVD-RGCLYVHSHYGMGRSAGCGEMIVVVEVAPGAGDGEREPFRDYGEHT-----VLNDWYHRST	166
AT5g21105	WNGTRCIGTSPWADGEGVWCCFHPGSEVTVQFVVD-RGCLYVHSHYGMGRSAGCGEMIVVVEVAPGAGDGEREPFRDYGEHT-----VLNDWYHRST	183
Os01g0816700	TVLAKNDAGK-----SILGRPACTVINGKN-----EKDASNPMTMEAGRY	216
Os07g0510900	TDLKYMDSGK-----AGFPDCLINGR-----SWDGYTFVQQGRY	131
Os07g0119400	KQLRQADAGGG---GAPPPEDALING-----MPSAAAFVQQRGY	216
AT4g12420	TALRKADGDK---DGMDFGVLINGKPYRYN-----DTL-----VADGIDFETITVHPGRY	221
Os09g0507300	YEQAVGASVYV---MVVGEFQSLINGR-----VFNCSF---PAASN-----GGGAACNAFG---GCCWPTLETASPCRY	236
Os09g0365900	YEQAVGASVYV---MVVGEFQSLINGR-----VFNCSN---SPAT-----AASCNVSH---PDC-ARAVPAVVPGRY	239
AT4g39830	SEKATGASIP---FKWGEFQSDIINGR-----RFNCSNLTTPPS-----LVSGVCNVSN---ADC-SRFLITVPGRY	247
Os06g0567200	YTCMVGLSNP---FRWGEFQSLINGR-----QFNCSLAAAH---PGAKCAAAG---NRHCAVILPVLNRY	237
Os06g0567900	YQAAGADGDRHFEMGEPQTIDINGR-----QFECTLGPARKSEFKLLNENVEVTDQDKMCSQKCLLRSECGYPSPRSQCAQVTVNVEQRY	275
AT5g21100	HAQELARSSRP---MRWGEFQSDIINGR-----QFNCSQAAYFNK---GGEKDVCTFKE---NDQCAQPTLVNPNRY	233
AT5g21105	PSQELGSSPK---MRWGEFQSDIINGR-----QFNCSLAAQFSN---NTSLPMCTFKE---GDQCAQILHVEPNRY	250
Os01g0816700	RFRVNVGIRKTSNVRIQGSLKLVEMESHTVQNSYDSLVHVAACVSELVTAQ-KPGVILVASTRFLK---EYSAIT---AIVRNGSNTPASP-KLP	310
Os07g0510900	RFRVNSVGLSTSNIRFOGHTLVVEVESHMTQTYSLDVLHICGSYSLVLTADQ-PAYDYAVVSTRFTS---KIISTT---AVHRSQSGGKSPA-ALP	225
Os07g0119400	LRVSNVGVKTSNVRIQGSLKLVEMESHTVQNSYDSLVHVAACVSELVTAQ-KPGVILVASTRFLK---EYSAIT---AIVRNGSNTPASP-KLP	312
AT4g12420	LRVSNVGVKTSNVRIQGSLKLVEMESHTVQNSYDSLVHVAACVSELVTAQ-KPGVILVASTRFLK---EYSAIT---AIVRNGSNTPASP-KLP	320
Os09g0507300	RFRVNSVGLSTSNIRFOGHTLVVEVESHMTQTYSLDVLHICGSYSLVLTADQ-PAYDYAVVSTRFTS---KIISTT---AVHRSQSGGKSPA-ALP	330
Os09g0365900	RFRVNSVGLSTSNIRFOGHTLVVEVESHMTQTYSLDVLHICGSYSLVLTADQ-PAYDYAVVSTRFTS---KIISTT---AVHRSQSGGKSPA-ALP	336
AT4g39830	RFRVNSVGLSTSNIRFOGHTLVVEVESHMTQTYSLDVLHICGSYSLVLTADQ-PAYDYAVVSTRFTS---KIISTT---AVHRSQSGGKSPA-ALP	341
Os06g0567200	RFRVNSVGLSTSNIRFOGHTLVVEVESHMTQTYSLDVLHICGSYSLVLTADQ-PAYDYAVVSTRFTS---KIISTT---AVHRSQSGGKSPA-ALP	330
Os06g0567900	RFRVNSVGLSTSNIRFOGHTLVVEVESHMTQTYSLDVLHICGSYSLVLTADQ-PAYDYAVVSTRFTS---KIISTT---AVHRSQSGGKSPA-ALP	371
AT5g21100	RFRVNSVGLSTSNIRFOGHTLVVEVESHMTQTYSLDVLHICGSYSLVLTADQ-PAYDYAVVSTRFTS---KIISTT---AVHRSQSGGKSPA-ALP	325
AT5g21105	RFRVNSVGLSTSNIRFOGHTLVVEVESHMTQTYSLDVLHICGSYSLVLTADQ-PAYDYAVVSTRFTS---KIISTT---AVHRSQSGGKSPA-ALP	343
Os01g0816700	EGPS---GWAWSINQWRSFRWNLTAARPNPQGSYHYQINIRTRIRCTSRGK-VDGKEFPALNSVSHVDDAGTFLKAEYFNASSGVFEYN-----	400
Os07g0510900	GGPTI---QIDVSLNQARSIRWNLTAARPNPQGSYHYQINIRTRIRCTSRGK-VDGKEFPALNSVSHVDDAGTFLKAEYFNASSGVFEYN-----	314
Os07g0119400	APPE---QAEWMSNQARSFRWNLTAARPNPQGSYHYQINIRTRIRCTSRGK-VDGKEFPALNSVSHVDDAGTFLKAEYFNASSGVFEYN-----	401
AT4g12420	PGQDEFDKMSNQARSIRWNLTAARPNPQGSYHYQINIRTRIRCTSRGK-VDGKEFPALNSVSHVDDAGTFLKAEYFNASSGVFEYN-----	412
Os09g0507300	TFPPTG---FRWNTASR---VAQSRFAALPGHVEPPAPRQSLKIDN-HTWALNVSLSF-EATVFLVAMKHCGR-GEFQR-PPDPS	419
Os09g0365900	TPPPAG---PAWNTASR---VRCSLATVAHPAHAVPPPTSDRTILDLNTQNKIGG-QIHWALNVSFTL-PHTVFLVAMKHCGR-GEFQR-PPPET	425
AT4g39830	TSESSNVFVWNTASR---LACSLAIKARRGFTHALPNSDKVIVLNTQNEVNG-YRWNSVNVVSHH-PHTVFLVAMKHCGR-GEFQR-PPPET	433
Os06g0567200	AAAPPAT---PAWNTASR---KAFYRILGRAGVTTPPPATSDRRIRLNTQNRMGGGHVRWSINNVSMVL-PATVFLVAMKHCGR-GEFQR-PPPET	420
Os06g0567900	AGEPPVT---PAWNTASR---KAFYRIRAKRDTNRPAAAADRIRLNTQNLMDG-RYRWSINNVSLTL-PATVFLVAMKHCGR-GEFQR-PPPET	461
AT5g21100	SHPPVT---PIWNTDTRS---KFSKIFAAKYG-PKPEKSHDQLLNTQNLVYD-YRWNSINNVSLSV-PATVFLVAMKHCGR-GEFQR-PPPET	413
AT5g21105	SSPPVT---PIWNTDTRS---KNSKIFSAKYG-PSPPKRYKRLLNTQNLIDG-YRWNSINNVSLVT-PATVFLVAMKHCGR-GEFQR-PPPET	431
Os01g0816700	----LIGDVPATT-VPQKLPANVLSAEFRTFIEVSEPEK-----SIDSEHINCAFFAAGMGEGHTPECKRT-----YNLLDVTVSRHTQV	482
Os07g0510900	----TISDPSGGGGGAYLQAVMGASYRDRYIVSENPEN-----EVQSNHIDCAFFVWVMDGGKSSASRQ-----YNLRDAVSRHTQV	397
Os07g0119400	----SVFAPDGT---AARSGTVPVWNLNHEFIEVSENPEN-----ELQSNHIDCAFFVWVMDGGKSSASRQ-----YNLRDAVSRHTQV	481
AT4g12420	----FPKRPLTG---PAKVATSIINGTYRGMVVDQNDT-----KMQSVMSCVAFVWVMDGGKSSASRQ-----YNLRDAVSRHTQV	491
Os09g0507300	YD-HGSLNLSPP---ASLAVRHAAYRLALGSDVVDVQNTAIPPPNGRSETHPWHLEHGFVWLVGCGGKRV-PEVDPGLNASARGGAVMNTVAFH	515
Os09g0365900	YAGAARFDVYAVQGNPNATSDAPYRRLRFSVVDVQNTAIPPPNGRSETHPWHLEHGFVWLVGCGGKRV-PEVDPGLNASARGGAVMNTVAFH	519
AT4g39830	YD-SRNYDIFAKFLANATSDGIYRRLRNSVDVQNTAIPPPNGRSETHPWHLEHGFVWLVGCGGKRV-PEVDPGLNASARGGAVMNTVAFH	526
Os06g0567200	DTFGRGVDVNRPPANNPTVGGDNVYLAHNAVDVQNTAIPPPNGRSETHPWHLEHGFVWLVGCGGKRV-PEVDPGLNASARGGAVMNTVAFH	515
Os06g0567900	AAPFDYDVMRPPANNPTASDRVRLRHGGVVDVQNTAIPPPNGRSETHPWHLEHGFVWLVGCGGKRV-PEVDPGLNASARGGAVMNTVAFH	555
AT5g21100	KLMDNIDMKNPPNPTTKGSGIYNFAGIYVDVQNTAIPPPNGRSETHPWHLEHGFVWLVGCGGKRV-PEVDPGLNASARGGAVMNTVAFH	507
AT5g21105	SYRMD-YDIMNPPNPTTNGIYVFPFNVVDVQNTAIPPPNGRSETHPWHLEHGFVWLVGCGGKRV-PEVDPGLNASARGGAVMNTVAFH	524
Os01g0816700	RSNTAVMLTFINAGMNIISNMWERYLCAQLVSVVSPARSLRDEYNNPEIARLCKGVVGLPMPSPYLPA-----	553
Os07g0510900	NSNTAVMLTFINAGMNIISNMWERYLCAQLVSVVSPARSLRDEYNNPEIARLCKGVVGLPMPSPYLPA-----	464
Os07g0119400	NCWNSALVSLNCGMNIISANWDRQYLCOQLYLRVWTSSTSWRDEYVPEKNALLCGRAAGRTRPL-----	545
AT4g12420	GWNSALLSILNCGMNIISRENLSWYLCQETVYRVWNPDENNKTEFGHPDNLVCCGALSKLQKPKQVSSASKSIGFTSLSMVVMALVMMMLQH	587
Os09g0507300	MGWAVRFRASNGVWLFHCHLEAHVIMGCG---VVVEEGVDVLP---RIPASIMCGKRTKGGH-----	574
Os09g0365900	FGWTAIRFRALNGVWAFHCHIEAHFVMGCG---IVVEEGVERVG---EPPPEIMCGKTRGGH-----	577
AT4g39830	FGWTAIRFRALNGVWAFHCHIESHFVMGCG---IVVEEGIDKVS---SIPSSIMCGKTR-----	582
Os06g0567200	YCWTAIRFRVADNGVWAFHCHIEPHLMGCG---VVEEAVDRVSLP---PKRAVSCGATATAMAGAGGHV-----	581
Os06g0567900	HGWTAIRFRVANNCGWAFHCHIEPHLMGCG---VVEEVEDRMLHDPKIDMAGCGLVARTATPLTPATLPPSPAPAP-----	633
AT5g21100	FGWTAIRFRVADNGVWAFHCHIEPHLMGCG---VVEEVEDRIGKMEIPDEALGCGLTRKWLNRGR-----	573
AT5g21105	YCWTAIRFRVADNGVWAFHCHIEPHLMGCG---VVEEAEGLNRIG---KVPDEALGCGLTRKQFLMNRNR-----	588

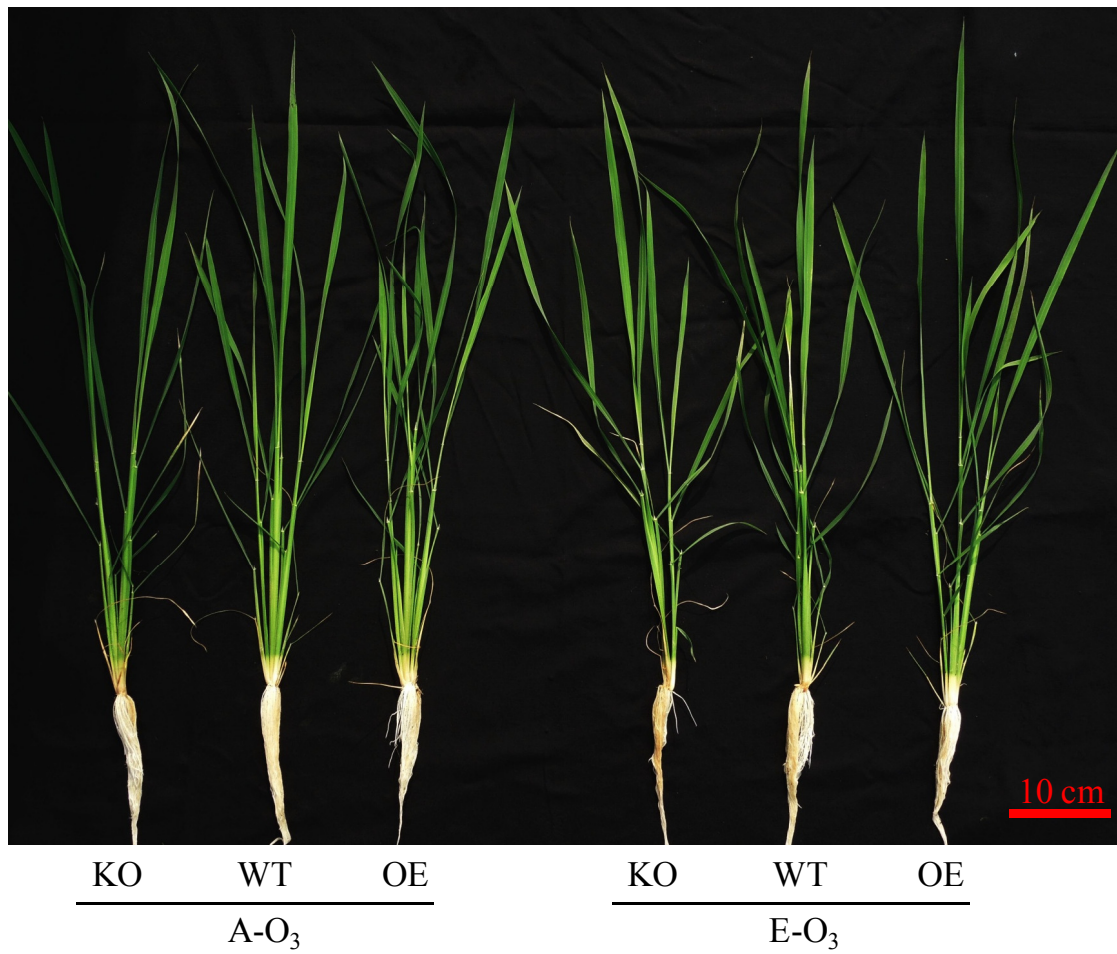
Multicopper-oxidases signature 1: G-x-[FYW]-x-[LIVMFYW]-x-[CST]-x-[PR]-{K}-x(2)-{S}-x-[LFH]-G-[LM]-x(3)-[LIVMFYW]

Multicopper-oxidases signature 2: H-C-H-x(3)-H-x(3)-[AG]-[LM]

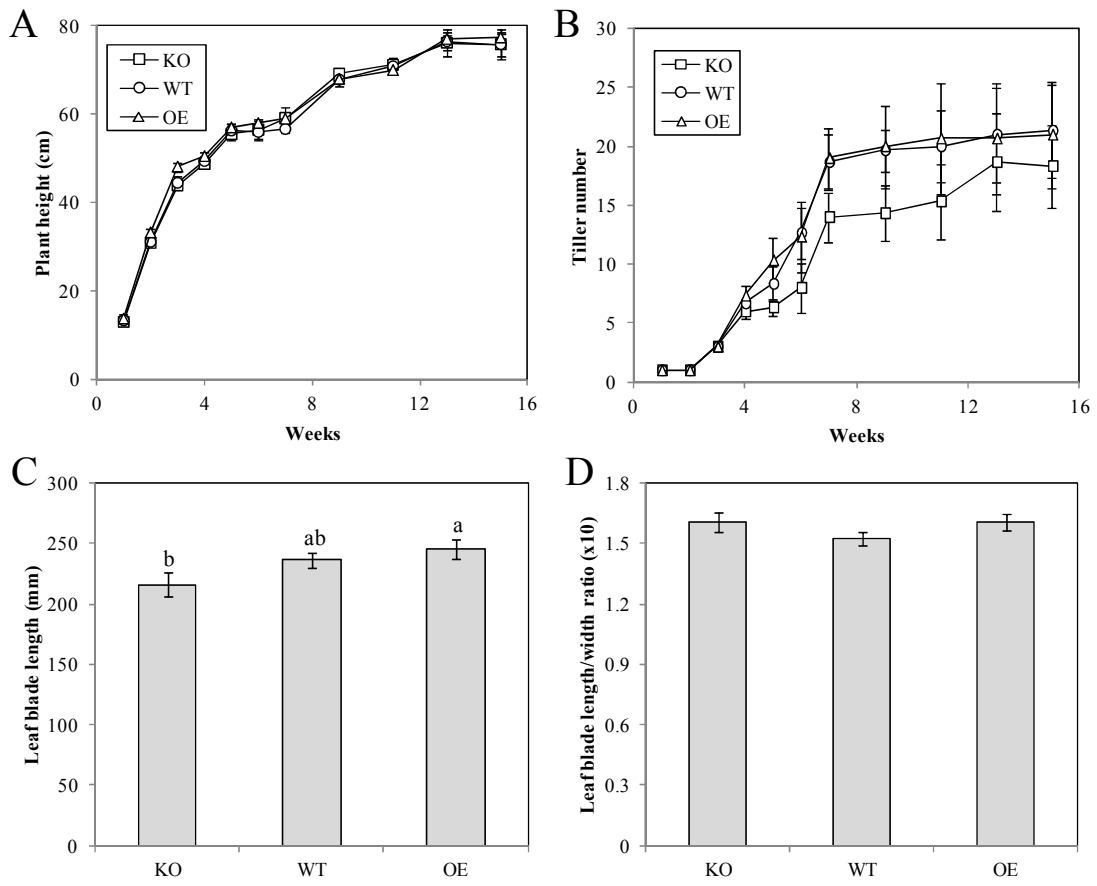
Supplementary Figure S4: Multiple alignment of proteins in clades II and III from *Arabidopsis* and rice. The sites with completely conserved amino acid are shown in black colour, and the sites with similar amino acids are shown in gray colour. Predicted copper-binding sites (Lin *et al.*, 2013) are indicated by asterisks with red background. The squared position contains Multicopper-oxidases signature 1 and 2, of which sequences are shown below. The denotation of signature is according to Prosite website (<http://prosite.expasy.org/>).



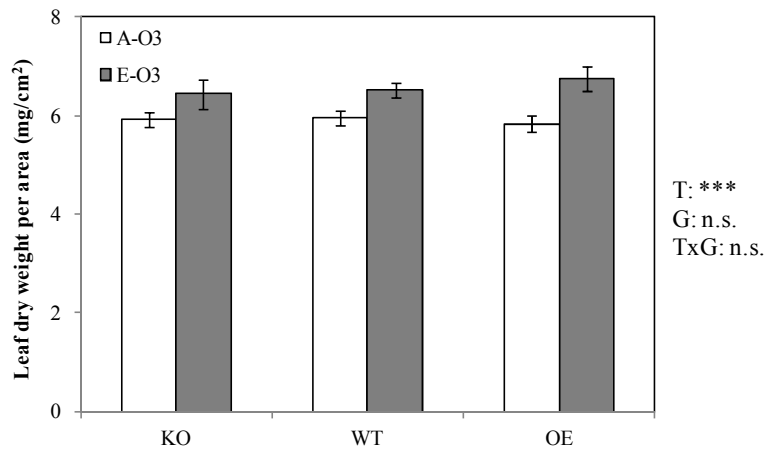
Supplementary Figure S5: Transient expression of *OsORAP1* in *Nicotiana benthamiana* plant. The leaves of *N. benthamiana* were infiltrated at an optical density of  $OD_{600} = 2.0$  of *Agrobacterium tumefaciens* carrying pMDC32-*OsORAP1* vector (*OsORAP1*). As empty vector control (EV), *A. tumefaciens* carrying pMDC32 was infiltrated. The infiltration was carried out together with *A. tumefaciens* carrying pBIN61-P19 at the same optical density to enhance the expression of the transgene. The plants were grown in a greenhouse after the infiltration, and the samples were taken after 10 days from the infiltrated area. Ascorbate oxidase (AO) activity and gene expression were analysed. *EF-1α* gene was used as a reference. A representative leaf picture is shown on the top. Values are means of three different leaves. Error bars indicate standard errors.



Supplementary Figure S6: Morphology of the three lines in the ambient ozone concentration (A-O<sub>3</sub>, 12 ppb) and the elevated ozone concentration (E-O<sub>3</sub>, 86 ppb). The plants were grown in hydroponic tanks for three weeks before the initiation of elevated ozone stress, and the picture was taken on DAY 15 of E-O<sub>3</sub> treatment. KO, knock-out line; WT, wildtype; and OE, over-expression line.

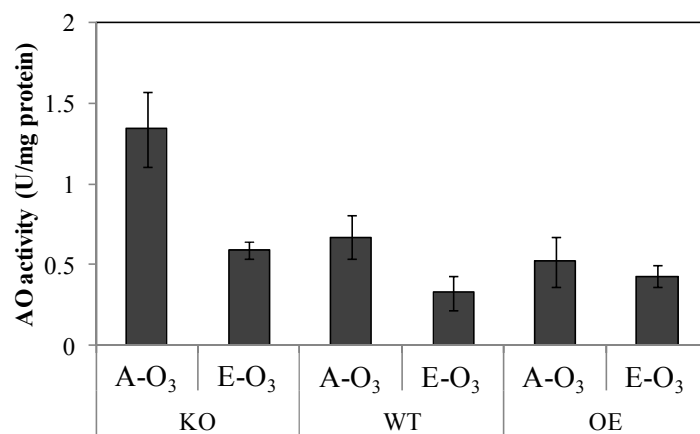


Supplementary Figure S7: Growth characteristics of wildtype and two mutant lines grown in the soil. (A) Plant height, (B) tiller number, (C) flag leaf blade length, and (D) flag leaf blade length/width ratio are shown. In A and B, values are average of three individuals, and in C and D, values are average of 27 to 30 different flag leaves from three individual plants. ANOVA was conducted for all the data, and significant differences are indicated with different alphabets in C. All error bars indicate standard errors.

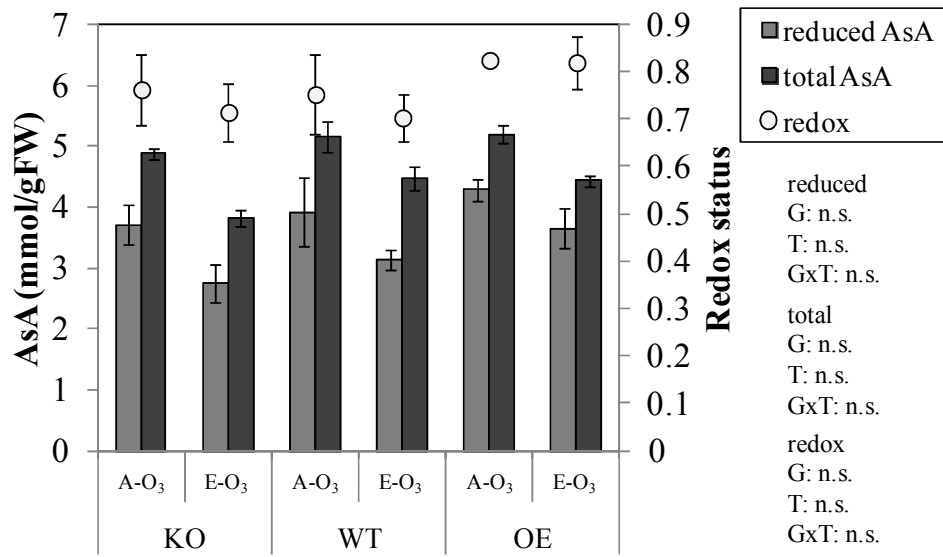


Supplementary Figure S8: Leaf dry weight per leaf area in the ambient ozone concentration (A-O<sub>3</sub>, 12 ppb) and the elevated ozone concentration (E-O<sub>3</sub>, 86 ppb). The plants were grown in hydroponic tanks for three weeks before the initiation of elevated ozone stress, and the samples were taken 20 days after the onset of elevated ozone treatment. Samples were dried at 70 °C for 3 days after the harvesting. Three to four leaves (1st and 2nd fully expanded leaves from the top) per plant were used for the measurement of dry weight and leaf area. Leaf area was measured using a scanner and OMA2.0 system (HGoTECH GmbH, Bonn, Germany). Values are means of 12 to 16 leaves deriving from four individual plants. Error bars indicate standard errors. KO, knock-out line; WT, wildtype; and OE, over-expression line. ANOVA was conducted, and the significance is denoted as follows: G, genotype; T, treatment; GxT, genotype and treatment interaction; n.s., not significant; and \*\*\*,  $P < 0.001$ .

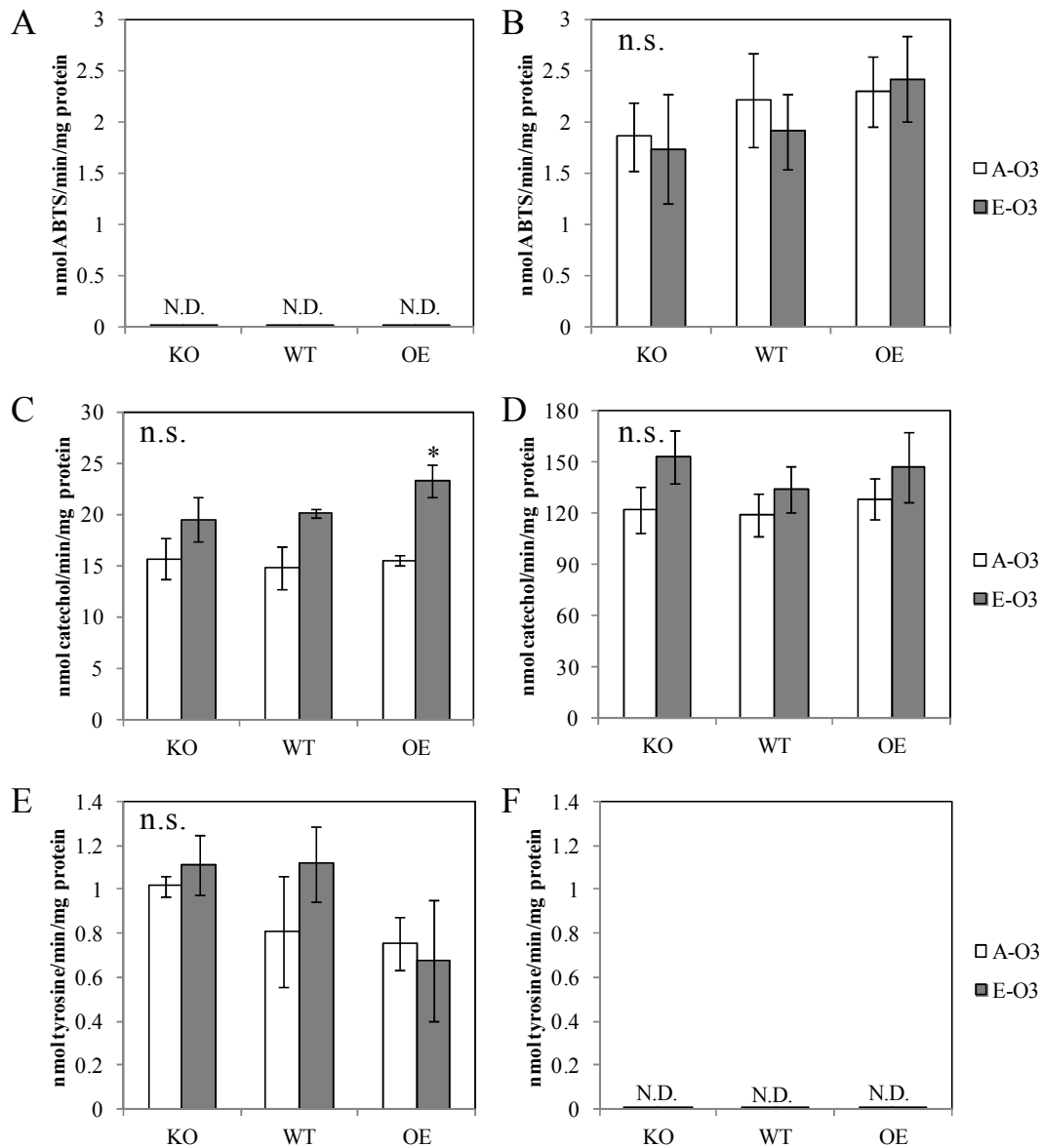




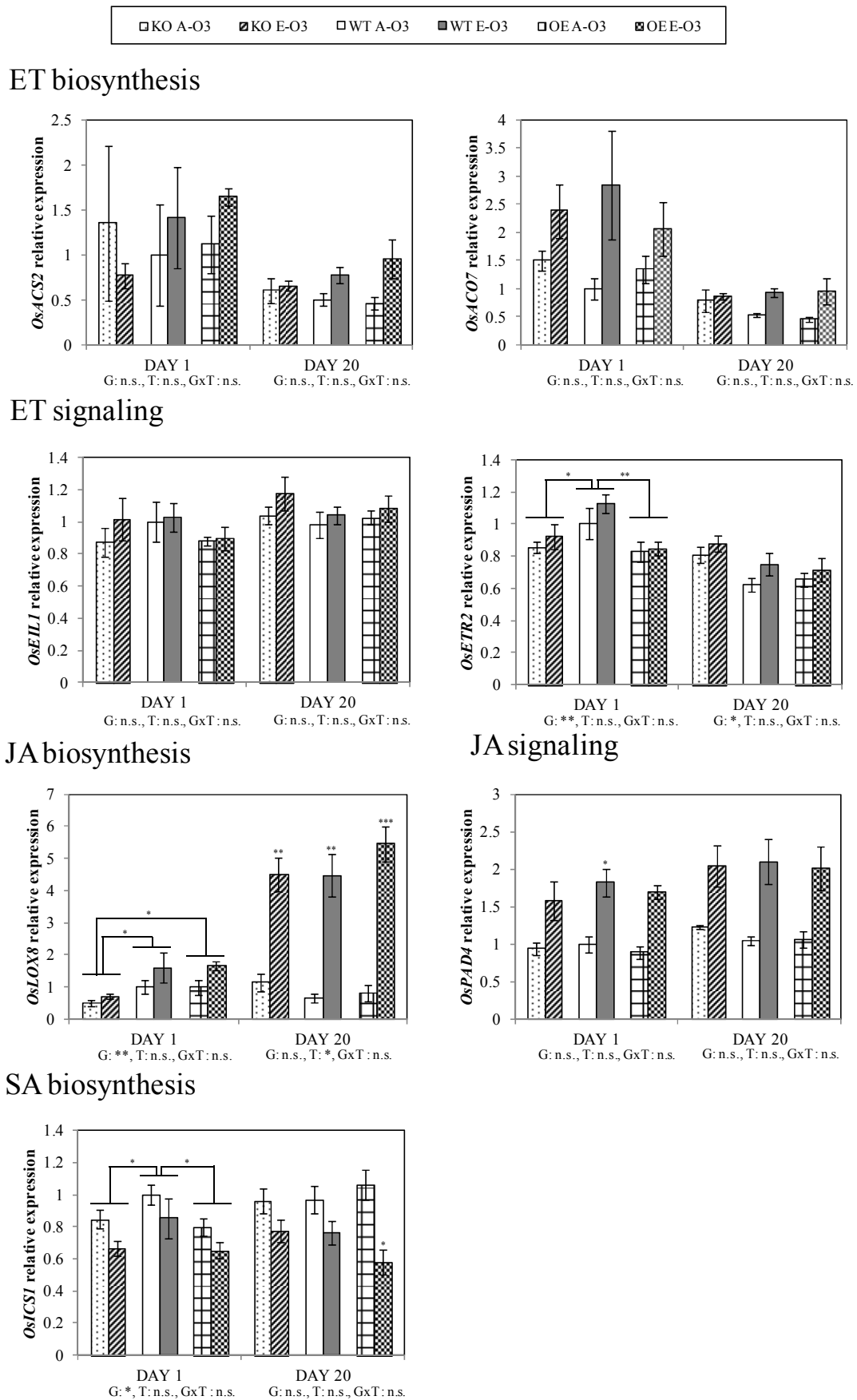
Supplementary Figure S9: Ascorbate oxidase (AO) activity in the apoplast in the ambient ozone concentration (A-O<sub>3</sub>, 40 ppb) and the elevated ozone concentration (E-O<sub>3</sub>, 159 ppb). The AO activity in the apoplastic washing fluid was measured according to Frei *et al.* (2010) on DAY 16. Values are means of three or four biological replicates. Error bars indicate standard errors. KO, knock-out line; WT, wildtype; and OE, over-expression line.



Supplementary Figure S10: Ascorbate (AsA) content and redox status in the whole tissue in the ambient ozone concentration (A-O<sub>3</sub>, 40 ppb) and the elevated ozone concentration (E-O<sub>3</sub>, 159 ppb). The samples were taken on DAY 20, and AsA content and redox status were measured. Values are means of four biological replicates. Error bars indicate standard errors. KO, knock-out line; WT, wildtype; and OE, over-expression line. ANOVA was conducted, and the result is shown as follows: G, genotype; T, treatment; GxT, genotype and treatment interaction; and n.s., not significant.



Supplementary Figure S11: Polyphenol oxidase activity of three lines using different substrates. The plants were grown in ambient ozone concentration (A-O<sub>3</sub>, 12 ppb) or elevated ozone concentration (E-O<sub>3</sub>, 86 ppb). The enzymatic activities were determined according to Supplementary Protocol 2. Values are means of four biological replicates. (A, B) Laccase activity, (C, D) catechol oxidase activity, (E, F) tyrosinase activity. A, C and E show the activity from the soluble fraction, and B, D and F show the activity from the ionically-bound fraction. Error bars indicate standard errors. KO, knock-out line; WT, wildtype; and OE, over-expression line. Laccase activity in the soluble fraction and tyrosinase activity in the ionically-bound fraction were not detected. ANOVA was conducted, and no significant effect of treatment, genotype and interaction between treatment and genotype was observed. The asterisk indicates the value was significantly affected by elevated ozone treatment ( $P < 0.05$ ). N.D., not detected; and n.s., not significant.



Supplementary Figure S12: Gene expression level of phytohormone-related genes on DAY 1 and DAY 20. Plants were treated with the ambient ozone concentration (A-O<sub>3</sub>, 40 ppb) or the elevated ozone

concentration (E-O<sub>3</sub>, 159 ppb) for 20 days. Total RNA was extracted from leaves and shoots on the indicated time points and qPCR was conducted with gene-specific primers (Table S1). ET, ethylene; JA, jasmonic acid; and SA, salicylic acid. Aminocyclopropane-1-carboxylic acid synthase (ACS) is the rate-limiting enzyme of ET production (Rzewuski and Sauter, 2008). It determines the production of ET under ozone stress together with another enzyme aminocyclopropane-1-carboxylic acid oxidase (ACO), which succeeds ACS in the biosynthetic pathway (Tuomainen *et al.*, 1997). Among several isoforms, the expression levels of *OsACS2* (*Os04g0578000*) and *OsACO7* (*Os01g0580500*) were previously shown to correlate with the formation of ET in rice in ozone stress (Cho *et al.*, 2008). OsEIL1 (Os03g0324300) is a cytosolic protein involved in ethylene signalling (Mao *et al.*, 2006; Rzewuski and Sauter, 2008). OsETR2 (Os04g0169100) is an ethylene receptor located on the plasma membrane, and its expression is induced by ethylene (Yau *et al.*, 2003). OsLOX8 (Os08g0509100) is involved in the first step of JA biosynthesis, and its expression is induced by ozone stress (Cho *et al.*, 2008). OsPAD4 (Os11g0195500) is supposedly involved in JA signalling (Ke *et al.*, 2014). OsICS1 (Os09g0361500) is involved in one of the SA biosynthetic pathways (Kyndt *et al.*, 2012). Values are means of four biological replicates. Error bars indicate standard errors. ANOVA was conducted for each day, and the significance is denoted as follows: G, genotype; T, treatment; GxT, genotype and treatment interaction; n.s., not significant; \*,  $P < 0.05$ ; \*\*,  $P < 0.01$ ; and \*\*\*,  $P < 0.001$ . KO, knock-out line; WT, wildtype; and OE, over-expression line.



Appendices

Nipponbare	CCATCAACGGCCACACCGGGGCCACCATCCGGCCGCTCAGGGGACACCCATCGTCTGCAACGCAAGCTCGTCTGACGGAGAAGCTGCCAT
Dongjin	CCATCAACGGCCACACCGGGGCCACCATCCGGCCGCTCAGGGGACACCCATCGTCTGCAACGCAAGCTCGTCTGACGGAGAAGCTGCCAT
Kasalath	CCATCAACGGCCACACCGGGGCCACCATCCGGCCGCTCAGGGGACACCCATCGTCTGCAACGCAAGCTCGTCTGACGGAGAAGCTGCCAT
SL41	CCATCAACGGCCACACCGGGGCCACCATCCGGCCGCTCAGGGGACACCCATCGTCTGCAACGCAAGCTCGTCTGACGGAGAAGCTGCCAT
Nipponbare	CCACTGGCAGGGCATCCGGCAGATCGGCACGCCGTGGGGGACGGCAGGAGGGCGTCAACCGATGCCCATCTCCCGGGGACACCTTCGCCTACACC
Dongjin	CCACTGGCAGGGCATCCGGCAGATCGGCACGCCGTGGGGGACGGCAGGAGGGCGTCAACCGATGCCCATCTCCCGGGGACACCTTCGCCTACACC
Kasalath	CCACTGGCAGGGCATCCGGCAGATCGGCACGCCGTGGGGGACGGCAGGAGGGCGTCAACCGATGCCCATCTCCCGGGGACACCTTCGCCTACACC
SL41	CCACTGGCAGGGCATCCGGCAGATCGGCACGCCGTGGGGGACGGCAGGAGGGCGTCAACCGATGCCCATCTCCCGGGGACACCTTCGCCTACACC
Nipponbare	TTCGTGTGCGACCGCCCGGACCTACATGTACCAAGCCCACTACGGGATGCAACGCTCGCGGGGCTCAACGGCATGATCGTCTGAGGTCGCCCCG
Dongjin	TTCGTGTGCGACCGCCCGGACCTACATGTACCAAGCCCACTACGGGATGCAACGCTCGCGGGGCTCAACGGCATGATCGTCTGAGGTCGCCCCG
Kasalath	TTCGTGTGCGACCGCCCGGACCTACATGTACCAAGCCCACTACGGGATGCAACGCTCGCGGGGCTCAACGGCATGATCGTCTGAGGTCGCCCCG
SL41	TTCGTGTGCGACCGCCCGGACCTACATGTACCAAGCCCACTACGGGATGCAACGCTCGCGGGGCTCAACGGCATGATCGTCTGAGGTCGCCCCG
Nipponbare	CGCCCGCGGGCAGCGGAGCGGAGCGGTTACAGTACGACGGGAGCACACCGTCTGCTCAACGACTGGTGGCACCAGGAGCAGTACGAGCAGGGGGC
Dongjin	CGCCCGCGGGCAGCGGAGCGGAGCGGTTACAGTACGACGGGAGCACACCGTCTGCTCAACGACTGGTGGCACCAGGAGCAGTACGAGCAGGGGGC
Kasalath	CGCCCGCGGGCAGCGGAGCGGAGCGGTTACAGTACGACGGGAGCACACCGTCTGCTCAACGACTGGTGGCACCAGGAGCAGTACGAGCAGGGGGC
SL41	CGCCCGCGGGCAGCGGAGCGGAGCGGTTACAGTACGACGGGAGCACACCGTCTGCTCAACGACTGGTGGCACCAGGAGCAGTACGAGCAGGGGGC
Nipponbare	GGGGCTCGCGTCCGTCGCCATGGTGTGGGTGGGGAGCGCAGTCTGCTCATCAACGGGGCGGGCGTGGTGGTGAACGCTGCTCGCCGGGAGC
Dongjin	GGGGCTCGCGTCCGTCGCCATGGTGTGGGTGGGGAGCGCAGTCTGCTCATCAACGGGGCGGGCGTGGTGGTGAACGCTGCTCGCCGGGAGC
Kasalath	GGGGCTCGCGTCCGTCGCCATGGTGTGGGTGGGGAGCGCAGTCTGCTCATCAACGGGGCGGGCGTGGTGGTGAACGCTGCTCGCCGGGAGC
SL41	GGGGCTCGCGTCCGTCGCCATGGTGTGGGTGGGGAGCGCAGTCTGCTCATCAACGGGGCGGGCGTGGTGGTGAACGCTGCTCGCCGGGAGC
Nipponbare	CGCGGTGCTGCAACGCTGTCGCAACCGGACTGCGCGCCGGGGTGTTCGCGTGGTCCCGGGGAAAGCAGTACCGTTCCCGCTCGCCAGGCTCACCTCC
Dongjin	CGCGGTGCTGCAACGCTGTCGCAACCGGACTGCGCGCCGGGGTGTTCGCGTGGTCCCGGGGAAAGCAGTACCGTTCCCGCTCGCCAGGCTCACCTCC
Kasalath	CGCGGTGCTGCAACGCTGTCGCAACCGGACTGCGCGCCGGGGTGTTCGCGTGGTCCCGGGGAAAGCAGTACCGTTCCCGCTCGCCAGGCTCACCTCC
SL41	CGCGGTGCTGCAACGCTGTCGCAACCGGACTGCGCGCCGGGGTGTTCGCGTGGTCCCGGGGAAAGCAGTACCGTTCCCGCTCGCCAGGCTCACCTCC
Nipponbare	CTCTCCGCGCTCAACTTCGAGATCGACTACCGCATGCAAGCTCATCCCCATCGCCATTGCGGCCATTATATATTTTACTTATACCCAAAATCBAAGT
Dongjin	CTCTCCGCGCTCAACTTCGAGATCGACTACCGCATGCAAGCTCATCCCCATCGCCATTGCGGCCATTATATATTTTACTTATACCCAAAATCBAAGT
Kasalath	CTCTCCGCGCTCAACTTCGAGATCGACTACCGCATGCAAGCTCATCCCCATCGCCATTGCGGCCATTATATATTTTACTTATACCCAAAATCBAAGT
SL41	CTCTCCGCGCTCAACTTCGAGATCGACTACCGCATGCAAGCTCATCCCCATCGCCATTGCGGCCATTATATATTTTACTTATACCCAAAATCBAAGT
Nipponbare	GAAAAGCACACAGCTGTAACCAAAAACAATGCTACTACATAAACCTCGATTTGATTAATCTCGATTCAAGAACATTAAGTGGCACACAGAGTAG
Dongjin	GAAAAGCACACAGCTGTAACCAAAAACAATGCTACTACATAAACCTCGATTTGATTAATCTCGATTCAAGAACATTAAGTGGCACACAGAGTAG
Kasalath	GAAAAGCACACAGCTGTAACCAAAAACAATGCTACTACATAAACCTCGATTTGATTAATCTCGATTCAAGAACATTAAGTGGCACACAGAGTAG
SL41	GAAAAGCACACAGCTGTAACCAAAAACAATGCTACTACATAAACCTCGATTTGATTAATCTCGATTCAAGAACATTAAGTGGCACACAGAGTAG
Nipponbare	TCATGGATCAGAAAACCATAGGGGTTCCACAAGATGCTGTAGCCAGATGATCTGGTTTCBAAGCTCACCTTCTAATTAATTAATATAGATCTTTTC
Dongjin	TCATGGATCAGAAAACCATAGGGGTTCCACAAGATGCTGTAGCCAGATGATCTGGTTTCBAAGCTCACCTTCTAATTAATTAATATAGATCTTTTC
Kasalath	TCATGGATCAGAAAACCATAGGGGTTCCACAAGATGCTGTAGCCAGATGATCTGGTTTCBAAGCTCACCTTCTAATTAATTAATATAGATCTTTTC
SL41	TCATGGATCAGAAAACCATAGGGGTTCCACAAGATGCTGTAGCCAGATGATCTGGTTTCBAAGCTCACCTTCTAATTAATTAATATAGATCTTTTC
Nipponbare	GTAAATATTTGTGTCTTTGTGTAGTATCGATCCACTTATCCCAAATTAAGTACAAATGAGATGGGACGCTGGGATAGGATTTACTAGTCTGTTA
Dongjin	GTAAATATTTGTGTCTTTGTGTAGTATCGATCCACTTATCCCAAATTAAGTACAAATGAGATGGGACGCTGGGATAGGATTTACTAGTCTGTTA
Kasalath	GTAAATATTTGTGTCTTTGTGTAGTATCGATCCACTTATCCCAAATTAAGTACAAATGAGATGGGACGCTGGGATAGGATTTACTAGTCTGTTA
SL41	GTAAATATTTGTGTCTTTGTGTAGTATCGATCCACTTATCCCAAATTAAGTACAAATGAGATGGGACGCTGGGATAGGATTTACTAGTCTGTTA
Nipponbare	ATTAGCATGTCTAACACATTTGCCATGCAAATGAATGGATGAAAAGCACCACATGCAAGAACTTGTAGGAAATTTGGACATTTGGTAGCTCTCGCGGTG
Dongjin	ATTAGCATGTCTAACACATTTGCCATGCAAATGAATGGATGAAAAGCACCACATGCAAGAACTTGTAGGAAATTTGGACATTTGGTAGCTCTCGCGGTG
Kasalath	ATTAGCATGTCTAACACATTTGCCATGCAAATGAATGGATGAAAAGCACCACATGCAAGAACTTGTAGGAAATTTGGACATTTGGTAGCTCTCGCGGTG
SL41	ATTAGCATGTCTAACACATTTGCCATGCAAATGAATGGATGAAAAGCACCACATGCAAGAACTTGTAGGAAATTTGGACATTTGGTAGCTCTCGCGGTG
Nipponbare	CGGTCAACCGGGTGAACCTTACAAGATTTGGGTTTTTCGCGTGGCATCTCGACCAGAGAGATGAGAGATCGCCAAAATCACGGTACATGTTTCGAGAAT
Dongjin	CGGTCAACCGGGTGAACCTTACAAGATTTGGGTTTTTCGCGTGGCATCTCGACCAGAGAGATGAGAGATCGCCAAAATCACGGTACATGTTTCGAGAAT
Kasalath	CGGTCAACCGGGTGAACCTTACAAGATTTGGGTTTTTCGCGTGGCATCTCGACCAGAGAGATGAGAGATCGCCAAAATCACGGTACATGTTTCGAGAAT
SL41	CGGTCAACCGGGTGAACCTTACAAGATTTGGGTTTTTCGCGTGGCATCTCGACCAGAGAGATGAGAGATCGCCAAAATCACGGTACATGTTTCGAGAAT
Nipponbare	CGCACCAATATCGAGACAGCAGCATCTTTTACTGTCCCGCAATTTGCCACTGCACGATATTCGGTAGGATTAGTATATTTTTGTACTACAAGTA
Dongjin	CGCACCAATATCGAGACAGCAGCATCTTTTACTGTCCCGCAATTTGCCACTGCACGATATTCGGTAGGATTAGTATATTTTTGTACTACAAGTA
Kasalath	CGCACCAATATCGAGACAGCAGCATCTTTTACTGTCCCGCAATTTGCCACTGCACGATATTCGGTAGGATTAGTATATTTTTGTACTACAAGTA
SL41	CGCACCAATATCGAGACAGCAGCATCTTTTACTGTCCCGCAATTTGCCACTGCACGATATTCGGTAGGATTAGTATATTTTTGTACTACAAGTA
Nipponbare	TATATATAATCCATCATGTTTGGGAGCGTCTCGAGCAAACTGCAAGCAAGCAGGTTGATTTGTCATGGAGAAATCTGTAAGCAAGCTGAATAGGCT
Dongjin	TATATATAATCCATCATGTTTGGGAGCGTCTCGAGCAAACTGCAAGCAAGCAGGTTGATTTGTCATGGAGAAATCTGTAAGCAAGCTGAATAGGCT
Kasalath	TATATATAATCCATCATGTTTGGGAGCGTCTCGAGCAAACTGCAAGCAAGCAGGTTGATTTGTCATGGAGAAATCTGTAAGCAAGCTGAATAGGCT
SL41	TATATATAATCCATCATGTTTGGGAGCGTCTCGAGCAAACTGCAAGCAAGCAGGTTGATTTGTCATGGAGAAATCTGTAAGCAAGCTGAATAGGCT
Nipponbare	GAAACAGTTAGCTGAATAGTGGGGATGATCTGACACAACTAATTTGGCCCTAGTTAGTGGGTTTGTACTTGGCTTTGGTGCATCAACTAGCTG
Dongjin	GAAACAGTTAGCTGAATAGTGGGGATGATCTGACACAACTAATTTGGCCCTAGTTAGTGGGTTTGTACTTGGCTTTGGTGCATCAACTAGCTG
Kasalath	GAAACAGTTAGCTGAATAGTGGGGATGATCTGACACAACTAATTTGGCCCTAGTTAGTGGGTTTGTACTTGGCTTTGGTGCATCAACTAGCTG
SL41	GAAACAGTTAGCTGAATAGTGGGGATGATCTGACACAACTAATTTGGCCCTAGTTAGTGGGTTTGTACTTGGCTTTGGTGCATCAACTAGCTG
Nipponbare	ACAACGAGTTTAAATTAATCTGGTAATAATGCCATCCAACCAAATGTGTTGACTCATATATCGAACATTGACTTGGGTACTACGTAGTATATGACGAGACT
Dongjin	ACAACGAGTTTAAATTAATCTGGTAATAATGCCATCCAACCAAATGTGTTGACTCATATATCGAACATTGACTTGGGTACTACGTAGTATATGACGAGACT
Kasalath	ACAACGAGTTTAAATTAATCTGGTAATAATGCCATCCAACCAAATGTGTTGACTCATATATCGAACATTGACTTGGGTACTACGTAGTATATGACGAGACT
SL41	ACAACGAGTTTAAATTAATCTGGTAATAATGCCATCCAACCAAATGTGTTGACTCATATATCGAACATTGACTTGGGTACTACGTAGTATATGACGAGACT
Nipponbare	AGCAACTCGTCAATGGGCTCATGGCCT---TCGCAATGAAGCTTCTTTCGCTGCCACCGAATAGTTCCGATTAAACAGCCCTACGGCCTTGACTTGC
Dongjin	AGCAACTCGTCAATGGGCTCATGGCCT---TCGCAATGAAGCTTCTTTCGCTGCCACCGAATAGTTCCGATTAAACAGCCCTACGGCCTTGACTTGC
Kasalath	AGCAACTCGTCAATGGGCTCATGGCCT---TCGCAATGAAGCTTCTTTCGCTGCCACCGAATAGTTCCGATTAAACAGCCCTACGGCCTTGACTTGC
SL41	AGCAACTCGTCAATGGGCTCATGGCCT---TCGCAATGAAGCTTCTTTCGCTGCCACCGAATAGTTCCGATTAAACAGCCCTACGGCCTTGACTTGC
Nipponbare	TATTACTCTATCTGTTTCATATTACAAGATTTTCTAGTATTGTCACATTCATATAGATGTAATGAATCTTGACATACATAATATATGCTAGATTCATT
Dongjin	TATTACTCTATCTGTTTCATATTACAAGATTTTCTAGTATTGTCACATTCATATAGATGTAATGAATCTTGACATACATAATATATGCTAGATTCATT
Kasalath	TATTA-----
SL41	TATTA-----
Nipponbare	AACATATATATGAATATAGCAATGCTAGAAAGTCTTATAATAAGAAAAGCAGAAAGTATTTTTTAAATATTCGTTACTAGATGATPATAAATAGTC
Dongjin	AACATATATATGAATATAGCAATGCTAGAAAGTCTTATAATAAGAAAAGCAGAAAGTATTTTTTAAATATTCGTTACTAGATGATPATAAATAGTC
Kasalath	-----TTTTTTTAAATATTCGTTACTAGATGATPATAAATAGTC
SL41	-----TTTTTTTAAATATTCGTTACTAGATGATPATAAATAGTC
Nipponbare	ACTAC---TAGAAAACATTTTCGACGGCGCTAAAATTCGCTGCTCCATGAAAACATTTTTTGAGCGGCTAAACTAGTTTACAAATPATAAACAATA
Dongjin	ACTAC---TAGAAAACATTTTCGACGGCGCTAAAATTCGCTGCTCCATGAAAACATTTTTTGAGCGGCTAAACTAGTTTACAAATPATAAACAATA
Kasalath	ACTACGACTAGAAAACATTTTCGACGGCGCTAAAATTCGCTGCTCCATGAAAACATTTTTTGAGCGGCTAAACTAGTTTACAAATPATAAACAATA
SL41	ACTACGACTAGAAAACATTTTCGACGGCGCTAAAATTCGCTGCTCCATGAAAACATTTTTTGAGCGGCTAAACTAGTTTACAAATPATAAACAATA

Supplementary Figure S13 (continued)







## Appendices

```
Nipponbare ACACACCTGCAGGCTGCACCATCCGCATCGAGTACTCCAGACCAAAAAGATAGC SCACTCCAGTTAAAAACAAAAAGAACATTAACATCATT  
Dongjin ACACACCTGCAGGCTGCACCATCCGCATCGAGTACTCCAGACCAAAAAGATAGC SCACTCCAGTTAAAAACAAAAAGAACATTAACATCATT  
Kasalath ACACACCTGCAGGCTGCACCATCCGCATCGAGTACTCCAGACCAAAAAGATAGC SCACTCCAGTTAAAAACAAAAAGAACATTAACATCATT  
SL41 ACACACCTGCAGGCTGCACCATCCGCATCGAGTACTCCAGACCAAAAAGATAGC SCACTCCAGTTAAAAACAAAAAGAACATTAACATCATT  
  
Nipponbare TAGTTATATTAAGGCTATATAGCTATATATTTACACATCTTTTTAGTTTCATACCACCACACTA-----TCCTTCCATCTGTGACGGCAC  
Dongjin TAGTTATATTAAGGCTATATAGCTATATATTTACACATCTTTTTAGTTTCATACCACCACACTA-----TCCTTCCATCTGTGACGGCAC  
Kasalath TAGTTATATTAAGGCTATATAGCTATATATTTACACATCTTTTTAGTTTCATACCACCACACTAETACAGTTCCTTCCATCTGTGACGGCAC  
SL41 TAGTTATATTAAGGCTATATAGCTATATATTTACACATCTTTTTAGTTTCATACCACCACACTAETACAGTTCCTTCCATCTGTGACGGCAC
```

### Supplementary Figure S13 (continued)

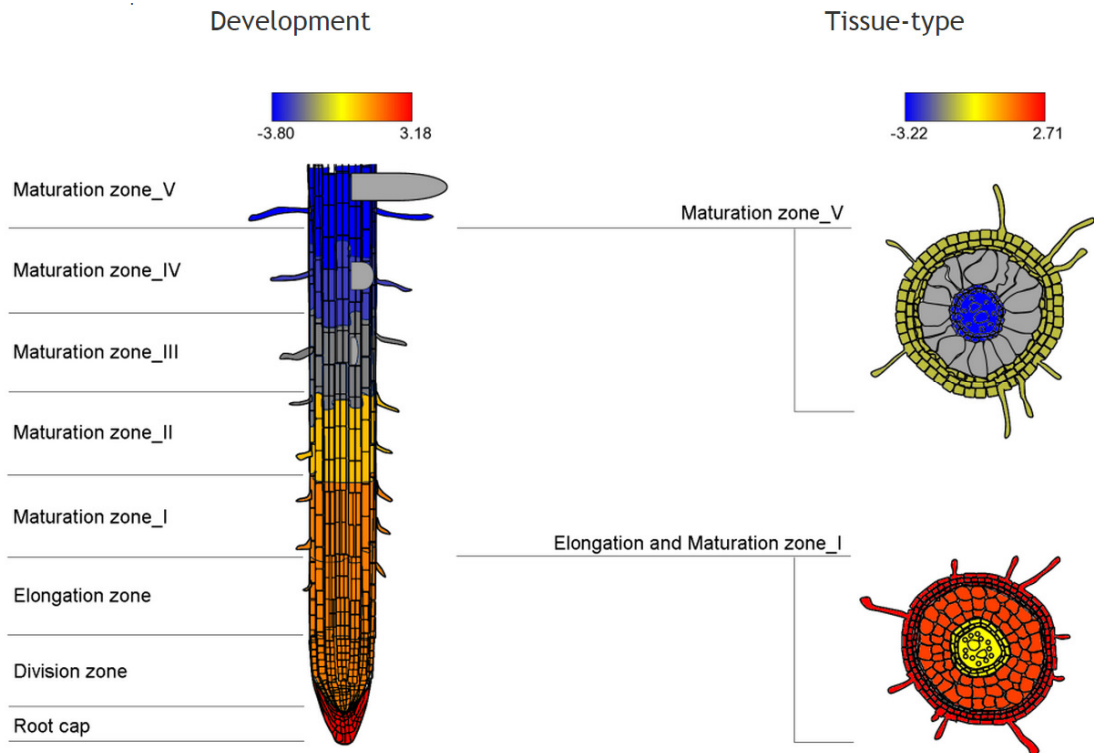
Upstream 1,500 bp, *OsORAPI* region and downstream 1,000 bp sequences were obtained either by sequencing experiment or from public database (RAP-DB, <http://rapdb.dna.affrc.go.jp/>, as of June 2014). Multiple alignment was conducted using MEGA5 software (Tamura *et al.*, 2011). Matched nucleotides are shown in black colour. Transcript and splicing sites information was obtained from RAP-DB based on Nipponbare sequence. Since annotated genome information of Kasalath was not available, the start codon was predicted as follows. First, the obtained Kasalath sequence was BLASTed against RNA-seq read archive of Kasalath (<http://www.ncbi.nlm.nih.gov/sra>, experiment ID DRA000685 (Oono *et al.*, 2013), as of September 2014). The most upstream reading was determined as the transcription initiation site. The start codon in Kasalath and SL41 was determined to provide the longest open reading frame in the transcript.

Appendices

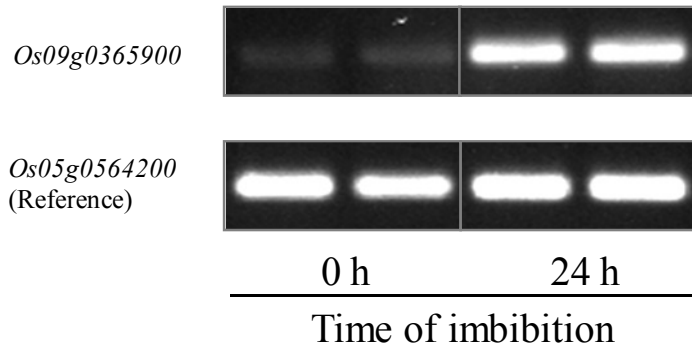
	signal peptide		
Nipponbare	MRCSDR-----LLCSLFLAALFGVAAATRRHDWDISYQFTSPDCVRKLAVTINGHTPGPTIRAVQGDTIVVNVKNSLLETENVAIHHWGIRQIGTPW	94	
Dongjin	MRCSDR-----LLCSLFLAALFGVAAATRRHDWDISYQFTSPDCVRKLAVTINGHTPGPTIRAVQGDTIVVNVKNSLLETENVAIHHWGIRQIGTPW	94	
Kasalath	MSGVASRSMERRLLCSLFLAALFGVAAATRRHDWDISYQFTSPDCVRKLAVTINGHTPGPTIRAVQGDTIVVNVKNSLLETENVAIHHWGIRQIGTPW	100	
SL41	MSGVASRSMERRLLCSLFLAALFGVAAATRRHDWDISYQFTSPDCVRKLAVTINGHTPGPTIRAVQGDTIVVNVKNSLLETENVAIHHWGIRQIGTPW	100	
			* *
Nipponbare	ADGTEGVTCPIILPGDTFAYTFVVDPRPGTYMYHAHYGMQRSAGLNGMIVVEVAPGAAGDGEREPFRYDGEHTVLLNDWWHRSTYEQAAGLASVPMVWVGE	194	
Dongjin	ADGTEGVTCPIILPGDTFAYTFVVDPRPGTYMYHAHYGMQRSAGLNGMIVVEVAPGAAGDGEREPFRYDGEHTVLLNDWWHRSTYEQAAGLASVPMVWVGE	194	
Kasalath	ADGTEGVTCPIILPGDTFAYTFVVDPRPGTYMYHAHYGMQRSAGLNGMIVVEVAPGAAGDGEREPFRYDGEHTVLLNDWWHRSTYEQAAGLASVPMVWVGE	200	
SL41	ADGTEGVTCPIILPGDTFAYTFVVDPRPGTYMYHAHYGMQRSAGLNGMIVVEVAPGAAGDGEREPFRYDGEHTVLLNDWWHRSTYEQAAGLASVPMVWVGE	200	
	# * *		
Nipponbare	PQSLLINGRGRFVNCSSSPA#AASCNVSHPDCAPAVFAVVPKTYRFRVASVTSLSALNFEIEGHEMTVVEADGHYVVPVVKLNLIYSGETYSVLITAD	294	
Dongjin	PQSLLINGRGRFVNCSSSPA#AASCNVSHPDCAPAVFAVVPKTYRFRVASVTSLSALNFEIEGHEMTVVEADGHYVVPVVKLNLIYSGETYSVLITAD	294	
Kasalath	PQSLLINGRGRFVNCSSSPA#AASCNVSHPDCAPAVFAVVPKTYRFRVASVTSLSALNFEIEGHEMTVVEADGHYVVPVVKLNLIYSGETYSVLITAD	300	
SL41	PQSLLINGRGRFVNCSSSPA#AASCNVSHPDCAPAVFAVVPKTYRFRVASVTSLSALNFEIEGHEMTVVEADGHYVVPVVKLNLIYSGETYSVLITAD	300	
	# # #		
Nipponbare	QDPNRNYWLASNVVSRKPATPTGTAVLAYYGRRNSPRARPPPTPPAGPAWNDTAYRVRQSLATVAHPAHAVPPPPTSDRTILLLNTQNKIGGQIKWALN	394	
Dongjin	QDPNRNYWLASNVVSRKPATPTGTAVLAYYGRRNSPRARPPPTPPAGPAWNDTAYRVRQSLATVAHPAHAVPPPPTSDRTILLLNTQNKIGGQIKWALN	394	
Kasalath	QDPNRNYWLASNVVSRKPATPTGTAVLAYYGRRNSPRARPPPTPPAGPAWNDTAYRVRQSLATVAHPAHAVPPPPTSDRTILLLNTQNKIGGQIKWALN	400	
SL41	QDPNRNYWLASNVVSRKPATPTGTAVLAYYGRRNSPRARPPPTPPAGPAWNDTAYRVRQSLATVAHPAHAVPPPPTSDRTILLLNTQNKIGGQIKWALN	400	
			* * *
Nipponbare	NVSFTLPHTPYLVAMKRGLLGAFDQRPPPEYAGAAAFDVIYVQGNPNATTSAPYRLRFGSVVDVVLQANMLAANSSETHPWHLHGHDFFVLGHGAGR	494	
Dongjin	NVSFTLPHTPYLVAMKRGLLGAFDQRPPPEYAGAAAFDVIYVQGNPNATTSAPYRLRFGSVVDVVLQANMLAANSSETHPWHLHGHDFFVLGHGAGR	494	
Kasalath	NVSFTLPHTPYLVAMKRGLLGAFDQRPPPEYAGAAAFDVIYVQGNPNATTSAPYRLRFGSVVDVVLQANMLAANSSETHPWHLHGHDFFVLGHGAGR	500	
SL41	NVSFTLPHTPYLVAMKRGLLGAFDQRPPPEYAGAAAFDVIYVQGNPNATTSAPYRLRFGSVVDVVLQANMLAANSSETHPWHLHGHDFFVLGHGAGR	500	
			* * *
Nipponbare	FDPVHPAAYNLRDPIMKNTVAVHPFGWTALRFRADNE#VWAFHCHIEAHFFMGMGIV#EEGVERVGEVLPPEIMCGCKTRGGH	577	
Dongjin	FDPVHPAAYNLRDPIMKNTVAVHPFGWTALRFRADNE#VWAFHCHIEAHFFMGMGIV#EEGVERVGEVLPPEIMCGCKTRGGH	577	
Kasalath	FDPVHPAAYNLRDPIMKNTVAVHPFGWTALRFRADNE#VWAFHCHIEAHFFMGMGIV#EEGVERVGEVLPPEIMCGCKTRGGH	583	
SL41	FDPVHPAAYNLRDPIMKNTVAVHPFGWTALRFRADNE#VWAFHCHIEAHFFMGMGIV#EEGVERVGEVLPPEIMCGCKTRGGH	583	
	*** * *		

Multicopper-oxidases signature 1/2

Supplementary Figure S14: Multiple alignment of OsORAP1 protein from Nipponbare, Dongjin, Kasalath and SL41. The amino acid sequences were obtained from the genomic sequences of OsORAP1, and multiple alignment was conducted using MEGA5 software (Tamura *et al.*, 2011). Prediction of signal peptide was conducted using SignalP 4.1 (<http://www.cbs.dtu.dk/services/SignalP/>, as of October 2014). The sites with completely conserved amino acids are shown in black colour, and the sites with similar amino acids are shown in gray colour. Multicopper-oxidases signature 1 and 2 and signal peptide are shown in red squares. Asterisk (\*) shows predicted copper-binding sites. Pound sign (#) indicates cysteine residues forming disulfide bonds (Lin *et al.*, 2013).



Supplementary Figure S15: Expression patterns of *OsORAPI* in rice root tissues. Red colour shows high expression, and blue colour shows low expression. The data was taken from RiceXPro database (<http://ricexpro.dna.affrc.go.jp/>). The values indicate the normalized signal intensity ( $\log_2$ ) when the average expression level was set to 0.



Supplementary Figure S16: Expression of *OsORAPI* during seed imbibition. The seeds of Dongjin were dehusked, soaked in deionized water, and incubated at 28 °C for 24 h in dark. RNA was extracted from the seeds, and RT-PCR was conducted. The expression levels of *OsORAPI* (*Os09g0365900*, using OsORAP1-F1/R1 primers) and reference gene (*Os05g0564200*) are shown.

Appendices

Supplementary Table S1: Primers used for the study.

Gene name	Gene ID	5'-Forward primer-3'	5'-Reverse primer-3'
<i>OsORAP1</i> -F1/R1	Os09g0365900	CAGTCGCTGCTCATCAACGGGC	CCACCACCGTCATCTCGTGCC
<i>OsORAP1</i> -F2/R2 (for qPCR)	Os09g0365900	TAGCTCAACAGGACGCACAC	ACACCGCATCATGTTCACCTCT
Rice AO homologue	Os09g0507300	GTGAGGTTTCAGGGCGAGCAA	TGACTAAGCTGTTGGACGTTTCG
Rice AO homologue	Os06g0567200	CGGCATCAGACAGATCGGGA	CGAAGCGATAGGTGAAGGTTTC
Rice AO homologue	Os06g0567900	TGACGTGGGACGTGGAGTA	GCGTGCCAAACTGTCTGATG
<i>Osmir528</i>	Osmir528	CCTGGAAGGGGCATGCA	GTGCAGGGTCCGAGGT
<i>OsACS2</i>	Os04g0578000	GGAGTCCGACACCAAATCAATG	GTCCAGAGAAAGCTGGTTCTC
<i>OsACO7</i>	Os01g0580500	CCTGTAAGGACTGGGGCTTC	TCCAGGTGCTCGTCGTAATG
<i>OsEIL1</i>	Os03g0324300	CAACCGTGTCTACACCTGCC	TTCCGGTCAAGGAACCCGTA
<i>OsETR2</i>	Os04g0169100	AGTCGCAGTCGCCCTATCAC	CAGCAAGTCCCTGTGTTGCG
<i>OsNPR1</i>	Os01g0194300	AGAAGGGACCCACAACCTCGG	TCCTCGCCAAAGCAACTCGG
<i>OsWRKY45</i>	Os05g0322900	GACGAGGTTGTCTTCGATCTG	CGTGGAATCCATCTTCTTTCGATC
<i>OsICS1</i>	Os09g0361500	AGTAAAGGTCGTACTIONGGCAAGG	AGGAGCATCAGGTGGCTGTA
<i>OsOPR7</i>	Os08g0459600	CATTGAAGCAGGTTTTGATGGCA	CCATACTCGTCAGTGC GGTC
<i>OsLOX8</i>	Os08g0509100	TCTCTCGATTCTGCACGCCT	GGCTGGACGATGGATTGAGC
<i>OsJAZ8</i>	Os09g0439200	CACACAACAGTCTTCCCAGATCTG	TCACCGTTAGCTTGCTTGGAC
<i>OsJAmyb</i>	Os11g0684000	GCAAGAGGTTCAAGGATGCCA	AGCTAGTACCATGCTCGGA
<i>OsPAD4</i>	Os11g0195500	GCTGTGCAGATCCCCTGAAT	TGACACAAAGCACCGGAGGA
<i>U2 snRNP</i> (Reference, rice)	Os05g0564200	CACAACAGGCCAACTGTGTC	GAGGGTCTCAACCTCACCAA
Arabidopsis AO homologue (for genotyping and RT-PCR)	At5g21100	ATCCACGTCGTCAACAAACTC	AGCAAGAGCAGTTGTGCTAGC
Arabidopsis AO homologue (for genotyping)	At4g39830	TCCACGGTTGAATTGAATCTC	GTATGTCAGAGAAAGCCACCG
Arabidopsis AO homologue (for RT-PCR)	At4g39830	GTCTCAAACGCTGATTGTTCG	CGTAGTGTCCGCTCTGCTTCA
<i>AtPP2AA3</i> (Reference, Arabidopsis)	At1g13320	AGCGTAATCGGTAGGGAGTG	CGATAAGCACAGCAATCGGG
<i>NbEF-1a</i> (Reference, tobacco)	AY206004	TGTGGAAGTTTGAGACCACC	GCAAGCAATGCGTGCTCAC

Gene name, gene ID and primer sequences are shown. The primer sequences for *NbEF-1a* were taken from Ishihama *et al.* (2011). The primer sequences for *Osmir528* were taken from Lima *et al.* (2011). The primers for genotyping of *Arabidopsis* mutants were used with a vector primer 5'-ATT TTG CCG ATT TCG GAA C-3' to confirm T-DNA insertion.

## Appendices

Supplementary Table S2: Expression levels of two *Arabidopsis* genes under several stress conditions.

Stress	<i>At4g39830</i>	<i>At5g21100</i>	Reference
Cold stress (12 h)	2.4	0.2	Kilian <i>et al.</i> , 2007
Salinity stress (12 h)	1.0	0.6	Kilian <i>et al.</i> , 2007
Drought stress (12 h)	1.3	1.0	Kilian <i>et al.</i> , 2007
Wound (12 h)	1.1	0.4	Kilian <i>et al.</i> , 2007
Ozone (125 ppb, 3 h)	4.2	0.8	Booker <i>et al.</i> , 2012
Pathogen ( <i>P. syringae</i> ) (12 h)	8.1	0.4	De Vos <i>et al.</i> , 2005
Chitin treatment (30 min)	4.9	1.1	Ramonell <i>et al.</i> , 2005
Elicitor (elf18) treatment (10 h)	19.3	0.2	Tintor <i>et al.</i> , 2013

Expression data were obtained from publicly available microarray data sources. The fold increase values under the denoted stress conditions are shown for *At4g39830* and *At5g21100*. The left column shows the type and duration of stress treatment.

## Appendices

Table S3: *Cis*-elements found only in Nipponbare *OsORAP1* promoter region.

**Only in Nipponbare**

Name	Sequence	PLACE ID	Description
CANBNA PA	CNAACAC	S000148	Core of "(CA) <sub>n</sub> element" in storage protein genes in <i>Brassica napus</i> (B.n.); embryo- and endosperm-specific transcription of napin (storage protein) gene, napA; seed specificity; activator and repressor
AGCBOXNP GLB	AGCCGCC	S000232	"AGC box" repeated twice in a 61 bp enhancer element in tobacco (N.p.) class I beta-1,3-glucanase (GLB) gene; "GCC-box"; Binding sequence of Arabidopsis AtERFs; AtERF1,2 and 5 functioned as activators of GCC box-dependent transcription; AtERF3 and 4 acted as repressors; AtERF proteins are stress signal-response factors; EREBP2 binding site; Conserved in most PR-protein genes; Rice MAPK (BWMK1) phosphorylates OS EREBP1, which enhance DNA-binding activity of the factor to the GCC box;
GCCCORE	GCCGCC	S000430	Core of GCC-box found in many pathogen-responsive genes such as PDF1.2, Thi2.1, and PR4; Has been shown to function as ethylene-responsive element; Appears to play important roles in regulating jasmonate-responsive gene expression; Tomato Pti4 (ERF) regulates defence-related gene expression via GCC box and non-GCC box cis elements (Myb1 (GITAGTT) and G-box(CACGTG))
CGACGOSA MY3	CGACG	S000205	"CGACG element" found in the GC-rich regions of the rice (O.s.) Amy3D and Amy3E amylase genes, but not in Amy3E gene; May function as a coupling element for the G box element
NODCON1 GM	AAAGAT	S000461	One of two putative nodulin consensus sequences
OSE1ROOT NODULE	AAAGAT	S000467	One of the consensus sequence motifs of organ-specific elements (OSE) characteristic of the promoters activated in infected cells of root nodules
CIACADIA NLELHC	CAANNNN ATC	S000252	Region necessary for circadian expression of tomato (L.e.) Lhc gene
IBOXCORE	GATAA	S000199	"I box"; "I-box"; Conserved sequence upstream of light-regulated genes; Conserved sequence upstream of light-regulated genes of both monocots and dicots
LEAFYATA G	CCAATGT	S000432	Target sequence of LEAFY in the intron of AGAMOUS gene in Arabidopsis
CPBCSPOR	TATTAG	S000491	The sequence critical for Cytokinin-enhanced Protein Binding in vitro, found in -490 to -340 of the promoter of the cucumber (CS) POR (NADPH-protochlorophyllide reductase) gene
SREATMSD	TTATCC	S000470	"sugar-repressive element (SRE)" found in 272 of the 1592 down-regulated genes after main stem decapitation in Arabidopsis
REBETALGL HCB21	CGGATA	S000363	"REbeta" found in <i>Lemma gibba</i> Lhcb21 gene promoter; Located at -114 to -109; A GATA sequence created at a position six nucleotides upstream could replace the function of REbeta; Required for phytochrome regulation
HEXAMERA TH4	CCGTCC	S000146	hexamer motif of Arabidopsis thaliana (A.t.) histone H4 promoter
POLASIG2	AATTAAG	S000081	"PolyA signal"; poly A signal found in rice alpha-amylase; -10 to -30 in the case of animal genes. AATAAA; AATAAT; AATTAAG; AATAAG



## Appendices

Table S3 (continued)

Name	Sequence	PLACE ID	Description
ANAERO1C ONSENSUS	AAACAAA	S000477	One of 16 motifs found in silico in promoters of 13 anaerobic genes involved in the fermentative pathway (anaerobic set 1)(Mohanty et al., 2005); Arbitrary named ANAERO1CONSENSUS by the PLACEdb curator
UPIATMSD	GGCCCAW WW	S000471	"Up1" motif found in 162 of the 1184 up-regulated genes after main stem decapitation in Arabidopsis
AMYBOX2 TATCCAYM OTIFOSRA MY3D	TATCCAT TATCCAY	S000021 S000256	"amylase box"; "amylase element"; Conserved sequence found in 5'upstream region of alpha-amylase gene of rice, wheat, barley; "amylase box" (Huang et al. 1990); "amylase element" (Hwang et al., 1998) "TATCCAY motif" found in rice (O.s.) RAmY3D alpha-amylase gene promoter; Y=T/C; a GATA motif as its antisense sequence; TATCCAY motif and G motif (see S000130) are responsible for sugar repression (Toyofuku et al. 1998)
SEF1MOTIF	ATATTTAW W	S000006	"SEF1 (soybean embryo factor 1)" binding motif, sequence found in 5'-upstream region (-640; -765) of soybean beta-conglucinin (7S globulin) gene
NTBBF1AR ROLB	ACTTTA	S000273	NtBBF1(Dof protein from tobacco) binding site in Agrobacterium rhizogenes (A.r.) rolB gene; Found in regulatory domain B (-341 to -306); Required for tissue-specific expression and auxin induction
TAAAGSTK ST1	TAAAG	S000387	TAAAG motif found in promoter of Solanum tuberosum (S.t.) KST1 gene; Target site for trans-acting StDof1 protein controlling guard cell-specific gene expression; KST1 gene encodes a K <sup>+</sup> influx channel of guard cells
BIHD1OS	TGTC A	S000498	Binding site of OsBIHD1, a rice BELL homeodomain transcription factor
AUXREPSIA A4	KGTCCCAT	S000026	"AuxRE (Auxine responsive element )" of pea (P.s.) PS-IAA4/5 gene; Indoleacetic acid-inducible genes; domain A; TGA1a is preferentially expressed in root tip meristems; TGA1a may contribute to the expression of GST isoenzymes, especially in root tip meristems
TATABOX3 ERELEE4	TATTAAT AWTTCAA A	S000110 S000037	"TATA box"; TATA box found in the 5'upstream region of sweet potato sporamin A gene "ERE (ethylene responsive element)" of tomato (L.e.) E4 and carnation GST1 genes; GST1 is related to senescence; Found in the 5'-LTR region of TLC1.1 retrotransposon family in Lycopersicon chilense (Tapia et al.); ERE motifs mediate ethylene-induced activation of the U3 promoter region
BP5OSWX	CAACGTG	S000436	OsBP-5 (a MYC protein) binding site in Wx promoter
T/GBOXATP IN2	AACGTG	S000458	"T/G-box" found in tomato proteinase inhibitor II (pin2) and leucine aminopeptidase (LAP) genes; Involved in jasmonate (JA) induction of these genes; bHLH-Leu zipper JAMYC2 and JAMYC10 proteins specifically recognize this motif (Boter et al., 2004)
SORLREP3A T	TGTATATA T	S000488	one of "Sequences Over-Represented in Light-Repressed Promoters (SORLREPs) in Arabidopsis; Computationally identified phyA-repressed motifs

Upstream 1,000 bp from the transcript initiation site of Nipponbare and Kasalath OsORAP1 was subjected to *cis*-element search through PLACE database (<http://www.dna.affrc.go.jp/PLACE/>, as of May 2015) using default settings. The *cis*-elements which appear only in Nipponbare are shown with name, ID and description. N = A/T/C/G; K = G/T; W = A/T; Y = C/T.

## Appendices

Table S4: *Cis*-elements common in Nipponbare and Kasalath *OsORAP1* promoter region.

### Nipponbare and Kasalath

Name	Sequence	PLACE ID	Description
ARRIAT	NGATT	S000454	"ARR1-binding element" found in Arabidopsis; ARR1 is a response regulator; N=G/A/C/T; AGATT is found in the promoter of rice non-symbiotic haemoglobin-2 (NSHB) gene (Ross et al., 2004)
RAVIAAT	CAACA	S000314	Binding consensus sequence of Arabidopsis (A.t.) transcription factor, RAV1; RAV1 specifically binds to DNA with bipartite sequence motifs of RAV1-A (CAACA) and RAV1-B (CACCTG); RAV1 protein contain AP2-like and B3-like domains; The AP2-like and B3-like domains recognize the CAACA and CACCTG motifs, respectively; The expression level of RAV1 were relatively high in rosette leaves and roots
POLASIG3	AATAAT	S000088	"Plant polyA signal"; Consensus sequence for plant polyadenylation signal
DOFCOREZ M	AAAG	S000265	Core site required for binding of Dof proteins in maize (Z.m.); Dof proteins are DNA binding proteins, with presumably only one zinc finger, and are unique to plants; Four cDNAs encoding Dof proteins, Dof1, Dof2, Dof3 and PBF, have been isolated from maize; PBF is an endosperm specific Dof protein that binds to prolamins box; Maize Dof1 enhances transcription from the promoters of both cytosolic orthophosphate kinase (C <sub>4</sub> PEPK) and a non-photosynthetic PEPC gene; Maize Dof2 suppressed the C <sub>4</sub> PEPK promoter
GATABOX	GATA	S000039	"GATA box"; GATA motif in CaMV 35S promoter; Binding with ASF-2; Three GATA box repeats were found in the promoter of Petunia (P.h.) chlorophyll a/b binding protein, Cab22 gene; Required for high level, light regulated, and tissue specific expression; Conserved in the promoter of all LHCII type I Cab genes
NODCON2 GM	CTCTT	S000462	One of two putative nodulin consensus sequences
OSE2ROOT NODULE	CTCTT	S000468	One of the consensus sequence motifs of organ-specific elements (OSE) characteristic of the promoters activated in infected cells of root nodules
CURECORE CR	GTAC	S000493	GTAC is the core of a CuRE (copper-response element) found in <i>Cyc6</i> and <i>Cpx1</i> genes in <i>Chlamydomonas</i> ; Also involved in oxygen-response of these genes
CACTFTPP CA1	YACT	S000449	Tetranucleotide (CACT) is a key component of Mem1 (mesophyll expression module 1) found in the cis-regulatory element in the distal region of the phosphoenolpyruvate carboxylase ( <i>ppcA1</i> ) of the C4 dicot <i>F. trinervia</i>
GTGANTG1 0	GTGA	S000378	"GTGA motif" found in the promoter of the tobacco (N.t.) late pollen gene <i>gl0</i> which shows homology to pectate lyase and is the putative homologue of the tomato gene <i>lat56</i> ; Located between -96 and -93
EECCRCAH 1	GANTINC	S000494	"EEC"; Consensus motif of the two enhancer elements, EE-1 and EE-2, both found in the promoter region of the <i>Chlamydomonas</i> <i>Cah1</i> (encoding a periplasmic carbonic anhydrase); Binding site of Myb transcription factor LCR1 (see Yoshioka et al., 2004)
GTICONSE NSUS	GRWAAW	S000198	Consensus GT-1 binding site in many light-regulated genes, e.g., RBCS from many species, PHYA from oat and rice, spinach RCA and PETA, and bean CHS15; For a compilation of related GT elements and factors, see Villain et al. (1996); GT-1 can stabilize the TFIIA-TBP-DNA (TATA box) complex; The activation mechanism of GT-1 may be achieved through direct interaction between TFIIA and GT-1; Binding of GT-1-like factors to the PR-1a promoter influences the level of SA-inducible gene expression
CAATBOX1	CAAT	S000028	"CAAT promoter consensus sequence" found in <i>legA</i> gene of pea
ROOTMOTI FTAPOX1	ATATT	S000098	Motif found both in promoters of <i>roLD</i>

## Appendices

Table S4 (continued)

Name	Sequence	PLACE ID	Description
SITEIIATCY TC	TGGGCY	S000474	"Site II element" found in the promoter regions of cytochrome genes (Cytc-1, Cytc-2) in Arabidopsis; Located between -147 and -156 from the translational starts sites (Welchen et al., 2005)
REALPHAL GLHCB21	AACCAA	S000362	"REalpha" found in Lemna gibba Lhcb21 gene promoter; Located at -134 to -129; Binding site of proteins of whole-cell extracts; The DNA binding activity is high in etiolated plants but much lower in green plants; Required for phytochrome regulation
CCAATBOX 1	CCAAT	S000030	Common sequence found in the 5'-non-coding regions of eukaryotic genes; "CCAAT box" found in the promoter of heat shock protein genes; Located immediately upstream from the most distal HSE of the promoter; "CCAAT box" act cooperatively with HSEs to increase the hs promoter activity
MYBST1	GGATA	S000180	Core motif of MybSt1 (a potato MYB homolog) binding site; MybSt1 cDNA clone was isolated by using CaMV 35S promoter domain A as a probe (Baranowskij et al. 1994); The Myb motif of the MybSt1 protein is distinct from the plant Myb DNA binding domain described so far
CBFHV	RYCGAC	S000497	Binding site of barley (H.v.) CBF1, and also of barley CBF2; CBF = C-repeat (CRT) binding factors; CBFs are also known as dehydration-responsive element (DRE) binding proteins (DREBs)
SORLIP2AT	GGGCC	S000483	one of "Sequences Over-Represented in Light-Induced Promoters (SORLIPs) in Arabidopsis; Computationally identified phyA-induced motifs
EBOXBNNNA PA	CANNTG	S000144	E-box of napA storage-protein gene of Brassica napus (B.n.); See S000042 (CACGTGMOTIF); see S000407 (Myc consensus: CANNTG); This sequence is also known as RRE (R response element)(Hartmann et al., 2005)
MYCCONS ENSUSAT	CANNTG	S000407	MYC recognition site found in the promoters of the dehydration-responsive gene rd22 and many other genes in Arabidopsis; Binding site of ATMYC2 (previously known as rd22BP1); see S000144 (E-box; CANNTG); S000174 (MYCATRD22); MYC recognition sequence in CBF3 promoter; Binding site of ICE1 (inducer of CBF expression 1) that regulates the transcription of CBF/DREB1 genes in the cold in Arabidopsis; ICE1 (Chinnusamy et al., 2004); This sequence is also known as RRE (R response element)(Hartmann et al., 2005)
POLLENILE LAT52	AGAAA	S000245	One of two co-dependent regulatory elements responsible for pollen specific activation of tomato (L.e.) lat52 gene; Found at -72 to -68 region; See S000246 (POLLEN2LELAT52); AGAAA and TCCACCATA (S000246) are required for pollen specific expression; Also found in the promoter of tomato endo-beta-mannanase gene (LeMAN5) gene (Filichkin et al. 2004)
TATCCAOS AMY	TATCCA	S000403	"TATCCA" element found in alpha-amylase promoters of rice (O.s.) at positions ca.90 to 150bp upstream of the transcription start sites; Binding sites of OsMYBS1, OsMYBS2 and OsMYBS3 which mediate sugar and hormone regulation of alpha-amylase gene expression
RYREPEAT BNNAPA	CATGCA	S000264	RY repeat" found in RY/G box (the complex containing the two RY repeats and the G-box) of napA gene in Brassica napus (B.n.); Found between -78 and -50; Required for seed specific expression; dist B ABRE mediated transactivation by ABI3 and ABI3-dependent response to ABA; a tetramer of the composite RY/G complex mediated only ABA-independent transactivation by ABI3; B2 domain of ABI3 is necessary for ABA-independent and ABA-dependent activation through the dist B ABRE
RYREPEATL EGUMINBO X	CATGCAY	S000100	"RY repeat (CATGCAY)" or legumin box found in seed-storage protein genes in legume such as soybean (G.m.)
RHERPATE XPA7	KCACGW	S000512	"Right part of RHEs (Root Hair-specific cis-Elements)" conserved among the Arabidopsis thaliana A7 (AtEXPA7) orthologous (and paralogous) genes from diverse angiosperm species with different hair distribution patterns
ABRELATE RD1	ACGTG	S000414	ABRE-like sequence (from -199 to -195) required for etiolation-induced expression of erd1 (early responsive to dehydration) in Arabidopsis
ACGTATER D1	ACGT	S000415	ACGT sequence (from -155 to -152) required for etiolation-induced expression of erd1 (early responsive to dehydration) in Arabidopsis

## Appendices

Table S4 (continued)

Name	Sequence	PLACE ID	Description
TATABOXO SPAL	TATTTAA	S000400	Binding site for OsTBP2, found in the promoter of rice pal gene encoding phenylalanine ammonia-lyase; OsTFIIB stimulated the DNA binding and bending activities of OsTBP2 and synergistically enhanced OsTBP2-mediated transcription from the pal promoter
ASF1MOTIF CAMV	TGACG	S000024	"ASF-1 binding site" in CaMV 35S promoter; ASF-1 binds to two TGACG motifs; See S000023 (AS1); Found in HBP-1 binding site of wheat histone H3 gene; TGACG motifs are found in many promoters and are involved in transcriptional activation of several genes by auxin and/or salicylic acid; May be relevant to light regulation; Binding site of tobacco TGA1a; TGA1a and b show homology to CREB; TGA6 is a new member of the TGA family; Abiotic and biotic stress differentially stimulate "as-1 element" activity
WBOXATN PR1	TTGAC	S000390	"W-box" found in promoter of Arabidopsis thaliana (A.t.) NPR1 gene; Located between +70 and +79 in tandem; They were recognized specifically by salicylic acid (SA)-induced WRKY DNA binding proteins; See S000142 (SQ=TTGACC); See S000310 (SQ=TTTGACY); A cluster of WRKY binding sites act as negative regulatory elements for the inducible expression of AtWRKY18 (Chen and Chen, 2002)
WRKY71OS -	TGAC	S000447	"A core of TGAC-containing W-box" of e.g., Amy32b promoter; Binding site of rice WRKY71, a transcriptional repressor of the gibberellin signaling pathway; Parsley WRKY proteins bind specifically to TGAC-containing W box elements within the Pathogenesis-Related Class10 (PR-10) genes (Eulgem et al., 1999)
300ELEMEN T	TGHAAARK	S000122	Present upstream of the promoter from the B-hordein gene of barley and the alpha-gliadin, gamma-gliadin, and low molecular weight glutenin genes of wheat
GT1GMSCA M4	GAAAAA	S000453	"GT-1 motif" found in the promoter of soybean (Glycine max) CaM isoform, SCaM-4; Plays a role in pathogen- and salt-induced SCaM-4 gene expression
TATABOX2	TATAAAT	S000109	"TATA box"; TATA box found in the 5'upstream region of pea legA gene; sporamin A of sweet potato; TATA box found in beta-phaseolin promoter (Grace et al.); sequence and spacing of TATA box elements are critical for accurate initiation (Grace et al.)
MYBCORE PYRIMIDIN EBOXOSRA MY1A	CNGTTR CCTTTT	S000176 S000259	Binding site for all animal MYB and at least two plant MYB proteins ATMYB1 and ATMYB2, both isolated from Arabidopsis; ATMYB2 is involved in regulation of genes that are responsive to water stress in Arabidopsis; A petunia MYB protein (MYB.Ph3) is involved in regulation of flavonoid biosynthesis (Solano et al. EMBO J 14:1773 (1995)) Pyrimidine box found in rice (O.s.) alpha-amylase (RAmy1A) gene; Gibberellin-respons cis-element of GARE and pyrimidine box are partially involved in sugar repression; Found in the promoter of barley alpha-amylase (Amy2/32b) gene which is induced in the aleurone layers in response to GA; BPBF protein binds specifically to this site
MYB2CONS ENSUSAT -	YAACKG	S000409	MYB recognition site found in the promoters of the dehydration-responsive gene rd22 and many other genes in Arabidopsis
10PEHVPSB D	TATTCT	S000392	"-10 promoter element" found in the barley (H.v.) chloroplast psbD gene promoter; Involved in the expression of the plastid gene psbD which encodes a photosystem II reaction center chlorophyll-binding protein that is activated by blue, white or UV-A light
MYBPZM	CCWACC	S000179	Core of consensus maize P (myb homolog) binding site; 6 bp core; Maize P gene specifies red pigmentation of kernel pericarp, cob, and other floral organs; P binds to A1 gene, but not Bz1 gene; Maize C1 (myb homolog) activates both A1 and Bz1 genes (Grotewold et al. 1994)
TATABOX4	TATATAA	S000111	"TATA box"; TATA box found in the 5'upstream region of sweet potato sporamin A gene; TATA box found in beta-phaseolin promoter (Grace et al.); sequence and spacing of TATA box elements are critical for accurate initiation (Grace et al.)
MYBCORE ATCYCB1	AACGG	S000502	"Myb core" in the 18 bp sequence which is able to activate reporter gene without leading to M-phase-specific expression, found in the promoter of Arabidopsis thaliana cyclin B1:1 gene; the 18 bp sequence share homology with a sequence found in the N. sylvestris cyclin B1 promoter (Trehin et al., 1999; see S000283)
MYCATRD2 2	CACATG	S000174	Binding site for MYC (rd22BP1) in Arabidopsis (A.t.) dehydration-responsive gene, rd22; MYC binding site in rd22 gene of Arabidopsis thaliana; ABA-induction; Located at ca. -200 of rd22 gene; Also MYB at ca. -141 of rd22 gene

## Appendices

Table S4 (continued)

Name	Sequence	PLACE ID	Description
MYCATERD 1	CATGTG	S000413	MYC recognition sequence (from -466 to -461) necessary for expression of <i>erd1</i> (early responsive to dehydration) in dehydrated <i>Arabidopsis</i> ; NAC protein bound specifically to the CATGTG motif (Tran et al., 2004); NAC protein bound specifically to the CATGTG motif (Tran et al., 2004)
MYBPLANT C	MACCWAM	S000167	Plant MYB binding site; Consensus sequence related to box P in promoters of phenylpropanoid biosynthetic genes such as PAL, CHS, CHI, DFR, CL, Bz1; Myb305; M=A/C; W=A/T; See S000355; The AmMYB308 and AmMYB330 transcription factors from <i>Antirrhinum majus</i> regulate phenylpropanoid and lignin biosynthesis in transgenic tobacco
BOXLCORE DCPAL	ACCWWCC	S000492	Consensus of the putative "core" sequences of box-L-like sequences in carrot ( <i>D.c.</i> ) PAL1 promoter region; DCMYB1 bound to these sequences in vitro
CGCGBOX AT	VCGCGB	S000501	"CGCG box" recognized by AtSR1-6 ( <i>Arabidopsis thaliana</i> signal-responsive genes); Multiple CGCG elements are found in promoters of many genes; Ca <sup>++</sup> /calmodulin binds to all AtSRs
MARTBOX	TTWTWTT WTT	S000067	"T-Box"; Motif found in SAR (scaffold attachment region; or matrix attachment region, MAR)
SEF4MOTIF GM7S	RITTTTR	S000103	"SEF4 binding site"; Soybean ( <i>G.m.</i> ) consensus sequence found in 5'upstream region (-199) of beta-conglycinin (7S globulin) gene ( <i>Gmg17.1</i> ); "Binding with SEF4 (soybean embryo factor 4)"
DPBFCORE DCDC3	ACACNNG	S000292	A novel class of bZIP transcription factors, DPBF-1 and 2 (Dc3 promoter-binding factor-1 and 2) binding core sequence; Found in the carrot ( <i>D.c.</i> ) Dc3 gene promoter; Dc3 expression is normally embryo-specific, and also can be induced by ABA; The <i>Arabidopsis</i> abscisic acid response gene ABI5 encodes a bZIP transcription factor; <i>abi5</i> mutant have a pleiotropic defects in ABA response; ABI5 regulates a subset of late embryogenesis-abundant genes; GIA1 (growth-insensitivity to ABA) is identical to ABI5
ABRERATC AL	MACGYGB	S000507	"ABRE-related sequence" or "Repeated sequence motifs" identified in the upstream regions of 162 Ca(2+)-responsive upregulated genes; see also ABRE
NAPINMOT IFBN	TACACAT	S000070	Sequence found in 5' upstream region (-6, -95, -188) of napin (2S albumin) gene in <i>Brassica napus</i> ( <i>B.n.</i> ); Interact with a protein present in crude nuclear extracts from developing <i>B. napus</i> seeds

Upstream 1,000 bp from the transcript initiation site of Nipponbare and Kasalath OsORAP1 was subjected to *cis*-element search through PLACE database (<http://www.dna.affrc.go.jp/PLACE/>, as of May 2015) using default settings. The *cis*-elements which are common in both cultivars are shown with name, ID and description. N = A/T/C/G; K = G/T; W = A/T; Y = C/T; B = C/G/T; M = A/C; R = A/G; V = A/C/G; H = A/C/T.

## Appendices

Table S5: *Cis*-elements found only in Kasalath *OsORAP1* promoter region.

**Only in Kasalath**

Name	Sequence	PLACE ID	Description
CACGTGM			"CACGTG motif"; "G-box"; Binding site of Arabidopsis GBF4; <i>C. roseus</i> G-box binding factor 1 (CrGBF1) and 1 (CrGBF2) can act as transcriptional repressors of the Str promoter via direct interaction with the G-box; See S000345; Essential for expression of beta-phaseolin gene during embryogenesis in bean, tobacco, Arabidopsis; Tomato Pti4 (ERF) regulates defense-related gene expression via GCC box and non-GCC box cis-element (Myb1 (GTTAGTT) and G-box (CACGTG)); A prominent hit by in silico analysis in both induced and repressed phyA-responsive promoters (Hudson and Quail 2003)
OTIF	CACGTG	S000042	
TATABOX5	TTATTT	S000203	"TATA box"; TATA box found in the 5'upstream region of pea ( <i>Pisum sativum</i> ) glutamine synthetase gene; a functional TATA element by in vivo analysis
CARGCW8	CWVWWW		
GAT	WWWG	S000431	A variant of CArG motif (see S000404), with a longer A/T-rich core; Binding site for AGL15 (AGAMOUS-like 15)
SORLPIAT	GCCAC	S000482	one of "Sequences Over-Represented in Light-Induced Promoters (SORLIPs) in Arabidopsis; Computationally identified phyA-induced motifs; SORLIP 1 is most over-represented, and most statistically significant; Over-represented in light-induced cotyledon and root common genes and root-specific genes (Jiao et al. 2005; see S000486)
CELLCYCL	CACGAAA		
ESC	A	S000031	"cell cycle box" found in URS2 (-940/-200) of HO gene of <i>S.cerevisiae</i> ; cell-cycle-specific activation of transcription
WBOXNTE			
RF3	TGACY	S000457	"W box" found in the promoter region of a transcriptional repressor ERF3 gene in tobacco; May be involved in activation of ERF3 gene by wounding
WBOXNTC			
HN48	CTGACY	S000508	"W box" identified in the region between -125 and -69 of a tobacco class I basic chitinase gene CHN48; NtWRKY1, NtWRKY2 and NtWRKY4 bound to W box; NtWRKYs possibly involved in elicitor-responsive transcription of defense genes in tobacco
MYB2AT	TAACTG	S000177	Binding site for ATMYB2, an Arabidopsis MYB homolog; ATMYB2 binds oligonucleotides that contained a consensus MYB recognition sequence (TAACTG), such as is in the SV40 enhancer and the maize bronze-1 promoter (Urao et al., Plant Cell 5:1529 (1993)); ATMYB2 is involved in regulation of genes that are responsive to water stress in Arabidopsis
SV40COREE	GTGGWWH		
NHAN	G	S000123	"SV40 core enhancer"; Similar sequences found in <i>rbcS</i> genes
MYBATRD2			
2	CTAACCA	S000175	Binding site for MYB (ATMYB2) in dehydration-responsive gene, rd22; MYB binding site in rd22 gene of Arabidopsis thaliana; ABA-induction; Located at ca. -141 of rd22 gene; Also MYC at ca. -200 of rd22 gene
MYB1AT	WAACCA	S000408	MYB recognition site found in the promoters of the dehydration-responsive gene rd22 and many other genes in Arabidopsis
L1BOXATP			
DF1	TAAATGYA	S000386	"L1 box" found in promoter of Arabidopsis thaliana (A.t.) PROTODERMAL FACTOR1 (PDF1) gene; Located between -134 and -127; Involved in L1 layer-specific expression; L1-specific homeodomain protein ATML can bind to the "L1 box"; A cotton fiber gene, RD22-like 1 (RDL1), contains a homeodomain binding L1 box and a MYB binding motif (Wang et al., 2004); HDZip IV
BS1EGCCR	AGCGGG	S000352	"BS1 (binding site 1)" found in <i>E. gunnii</i> Cinnamoyl-CoA reductase (CCR) gene promoter; nuclear protein binding site; Required for vascular expression
BOXCPSAS			
1	CTCCAC	S000226	Box C in pea ( <i>P.s.</i> ) asparagine synthetase (AS1) gene; Found at -45; AS1 is negatively regulated by light; Box C binds with nuclear proteins, which was competed by a putative repressor element RE1 (see S000195)

## Appendices

Table S5 (continued)

Name	Sequence	PLACE ID	Description
CRTDREHV CBF2	GTCGAC	S000411	Preferred sequence for AP2 transcriptional activator HvCBF2 of barley; "Core CRT/DRE motif"; HvCBF2 bound to a (G/a)(T/c)CGAC core motif(Xue, 2003); DNA binding is regulated by temperature
SURECORE ATSULTR11	GAGAC	S000499	Core of sulfur-responsive element (SURE) found in the promoter of SULTR1;1 high-affinity sulfate transporter gene in Arabidopsis; SURE contains auxin response factor (ARF) binding sequence (GAGACA)(see S000270 ARF:TGTCTC; its complementary seq is GAGACA), and this core sequence is a part of it; this core seq is involved in -S response
RYREPEAT GMGY2	CATGCAT	S000105	"RY repeat motif (CATGCAT)"; Present in the 5' region of the soybean (G.m.) glycinin gene (Gy2)
SEF3MOTIF GM	AACCCA	S000115	"SEF3 binding site"; Soybean (G.m.) consensus sequence found in the 5' upstream region of beta-conglycinin (7S globulin) gene; AACCCA(-27bp-)AACCCA; SEF=soybean embryo factor; SEF2; SEF3; SEF4
E2FCONSE NSUS	WTSSCSS	S000476	"E2F consensus sequence" of all different E2F-DP-binding motifs that were experimentally verified in plants (Vandepoel et al., 2005)
IRO2OS	CACGTGG	S000505	OsIRO2-binding core sequence; "G-box plus G"; Transcription factor OsIRO2 is induced exclusively by Fe deficiency

Upstream 1,000 bp from the transcript initiation site of Nipponbare and Kasalath OsORAP1 was subjected to *cis*-element search through PLACE database (<http://www.dna.affrc.go.jp/PLACE/>, as of May 2015) using default settings. The *cis*-elements which appear only in Kasalath are shown with name, ID and description. W = A/T; Y = C/T; H = A/C/T; S = G/C.

## Appendices

Supplementary Table S6: Expression levels of rice *OsORAP1* and *Os06g0567900* gene under several stress conditions.

Stress	<i>Os09g0365900</i>	<i>Os06g0567900</i>	Reference
Cold stress (12 h)	1.0	0.9	Yun <i>et al.</i> , 2010
Salinity stress (30 days)	0.7	0.6	Walia <i>et al.</i> , 2005
Drought stress (12 h)	1.3	1.7	Minh-Thu <i>et al.</i> , 2013
Zinc deficiency (4 weeks)	1.0	1.4	Widodo <i>et al.</i> , 2010
Iron toxicity (1 g/L Fe <sup>2+</sup> , 4 days)	1.8	1.7	Wu <i>et al.</i> , unpublished
Ozone (120 ppb, 7 h, 13 days)	39.1	0.3	Frei <i>et al.</i> , 2010
Methyl viologen (24 h)	2.7	3.1	This study
Blast fungus (48 h)	5.9	2.1	Chujo <i>et al.</i> , 2013

Expression data were obtained from publicly available microarray data sources, or experimentally determined for methyl viologen (MV) treatment. The fold increase values under the denoted stress conditions are shown for *Os09g0365900* and *Os06g0567900*. The left column shows the type and duration of stress treatment. For MV treatment, plants were sprayed with 50 mM MV added with 0.1% (v/v) Tween 20, or 0.1% (v/v) Tween 20 alone as a mock treatment. The shoot samples were taken after 24 h and the gene expression levels were analysed by real-time PCR.

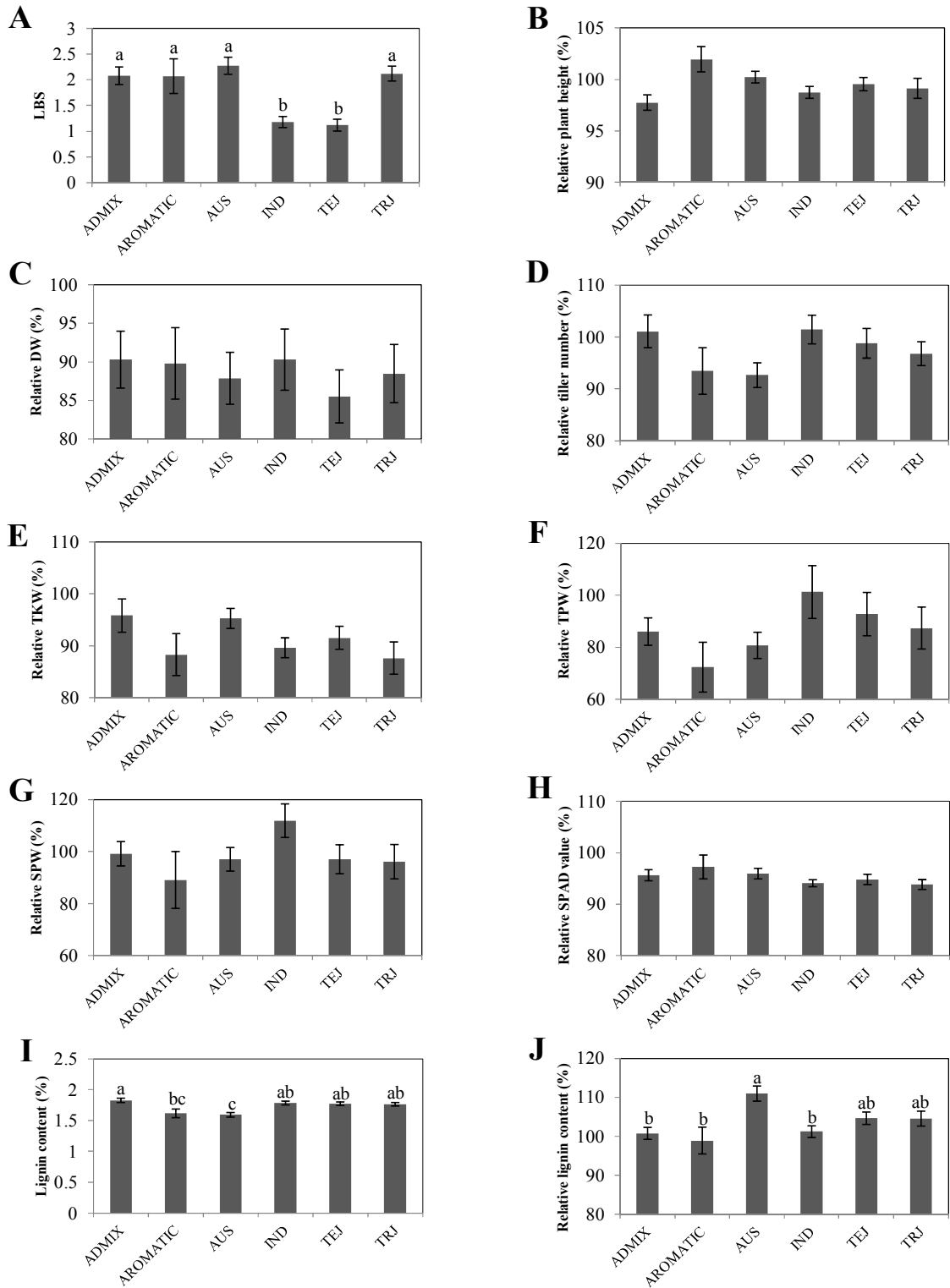
Supplementary Table S7: Germination rate of heterozygous knock-out line of *OsORAP1* in Tainung 67 genetic background.

	Germinated	Not germinated	Predicted ratio	Germination rate
Plate 1	56	18	3:1	75.70%
Plate 2	48	18	3:1	72.70%
Plate 3	53	17	3:1	75.70%
Total	157	53	3:1	74.80%

Seeds were obtained from *OsORAP1* heterozygous knock-out plants with the genetic background of Tainung 67. Seeds were sterilized with 5% (w/v) NaClO for 5 min, rinsed with water 5 times and sown on 0.8% (w/v) agar plates. The number of seedlings was counted after 16 days of incubation at 28 °C in dark. The seeds were considered germinated when either coleoptile or radicle emerged from the embryo. Chi-square test was conducted with the null hypothesis that the germination rate was 75%. The parameters used were:  $d$  (degrees of freedom) = 1 and  $\chi^2 = 0.0063$ . It rendered  $P = 0.9365$  and therefore it was concluded that the homozygous seeds were lethal. Genotyping of 43 randomly chosen germinated seeds from another experiment did not contain any homozygous mutant (15 null, 28 heterozygous).

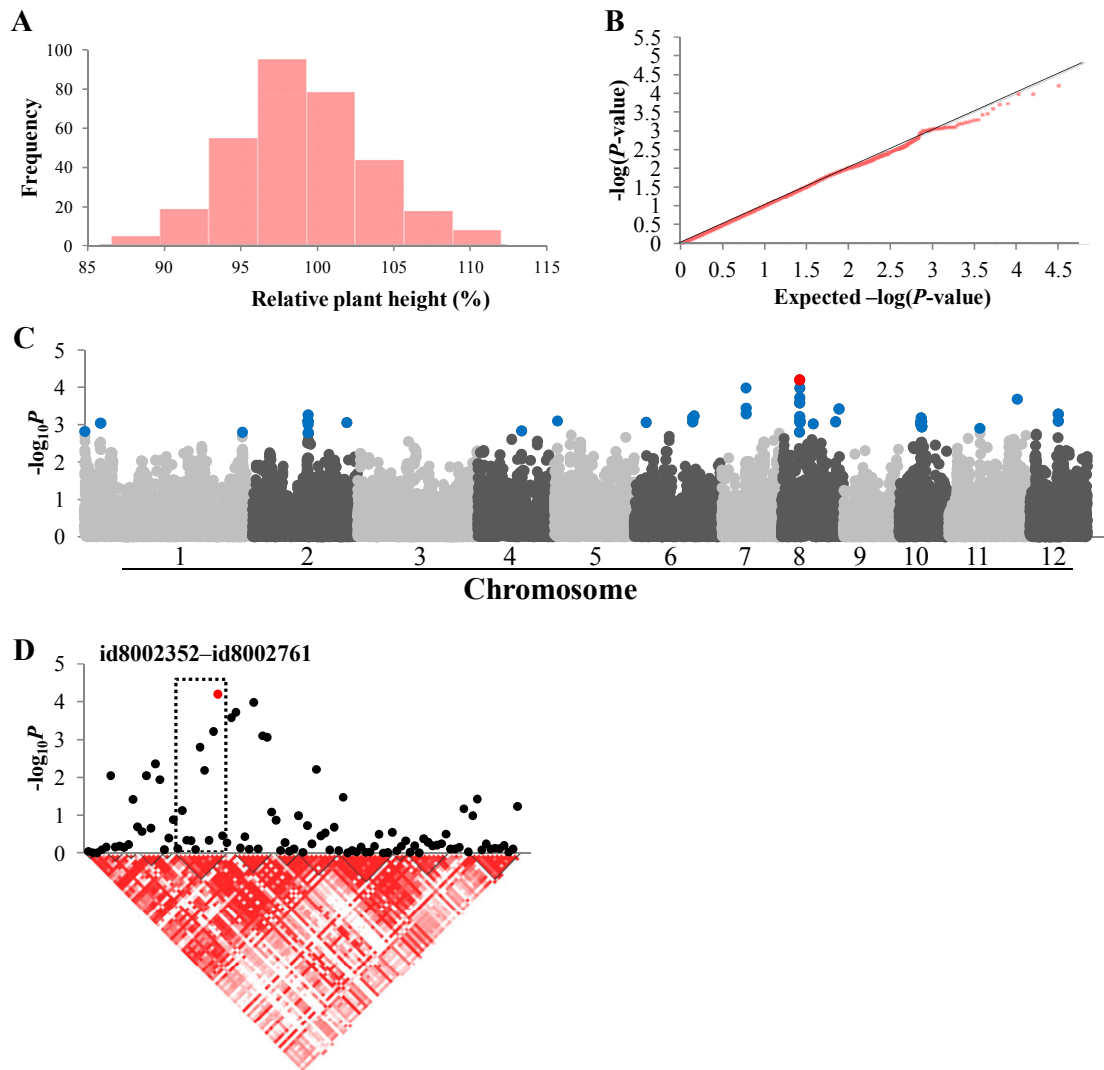


Supplementary data for Chapter 4

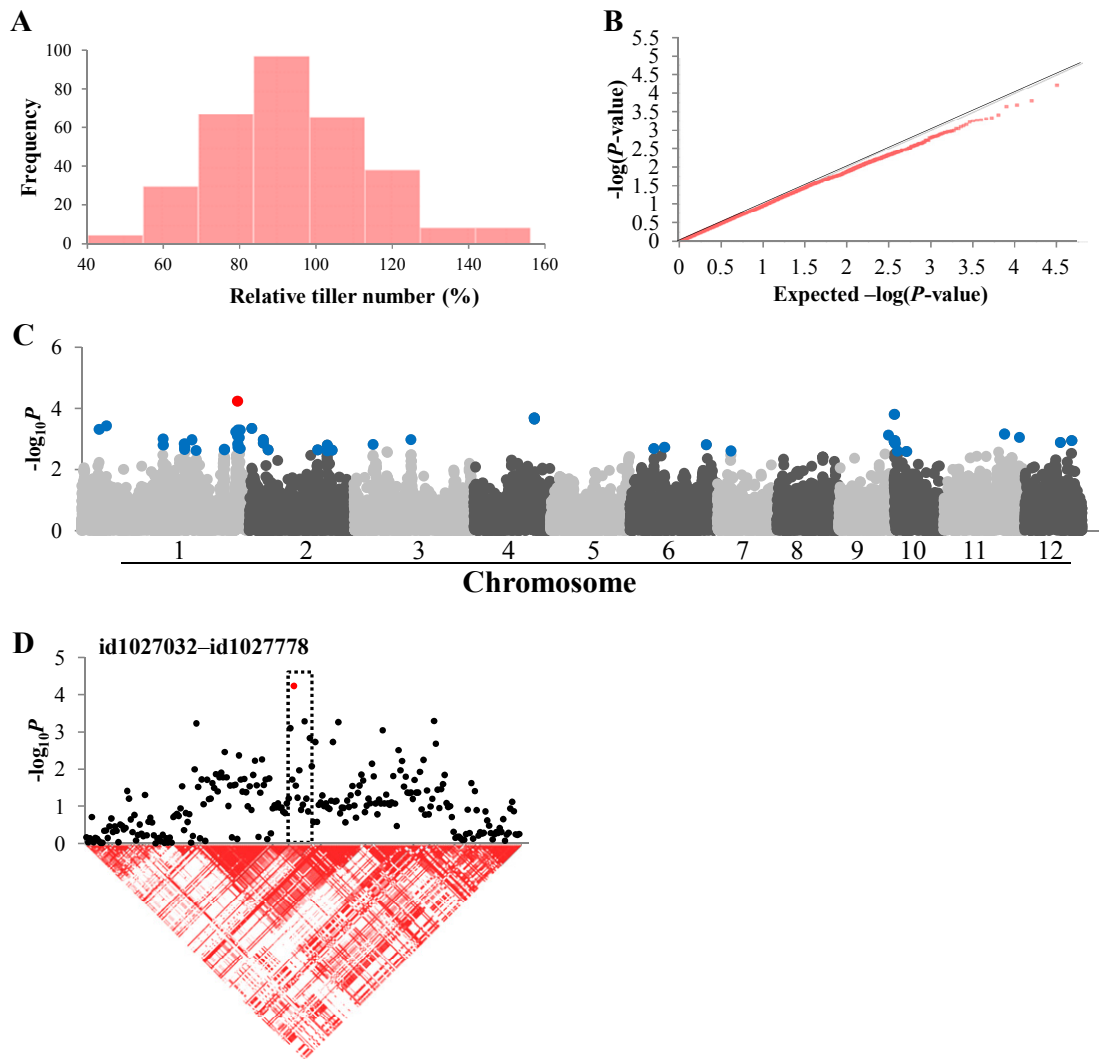


Supplementary Figure S17: Subpopulation comparison of all phenotypes. The whole population was classified into five subpopulations or admixed group as proposed by Zhao *et al.* (2010). Mean values and standard errors are shown. The subpopulations were composed as follows: ADMIX (admixed group, n =

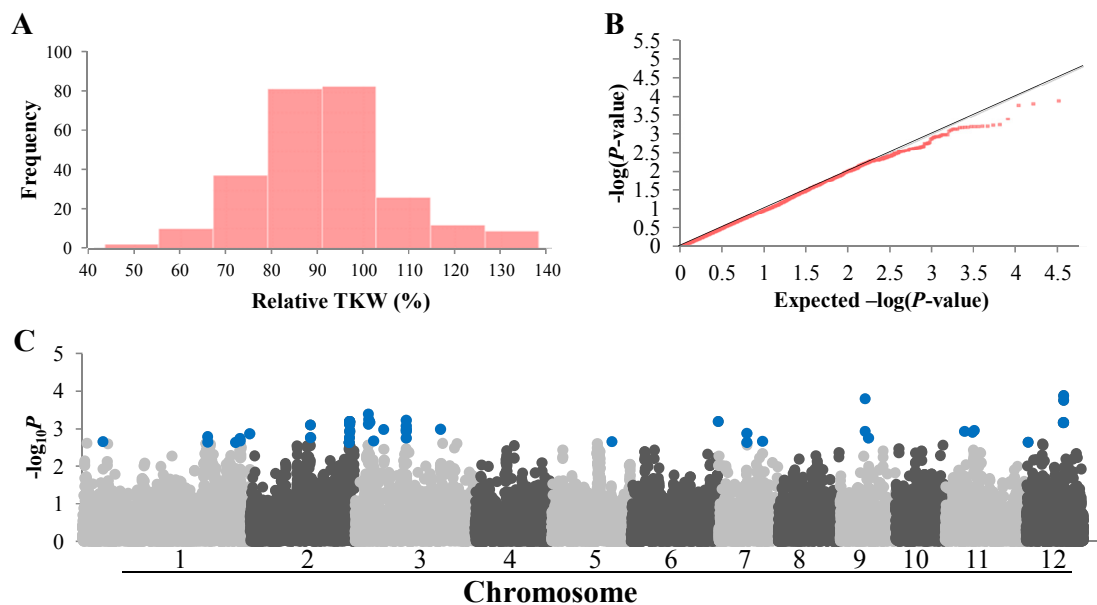
48), AROMATIC (n = 12), AUS (n = 55), IND (*indica*, n = 74), TEJ (*temperate japonica*, n = 69), TRJ (*tropical japonica*, n = 70). In E-G, 63 lines with thousand kernel weight (TKW) less than 10 g (ten ADMIX, four AROMATIC, three AUS, 26 IND, four TEJ and 16 TRJ) were eliminated to evaluate only matured grains. In F and G, lines with high grain shattering (one ADMIX, six AUS and one IND) were further eliminated. For A, I and J, letters above the bars indicate significant differences at  $P < 0.05$ . All other parameters showed no significant differences. (A) leaf bronzing score (LBS), (B) relative plant height, (C) relative dry weight (DW), (D) relative tiller number, (E) relative TKW, (F) relative total panicle weight (TPW), (G) relative single panicle weight (SPW), (I) relative SPAD value, (H) constitutive lignin content, (J) relative lignin content.



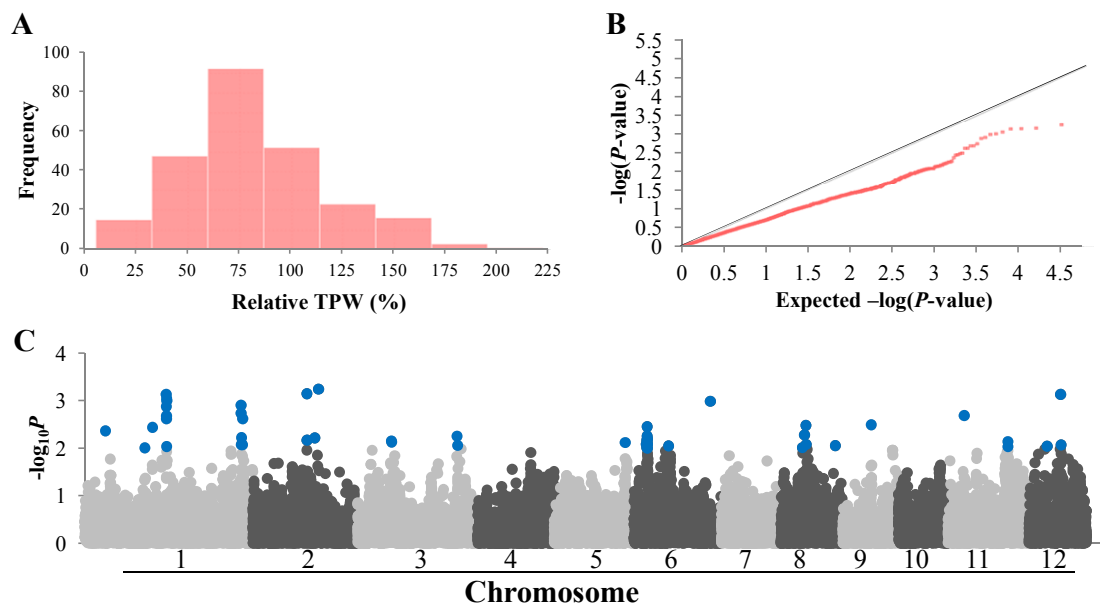
Supplementary Figure S18: Association mapping result for relative plant height. (A) Frequency distribution of observed relative plant height. (B) QQ plot of expected and observed  $P$  values. (C) Manhattan plots from association mapping using the Mixed Linear Model. The top 50 SNPs are shown in blue and the SNP exceeding the significance threshold of  $P < 0.0001$  is shown in red. (D) The peak region on chromosome 8. In D, pair-wise linkage disequilibrium between SNP markers is indicated as  $D'$  values: dark red indicates a value of 1 and white indicates 0. The dotted square in D denotes the linkage disequilibrium block which contains the significant SNP.



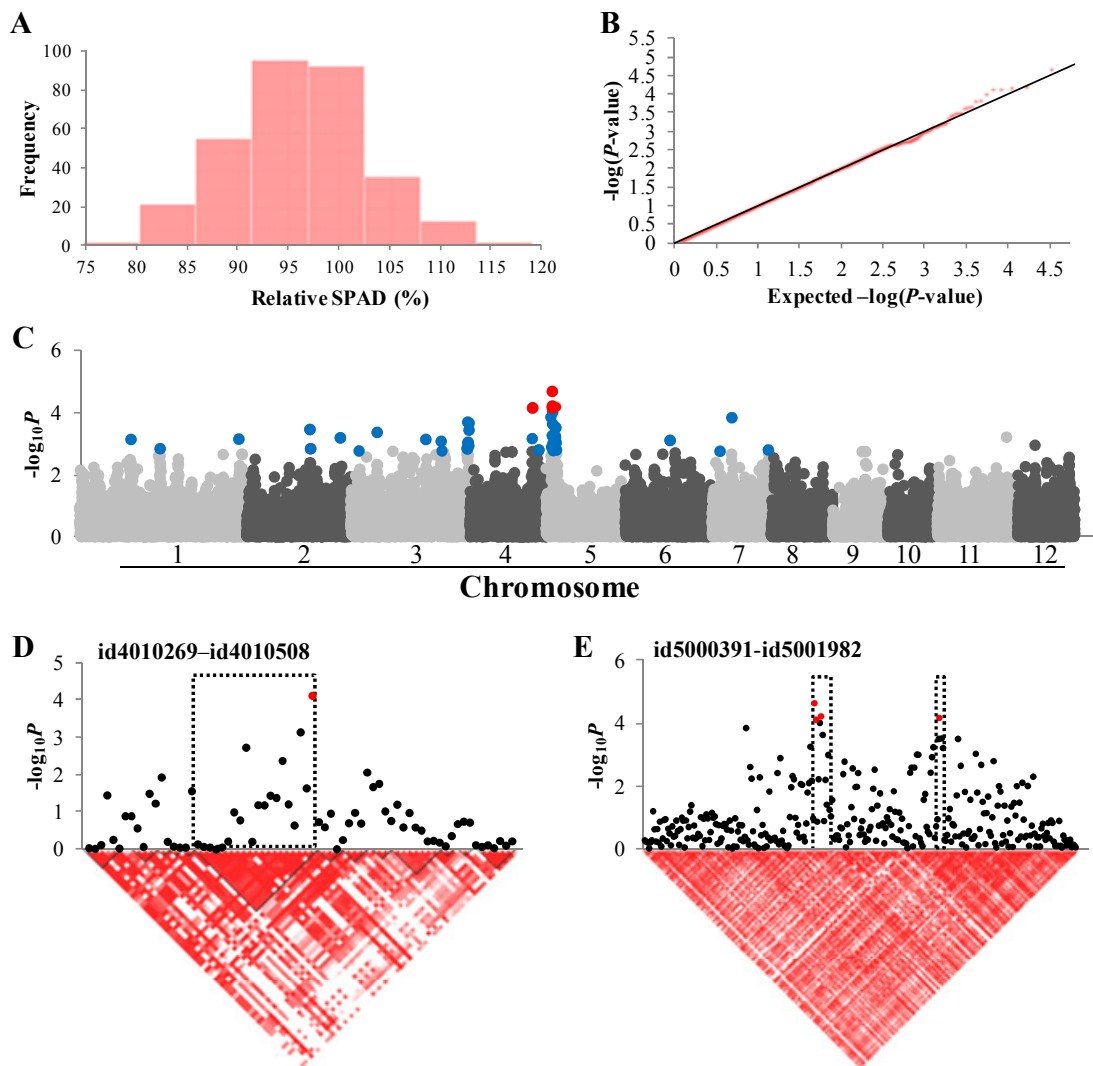
Supplementary Figure S19: Association mapping result for relative tiller number. (A) Frequency distribution of observed relative tiller number. (B) QQ plot of expected and observed  $P$  values. (C) Manhattan plots from association mapping using the Mixed Linear Model. The top 50 SNPs are shown in blue and the SNP exceeding the significance threshold of  $P < 0.0001$  is shown in red. (D) The peak region on chromosome 1. In D, pair-wise linkage disequilibrium between SNP markers is indicated as  $D'$  values: dark red indicates a value of 1 and white indicates 0. The dotted square in D denotes the linkage disequilibrium block which contains the significant SNP.



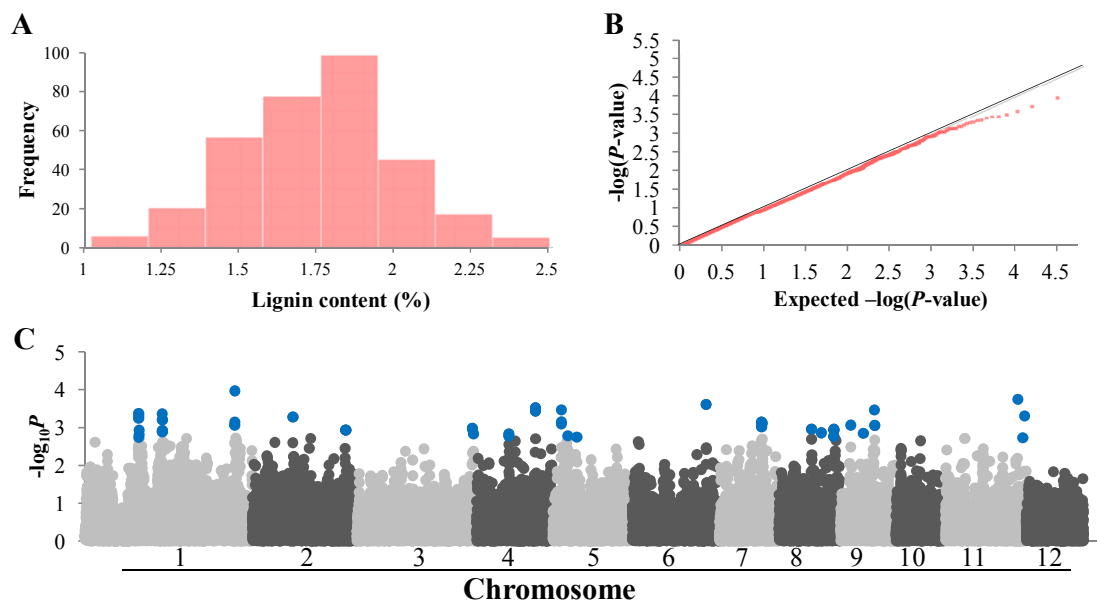
Supplementary Figure S20: Association mapping result for relative thousand kernel weight (TKW). (A) Frequency distribution of observed relative TKW. (B) QQ plot of expected and observed  $P$  values. (C) Manhattan plots from association mapping using the Mixed Linear Model. The top 50 SNPs are shown in blue.



Supplementary Figure S21: Association mapping result for relative total panicle weight (TPW). (A) Frequency distribution of observed relative TPW. (B) QQ plot of expected and observed  $P$  values. (C) Manhattan plots from association mapping using the Mixed Linear Model. The top 50 SNPs are shown in blue.

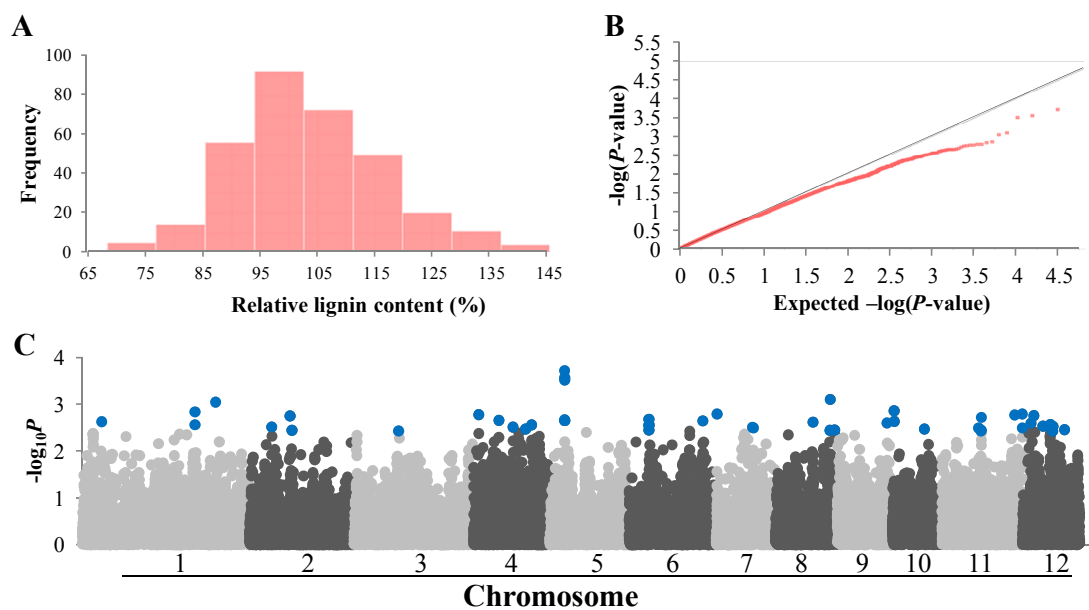


Supplementary Figure S22: Association mapping result for relative SPAD value. (A) Frequency distribution of observed relative SPAD value. (B) QQ plot of expected and observed  $P$  values. (C) Manhattan plots from association mapping using the Mixed Linear Model. The top 50 SNPs are shown in blue and the SNPs exceeding the significance threshold of  $P < 0.0001$  are shown in red. (D) The peak region on chromosome 4. (E) The peak region on chromosome 5. In D and E, pair-wise linkage disequilibrium between SNP markers is indicated as  $D'$  values: dark red indicates a value of 1 and white indicates 0. The dotted squares in D and E denote the linkage disequilibrium blocks which contain significant SNPs.



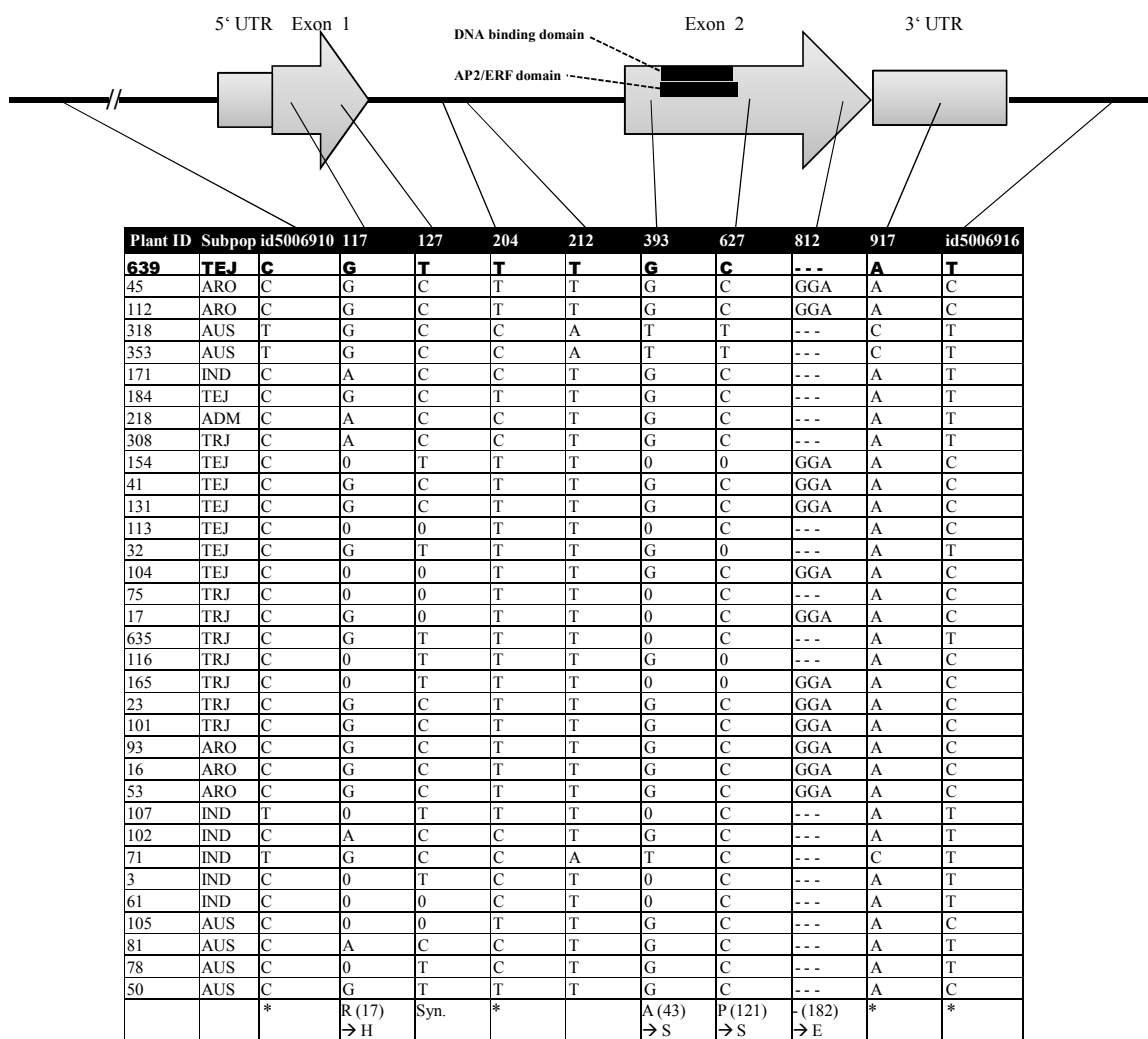
Supplementary Figure S23: Association mapping result for constitutive lignin content. (A) Frequency distribution of observed constitutive lignin content. (B) QQ plot of expected and observed  $P$  values. (C) Manhattan plots from association mapping using the Mixed Linear Model. The top 50 SNPs are shown in blue.



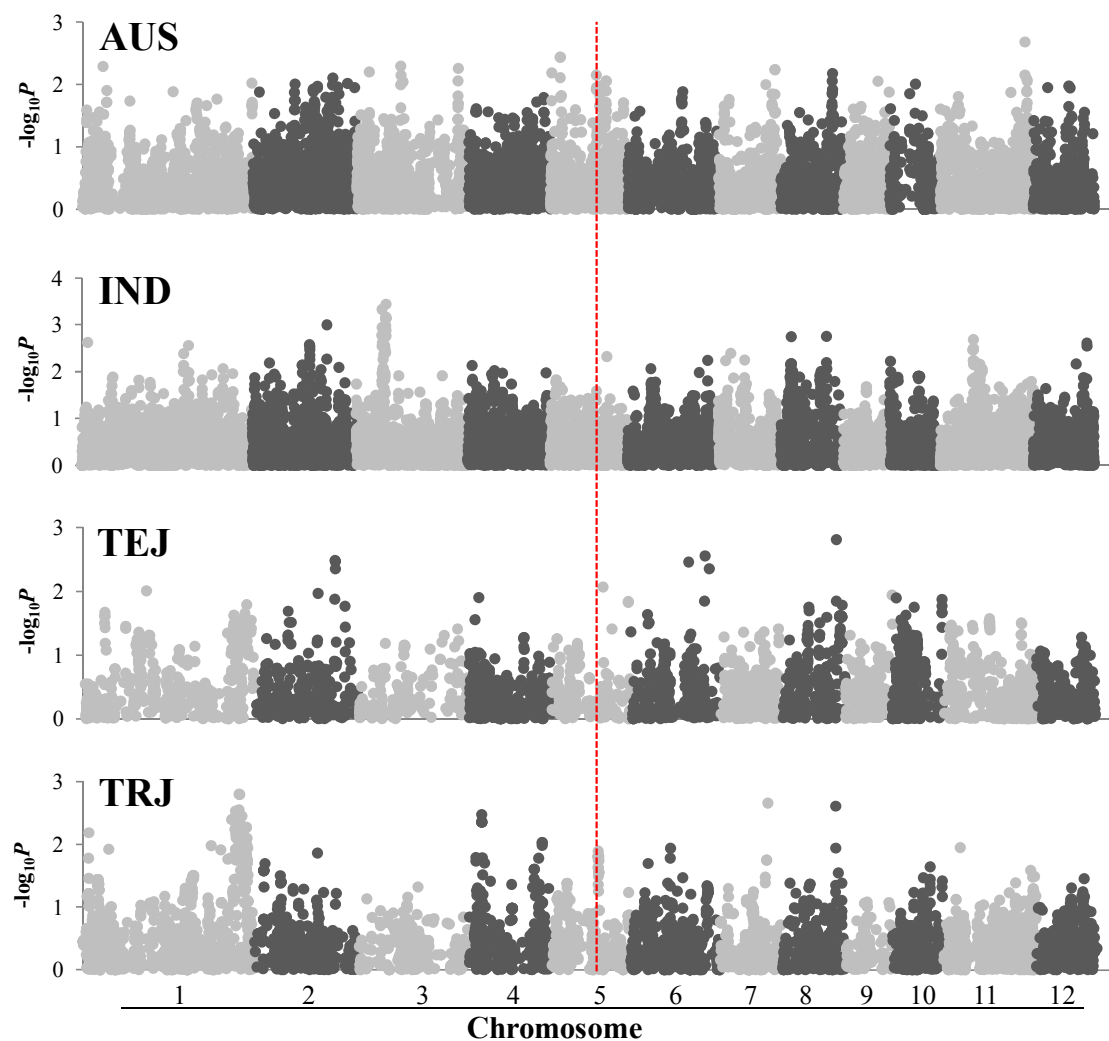


Supplementary Figure S24: Association mapping result for relative lignin content. (A) Frequency distribution of observed relative lignin content. (B) QQ plot of expected and observed  $P$  values. (C) Manhattan plots from association mapping using the Mixed Linear Model. Top 50 SNPs are shown in blue.

Appendices

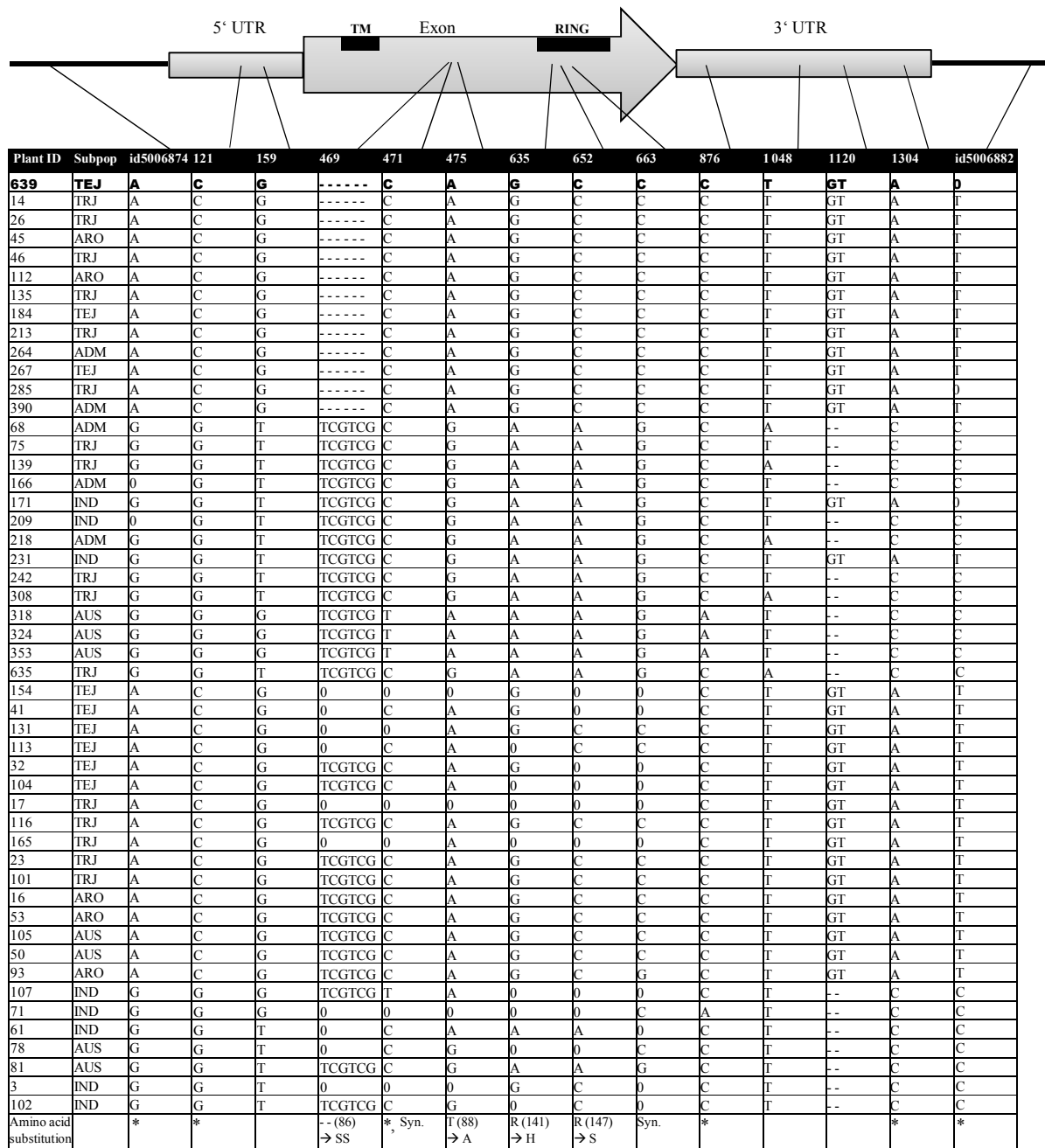


Supplementary Figure S25: Sequence variation of *EREBP* gene. The genomic sequences of *EREBP* from a total of 34 lines are shown together with two adjacent SNPs. The amino acid sequence 53 to 111 is a DNA binding domain, and 53 to 116 is an AP2/ERF domain. The reference sequence from Nipponbare is shown in boldface on the top. The possible amino acid substitution in the coding sequence is shown in the bottom row. The amino acid in the reference sequence, its position and the substituted amino acid are shown. ‘0’ stands for missing data. ‘Syn.’ denotes that the SNP causes silent mutation. Asterisks show that the SNP position has been already reported by OryzaSNP project (McNally *et al.*, 2009).



Supplementary Figure S26: Association mapping result in each subpopulation for square-root transformed leaf bronzing score (t-LBS). The subpopulations consisted of AUS ( $n = 55$ ), IND (*indica*,  $n = 74$ ), TEJ (*temperate japonica*,  $n = 69$ ) and TRJ (*tropical japonica*,  $n = 70$ ). Association mapping was not conducted in ADMIX and AROMATIC subpopulation. The dotted red line on chromosome 5 denotes the position of the *RING* (*LOC\_Os05g29710*).

Appendices



Supplementary Figure S27: Sequence variation of *RING* gene. The genomic sequences of *RING* from 50 lines are shown together with two adjacent SNPs. The amino acid sequence 29 to 50 is a transmembrane domain (TM), and 133 to 175 is a zinc-finger motif (RING). The reference sequence from Nipponbare is shown in boldface on the top. The possible amino acid substitution in the coding sequence is shown in the bottom row. The amino acid in the reference sequence, its position and the substituted amino acid are shown. ‘0’ stands for missing data. ‘Syn.’ denotes that the SNP causes silent mutation. Asterisks show that the SNP position has been already reported by OryzaSNP project (McNally *et al.*, 2009).

Appendices

Supplementary Table S8: All the accessions and phenotypic data used for the mapping.

NSFLV/D	Accession Name	Country of Origin	Subpopulation	Leaf bronzing score	Control plant height	Ozone plant height	Control dry weight	Ozone dry weight	Control tiller number	Ozone tiller number	Control thousand kernel weight	Ozone thousand kernel weight	Control total panicle weight	Ozone total panicle weight	Control single panicle weight	Ozone single panicle weight	Control SPAD	Ozone SPAD	Control lignin content	Ozone lignin content
3	Ai-Chiao-Hong	China	IND	0.7	197.0	191.7	70.7	49.4	11.3	8.3	21.4	18.2	31.8	15.9	2.9	2.2	425.0	417.0	1.6	1.4
4	ARC 10177	India	AUS	0.3	187.0	184.7	42.8	26.0	5.7	4.0	9.2	11.9	11.2	8.2	0.8	1.2	374.0	415.5	1.7	1.8
5	ARC 10352	India	AROMATIC	3.7	223.7	230.3	102.5	76.7	13.7	9.7	19.8	19.3	26.9	21.0	2.1	2.1	405.7	377.3	1.6	1.6
6	ARC 7229	India	AUS	4.3	212.3	217.3	33.7	34.2	3.7	4.0	22.4	18.6	14.7	14.3	3.4	3.9	347.0	382.5	1.8	1.9
8	Asse Y Pung	Philippines	TRJ	3.3	225.0	205.0	56.4	39.5	5.0	5.0	21.6	16.8	12.6	6.4	2.3	1.6	373.0	303.7	1.9	2.2
9	Baber	India	TEJ	2.0	205.0	206.7	52.6	32.3	7.0	6.7	23.8	19.1	35.3	25.8	4.8	3.7	432.3	406.3	1.7	2.1
10	Baghlani Nangarhar	Afghanistan	TEJ	2.0	146.7	147.0	27.1	17.9	8.7	6.7	16.8	14.1	11.3	2.9	1.3	0.5	445.0	400.0	1.8	1.9
12	Basmati	Pakistan	AROMATIC	2.0	226.7	209.0	70.8	57.9	12.5	10.3	20.9	14.0	53.8	9.1	2.6	0.9	385.3	348.0	1.5	1.7
13	Basmati 1	Pakistan	AUS	2.0	210.0	201.7	66.3	64.1	12.0	12.0	20.6	14.2	19.6	13.4	1.0	0.9	383.0	343.3	1.4	1.5
14	Basmati 217	India	TRJ	4.7	219.0	189.7	65.5	31.5	12.7	8.3							378.0	321.7	1.9	1.9
16	Bico Branco	Brazil	AROMATIC	2.3	238.0	234.3	137.6	109.5	14.3	13.7							379.3	390.3	1.4	1.6
17	Binulawan	Philippines	IND	0.3	91.3	84.0	17.4	6.8	5.7	5.0							372.3	348.0	1.7	1.9
18	BJ 1	India	AUS	3.3	208.0	204.0	86.2	66.2	26.7	17.7	22.1	21.0					387.0	360.7	1.5	1.9
19	Black Gora	India	AUS	2.0	191.2	198.7	44.8	35.0	8.7	7.7	25.4	22.3	37.0	24.1	2.8	2.3	373.7	364.3	1.6	1.8
21	Byakkoku Y 5006 Seln	Australia	IND	2.7	190.7	186.3	60.0	42.8	11.0	8.7	20.0	16.3	15.0	13.7	1.7	2.5	413.0	370.0	1.5	1.6
22	Caawa/Fortuna 6-103-15	Taiwan	TRJ	3.0	210.3	209.0	81.4	51.3	9.7	7.0	22.1	21.2	10.0	11.5	1.7	1.7	338.5	343.7	1.5	1.8
23	Canella De Ferro	Brazil	TRJ	2.0	239.3	232.0	107.6	47.8	7.5	5.7	17.6	14.6	26.9	13.6	2.8	2.3	385.7	368.7	1.8	1.7
24	Carolina Gold	United States	TRJ	2.3	229.0	213.3	62.2	53.0	6.0	5.7	23.0	19.1	20.2	13.7	3.2	2.3	376.3	361.0	1.8	1.8
25	Carolina Gold	United States	TRJ	3.3	229.0	223.7	45.3	50.2	5.7	6.7	19.5	13.7	19.8	12.7	3.6	2.1	387.0	383.0	1.8	1.7
26	Carolina Gold Sel	United States	TRJ	2.0	232.3	218.5	48.1	48.9	5.7	5.3	24.8	18.4	14.9	10.9	3.4	2.3	377.0	377.7	1.8	1.9
27	Chahora 144	Pakistan	TRJ	2.7	159.7	153.0	21.3	16.2	5.0	4.3	22.5	17.9	6.4	4.2	1.8	1.1	351.7	355.3	2.0	1.8
29	Chau	Vietnam	IND	0.3	226.7	227.0	55.7	44.1	8.7	7.0							378.3	383.0	1.9	2.0
30	Chiem Chanh	Vietnam	IND	2.0	245.3	228.7	78.5	69.4	16.7	16.3	20.3	18.4	31.2	24.1	2.2	1.8	394.0	416.0	2.3	2.0
31	Chinese	China	TEJ	0.7	143.7	147.7	22.3	20.0	6.7	6.7	12.1	15.5	4.2	3.7	0.6	0.6	396.0	373.0	1.9	1.9
32	Chodongji	South Korea	TEJ	1.7	174.3	167.7	38.4	30.0	8.3	6.3	18.0	15.3	11.9	6.2	1.8	1.4	380.3	396.7	2.1	2.1
33	Chuan 4	Taiwan	AUS	3.3	184.7	186.3	50.2	56.3	13.7	12.7	18.9	18.3	23.0	16.1	1.5	1.3	369.0	342.0	1.5	1.9
35	CO18	India	IND	1.3	243.5	225.5	68.6	125.5	9.0	12.7	17.8	13.1	25.0	39.5	2.5	2.5	349.3	350.7	2.2	2.1
36	CS-M3	United States	TEJ	1.0	179.7	163.7	31.3	14.3	7.5	5.0	24.9	16.8	11.6	2.9	1.2	0.8	428.7	429.7	2.1	2.3
37	Cuba 65	Cuba	TRJ	2.7	148.0	153.3	21.8	14.3	5.3	4.3	10.6	9.5	4.1	1.8	0.6	0.5	360.3	402.5	2.1	2.0
39	DA 16	Bangladesh	ADMIX	3.0	235.7	229.0	90.6	76.1	16.3	12.7	33.0	33.0	31.9	29.4	2.3	2.8	371.7	359.7	2.1	2.0
40	Dam	Thailand	ADMIX	1.3	202.3	193.0	23.1	32.2	4.3	6.0	17.5	20.6	6.5	4.7	1.3	0.9	365.3	351.7	1.5	1.4
41	Darmali	Nepal	ADMIX	2.3	281.0	270.0	81.1	82.7	8.0	9.3	20.6	16.4	38.6	34.5	4.7	4.9	429.0	386.7	1.7	1.8
43	Dee Geo Woo Gen	Taiwan	IND	0.0	101.7	99.3	13.9	13.0	9.7	10.0							375.7	372.3	1.1	1.3
44	Dhala Shaitta	Bangladesh	AUS	0.5	147.7	154.0	20.1	17.3	5.0	5.0	12.1	13.1	6.0	2.0	1.1	0.4	403.0	370.3	1.5	1.9
45	Dom-sufid	Iran	AROMATIC	0.0	201.0	213.3	46.6	45.4	8.7	7.3	23.5	19.7	26.1	17.3	2.9	1.8	392.0	426.3	1.4	1.4
46	Dourado Agulha	Brazil	TRJ	1.0	212.3	217.0	62.6	57.7	7.7	8.7	28.4	20.7	19.6	10.8	3.1	1.3	366.7	370.0	1.8	1.7
49	DV85	Bangladesh	AUS	0.7	174.0	178.3	26.4	20.4	9.0	11.3	18.2	19.0					347.0	357.7	1.5	1.6
50	DZ78	Bangladesh	AUS	1.7	195.5	197.3	38.5	38.7	7.3	6.7	27.1	26.6	31.3	23.3	5.3	2.5	378.7	419.7	2.1	1.7
51	Early Wataribune	Japan	TEJ	0.7	175.0	171.0	45.6	30.5	10.3	8.0	22.9	18.7	15.8	11.2	1.7	1.4	382.0	425.3	1.8	1.9
53	Firooz	Iran	AROMATIC	1.0	226.7	238.7	120.7	121.9	14.3	12.0							371.0	366.0	1.4	1.4

Appendices

Supplementary Table S8 (continued)

NSR/TV ID	Accession Name	Country of Origin	Subpopulation	Leaf bronzing score	Control plant height	Ozone plant height	Control dry weight	Ozone dry weight	Control tiller number	Ozone tiller number	Control thousand kernel weight	Ozone thousand kernel weight	Control total panicle weight	Ozone total panicle weight	Control single panicle weight	Ozone single panicle weight	Control SPAD	Ozone SPAD	Control lignin content	Ozone lignin content
54	Fortuna	United States	TRJ	1.7	196.3	205.5	29.0	37.4	4.7	6.0	8.8	18.0	1.6	7.1	0.4	1.4	402.0	383.0	1.8	1.8
56	Geumobyeo	South Korea	TEJ	0.7	108.7	112.3	6.3	9.8	3.7	5.7							400.3	385.0	2.1	1.9
57	Gharib	Iran	IND	0.0	193.7	191.0	61.5	73.1	9.0	10.7							395.3	372.0	1.3	1.5
58	Ghati Kamma Nangarhar	Afghanistan	AUS	2.7	183.7	197.7	48.8	85.2	8.0	12.0	12.9	16.7	16.9	25.9	1.3	1.3	373.7	341.3	1.4	1.3
59	Gogo Lempuk	Indonesia	TRJ	1.7	214.0	219.0	87.5	88.1	8.0	7.7	21.2	23.8	32.5	32.4	4.3	4.1	371.7	344.0	1.9	2.3
61	Guan-Yin-Tsan	China	IND	1.3	206.7	196.3	75.0	59.1	10.3	10.0	21.6	20.9	28.1	23.6	1.1	1.4	393.0	325.0	1.7	1.9
65	Honduras	Honduras	TRJ	1.7	235.5	242.3	64.9	54.9	6.0	5.0	23.2	23.5	22.0	19.4	3.7	3.9	365.0	341.5	1.8	1.9
66	Hsia Chioh Keh Tu	Taiwan	IND	0.3	201.3	198.0	36.2	47.5	8.0	8.0							397.0	353.5	1.8	2.0
67	Hu Lo Tao	China	TEJ	0.0	213.3	207.2	53.3	57.3	9.7	9.0	19.2	16.7	15.3	12.9	1.6	2.2	416.3	389.7	1.8	1.8
68	I-Geo-Tze	Taiwan	ADMIX	1.0	171.7	179.3	47.8	33.6	11.7	7.7	18.3	14.5	11.4	3.8	0.9	0.7	354.3	360.0	1.7	1.9
69	IAC 25	Brazil	TRJ	1.0	225.7	215.8	40.7	35.9	6.0	4.5	28.7	26.9	18.3	13.3	3.0	3.4	394.7	409.3	1.5	1.8
70	Iguape Cateto	Haiti	TRJ	3.7	197.0	196.3	35.3	40.6	7.7	7.7	13.5	13.1	9.9	9.5	1.5	1.3	335.7	339.7	1.6	1.7
71	IR 36	Philippines	IND	0.0	105.7	114.0	10.8	17.2	7.3	10.7							388.5	360.0	1.5	1.6
72	IR 8	Philippines	IND	0.3	124.3	112.0	10.5	10.9	5.3	8.3							387.7	378.7	1.3	1.7
73	IRAT 177	French Guiana	TRJ	2.0	184.7	184.7	26.2	31.8	5.0	6.0	25.8	20.2	9.9	8.5	2.4	0.9	379.3	331.0	1.6	2.0
74	IRGA 409	Brazil	IND	2.0	129.0	125.7	19.1	27.0	6.3	8.0	15.7	14.8	3.5	9.9	0.6	0.8	396.7	383.0	1.2	1.4
75	Jambu	Indonesia	TRJ	4.5	203.0	204.0	41.2	33.8	5.0	4.0	15.3	10.9	5.9	5.1	1.4	1.3	359.0	377.0	1.9	2.2
76	Jaya	India	IND	1.3	111.3	112.0	25.7	20.6	10.3	10.0							384.0	374.0	1.5	1.6
77	JC149	India	IND	1.7	239.7	248.0	82.7	58.5	9.0	6.7	17.7	12.0	22.5	11.9	2.5	2.4	380.3	405.0	1.6	1.7
78	Jhona 349	India	AUS	0.7	193.7	192.0	72.4	52.7	16.0	13.7	22.5	20.7	42.5	30.7	1.5	1.5	386.7	380.3	0.6	1.0
79	Jouiku 393G	Japan	TEJ	0.7	129.7	128.7	16.3	6.7	7.0	3.7	12.6	10.0	9.0	2.3	1.3	0.8	476.0	390.3	1.9	2.0
81	Kalamkati	India	AUS	0.7	194.7	205.3	48.5	35.7	10.0	6.7	12.0	11.7	8.2	6.1	0.7	0.4	361.0	350.3	2.0	2.1
83	Kamenoo	Japan	TEJ	1.7	165.7	160.0	18.8	17.0	4.7	5.7	12.2	14.5	10.4	7.3	1.8	1.2	385.0	402.0	1.7	1.9
85	Kasalath	India	AUS	0.3	210.7	213.0	56.2	49.8	11.7	12.3	16.3	16.5	26.8	30.8	2.2	2.7	386.0	368.7	2.2	2.0
87	Keriting Tingii	Indonesia	ADMIX	3.0	207.7	209.7	25.5	36.5	3.7	4.3	23.3	27.1					406.7	365.0	1.9	1.9
88	Khao Gaew	Thailand	AUS	2.5	193.0	202.0	27.9	26.6	4.0	3.0	17.1	16.2					391.0	371.3	1.6	2.1
89	Khao Hawn	Thailand	TRJ	1.5	205.7	195.7	45.2	36.3	4.7	5.7	12.9	12.2	8.2	6.6	1.8	1.1	428.0	407.5	1.5	1.9
90	Kiang-Chou-Chiu	Taiwan	IND	1.0	184.7	180.0	40.2	27.6	9.7	7.3	23.6	22.5	34.1	21.6	3.6	2.7	397.3	360.0	1.7	1.6
92	Kinastano	Philippines	TRJ	2.0	205.3	195.7	36.5	24.5	4.0	3.7	26.3	18.0	12.4	6.7	3.1	1.8	357.0	362.7	1.8	2.3
93	Kitrana 508	Madagascar	AROMATIC	1.5	222.0	226.3	91.3	80.1	10.0	11.7	16.7	15.2	14.0	14.6	1.0	1.2	357.3	376.0	2.1	1.5
96	KU115	Thailand	ADMIX	1.7	212.0	203.7	31.2	23.2	4.3	4.0	24.2	26.1	8.4	6.3	2.3	1.3	384.3	363.7	2.1	2.2
97	Kun-Min-Tsieh-Hunan	China	IND	2.3	210.7	209.7	47.2	31.3	9.0	7.0	21.8	20.8	31.5	11.5	3.0	1.8	376.3	399.0	1.6	1.6
98	L-202	United States	TRJ	0.3	120.3	121.3	14.5	7.9	6.3	5.3	13.3	7.5	3.4	0.9	0.8	0.4	335.7	369.7	1.6	1.7
99	LAC 23	Liberia	TRJ	1.7	200.7	191.3	35.4	27.6	4.3	4.7	25.7	23.7	7.7	5.5	1.7	1.4	398.7	337.0	1.3	2.2
100	Lacrosse	United States	ADMIX	2.7	193.0	194.3	29.7	44.2	4.3	6.0							360.3	375.7	1.8	1.8
101	Lemont	United States	TRJ	0.3	99.5	101.5	6.7	9.9	3.0	5.5							446.7	379.3	1.5	1.0
102	Leung Pratew	Thailand	IND	0.0	264.3	280.3	84.7	107.7	12.0	11.3	19.0	19.2	38.0	37.8	2.6	3.1	394.0	372.3	1.9	2.2
103	Luk Takhar	Afghanistan	TEJ	0.0	121.0	119.0	13.0	13.5	5.7	6.3							391.0	352.7	1.6	1.5
104	Mansaku	Japan	TEJ	2.7	177.3	178.0	24.8	18.9	6.0	4.3	17.1	16.7	16.8	12.3	2.9	2.7	427.3	384.0	1.7	2.1
105	Mehr	Iran	AUS	1.3	188.5	190.0	46.7	41.0	8.7	7.3	11.9	10.0	17.3	15.2	0.9	1.1	350.3	374.7	1.4	1.3

Appendices

Supplementary Table S8 (continued)

NSR/TV ID	Accession Name	Country of origin	Subpopulation	Leaf bronzing score	Control plant height	Ozone plant height	Control dry weight	Ozone dry weight	Control tiller number	Ozone tiller number	Control thousand kernel weight	Ozone thousand kernel weight	Control total panicle weight	Ozone total panicle weight	Control single panicle weight	Ozone single panicle weight	Control SPAD	Ozone SPAD	Control lignin content	Ozone lignin content
106	Ming Hui	China	IND	0.3	118.3	111.3	22.9	14.3	9.0	7.0							392.0	356.0	2.0	1.9
107	Miriti	Bangladesh	TRJ	1.0	190.3	184.2	31.9	32.3	6.7	7.0	27.4	20.2	13.0	20.1	2.3	3.1	383.3	358.0	1.3	1.6
108	Moroberekan	Guinea	TRJ	0.0	148.7	227.0	33.8	29.8	3.7	3.3	26.1	23.7	6.6	8.3	1.7	3.2	393.7	401.7	1.6	2.0
109	MTU9	India	IND	1.5	218.7	214.0	78.4	51.2	12.3	8.0	25.6	23.2	58.3	33.6	3.0	4.0	367.7	338.7	1.7	1.6
110	Mudgo	India	IND	0.3	235.3	238.0	76.6	71.2	8.7	8.0	33.7	29.9	27.9	25.6	2.6	3.7	442.0	418.0	1.5	2.0
112	N12	India	AROMATIC	3.7	218.0	210.3	56.2	67.7	11.7	7.0							372.3	328.0	1.9	1.9
113	Norin 20	Japan	TEJ	1.0	144.7	133.5	14.8	11.2	5.7	5.3	15.8	15.6	11.2	7.1	2.4	1.9	422.7	357.3	1.9	2.3
114	Nova	United States	ADMIX	1.7	200.3	198.7	39.1	38.3	4.7	4.3							380.7	380.7	2.0	1.6
116	NPE 844	Pakistan	TRJ	1.7	221.7	217.7	37.7	38.6	4.0	4.7	25.0	22.9	15.3	12.6	3.8	2.7	416.0	389.7	1.8	2.0
117	O-Luen-Cheung	Taiwan	IND	1.0	186.7	185.0	52.5	37.6	11.7	10.3	22.6	19.9	36.9	30.8	2.8	3.6	388.0	360.0	1.6	1.7
118	Oro	Chile	TEJ	1.7	159.0	172.5	25.8	20.2	7.7	7.3	26.0	22.8	23.0	18.6	3.0	2.5	435.7	375.7	1.8	1.7
119	Oryzica Llanos 5	Colombia	IND	0.7	115.7	129.2	20.0	15.3	5.3	5.7							373.3	377.3	1.8	1.7
120	OS6	Nigeria	TRJ	4.7	226.5	226.7	61.0	48.0	8.0	6.3	26.1	25.0	17.9	10.5	2.3	2.4	368.0	340.7	2.0	1.9
121	Ostiglia	Argentina	TEJ	0.5	163.7	170.5	31.0	17.3	6.0	5.3	19.9	18.5	13.3	8.2	1.6	1.6	414.0	394.0	2.0	2.0
122	Padi Kasalle	Indonesia	TRJ	3.0	244.3	246.7	54.7	40.7	8.7	6.3							377.7	333.0	1.9	2.1
123	Pagaiyahan	Taiwan	IND	0.7	198.7	187.0	68.0	51.0	10.7	9.0							397.0	384.3	1.7	1.6
125	Pao-Tou-Hung	China	IND	1.3	237.0	226.0	75.9	86.8	12.0	15.0	22.0	19.8					363.3	369.0	2.1	2.0
126	Pappaku	Taiwan	IND	2.3	220.3	227.7	54.0	59.8	6.0	6.7	21.3	23.1	19.1	21.1	2.8	3.5	401.0	392.0	1.9	1.9
128	Pato De Gallinazo	Australia	ADMIX	1.3	179.3	167.7	15.4	16.5	4.7	4.7	14.2	11.4	4.4	5.6	0.9	0.9	402.7	393.3	1.9	1.8
129	Peh-Kuh	Taiwan	IND	1.0	194.7	194.7	74.5	71.1	10.3	11.7							396.0	355.0	1.8	1.4
130	Peh-Kuh-Tsao-Tu	Taiwan	IND	1.0	194.7	191.3	88.2	64.8	13.0	11.3							372.3	369.0	1.6	1.6
131	Phudugey	Bhutan	AUS	4.7	196.3	202.7	61.2	42.5	11.7	7.7	15.5	13.9	34.2	22.7	2.4	2.5	358.7	340.3	1.4	1.5
132	Rathuwee	Sri Lanka	IND	2.5	198.0	192.0	61.2	36.3	7.3	5.0	20.8	17.0	16.0	9.6	2.2	1.9	370.0	346.0	2.4	2.3
133	Rikuto Kemochi	Japan	TEJ	1.3	217.0	202.7	83.9	44.4	10.3	5.7	21.0	19.8	36.8	21.0	3.5	3.9	399.3	365.3	1.7	2.2
135	RT 1031-69	Zaire	TRJ	0.7	165.0	165.9	49.9	19.1	9.0	3.7	9.8	6.5	11.9	2.2	1.4	0.6	377.0	361.7	1.5	1.5
137	RTS14	Vietnam	IND	0.3	192.0	190.0	75.8	43.6	12.0	9.7	18.4	16.4	49.4	35.1	2.3	2.9	387.3	357.3	1.6	1.7
138	RTS4	Vietnam	IND	1.3	270.7	269.0	97.9	70.8	12.7	9.3	20.5	19.8	31.9	27.2	2.4	3.7	392.7	383.0	2.1	2.4
139	S4542A3-49B-2B12	United States	TRJ	1.7	153.7	150.0	16.4	16.9	3.3	5.0							407.3	359.7	1.8	1.9
140	Satum	United States	ADMIX	1.5	166.0	167.7	32.1	29.4	6.0	6.7							393.7	373.0	1.8	1.9
141	Seratoes Hari	Indonesia	IND	2.3	264.3	283.7	82.8	93.0	9.3	8.0							397.3	354.0	2.3	2.5
142	Shai-Kuh	China	IND	2.0	261.0	262.7	106.8	101.3	14.0	13.0	15.2	18.4	22.2	34.0	1.5	2.7	390.7	348.7	1.9	2.1
143	Shinriki	Japan	TEJ	0.0	155.7	156.3	35.4	22.9	11.0	8.3	19.9	14.4	6.7	3.4	0.8	0.7	399.0	381.0	2.0	2.3
144	Shoemed	United States	TEJ	1.3	151.7	150.7	28.2	17.2	8.7	6.3	17.5	10.4	5.8	1.3	0.8	0.3	395.7	353.7	1.7	1.8
145	Short Grain	Thailand	IND	2.3	253.7	243.7	146.8	115.2	13.3	10.0	25.5	22.9	52.4	35.9	3.8	3.8	343.7	329.3	1.8	1.7
147	Sinampaga Selection	Philippines	TRJ	2.3	172.7	173.7	39.4	24.8	6.0	4.7	16.0	5.7	4.7	1.5	0.9	0.3	376.3	366.0	2.0	2.0
148	Sintane Diofor	Burkina Faso	IND	2.7	227.3	226.7	134.9	87.3	15.7	8.7							327.0	312.3	1.8	1.9
150	Sultani	Egypt	TRJ	3.0	158.3	161.4	20.0	17.2	3.7	3.7	18.4	18.0	12.0	10.2	1.8	1.5	384.7	360.0	1.9	2.0
152	T 1	India	AUS	1.7	194.7	196.3	28.4	27.8	6.3	6.0	18.0	15.9	5.1	9.2	0.8	1.2	354.7	367.3	1.3	1.7
153	T26	India	AUS	2.0	157.7	188.7	26.6	40.3	6.0	8.3	28.7	28.1	37.8	49.5	4.7	4.7	360.7	322.7	2.0	1.8
154	Ta Hung Ku	China	TEJ	1.7	196.3	193.0	55.2	53.3	7.3	12.0	22.1	26.0	24.8	36.2	4.3	3.9	416.0	391.3	1.6	1.9

Appendices

Supplementary Table S8 (continued)

NSRFV ID	Accession Name	Country of origin	Subpopulation	Leafhoppering score	Control plant height	Oxone plant height	Control dry weight	Oxone dry weight	Control tiller number	Oxone tiller number	Control thousand kernel weight	Oxone thousand kernel weight	Control total panicle weight	Oxone total panicle weight	Control single panicle weight	Oxone single panicle weight	Control SPAD	Oxone SPAD	Control lignin content	Oxone lignin content
155	Ta Mao Tsao	China	TEJ	0.3	208.3	212.0	69.9	67.0	11.0	9.0							408.3	432.0	1.8	1.5
156	Taichung Native 1	Taiwan	IND	0.7	118.0	110.2	11.0	15.3	8.0	8.7							381.3	401.3	1.7	1.8
157	Tainan Iku 487	Taiwan	TEJ	0.7	145.0	137.5	18.4	14.7	6.3	5.7	18.8	17.1	9.1	3.4	1.5	0.7	385.3	384.0	1.9	1.7
158	Taipei 309	Taiwan	TEJ	1.0	147.3	138.0	29.6	13.9	8.0	5.7	19.1	8.3	11.4	0.6	1.6	0.2	405.3	424.0	1.6	1.8
161	TeQing	China	IND	0.7	109.2	102.3	21.2	11.7	8.3	7.7							432.7	362.0	1.7	1.5
162	TKM6	India	IND	1.3	212.0	194.7	52.1	39.9	10.3	10.0	17.1	13.7	21.1	14.4	2.5	1.4	390.3	359.0	1.8	1.7
163	Taducan	Philippines	IND	1.3	237.7	218.7	112.5	48.8	25.0	14.0	16.8	15.0	50.9	12.8	1.9	1.0	377.0	380.0	1.8	1.9
165	Trembese	Indonesia	TRJ	0.3	181.0	180.7	27.2	24.3	4.0	3.0	16.3	10.4	3.7	2.8	0.9	0.9	455.0	391.7	1.8	1.8
166	Tsipala 421	Madagascar	ADMIX	3.0	263.0	243.3	104.2	76.4	12.0	9.3	24.4	21.6	79.1	55.0	6.2	6.5	370.3	358.3	2.2	2.2
167	B6616A4-22-Bk-5-4	United States	TRJ	0.3	136.3	137.7	11.8	19.5	3.0	3.0							390.0	389.3	1.6	1.5
168	Vary Vato 462	Madagascar	ADMIX	4.7	235.0	223.0	44.4	46.3	8.3	9.0	25.0	21.7	21.8	25.9	2.8	3.0	418.7	391.7	2.0	2.0
171	ZHE 733	China	IND	0.7	114.5	113.7	13.8	11.1	6.7	7.0	17.3	16.3	4.2	6.4	0.4	1.0	422.0	407.0	2.1	1.8
172	Zhenshan 2	China	IND	1.0	92.3	94.0	12.1	11.9	8.3	10.3							414.7	358.7	2.1	1.6
176	583	Ecuador	TRJ	1.0	143.3	147.0	19.7	17.7	7.0	7.3	16.0	18.3	12.6	9.6	1.4	1.3	463.0	427.7	1.9	1.7
177	68-2	France	TEJ	2.3	142.3	141.7	23.8	14.6	8.7	6.0	17.6	11.4	18.1	5.8	2.0	0.9	447.7	418.0	1.8	2.0
178	ARC 6578	India	AUS	0.7	205.0	209.2	44.5	21.7	6.3	3.3	16.1	15.0	14.5	8.3	2.3	2.8	350.3	350.3	1.9	1.7
179	Bellardone	France	TEJ	0.0	168.0	171.2	32.0	20.4	9.0	6.7	24.0	19.0	33.3	17.4	3.4	2.8	438.3	394.3	1.8	1.8
180	Benllok	Peru	TEJ	2.0	166.0	166.3	36.9	19.4	10.0	6.3	20.4	15.7	19.7	7.4	2.0	1.2	446.0	381.7	1.9	1.7
183	Boa Vista	El Salvador	TRJ	3.3	193.3	176.7	29.7	18.8	5.3	3.7	25.9	22.1	6.2	2.9	1.2	1.0	359.7	374.0	1.7	1.5
184	Bombon	Spain	TEJ	2.7	212.7	209.7	46.0	46.1	5.3	5.3	22.4	20.6	14.4	14.9	2.5	2.6	401.7	384.0	1.6	1.6
185	British Honduras Creole	Belize	TRJ	2.0	220.0	223.0	37.7	55.6	5.0	7.3	22.4	19.0	12.7	21.1	2.6	3.0	357.7	372.7	2.0	2.0
186	Bul Zo	South Korea	TEJ	1.3	159.3	154.0	19.8	14.6	5.0	4.3	17.4	13.6	4.0	3.5	0.8	0.8	394.0	383.7	1.7	1.7
187	C57-5043	United States	TRJ	3.7	174.3	173.7	15.8	18.9	3.7	3.7							411.3	412.5	1.8	1.8
188	Coppocina	Bulgaria	TRJ	3.3	167.3	180.5	23.9	37.3	3.7	4.7							406.7	379.0	1.8	1.9
189	Criollo La Fria	Venezuela	IND	2.0	186.3	189.8	71.9	60.8	12.0	9.7	13.4	16.0	31.9	33.0	1.6	2.0	374.0	357.3	1.6	1.5
190	Delrex	United States	TRJ	4.0	190.8	192.0	38.7	33.4	5.7	4.0							381.0	354.5	1.8	1.7
191	Dom Zard	Iran	AROMATIC	1.3	205.3	214.7	64.1	52.0	11.3	8.0	25.6	23.0	34.3	20.1	2.7	2.1	426.3	397.0	1.4	1.5
192	Erythroceros Hokkaido	Poland	TEJ	0.3	127.8	134.5	10.6	8.5	5.7	5.0	26.7	24.1	10.1	7.9	1.7	1.9	265.5	260.5	1.9	2.3
193	Fossa Av	Burkina Faso	TRJ	1.0	230.3	210.5	39.6	32.4	4.3	5.0	18.1	12.8	9.7	8.5	2.0	1.8	387.3	394.0	1.7	2.0
195	IRAT 13	Cote D'Ivoire	TRJ	1.3	160.0	147.3	22.9	14.7	5.3	4.3	25.2	19.0	6.7	5.0	1.5	1.2	385.7	358.7	1.9	1.7
196	JM70	Mali	IND	3.3	240.3	229.3	86.7	66.5	8.7	8.3							374.7	346.0	2.2	2.1
197	Kaukyi Ani	Myanmar	ADMIX	2.0	201.7	162.3	33.8	39.3	4.7	5.0							388.0	376.7	2.0	2.0
198	Leah	Bulgaria	TRJ	0.3	133.3	128.5	16.7	15.5	4.7	5.7							358.0	349.3	1.9	1.7
199	Mojito Colorado	Bolivia	TRJ	3.0	201.0	173.7	42.6	17.2	6.0	3.7							367.0	357.0	1.8	2.0
201	Pate Blanc Mn 1	Cote D'Ivoire	TRJ	1.7	222.0	235.0	45.3	35.1	5.0	3.3	21.9	24.5	10.5	9.6	2.2	3.2	471.0	406.0	1.6	1.7
202	Pratao	Brazil	TRJ	3.0	216.3	226.0	72.2	43.1	10.0	6.7	28.3	27.5	26.5	14.9	2.4	2.9	382.0	361.3	1.6	1.7
203	Radin Ebos 33	Malaysia	IND	1.3	210.0	217.3	84.2	46.7	10.5	9.3	17.7	15.1	60.4	40.8	2.5	1.9	384.0	421.5	1.9	2.1
204	Razza 77	Italy	TEJ	1.0	177.0	192.7	43.0	26.6	7.5	6.0	26.5	23.2	23.7	11.0	3.1	1.8	426.0	383.3	1.5	1.7
205	Rinaldo Bersani	Italy	ADMIX	1.3	177.8	173.7	41.8	25.3	7.7	5.0	29.1	26.5	29.9	18.4	3.9	3.8	455.3	404.7	1.6	1.7
206	Rojofofotsy 738	Madagascar	ADMIX	4.0	237.7	205.7	70.2	22.5	14.0	6.3	25.0	20.0	50.7	9.2	4.3	2.1	405.7	398.5	1.9	2.1



Appendices

Supplementary Table S8 (continued)

NSRTV ID	Accession Name	Country of origin	Subpopulation	Leafhoppering score	Control plant height	Oxone plant height	Control dry weight	Oxone dry weight	Control tiller number	Oxone tiller number	Control thousand kernel weight	Oxone thousand kernel weight	Control total particle weight	Oxone total particle weight	Control single particle weight	Oxone single particle weight	Control SPAD	Oxone SPAD	Control lignin content	Oxone lignin content
207	Sigadis	Indonesia	IND	1.0	215.8	204.7	59.4	32.2	8.7	5.7	22.8	19.2	22.7	10.1	2.7	1.8	357.3	338.0	2.2	1.6
208	SLO 17	India	IND	0.7	234.7	221.0	90.5	54.8	11.7	8.3	20.9	18.9	32.5	23.0	3.8	2.7	380.0	365.7	1.6	1.5
209	Tchibanga	Gabon	IND	1.0	112.0	114.0	18.3	40.5	8.0	11.0	13.5	11.1	4.3	15.7	0.5	0.9	440.3	377.7	1.5	1.5
211	Tokyo Shino Mochi	Japan	ADMIX	1.0	190.2	186.3	33.0	35.5	9.3	8.3	24.6	24.0	31.9	37.2	3.7	3.5	438.3	390.0	2.1	2.0
213	WC 3397	Jamaica	TRJ	0.7	209.5	193.0	71.1	39.0	7.0	7.0	20.7	14.3	23.9	20.0	3.5	3.7	386.7	384.3	1.9	1.7
214	WC 4419	Honduras	TRJ	3.0	157.8	164.5	25.0	25.8	5.3	4.0	12.9	14.1	4.4	7.3	1.0	1.6	347.3	413.0	1.9	1.5
215	WC 4443	Bolivia	TRJ	1.3	192.5	186.3	39.6	27.9	7.3	4.7	27.8	22.6	14.3	6.3	2.4	1.9	315.3	360.7	1.8	1.4
216	Yabani Montakhab 7	Egypt	TEJ	0.3	142.5	138.7	27.6	18.6	8.7	7.3	11.6	8.7	3.7	2.4	0.4	0.4	399.7	387.3	1.8	1.9
217	YRL-1	Australia	ADMIX	2.3	169.0	177.7	32.8	20.0	7.3	4.7	18.2	22.6	14.1	11.4	1.9	2.6	344.5	375.5	1.3	1.4
218	PI 298967-1	Australia	ADMIX	4.3	169.0	159.0	21.8	19.1	6.7	6.3	20.3	15.7	14.2	6.4	1.9	1.2	386.0	385.0	2.0	1.9
220	Azerbaijanica	Azerbaijan	TEJ	0.3	161.7	166.0	40.8	29.7	13.7	11.7	26.3	25.5	36.6	28.6	2.3	2.6	399.7	397.0	1.8	1.9
221	Sadri Belyi	Azerbaijan	AROMATIC	1.0	185.0	188.5	39.5	45.7	9.0	7.7	20.9	19.7	35.2	33.1	2.9	3.3	386.7	428.0	1.4	1.3
222	Paraiba Chines Nova	Brazil	IND	0.7	212.7	198.0	63.3	23.6	10.7	10.0	21.6	16.2	50.7	27.1	4.6	3.9	382.0	388.0	2.0	1.8
226	IRAT 44	Burkina Faso	TRJ	2.0	173.0	154.7	23.9	10.7	5.7	5.7	30.8	24.8	18.9	21.4	3.2	3.8	355.7	382.3	1.7	1.8
227	Riz Local	Burkina Faso	ADMIX	1.7	208.0	205.3	78.4	69.3	7.7	9.0	31.7	24.9	39.3	40.0	4.2	4.5	367.7	377.7	1.7	1.5
228	CA 902/B/2/1	Chad	AUS	2.0	174.0	174.3	30.3	20.9	9.3	6.0	22.2	20.2					389.3	403.0	1.3	1.5
229	Niquen	Chile	TRJ	1.7	140.7	132.7	17.7	20.0	8.3	10.3	25.5	23.5	17.4	20.7	2.0	1.8	401.7	383.3	2.0	1.6
231	Hunan Early Dwarf No. 3	China	IND	0.7	83.7	91.0	14.5	9.4	7.0	7.0	14.2	15.2	10.5	9.3	0.9	1.2	373.7	279.3	1.6	2.0
232	Shangyu 394	China	TEJ	0.0	113.7	113.0	7.2	7.1	5.0	5.7	14.7	12.5	6.7	7.1	1.1	1.3	420.7	387.0	2.4	2.3
234	Ajjiaonante	China	IND	0.0	101.0	96.3	26.0	17.8	14.0	10.7	11.8	9.4	12.1	14.0	1.0	1.1	429.0	396.7	1.8	2.2
235	Sze Guen Zim	China	IND	0.3	186.5	184.8	75.5	63.4	12.7	13.0	20.1	15.5	46.0	38.1	1.9	2.4	394.3	384.7	1.7	1.5
236	WC 521	China	ADMIX	1.3	156.3	153.2	31.4	30.3	5.3	4.5							397.7	378.3	2.2	1.9
239	WAB 502-13-4-1	Cote D'Ivoire	TRJ	5.0	173.0	166.0	19.9	23.1	6.7	5.7	19.2	24.6	13.4	19.1	2.2	3.1	388.0	323.3	1.8	1.9
240	WAB 501-11-5-1	Cote D'Ivoire	TRJ	4.3	170.8	167.3	21.4	22.3	5.3	5.7	25.7	24.2	16.6	20.4	3.2	3.6	391.3	332.7	1.9	2.1
241	ECIA76-S89-1	Cuba	IND	0.3	105.0	105.7	14.9	24.6	6.0	11.0							381.3	369.3	1.4	1.3
242	27	Dominican Republic	TRJ	1.0	199.3	191.8	39.5	29.6	4.7	4.7	22.6	22.2	18.7	14.4	4.3	3.2	402.0	370.0	1.9	1.9
244	Arabi	Egypt	ADMIX	4.0	150.8	169.0	30.2	26.6	9.0	6.3	19.0	17.7	5.3	4.7	0.6	0.9	384.7	337.0	1.6	1.9
245	Sab Ini	Egypt	TEJ	1.3	177.7	187.0	34.3	35.8	8.7	7.3	27.9	25.9	27.6	26.2	3.2	3.4	424.0	389.0	1.5	1.5
246	Saraya	Fiji	AUS	3.0	191.3	191.0	38.1	51.5	11.3	14.7	23.5	21.0	26.2	32.7	2.0	2.1	358.0	320.0	1.6	1.7
247	Desvauxii	Former Soviet Union	TEJ	0.3	165.7	173.0	29.1	27.3	6.3	8.0	24.8	18.9	17.2	20.0	2.3	2.3	393.3	345.7	1.5	1.6
248	Caucasica	Former Soviet Union	TEJ	1.0	180.5	187.0	36.7	33.5	8.0	6.7	25.3	24.5	21.6	27.9	2.6	4.2	431.0	412.3	1.3	1.6
249	Pirinae 69	Former Yugoslavia	ADMIX	1.3	181.3	174.3	50.8	47.9	8.3	7.0	30.1	19.4	26.0	15.6	3.2	1.6	411.7	375.0	1.8	1.6
251	H256-76-1-1-1	Argentina	TRJ	0.5	127.3	126.0	12.1	26.5	6.0	7.0							398.0	401.7	1.8	1.7
252	Djimoron	Guinea	IND	2.7	205.7	194.2	69.4	67.0	10.7	13.0	17.2	15.1	26.7	32.5	1.1	1.1	391.3	366.0	2.0	1.9
254	Hon Chim	Hong Kong	IND	1.0	205.3	195.0	37.0	25.8	8.0	6.7	14.1	14.1	22.3	10.4	2.0	1.3	392.7	389.0	2.0	2.1
255	Pai Hok Glutinous	Hong Kong	IND	0.7	184.7	189.7	80.8	85.0	14.3	14.3	23.0	11.8	23.0	30.1	0.8	1.1	385.3	392.0	1.7	1.9
257	Agusita	Hungary	TEJ	1.0	152.8	163.7	18.0	14.8	5.3	4.7	24.7	20.2	18.3	12.6	2.8	2.1	402.7	368.3	1.8	1.5
258	Tia Bura	Indonesia	TRJ	2.7	213.3	211.3	42.4	34.3	6.7	6.7	20.8	17.7	14.7	14.3	2.2	2.3	362.3	317.0	2.3	2.2
259	Sadri Tor Misri	Iran	ADMIX	2.3	191.7	210.0	73.4	83.0	10.0	9.7	29.3	24.3	44.3	33.3	4.5	5.8	374.7	378.3	1.8	1.7
260	205	Iran	AROMATIC	3.0	248.7	261.0	176.5	142.2	20.0	16.3							371.5	312.0	2.0	1.7

Appendices

Supplementary Table S8 (continued)

NSRFV ID	Accession Name	Country of origin	Subpopulation	Leaf bronzing score	Control plant height	Ozone plant height	Control dry weight	Ozone dry weight	Control tiller number	Ozone tiller number	Control thousand kernel weight	Ozone thousand kernel weight	Control total panicle weight	Ozone total panicle weight	Control single panicle weight	Ozone single panicle weight	Control SPAD	Ozone SPAD	Control lignin content	Ozone lignin content
261	Shim Balte	Iraq	AUS	2.0	168.5	168.8	54.6	42.4	13.3	11.7	19.9	18.3					380.7	317.0	1.2	1.4
262	Halwa Gose Red	Iraq	AUS	1.3	135.7	132.3	16.2	22.8	10.3	11.5	21.9	20.7	15.3	8.9	1.2	0.8	378.7	340.0	1.3	1.5
263	Maratelli	Italy	TEJ	0.3	165.3	161.2	29.7	21.0	6.7	9.0	23.9	20.7	23.6	14.7	3.1	2.4	476.3	459.0	1.8	1.8
264	Baldo	Italy	ADMIX	0.3	183.0	184.7	36.6	35.2	6.0	6.7	31.1	34.3	35.9	31.0	4.1	4.5	472.7	445.7	1.6	1.7
265	Vialone	Italy	TEJ	0.3	202.0	195.2	44.0	58.4	7.3	8.0	27.7	28.9	30.6	35.8	4.5	4.5	410.7	398.0	1.6	1.7
266	Hiderisirazu	Japan	ADMIX	0.7	164.7	160.0	13.0	12.3	4.7	4.0	16.8	16.7	9.8	11.2	2.2	3.2	397.3	442.0	1.6	1.8
267	Hatsunishiki	Japan	TEJ	2.3	172.2	163.0	25.5	23.0	8.7	8.0	20.3	18.6	21.0	13.7	2.1	1.7	392.5	385.0	1.5	2.1
268	Vavilovi	Kazakhstan	TEJ	1.0	179.2	196.0	36.1	33.0	8.3	8.3	29.7	26.3	28.9	31.8	3.9	3.1	412.3	400.7	1.6	1.7
269	Sundensis	Kazakhstan	IND	1.0	145.0	143.0	18.3	21.0	5.7	5.0	22.1	22.0	12.2	5.9	2.3	0.7	447.0	397.3	1.6	1.9
270	Osogovka	Macedonia	ADMIX	1.3	170.3	155.0	12.7	14.2	4.0	4.0	29.3	19.9	14.3	9.6	2.6	2.8	446.3	436.7	1.8	1.8
271	M. Blatec	Macedonia	ADMIX	2.5	196.3	196.7	30.8	36.6	5.0	5.3	32.2	33.3	13.2	16.5	3.2	3.3	405.0	368.7	1.9	1.6
273	Varyla	Madagascar	ADMIX	2.0	200.5	191.3	46.1	34.2	7.7	7.3	25.8	22.3	12.7	13.8	2.4	1.9	400.3	370.0	1.8	1.6
274	Padi Pagalong	Malaysia	TRJ	2.0	191.0	209.7	48.1	57.4	7.0	7.3	23.3	22.1	12.6	9.7	2.4	3.0	418.7	386.5	1.9	1.8
275	Sri Malaysia Dua	Malaysia	TEJ	0.7	165.3	153.5	29.8	15.5	7.7	8.5	23.1	21.5	21.1	18.0	2.9	2.6	388.7	420.0	1.4	1.7
276	Kaukau	Mali	AUS	1.0	216.7	211.7	82.6	82.8	6.7	8.0	18.8	16.4	35.2	34.8	1.7	2.0	375.7	385.7	1.8	1.6
277	Gambiaka Sebel	Mali	TEJ	0.0	127.7	129.9	13.3	21.0	4.0	6.7	22.9	21.4	4.1	15.3	1.0	2.0	407.7	402.7	1.6	1.4
278	CI-6-5-3	Mexico	ADMIX	1.0	124.0	116.7	12.9	14.6	5.0	6.3							375.7	386.0	1.9	1.8
279	Kon Suito	Mongolia	TEJ	3.3	139.3	144.3	14.5	17.9	6.0	7.0	26.7	23.8	12.2	41.2	2.0	5.0	418.0	366.3	2.0	1.9
280	Saku	Mongolia	ADMIX	2.0	174.7	171.3	24.9	15.8	3.7	4.7	18.4	15.9	4.4	6.9	1.2	1.6	386.3	385.3	1.8	1.6
282	Triomphe Du Maroc	Morocco	TEJ	0.3	113.2	124.7	12.0	11.7	4.3	4.3	18.9	16.1	2.7	4.6	0.8	1.3	414.7	402.0	1.6	1.5
283	Chibica	Mozambique	TEJ	2.0	143.2	136.3	25.5	22.0	7.0	8.0	22.2	16.4	8.9	9.6	1.3	1.3	384.7	397.0	1.5	2.0
284	IR-44595	Nepal	IND	0.0	101.0	119.0	14.5	22.4	7.3	11.0							409.3	373.3	1.7	1.8
285	Tox 782-20-1	Nigeria	TRJ	1.3	151.0	155.7	17.0	11.9	4.3	5.0	18.1	14.5	6.8	10.5	1.4	2.0	415.3	371.0	1.4	1.8
288	Italica Carolina	Poland	TEJ	1.7	143.0	141.7	22.6	17.9	8.3	8.0	22.9	24.0	21.4	22.6	1.8	2.5	409.7	366.5	1.5	1.4
289	Lusitano	Portugal	TEJ	1.7	168.0	160.0	26.9	19.9	10.7	7.3	22.5	21.2	30.6	20.6	3.0	2.3	448.3	430.0	1.7	1.6
290	Amposta	Puerto Rico	TEJ	0.3	141.3	134.7	8.9	13.8	5.0	5.3	12.3	16.8	5.7	12.7	1.1	2.6	376.5	434.3	2.0	1.7
291	Toploea 70/76	Romania	TEJ	0.0	106.0	112.3	7.6	11.0	5.7	6.7	9.3	11.2	3.7	10.7	0.6	1.3	417.3	433.3	1.8	2.1
293	TOg 7178	Senegal	ADMIX	2.7	217.0	208.0	88.9	73.3	9.7	9.3	31.3	31.6	41.7	42.2	5.4	6.3	409.0	411.0	1.7	1.7
294	SL 22-613	Sierra Leone	ADMIX	3.3	157.3	150.2	19.4	15.3	4.3	4.7	15.5	13.2	3.1	3.4	0.5	0.8	358.7	343.0	1.8	2.0
295	Bombilla	Spain	TEJ	3.3	172.7	164.0	35.1	25.9	9.0	6.3	22.5	24.5	14.8	10.9	2.0	1.7	419.7	409.3	1.6	1.6
296	Dosel	Spain	TEJ	0.7	137.3	140.0	15.0	8.8	6.0	5.3	20.5	20.0	5.3	7.9	1.0	1.2	415.0	403.7	1.5	1.6
297	Bahia	Spain	TEJ	0.3	128.7	129.5	14.2	13.0	4.0	4.7	24.6	23.2	4.3	6.1	1.0	1.5	396.3	412.3	1.4	1.5
298	LD 24	Sri Lanka	IND	1.0	178.3	175.2	46.4	46.5	6.7	8.0							416.3	348.0	1.9	1.7
299	SML 242	Suriname	IND	0.3	189.0	184.0	43.7	48.1	10.0	14.3	18.2	19.7	44.9	56.5	2.8	3.7	395.7	387.7	1.8	1.7
301	Melanotrix	Tajikistan	TEJ	1.0	196.8	195.0	40.7	37.7	9.0	10.3	22.6	23.1	32.6	30.9	3.7	3.4	432.3	358.7	1.7	1.8
303	Kihogo	Tanzania	TEJ	0.0	123.3	121.0	15.2	11.4	4.3	4.0	20.4	25.0	4.1	4.4	0.8	1.2	404.0	357.0	1.2	1.2
304	519	Uruguay	IND	2.3	202.7	193.0	65.5	44.5	11.7	9.7	18.0	16.8	36.6	26.3	1.9	2.0	368.3	345.3	1.6	1.9
305	Doble Carolina Rinaldo Barsan	Uruguay	ADMIX	0.0	175.0	172.7	25.3	32.2	6.0	5.7	26.3	22.5	14.7	15.5	2.3	2.5	416.7	405.3	1.4	1.5
306	WIR 3764	Uzbekistan	TEJ	1.3	180.7	172.0	31.0	30.0	8.7	9.7	22.1	23.3	26.5	28.3	2.9	3.6	432.3	424.0	1.4	2.0
307	Uzbekskij 2	Uzbekistan	TEJ	1.3	177.5	175.0	18.9	20.8	4.3	4.0	22.1	26.5	9.4	6.9	2.9	1.7	467.0	376.3	1.7	1.9

Appendices

Supplementary Table S8 (continued)

NSRFV ID	Accession Name	Country of origin	Subpopulation	Leaf bronzing score	Control plant height	Oxone plant height	Control dry weight	Oxone dry weight	Control tiller number	Oxone tiller number	Control thousand kernel weight	Oxone thousand kernel weight	Control total panicle weight	Oxone total panicle weight	Control single panicle weight	Oxone single panicle weight	Control SPAD	Oxone SPAD	Control lignin content	Oxone lignin content
308	Llanero 501	Venezuela	TRJ	3.0	161.7	158.7	19.3	14.7	4.3	4.0							408.3	394.0	2.3	2.4
310	R 101	Zaire	TRJ	2.7	171.7	166.0	21.5	15.5	4.0	3.3							376.7	317.7	1.8	1.9
311	56-122-23	Thailand	TEJ	2.7	138.5	138.5	18.5	13.7	6.7	6.3	14.0	10.6	6.2	3.2	1.1	0.6	377.3	415.3	1.9	2.1
312	Aswina 330	Bangladesh	AUS	3.3	192.7	186.0	43.7	40.7	11.7	13.3	19.3	22.1	36.7	33.6	2.7	2.2	381.3	377.0	1.9	2.2
313	BR24	Bangladesh	IND	2.7	147.3	144.0	25.3	41.7	5.0	7.7	17.6	15.4	9.3	13.7	1.8	1.7	345.3	327.0	1.6	2.0
314	CTG 1516	Bangladesh	AUS	2.3	162.2	159.3	26.4	20.3	9.0	8.0	16.2	11.8	5.8	3.0	0.7	0.4	368.3	323.7	1.6	1.9
315	Dawebyan	Myanmar	IND	1.0	210.7	197.3	105.1	47.4	11.3	8.3	25.9	16.4	35.4	15.6	1.2	1.4	380.3	374.7	1.4	1.5
316	DD 62	Bangladesh	AUS	3.7	170.0	160.7	44.4	25.9	6.0	5.3							362.3	328.0	1.6	1.5
317	DJ 123	Bangladesh	AUS	3.3	196.0	189.7	31.2	32.5	6.7	7.0	26.0	29.2	16.8	21.4	3.3	3.6	389.0	360.0	1.6	1.9
318	DJ 24	Bangladesh	AUS	0.7	208.3	198.2	62.7	43.2	6.3	5.7							351.0	366.3	1.5	1.7
319	DK 12	Bangladesh	AUS	3.0	201.3	195.3	55.0	47.1	9.3	7.7	15.6	12.6	13.7	7.4	1.0	0.8	342.7	352.3	1.8	2.1
320	DM 43	Bangladesh	AUS	2.0	198.0	186.0	77.3	27.8	14.3	8.0	22.1	16.1	33.4	13.6	1.5	1.4	405.3	360.3	1.3	1.8
321	DM 56	Bangladesh	AUS	2.3	157.0	153.2	19.8	8.9	5.3	4.3	14.4	14.0	2.9	1.1	0.4	0.2	381.0	298.0	1.7	1.9
322	DM 59	Bangladesh	AUS	2.0	155.7	160.0	24.8	25.3	8.3	8.0	13.8	17.9	3.6	4.8	0.5	0.9	357.7	347.0	1.3	1.9
323	DNJ 140	Bangladesh	AUS	2.0	197.3	185.8	84.9	87.6	12.3	12.5	19.4	19.4	31.9	21.0	1.5	2.0	375.3	393.5	1.6	1.5
324	DV 123	Bangladesh	AUS	5.7	159.2	163.1	21.4	24.1	5.3	5.7	10.1	11.5	2.9	5.5	0.4	0.6	388.7	327.7	1.6	1.8
325	EMATA A 16-34	Myanmar	IND	5.0	182.3	182.7	60.9	44.0	8.7	9.0							352.7	349.7	2.2	2.1
326	Ghorbhai	Bangladesh	AUS	1.3	174.8	168.7	31.0	17.8	8.0	4.7	14.6	15.6	8.7	4.8	0.8	0.7	353.7	322.0	2.0	2.2
327	Goria	Bangladesh	AUS	0.7	173.8	180.3	32.0	22.4	11.7	8.7	22.8	21.2	28.9	17.0	2.8	1.9	388.3	399.7	1.9	1.9
328	Jamir	Bangladesh	AUS	1.7	204.0	191.8	55.1	51.8	16.7	16.3	22.9	21.5					393.3	415.3	1.4	1.6
329	Kachilon	Bangladesh	AUS	4.0	202.7	196.3	29.0	26.3	9.7	9.0	19.0	16.5	19.4	12.3	2.0	2.0	374.3	370.5	1.8	2.3
331	Khao Tot Long 227	Thailand	AUS	3.0	191.0	184.5	40.3	25.4	10.3	8.3	22.1	23.3	21.6	14.9	1.9	2.3	363.0	375.3	2.1	2.3
332	KPF-16	Bangladesh	ADMIX	2.5	184.3	178.7	61.4	32.4	14.3	10.0	11.5	18.5	12.8	6.0	0.4	0.5	390.0	341.0	1.9	1.7
333	Leuang Hawn	Thailand	TEJ	0.0	108.0	117.5	5.2	8.7	4.0	4.5	16.2	11.7	4.7	5.3	1.2	1.1	347.7	303.7	2.3	2.1
334	Lomello	Thailand	TEJ	0.7	170.0	162.0	25.2	15.1	4.0	4.7	20.3	23.4	13.7	8.6	3.6	3.1	434.0	462.0	1.7	1.6
335	Okshitmayin	Myanmar	ADMIX	1.3	156.2	148.0	22.0	21.1	6.0	5.3	20.5	17.0	8.2	9.2	1.2	1.5	465.0	382.0	1.7	1.9
336	Paung Malaung	Myanmar	AUS	1.3	172.0	181.2	40.2	44.7	8.3	8.7	23.0	16.6	13.7	14.7	1.3	1.1	409.3	354.0	1.7	1.7
337	Sabharaj	Bangladesh	IND	2.0	196.0	202.8	79.3	52.5	11.3	9.7	23.1	20.5	36.6	29.0	1.2	1.2	403.3	392.7	1.7	1.7
338	Sitpwa	Myanmar	TEJ	1.7	158.0	153.3	19.9	15.1	7.0	5.0	16.8	21.6	10.9	7.6	1.9	1.6	422.3	417.0	2.1	2.0
339	Yodanya	Myanmar	IND	1.3	199.3	199.0	43.0	46.5	11.3	9.7	22.5	24.4	35.8	30.1	3.2	3.3	429.0	418.3	1.6	1.7
340	Berenj	Afghanistan	ADMIX	4.0	230.0	227.0	66.6	50.8	8.7	8.0	18.2	12.5	14.5	8.2	1.4	0.8	347.3	349.5	1.5	1.6
341	Shirkati	Afghanistan	AUS	0.5	199.7	191.3	58.5	56.7	9.7	11.0	19.7	15.0	14.9	14.6	0.6	0.7	357.5	364.7	1.0	1.0
342	Cenit	Argentina	TRJ	2.0	191.0	189.3	27.6	27.1	3.7	3.7	11.5	11.0	4.7	5.0	1.3	1.4	360.7	359.0	1.8	1.9
343	Victoria F.A.	Argentina	ADMIX	1.3	193.0	188.0	26.3	21.2	4.7	4.7	19.6	25.0	20.9	13.1	4.1	2.7	431.0	413.7	2.0	1.9
344	Habiganj Boro 6	Bangladesh	ADMIX	4.7	196.0	205.0	77.5	65.8	13.0	14.0	17.9	19.4	25.0	27.6	1.8	1.5	403.3	362.0	1.7	2.0
345	DZ 193	Bangladesh	AUS	4.3	184.0	195.7	35.1	30.4	7.0	5.7	22.6	27.1	23.1	16.8	2.5	2.5	397.0	378.7	2.0	1.9
346	Karkati 87	Bangladesh	AUS	2.0	185.0	187.3	55.3	64.7	11.3	10.0	21.8	18.5	25.3	23.6	1.2	0.9	382.3	376.0	1.0	1.2
348	China 1039	China	IND	0.3	191.7	187.7	49.2	48.8	10.3	9.0	18.7	19.1	48.1	42.7	4.3	3.6	392.7	399.5	2.0	2.2
349	Chang Ch'Sang Hsu Tao	China	IND	1.7	184.0	177.3	61.0	52.8	9.7	9.3	20.2	14.5	19.4	15.1	1.1	0.9	338.0	362.3	1.9	1.7
353	ARC 10376	India	AUS	4.3	191.3	197.0	32.0	23.3	7.0	4.3	17.5	18.6	22.0	13.9	2.1	1.9	395.3	389.3	1.7	1.9

Appendices

Supplementary Table S8 (continued)

NSFT/VID	Accession Name	Country of Origin	Subpopulation	Leaf bronzing score	Control plant height	Ozone plant height	Control dry weight	Ozone dry weight	Control tiller number	Ozone tiller number	Control thousand kernel weight	Ozone thousand kernel weight	Control total panicle weight	Ozone total panicle weight	Control single panicle weight	Ozone single panicle weight	Control SPAD	Ozone SPAD	Control lignin content	Ozone lignin content
355	ASD 1	India	TEJ	1.3	184.7	177.3	33.6	24.9	9.3	7.0	22.6	19.5	27.5	20.0	2.7	3.0	477.7	423.0	1.9	2.0
356	JC 117	India	IND	0.7	199.0	174.3	48.3	45.4	11.0	9.3	19.1	19.1	41.3	36.0	4.3	4.0	398.3	399.3	1.9	1.3
357	9524	India	AUS	1.5	224.3	218.5	56.0	46.3	6.3	6.7	24.7	21.7	31.5	18.2	5.3	2.6	333.3	374.0	1.9	1.8
358	ARC 10086	India	ADMIX	1.0	192.7	185.3	35.5	26.3	4.7	4.0	11.2	10.6	3.4	3.6	0.8	0.8	379.3	388.0	2.2	2.2
359	Surjamkuhi	India	AUS	2.0	160.7	159.7	19.8	13.9	5.3	5.0							338.3	352.3	1.4	1.7
360	PTB 30	India	AUS	3.0	196.3	197.0	36.1	30.7	9.3	7.3	19.9	17.6	12.5	8.6	1.3	1.2	342.0	348.3	2.0	2.1
361	F.R. 13A	India	TEJ	4.7	209.7	233.7	130.9	117.0	10.0	9.3							353.3	357.0	1.9	1.8
363	Edomen Scented	Japan	TEJ	2.3	204.0	157.7	26.5	29.6	5.0	6.3	22.1	20.4	13.4	22.4	4.5	3.7	397.0	377.3	2.2	2.1
364	Rikuto Norin 21	Japan	ADMIX	3.3	178.0	174.7	32.7	26.5	6.7	5.3	21.4	19.9	28.1	24.3	4.2	4.3	412.7	347.0	1.8	2.1
365	Shirogane	Japan	TEJ	0.3	122.7	123.5	12.9	10.7	6.7	7.3	11.9	13.5	6.6	5.5	0.7	0.6	461.0	449.7	1.4	2.2
366	Kiuki No. 46	Japan	TEJ	0.7	166.3	164.0	39.1	16.8	10.0	6.3	19.3	14.2	23.3	3.7	2.0	0.7	414.0	403.0	2.0	1.8
367	Sanbyang-Daeme	Korea	ADMIX	2.3	249.0	230.0	54.4	13.9	5.3	3.5	21.6	20.2	33.3	14.5	4.5	5.7	407.3	356.7	1.8	1.9
368	Deokjeokjodo	Korea	TEJ	1.3	182.5	193.7	38.9	56.5	7.7	7.7	17.3	12.8	10.1	10.9	1.6	1.4	398.0	387.7	1.8	1.9
369	Sathi	Pakistan	AUS	3.0	192.0	190.0	37.4	29.4	11.0	9.7	24.5	20.1	29.9	18.6	2.7	2.7	385.7	348.7	1.5	1.8
370	Coarse	Pakistan	AUS	3.0	208.3	209.0	63.4	65.2	11.0	11.3	18.6	19.0	42.4	27.4	3.0	2.8	363.7	366.7	1.2	1.0
371	Santhi Sufaid	Pakistan	AUS	2.3	184.3	188.0	51.4	42.6	10.3	9.3	15.1	13.9	20.0	10.0	1.1	0.7	376.3	378.3	1.3	1.7
372	Sufaid	Pakistan	AUS	2.7	207.7	203.7	48.7	39.7	10.3	9.7	17.4	16.9	18.3	13.3	1.6	1.5	352.3	330.7	1.2	1.5
373	Lambayeque 1	Peru	AROMATIC	2.0	233.7	248.0	99.8	67.9	12.0	10.7	21.9	17.6	37.0	26.0	3.2	2.5	363.7	355.3	1.5	1.7
376	Breviaristata	Portugal	ADMIX	1.3	200.0	202.0	34.1	42.1	5.0	5.5	31.6	31.4	20.5	30.1	4.1	3.8	445.3	427.7	1.5	1.5
377	PR 304	Puerto Rico	TRJ	2.7	208.7	203.0	50.8	40.2	5.7	5.0	16.8	14.0	9.9	9.2	2.2	2.0	396.5	330.0	2.0	2.1
378	Kalubala Vee	Sri Lanka	AUS	2.7	194.0	195.7	93.5	67.0	14.3	13.7	22.1	20.5	63.1	44.0	3.4	3.9	401.3	380.3	1.4	1.7
380	Tainan-Iku No. 512	Taiwan	TEJ	1.7	149.7	143.3	22.1	15.8	5.7	5.0	17.5	17.8	3.6	2.6	0.7	0.6	425.0	392.0	2.1	1.9
384	318	TURKEY	TRJ	3.0	200.7	185.0	48.9	30.1	7.7	5.0	24.0	18.8	15.7	6.8	2.0	1.3	399.7	320.3	1.9	1.7
385	Nira	United States	IND	1.3	178.7	189.0	43.6	45.8	8.0	11.3	23.6	19.2	33.8	41.9	3.7	3.0	395.0	345.0	1.8	1.9
386	Palmyra	United States	ADMIX	3.3	185.3	184.3	27.7	29.5	4.0	4.3							376.7	387.0	2.0	1.9
387	M-202	United States	ADMIX	0.0	121.3	120.7	9.5	9.5	4.3	5.0	14.9	20.6	2.6	1.4	0.7	0.4	467.0	412.5	1.8	1.8
389	CI 11011	United States	ADMIX	1.7	182.0	178.3	24.5	19.5	6.0	3.7							496.0	458.7	2.5	2.1
390	CI 11026	United States	ADMIX	0.3	151.7	159.5	17.5	14.7	5.0	5.5							318.3	322.3	2.3	2.1
392	Edith	United States	TRJ	0.7	196.7	200.0	36.7	41.5	6.0	6.3	20.0	18.2	13.5	12.5	2.1	2.3	380.3	385.0	1.9	2.0
394	Lady Wright Seln	United States	TRJ	0.5	169.0	160.5	26.7	22.9	5.7	5.3	22.1	18.6	11.3	9.0	2.3	2.1	386.7	395.0	1.7	2.0
395	OS 6 (WC 10296)	Zaire	TRJ	1.7	179.3	164.0	46.0	19.3	6.0	4.3	16.9	16.5	23.6	5.4	1.7	1.3	368.0	314.0	1.9	1.8
396	Cocodrie	United States	TRJ	1.7	113.0	120.7	18.6	14.1	6.3	6.0	12.5	7.1	2.0	0.7	0.3	0.2	386.3	373.7	1.6	1.7
397	Cybonnet	United States	TRJ	1.0	108.0	116.7	13.2	11.1	4.7	5.3							386.0	371.0	1.6	1.6
635	Azucena	Philippines	TRJ	3.0	224.5	207.3	48.8	35.6	6.7	4.7	22.5	19.4	13.2	10.4	3.3	2.2	417.0	363.0	1.8	1.7
636	Sadu Cho	Korea	IND	1.7	171.3	180.5	50.0	40.2	13.0	11.3	13.5	12.6	18.9	21.6	0.8	1.7	408.3	404.0	2.0	2.3
637	N 22	India	AUS	2.7	193.0	194.0	44.6	38.4	11.0	10.7	18.1	16.5	26.4	19.3	2.3	1.8	373.0	359.3	1.9	2.0
638	Moroberekan	Guinea	TRJ	2.5	224.0	210.7	40.5	25.3	3.7	3.0	25.0	22.9	9.5	4.7	2.6	2.0	437.7	404.5	1.8	1.7
639	Nipponbare	Japan	TEJ	0.3	136.0	134.0	17.5	13.8	6.0	6.3							388.0	368.5	1.9	1.8
640	Dom-Sofid	Iran	AROMATIC	3.3	220.3	226.0	87.7	78.3	10.3	10.0	10.7	11.1	11.5	10.4	0.9	1.0	406.3	389.0	1.7	1.6
641	Tainung 67	Taiwan	TEJ	0.3	134.0	129.0	18.7	13.9	6.0	5.7	13.3	8.8	3.0	0.6	0.4	0.2	392.0	366.0	2.2	2.1

Appendices

Supplementary Table S8 (continued)

NSFTV ID	Accession Name	Country of origin	Subpopulation	Leaf bronzing score	Control plant height	Ozone plant height	Control dry weight	Ozone dry weight	Control tiller number	Ozone tiller number	Control thousand kernel weight	Ozone thousand kernel weight	Control total panicle weight	Ozone total panicle weight	Control single panicle weight	Ozone single panicle weight	Control SPAD	Ozone SPAD	Control lignin content	Ozone lignin content
642	Zhenshan 97B	China	IND	0.0	93.7	92.0	11.6	10.9	8.3	8.7							408.3	398.3	1.9	1.8
643	Minghui 63	China	IND	1.0	130.0	126.0	36.9	32.5	12.3	13.0	12.3	9.6	1.4	4.9	0.3	0.5	402.0	364.0	2.1	1.7
644	IR64	Philippines	IND	1.0	105.0	108.7	18.6	12.4	8.3	7.0							417.7	362.7	1.9	1.8
645	M202	United States	ADMIX	1.3	125.3	125.3	16.8	10.5	6.3	4.7							441.0	460.0	1.5	1.9
647	Cypress	United States	TRJ	3.3	124.0	129.3	11.4	13.8	7.7	6.7							385.0	375.3	1.7	1.5
648	Shan-Huang-Zhan-2	China	IND	0.3	108.7	109.7	15.2	11.8	7.0	6.7							429.3	394.0	1.8	1.8
651	Dular	India	AUS	4.0	186.7	183.3	32.6	24.2	7.3	6.3	20.2	17.9	18.3	11.5	2.7	2.0	412.3	393.0	1.3	1.6
652	Li-Jiang-Xin-Tuan-Hei-Gu	China	ADMIX	2.7	218.0	207.0	43.3	27.8	9.3	8.0	19.5	19.6	28.6	15.7	2.5	2.4	402.0	371.7	1.4	1.6

The mean value of three biological replicates is shown. For mapping, raw value was used for lignin content, square-root transformed value was used for leaf bronzing score, and the ratio (ozone/control) was used for the rest of the traits. Gray cells are extreme values which were removed prior to the mapping. Empty cells from thousand kernel weight, total panicle weight and single panicle weight are the accessions which had less than 10 g of average thousand kernel weight or showed high shattering habit, which were removed from the original dataset.

Appendices

Supplementary Table S9: Correlation matrix in each subpopulation.

<i>admix</i>	Leaf bronzing score	Relative plant height	Relative dry weight	Relative tiller number	Relative thousand kernel weight	Relative total panicle weight	Relative single panicle weight	Relative SPAD	Lignin content	Relative lignin content
Leaf bronzing score	1.00	0.912	0.241	0.416	0.376	0.536	0.956	0.395	0.823	0.204
Relative plant height	-0.02	1.00	0.463	0.842	0.200	0.327	0.167	0.727	0.117	0.673
Relative dry weight	-0.17	0.11	1.00	<0.001	0.939	0.006	0.911	0.752	0.938	0.033
Relative tiller number	-0.12	0.03	0.70	1.00	0.693	<0.001	0.868	0.442	0.787	0.027
Relative thousand kernel weight	-0.15	0.21	-0.01	0.07	1.00	0.644	0.990	0.312	0.937	0.578
Relative total panicle weight	-0.11	0.17	0.45	0.53	-0.08	1.00	0.002	0.791	0.949	0.106
Relative single panicle weight	0.01	0.23	-0.02	-0.03	0.00	0.49	1.00	0.423	0.529	0.812
Relative SPAD	-0.13	0.05	0.05	0.11	-0.17	0.05	0.14	1.00	0.449	0.787
Lignin content	0.03	-0.23	-0.01	-0.04	0.01	0.01	-0.11	-0.11	1.00	<0.001
Relative lignin content	0.19	0.06	-0.31	-0.32	-0.09	-0.27	0.04	-0.04	-0.54	1.00

<i>aromatic</i>	Leaf bronzing score	Relative plant height	Relative dry weight	Relative tiller number	Relative thousand kernel weight	Relative total panicle weight	Relative single panicle weight	Relative SPAD	Lignin content	Relative lignin content
Leaf bronzing score	1.00	0.295	0.624	0.365	0.360	0.852	0.504	0.011	0.100	0.791
Relative plant height	-0.33	1.00	0.552	0.720	0.194	0.131	0.345	0.434	0.875	0.519
Relative dry weight	-0.16	-0.19	1.00	0.424	0.545	0.402	0.477	0.434	0.875	0.519
Relative tiller number	-0.29	0.12	-0.25	1.00	0.790	0.190	0.251	0.077	0.539	0.194
Relative thousand kernel weight	0.38	0.51	0.25	0.11	1.00	0.013	0.006	0.632	0.554	0.241
Relative total panicle weight	0.08	0.58	0.35	0.52	0.82	1.00	<0.001	0.132	0.248	0.045
Relative single panicle weight	0.28	0.39	0.30	0.46	0.86	0.95	1.00	0.343	0.198	0.044
Relative SPAD	-0.70	0.25	0.25	0.53	0.20	0.58	0.39	1.00	0.182	0.934
Lignin content	0.50	-0.10	0.05	0.20	0.25	0.46	0.51	-0.41	1.00	0.002
Relative lignin content	-0.09	-0.22	-0.21	-0.40	-0.47	-0.72	-0.72	-0.03	-0.79	1.00

Appendices

Supplementary Table S9 (continued)

<i>aus</i>	Leaf bronzing score	Relative plant height	Relative dry weight	Relative tiller number	Relative thousand kernel weight	Relative total panicle weight	Relative single panicle weight	Relative SPAD	Lignin content	Relative lignin content
Leaf bronzing score	1.00	0.883	0.391	0.906	0.504	0.271	0.443	0.062	0.799	0.351
Relative plant height	0.02	1.00	0.001	0.081	0.086	0.023	0.926	0.288	0.116	0.105
Relative dry weight	0.12	0.42	1.00	<0.001	0.228	<0.001	0.573	0.450	0.676	0.097
Relative tiller number	-0.02	0.24	0.78	1.00	0.352	<0.001	0.605	0.652	0.742	0.049
Relative thousand kernel weight	0.09	0.24	0.17	0.13	1.00	0.045	0.027	0.736	0.148	0.539
Relative total panicle weight	0.17	0.34	0.61	0.56	0.30	1.00	<0.001	0.589	0.760	0.641
Relative single panicle weight	0.12	-0.01	0.09	0.08	0.33	0.62	1.00	0.383	0.352	0.585
Relative SPAD	-0.25	-0.15	-0.10	-0.06	0.05	-0.08	0.13	1.00	0.320	0.117
Lignin content	0.04	0.21	-0.06	-0.05	0.20	-0.05	-0.14	0.14	1.00	<0.001
Relative lignin content	0.13	-0.22	-0.23	-0.27	-0.09	-0.07	0.08	-0.21	-0.54	1.00

<i>indica</i>	Leaf bronzing score	Relative plant height	Relative dry weight	Relative tiller number	Relative thousand kernel weight	Relative total panicle weight	Relative single panicle weight	Relative SPAD	Lignin content	Relative lignin content
Leaf bronzing score	1.00	0.687	0.322	0.166	0.542	0.978	0.689	0.510	0.008	0.715
Relative plant height	-0.05	1.00	0.029	0.071	0.241	0.315	0.013	0.117	0.623	0.140
Relative dry weight	-0.12	0.25	1.00	<0.001	0.689	<0.001	0.230	0.494	0.128	0.178
Relative tiller number	-0.16	0.21	0.76	1.00	0.913	<0.001	0.163	0.345	0.081	0.377
Relative thousand kernel weight	0.09	0.17	0.06	-0.02	1.00	0.809	0.557	0.069	0.916	0.679
Relative total panicle weight	0.00	0.15	0.68	0.62	-0.04	1.00	<0.001	0.062	0.504	0.909
Relative single panicle weight	-0.06	0.36	0.18	0.21	0.09	0.55	1.00	0.092	0.783	0.765
Relative SPAD	0.08	-0.18	-0.08	-0.11	-0.26	-0.27	-0.25	1.00	0.511	0.625
Lignin content	0.31	-0.06	-0.18	-0.20	0.02	-0.10	0.04	0.08	1.00	<0.001
Relative lignin content	-0.04	0.17	0.16	0.10	0.06	0.02	0.04	-0.06	-0.47	1.00

Appendices

Supplementary Table S9 (continued)

<i>temperate japonica</i>	Leaf bronzing score	Relative plant height	Relative dry weight	Relative tiller number	Relative thousand kernel weight	Relative total panicle weight	Relative single panicle weight	Relative SPAD	Lignin content	Relative lignin content
Leaf bronzing score	1.00	0.521	0.308	0.158	0.823	0.637	0.145	0.767	0.981	0.497
Relative plant height	-0.08	1.00	0.068	0.721	0.632	0.162	0.097	0.181	0.372	0.235
Relative dry weight	-0.12	0.22	1.00	<0.001	0.008	<0.001	<0.001	0.572	0.491	0.133
Relative tiller number	-0.17	0.04	0.64	1.00	0.008	<0.001	<0.001	0.273	0.466	0.742
Relative thousand kernel weight	-0.03	-0.06	0.33	0.33	1.00	0.003	<0.001	0.418	0.230	0.820
Relative total panicle weight	-0.06	0.18	0.73	0.65	0.37	1.00	<0.001	0.300	0.342	0.235
Relative single panicle weight	-0.18	0.21	0.59	0.42	0.44	0.86	1.00	0.259	0.276	0.332
Relative SPAD	-0.04	-0.16	0.07	0.13	0.10	0.13	0.14	1.00	0.562	0.565
Lignin content	0.00	-0.11	0.08	-0.09	-0.15	-0.12	-0.14	-0.07	1.00	<0.001
Relative lignin content	0.08	-0.14	-0.18	-0.04	-0.03	-0.15	-0.12	0.07	-0.42	1.00

<i>tropical japonica</i>	Leaf bronzing score	Relative plant height	Relative dry weight	Relative tiller number	Relative thousand kernel weight	Relative total panicle weight	Relative single panicle weight	Relative SPAD	Lignin content	Relative lignin content
Leaf bronzing score	1.00	0.054	0.337	0.012	0.285	0.916	0.904	0.125	0.003	0.791
Relative plant height	-0.23	1.00	0.039	0.352	0.302	0.155	0.005	0.223	0.330	0.514
Relative dry weight	-0.12	0.25	1.00	<0.001	0.003	<0.001	0.006	0.727	0.781	0.315
Relative tiller number	-0.30	0.11	0.62	1.00	0.157	<0.001	0.143	0.494	0.482	0.764
Relative thousand kernel weight	0.15	0.14	0.40	0.19	1.00	<0.001	<0.001	0.343	0.792	0.898
Relative total panicle weight	0.01	0.19	0.55	0.47	0.75	1.00	<0.001	0.946	0.744	0.460
Relative single panicle weight	-0.02	0.37	0.37	0.20	0.78	0.89	1.00	0.867	0.688	0.826
Relative SPAD	-0.18	0.15	0.04	-0.08	-0.13	0.01	0.02	1.00	0.984	0.126
Lignin content	0.35	-0.12	-0.03	-0.09	0.04	-0.05	-0.06	0.00	1.00	<0.001
Relative lignin content	-0.03	0.08	-0.12	0.04	-0.02	0.10	0.03	-0.18	-0.45	1.00

The population was divided into five main subpopulations and the admixed group, and the correlation coefficient and its significance were calculated. The lower triangle shows the correlation coefficient between two traits, and the upper triangle shows the *P* values of the correlation. The correlation coefficient was calculated using Pearson's correlation coefficient, and *P* values were obtained using two-tailed Student's *t*-test.



Appendices

Supplementary Table S10: List of significant SNPs identified through association mapping.

Trait	SNP marker ID	Chr	Position (MSU7)	$-\log_{10}P$ value	MAF	Major allele	Minor allele	Location
Square-root transformed leaf bronzing score	id1026704	1	41535807	5.39	0.11	C	T	188 bp upstream LOC_Os01g71670
Square-root transformed leaf bronzing score	id1027269	1	42082183	4.20	0.24	A	G	intron LOC_Os01g72560
Square-root transformed leaf bronzing score	id5006917	5	17249762	4.09	0.48	C	T	intergenic region
Relative plant height	id8002494	8	7984606	4.20	0.24	C	T	exon LOC_Os08g13420 (T683M)
Relative dry weight	id6015530	6	27382490	4.88	0.10	C	T	intergenic region
Relative dry weight	id8002877	8	9107117	4.18	0.18	C	T	intergenic region
Relative dry weight	id12008228	12	23661669	4.87	0.31	T	A	intergenic region
Relative tiller number	id1027513	1	42325443	4.23	0.29	A	C	380 bp upstream LOC_Os01g72970
Relative SPW	ud2001239	2	21778775	4.68	0.34	T	C	intergenic region
Relative SPW	id2008679	2	21812170	5.12	0.13	G	A	intron LOC_Os02g36190
Relative SPW	id10004968	10	17366969	4.27	0.33	T	C	86 bp upstream LOC_Os10g33140
Relative SPAD	wd4003148	4	30724662	4.12	0.40	A	C	3'-UTR LOC_Os04g51820
Relative SPAD	id5000986	5	1545155	4.66	0.42	G	A	intergenic region
Relative SPAD	id5000988	5	1546671	4.12	0.28	A	C	762 bp upstream LOC_Os05g03620
Relative SPAD	id5001009	5	1614147	4.20	0.45	G	A	intergenic region
Relative SPAD	id5001440	5	2539289	4.17	0.47	C	T	intron LOC_Os05g05210

The SNPs showing  $-\log_{10}P$  value  $> 4.0$  are listed together with the corresponding trait, SNP marker ID (used in rice diversity panel), chromosome number, physical position (bp, as in MSU 7 database),  $-\log_{10}P$  value, minor allele frequency, minor and major allele and the location of the SNPs on the chromosome. The location of the SNP marker was classified as exon, intron, untranslated region, upstream or downstream if the SNP was located within 1,000 bp from a gene, or intergenic region otherwise. If the SNP was located in an exon of a gene, amino acid substitution was shown if applicable (original amino acid, amino acid position and the resultant amino acid).

Appendices

Supplementary Table S11: List of the top 50 SNPs from each trait.

Trait	SNP marker ID	Chr	Position (MSU7)	-log10P value	LD block start (bp)	LD block end (bp)	LD block size (bp)
Relative plant height	id100058	1	204126	2.82	174692	401599	226907
Relative plant height	id1003397	1	4090558	3.04	<b>4005917</b>	<b>4173403</b>	167486
Relative plant height	id1003490	1	4173403	3.04	<b>4005917</b>	<b>4173403</b>	167486
Relative tiller number	id1003733	1	4427772	3.31	4408400	4427772	19372
Relative lignin content	id1004041	1	4971993	2.63	4969392	4975371	5979
Relative thousand kernel weight	id1004242	1	5326062	2.66	<b>5326062</b>	<b>5475749</b>	149687
Relative total panicle weight	id1004242	1	5326062	2.36	<b>5326062</b>	<b>5475749</b>	149687
Relative dry weight	id1005142	1	6668083	2.66	<b>6661627</b>	<b>6668083</b>	6456
Relative tiller number	id1005142	1	6668083	3.43	<b>6661627</b>	<b>6668083</b>	6456
Relative dry weight	id1005178	1	6794133	2.98	6787032	7054453	267421
Square-root transformed leaf bronzing score	id1005516	1	7180947	2.81	7177403	7332852	155449
Relative single panicle weight	id1006289	1	8174333	3.39	8137725	8510834	373109
Relative SPAD	id1007879	1	10998909	3.12	10939343	11357494	418151
Lignin content	ud1000550	1	11906109	3.24	<b>11856807</b>	<b>12308329</b>	451522
Lignin content	id1008322	1	11924993	3.37	<b>11856807</b>	<b>12308329</b>	451522
Lignin content	id1008336	1	11931155	2.74	<b>11856807</b>	<b>12308329</b>	451522
Lignin content	id1008346	1	11952182	3.31	<b>11856807</b>	<b>12308329</b>	451522
Lignin content	id1008401	1	12065469	2.82	<b>11856807</b>	<b>12308329</b>	451522
Lignin content	id1008403	1	12066168	2.93	<b>11856807</b>	<b>12308329</b>	451522
Relative total panicle weight	id1009376	1	14311295	2.00	14172690	14337515	164825
Relative total panicle weight	ud1000811	1	18075175	2.44	15438604	18235531	2796927
Relative single panicle weight	id1012723	1	22418794	3.73	22369525	22498177	128652
Lignin content	id1012795	1	22557082	3.36	<b>22557082</b>	<b>22721951</b>	164869
Lignin content	id1012821	1	22563986	2.88	<b>22557082</b>	<b>22721951</b>	164869
Lignin content	ud1001004	1	22591363	3.20	<b>22557082</b>	<b>22721951</b>	164869
Lignin content	id1012822	1	22591601	2.92	<b>22557082</b>	<b>22721951</b>	164869
Lignin content	id1012834	1	22594722	2.92	<b>22557082</b>	<b>22721951</b>	164869
Lignin content	id1012836	1	22595242	3.20	<b>22557082</b>	<b>22721951</b>	164869
Relative SPAD	id1013296	1	23193989	2.82	23116088	23248184	132096
Relative total panicle weight	id1013335	1	23315502	3.13	<b>23313092</b>	<b>23315780</b>	2688
Relative total panicle weight	ud1001043	1	23315780	2.87	<b>23313092</b>	<b>23315780</b>	2688
Relative total panicle weight	id1013354	1	23338226	2.61	<b>23337421</b>	<b>23338972</b>	1551
Relative total panicle weight	id1013362	1	23338972	2.68	<b>23337421</b>	<b>23338972</b>	1551
Relative dry weight	id1013402	1	23361499	2.61	<b>23361499</b>	<b>23363919</b>	2420
Relative tiller number	id1013402	1	23361499	3.00	<b>23361499</b>	<b>23363919</b>	2420
Relative total panicle weight	id1013402	1	23361499	3.05	<b>23361499</b>	<b>23363919</b>	2420
Relative total panicle weight	id1013404	1	23361760	2.03	<b>23361499</b>	<b>23363919</b>	2420
Relative tiller number	id1013422	1	23367451	2.79	<b>23366322</b>	<b>23367451</b>	1129
Relative total panicle weight	id1013422	1	23367451	3.00	<b>23366322</b>	<b>23367451</b>	1129
Relative single panicle weight	id1013546	1	23579131	2.70	<b>23518306</b>	<b>23609631</b>	91325
Relative single panicle weight	id1013566	1	23583742	2.71	<b>23518306</b>	<b>23609631</b>	91325
Square-root transformed leaf bronzing score	id1016608	1	28367634	2.81	28347716	28429542	81826
Relative tiller number	id1017391	1	29441562	2.84	29324976	29445755	120779
Relative tiller number	id1017422	1	29449009	2.65	<b>29448630</b>	<b>29488546</b>	39916
Relative tiller number	id1017430	1	29482477	2.73	<b>29448630</b>	<b>29488546</b>	39916
Relative tiller number	id1018950	1	31421262	2.97	none	none	0
Relative lignin content	id1019385	1	31921430	2.56	<b>31876884</b>	<b>32019849</b>	142965
Relative lignin content	id1019401	1	31939109	2.84	<b>31876884</b>	<b>32019849</b>	142965
Relative tiller number	ud1001373	1	32300029	2.62	32172130	32326843	154713
Relative dry weight	id1020214	1	32698021	2.61	none	none	0
Relative thousand kernel weight	id1021758	1	34786169	2.79	<b>34690632</b>	<b>34788248</b>	97616
Relative thousand kernel weight	id1021759	1	34788248	2.64	<b>34690632</b>	<b>34788248</b>	97616
Relative lignin content	id1023570	1	37391135	3.05	<b>37312393</b>	<b>38233157</b>	920764
Square-root transformed leaf bronzing score	id1023791	1	37686259	2.80	<b>37312393</b>	<b>38233157</b>	920764
Square-root transformed leaf bronzing score	id1025077	1	39548414	2.99	none	none	0
Square-root transformed leaf bronzing score	id1025088	1	39553459	2.81	<b>39549203</b>	<b>39825564</b>	276361
Square-root transformed leaf bronzing score	id1025198	1	39620806	2.82	<b>39549203</b>	<b>39825564</b>	276361
Relative tiller number	id1025292	1	39799820	2.66	<b>39549203</b>	<b>39825564</b>	276361
Relative tiller number	id1025321	1	39824649	2.64	<b>39549203</b>	<b>39825564</b>	276361
Relative single panicle weight	id1025861	1	40614386	2.71	<b>40253277</b>	<b>40614386</b>	361109
Relative single panicle weight	id1025863	1	40623063	2.66	<b>40623063</b>	<b>40623668</b>	605
Square-root transformed leaf bronzing score	id1026656	1	41349739	3.46	<b>41349739</b>	<b>41535420</b>	185681
Lignin content	id1026656	1	41349739	3.06	<b>41349739</b>	<b>41535420</b>	185681
Lignin content	id1026660	1	41386306	3.15	<b>41349739</b>	<b>41535420</b>	185681
Lignin content	id1026685	1	41396262	3.97	<b>41349739</b>	<b>41535420</b>	185681
Square-root transformed leaf bronzing score	id1026704	1	41535807	5.39	41535729	41535835	106
Relative thousand kernel weight	id1027233	1	42036835	2.64	42036835	42062369	25534
Square-root transformed leaf bronzing score	id1027269	1	42082183	4.20	42082183	42086346	4163
Relative tiller number	id1027397	1	42256178	3.23	42255303	42256178	875
Square-root transformed leaf bronzing score	dd1001373	1	42256875	3.06	none	none	0

## Appendices

Supplementary Table S11 (continued)

Trait	SNP marker ID	Chr	Position (MSU7)	-log10P value	LD block start (bp)	LD block end (bp)	LD block size (bp)
Square-root transformed leaf bronzing score	dd1001565	1	42316278	2.92	<b>42316278</b>	<b>42336093</b>	19815
Relative tiller number	id1027507	1	42324402	3.10	<b>42316278</b>	<b>42336093</b>	19815
Relative total panicle weight	id1027507	1	42324402	2.90	<b>42316278</b>	<b>42336093</b>	19815
Relative tiller number	id1027513	1	42325443	4.23	<b>42316278</b>	<b>42336093</b>	19815
Relative total panicle weight	id1027513	1	42325443	2.73	<b>42316278</b>	<b>42336093</b>	19815
Square-root transformed leaf bronzing score	id1027525	1	42328671	3.43	<b>42316278</b>	<b>42336093</b>	19815
Relative tiller number	id1027529	1	42329156	3.28	<b>42316278</b>	<b>42336093</b>	19815
Relative total panicle weight	id1027529	1	42329156	2.07	<b>42316278</b>	<b>42336093</b>	19815
Relative tiller number	dd1001675	1	42336093	2.83	<b>42316278</b>	<b>42336093</b>	19815
Relative tiller number	id1027563	1	42339408	2.73	<b>42336674</b>	<b>42340565</b>	3891
Relative total panicle weight	id1027563	1	42339408	2.22	<b>42336674</b>	<b>42340565</b>	3891
Square-root transformed leaf bronzing score	id1027567	1	42351580	2.79	<b>42340608</b>	<b>42374798</b>	34190
Square-root transformed leaf bronzing score	id1027571	1	42352040	3.36	<b>42340608</b>	<b>42374798</b>	34190
Relative tiller number	id1027571	1	42352040	2.73	<b>42340608</b>	<b>42374798</b>	34190
Relative tiller number	id1027576	1	42352787	3.26	<b>42340608</b>	<b>42374798</b>	34190
Relative total panicle weight	id1027576	1	42352787	2.08	<b>42340608</b>	<b>42374798</b>	34190
Square-root transformed leaf bronzing score	id1027585	1	42354084	2.78	<b>42340608</b>	<b>42374798</b>	34190
Relative total panicle weight	id1027630	1	42376686	2.07	none	none	0
Relative thousand kernel weight	id1027633	1	42377009	2.74	<b>42377009</b>	<b>42425393</b>	48384
Relative plant height	id1027640	1	42378501	2.80	<b>42377009</b>	<b>42425393</b>	48384
Relative tiller number	id1027640	1	42378501	3.04	<b>42377009</b>	<b>42425393</b>	48384
Relative total panicle weight	id1027640	1	42378501	2.62	<b>42377009</b>	<b>42425393</b>	48384
Relative single panicle weight	id1027640	1	42378501	3.38	<b>42377009</b>	<b>42425393</b>	48384
Relative thousand kernel weight	id1027649	1	42380579	2.68	<b>42377009</b>	<b>42425393</b>	48384
Relative single panicle weight	id1027656	1	42393687	3.52	<b>42377009</b>	<b>42425393</b>	48384
Relative single panicle weight	id1027666	1	42397035	2.88	<b>42377009</b>	<b>42425393</b>	48384
Square-root transformed leaf bronzing score	dd1001865	1	42397374	2.88	<b>42377009</b>	<b>42425393</b>	48384
Relative single panicle weight	id1027668	1	42397407	2.98	<b>42377009</b>	<b>42425393</b>	48384
Relative tiller number	id1027703	1	42434413	3.29	none	none	0
Relative tiller number	dd1001952	1	42435589	2.68	<b>42435589</b>	<b>42443477</b>	7888
Relative single panicle weight	id1001952	1	42435589	3.92	<b>42435589</b>	<b>42443477</b>	7888
Relative single panicle weight	id1027708	1	42436371	2.80	<b>42435589</b>	<b>42443477</b>	7888
Relative single panicle weight	id1027716	1	42439601	3.63	<b>42435589</b>	<b>42443477</b>	7888
Square-root transformed leaf bronzing score	dd1001979	1	42439864	3.15	<b>42435589</b>	<b>42443477</b>	7888
Relative SPAD	id1027775	1	42572243	3.12	42484324	42581918	97594
Relative thousand kernel weight	id1028484	1	43142537	2.87	43121356	43252778	131422
Relative tiller number	id2000443	2	629586	3.34	none	none	0
Relative tiller number	id2002594	2	4869035	2.86	<b>4851178</b>	<b>4870186</b>	19008
Relative tiller number	id2002597	2	4870186	2.97	<b>4851178</b>	<b>4870186</b>	19008
Relative tiller number	id2003314	2	6481090	2.64	6440863	6494147	53284
Relative single panicle weight	id2003743	2	7286487	2.67	7249337	7367879	118542
Relative lignin content	id2003809	2	7437761	2.51	7436591	7442135	5544
Square-root transformed leaf bronzing score	id2004165	2	8247250	3.04	8245076	8249418	4342
Relative lignin content	id2006786	2	17038133	2.75	<b>17038133</b>	<b>17042470</b>	4337
Lignin content	id2006793	2	17042470	3.28	<b>17038133</b>	<b>17042470</b>	4337
Relative lignin content	id2006996	2	17497082	2.44	none	none	0
Square-root transformed leaf bronzing score	id2008053	2	20713818	3.51	20713818	20764778	50960
Square-root transformed leaf bronzing score	id2008457	2	21116832	2.93	21100935	21116832	15897
Relative single panicle weight	ud2001239	2	21778775	4.68	<b>21714292</b>	<b>21856224</b>	141932
Relative total panicle weight	id2008679	2	21812170	3.14	<b>21714292</b>	<b>21856224</b>	141932
Relative single panicle weight	id2008679	2	21812170	5.12	<b>21714292</b>	<b>21856224</b>	141932
Relative total panicle weight	id2008710	2	21946539	2.17	21945345	21946769	1424
Relative plant height	id2008858	2	22329854	3.09	<b>22262297</b>	<b>22410305</b>	148008
Relative plant height	id2008860	2	22330712	3.09	<b>22262297</b>	<b>22410305</b>	148008
Relative plant height	id2008881	2	22350598	3.01	<b>22262297</b>	<b>22410305</b>	148008
Relative plant height	id2008883	2	22353205	3.26	<b>22262297</b>	<b>22410305</b>	148008
Relative plant height	id2008897	2	22361733	2.79	<b>22262297</b>	<b>22410305</b>	148008
Square-root transformed leaf bronzing score	id2009604	2	23690576	2.85	23605507	23711733	106226
Square-root transformed leaf bronzing score	id2009675	2	23746901	3.52	23731042	23746901	15859
Square-root transformed leaf bronzing score	id2009700	2	23767137	2.84	<b>23767137</b>	<b>23818687</b>	51550
Square-root transformed leaf bronzing score	id2009720	2	23776189	3.39	<b>23767137</b>	<b>23818687</b>	51550
Relative thousand kernel weight	id2009748	2	23818687	3.10	<b>23767137</b>	<b>23818687</b>	51550
Relative thousand kernel weight	id2009750	2	23819881	2.76	23819009	23819881	872
Relative total panicle weight	id2010101	2	24167855	2.22	24167855	24174658	6803
Relative SPAD	id2010410	2	24565561	3.43	none	none	0
Relative SPAD	id2010490	2	24629502	2.82	24628475	24629502	1027
Relative total panicle weight	id2010691	2	24776791	3.24	24776000	24776791	791
Relative single panicle weight	id2010974	2	25258215	2.81	25256777	25258215	1438
Relative tiller number	id2011084	2	25458438	2.64	25451465	25459484	8019
Relative tiller number	id2012482	2	28705134	2.79	<b>28702089</b>	<b>28725037</b>	22948

## Appendices

Supplementary Table S11 (continued)

Trait	SNP marker ID	Chr	Position (MSU7)	-log10P value	LD block start (bp)	LD block end (bp)	LD block size (bp)
Relative tiller number	id2012484	2	28725037	2.60	<b>28702089</b>	<b>28725037</b>	22948
Relative tiller number	id2013255	2	29933912	2.63	29875711	30074445	198734
Lignin content	id2014816	2	33386734	2.94	<b>32836722</b>	<b>33433823</b>	597101
Lignin content	id2014824	2	33393059	2.94	<b>32836722</b>	<b>33433823</b>	597101
Relative plant height	id2014909	2	33575539	3.06	<b>33436701</b>	<b>33666861</b>	230160
Relative SPAD	id2014918	2	33577618	3.16	<b>33436701</b>	<b>33666861</b>	230160
Relative thousand kernel weight	id2015653	2	34707350	2.63	<b>34682847</b>	<b>34843840</b>	160993
Relative thousand kernel weight	id2015660	2	34708959	2.63	<b>34682847</b>	<b>34843840</b>	160993
Relative thousand kernel weight	id2015690	2	34759038	2.76	<b>34682847</b>	<b>34843840</b>	160993
Relative thousand kernel weight	id2015695	2	34795012	3.19	<b>34682847</b>	<b>34843840</b>	160993
Relative thousand kernel weight	id2015696	2	34795072	3.12	<b>34682847</b>	<b>34843840</b>	160993
Relative thousand kernel weight	id2015718	2	34820449	3.17	<b>34682847</b>	<b>34843840</b>	160993
Relative thousand kernel weight	id2015722	2	34825306	3.12	<b>34682847</b>	<b>34843840</b>	160993
Relative thousand kernel weight	id2015724	2	34825826	3.19	<b>34682847</b>	<b>34843840</b>	160993
Relative thousand kernel weight	id2015729	2	34834516	2.91	<b>34682847</b>	<b>34843840</b>	160993
Relative thousand kernel weight	id2015739	2	34839061	3.19	<b>34682847</b>	<b>34843840</b>	160993
Relative thousand kernel weight	id2015743	2	34840365	2.95	<b>34682847</b>	<b>34843840</b>	160993
Relative dry weight	id2016070	2	35188325	2.82	35186964	35216508	29544
Relative dry weight	id2016104	2	35247681	2.63	<b>35227548</b>	<b>35254247</b>	26699
Relative dry weight	id2016108	2	35250486	3.09	<b>35227548</b>	<b>35254247</b>	26699
Relative dry weight	id2016129	2	35257403	3.50	<b>35255920</b>	<b>35264739</b>	8819
Relative dry weight	id2016152	2	35261836	2.53	<b>35255920</b>	<b>35264739</b>	8819
Relative dry weight	id2016513	2	35797762	3.85	35725772	35932195	206423
Relative SPAD	id3001415	3	2573901	2.75	2518677	3076493	557816
Relative thousand kernel weight	id3002151	3	3977709	3.12	<b>3817054</b>	<b>4079193</b>	262139
Relative thousand kernel weight	id3002164	3	3983734	3.39	<b>3817054</b>	<b>4079193</b>	262139
Relative thousand kernel weight	id3002208	3	4033977	3.25	<b>3817054</b>	<b>4079193</b>	262139
Relative thousand kernel weight	id3002450	3	4330054	3.19	<b>4266228</b>	<b>4433684</b>	167456
Relative thousand kernel weight	id3002476	3	4342381	3.17	<b>4266228</b>	<b>4433684</b>	167456
Relative single panicle weight	id3003082	3	5202873	2.73	<b>5042359</b>	<b>5708237</b>	665878
Relative thousand kernel weight	id3003194	3	5379379	2.67	<b>5042359</b>	<b>5708237</b>	665878
Relative tiller number	id3003238	3	5512729	2.82	<b>5042359</b>	<b>5708237</b>	665878
Relative SPAD	id3004253	3	7886467	3.34	7849199	7920201	71002
Relative thousand kernel weight	id3004451	3	8432883	2.98	8250082	8570874	320792
Square-root transformed leaf bronzing score	id3004757	3	9051553	2.79	<b>8839795</b>	<b>9274277</b>	434482
Square-root transformed leaf bronzing score	id3004807	3	9199361	2.85	<b>8839795</b>	<b>9274277</b>	434482
Square-root transformed leaf bronzing score	id3005005	3	9680089	3.62	<b>9587915</b>	<b>10002203</b>	414288
Square-root transformed leaf bronzing score	id3005012	3	9681555	3.62	<b>9587915</b>	<b>10002203</b>	414288
Square-root transformed leaf bronzing score	id3005034	3	9708735	3.62	<b>9587915</b>	<b>10002203</b>	414288
Square-root transformed leaf bronzing score	id3005045	3	9715853	3.74	<b>9587915</b>	<b>10002203</b>	414288
Square-root transformed leaf bronzing score	id3005104	3	9794206	3.72	<b>9587915</b>	<b>10002203</b>	414288
Square-root transformed leaf bronzing score	id3005120	3	9818620	3.19	<b>9587915</b>	<b>10002203</b>	414288
Square-root transformed leaf bronzing score	id3005127	3	9845599	3.68	<b>9587915</b>	<b>10002203</b>	414288
Square-root transformed leaf bronzing score	id3005145	3	9913627	3.63	<b>9587915</b>	<b>10002203</b>	414288
Relative total panicle weight	id3005158	3	9939669	2.15	<b>9587915</b>	<b>10002203</b>	414288
Relative total panicle weight	id3005193	3	10000880	2.13	<b>9587915</b>	<b>10002203</b>	414288
Relative lignin content	id3006917	3	13655639	2.43	13237358	13655639	418281
Relative thousand kernel weight	id3007831	3	15618492	2.98	<b>15610856</b>	<b>15824022</b>	213166
Relative thousand kernel weight	id3007832	3	15618508	3.22	<b>15610856</b>	<b>15824022</b>	213166
Relative thousand kernel weight	id3007862	3	15644405	2.75	<b>15610856</b>	<b>15824022</b>	213166
Relative thousand kernel weight	id3007881	3	15674475	3.07	<b>15610856</b>	<b>15824022</b>	213166
Relative thousand kernel weight	id3007883	3	15675533	2.93	<b>15610856</b>	<b>15824022</b>	213166
Relative thousand kernel weight	id3007889	3	15678743	2.98	<b>15610856</b>	<b>15824022</b>	213166
Relative tiller number	id3008579	3	17600978	2.97	17554346	17773502	219156
Relative single panicle weight	id3011299	3	26877848	2.68	<b>26865467</b>	<b>27051135</b>	185668
Relative SPAD	id3011300	3	26877959	3.12	<b>26865467</b>	<b>27051135</b>	185668
Relative thousand kernel weight	id3012205	3	27698278	2.98	27692870	27774249	81379
Relative SPAD	dd3001192	3	27885788	3.06	<b>27775008</b>	<b>28275789</b>	500781
Relative SPAD	id3012596	3	27912252	2.75	<b>27775008</b>	<b>28275789</b>	500781
Relative total panicle weight	id3014280	3	30224099	<b>2.25</b>	<b>29783920</b>	<b>30322184</b>	<b>538264</b>
Relative single panicle weight	id3014280	3	30224099	<b>2.73</b>	<b>29783920</b>	<b>30322184</b>	<b>538264</b>
Relative total panicle weight	id3014412	3	30396260	2.06	30348817	30456968	108151
Relative single panicle weight	id3015855	3	32881854	3.28	<b>32757372</b>	<b>33043750</b>	286378
Relative single panicle weight	id3015859	3	32886090	2.84	<b>32757372</b>	<b>33043750</b>	286378
Relative single panicle weight	id3015864	3	32926134	2.93	<b>32757372</b>	<b>33043750</b>	286378
Relative single panicle weight	id3015865	3	32926244	2.75	<b>32757372</b>	<b>33043750</b>	286378
Lignin content	id3017560	3	35433033	2.97	<b>35433033</b>	<b>35465246</b>	32213
Lignin content	id3017564	3	35433453	2.98	<b>35433033</b>	<b>35465246</b>	32213
Lignin content	id3017866	3	35771770	2.83	35769794	35771770	1976
Relative SPAD	id3017899	3	35824355	2.83	none	none	0

Appendices

Supplementary Table S11 (continued)

Trait	SNP marker ID	Chr	Position (MSU7)	-log10P value	LD block start (bp)	LD block end (bp)	LD block size (bp)
Relative SPAD	id3018013	3	35882893	2.81	35827861	35902029	74168
Relative SPAD	id3018096	3	35963966	3.67	35909353	35976506	67153
Relative SPAD	id3018154	3	35979532	2.96	<b>35979532</b>	<b>36100266</b>	120734
Relative SPAD	id3018157	3	35979857	3.03	<b>35979532</b>	<b>36100266</b>	120734
Relative SPAD	id3018168	3	35982080	3.01	<b>35979532</b>	<b>36100266</b>	120734
Relative SPAD	id3018359	3	36136637	2.91	36106430	36136637	30207
Relative SPAD	id3018393	3	36187187	3.42	<b>36155000</b>	<b>36288832</b>	133832
Relative SPAD	id3018399	3	36188014	3.64	<b>36155000</b>	<b>36288832</b>	133832
Relative lignin content	id4000806	4	1758758	2.78	1758758	1760163	1405
Relative dry weight	ud4000543	4	7521880	2.61	<b>7356732</b>	<b>11879743</b>	4523011
Relative dry weight	id4002885	4	7558749	2.67	<b>7356732</b>	<b>11879743</b>	4523011
Relative dry weight	id4003021	4	8682949	2.77	<b>7356732</b>	<b>11879743</b>	4523011
Relative dry weight	id4003033	4	8762568	2.58	<b>7356732</b>	<b>11879743</b>	4523011
Relative dry weight	id4003349	4	10564642	2.74	<b>7356732</b>	<b>11879743</b>	4523011
Relative lignin content	id4003766	4	12196453	2.66	ND	12214567	ND
Square-root transformed leaf bronzing score	id4004207	4	14183946	3.57	14137882	14262565	124683
Lignin content	id4004892	4	17183360	2.77	<b>16933227</b>	<b>17185622</b>	252395
Lignin content	id4004901	4	17185622	2.83	<b>16933227</b>	<b>17185622</b>	252395
Relative dry weight	id4005769	4	19741992	2.73	19565554	19795048	229494
Relative lignin content	id4006026	4	20132588	2.51	20014349	20342542	328193
Relative plant height	id4006835	4	21320269	2.83	21319507	21342089	22582
Relative dry weight	id4007370	4	22371291	3.04	22371291	22435296	64005
Relative lignin content	id4008536	4	26042668	2.47	25746825	26526299	779474
Relative lignin content	id4009840	4	29564914	2.56	29457811	29727137	269326
Lignin content	id4009930	4	29798036	3.52	<b>29776353</b>	<b>29799783</b>	23430
Lignin content	id4009933	4	29799783	3.44	<b>29776353</b>	<b>29799783</b>	23430
Relative tiller number	id4010137	4	30213031	3.69	<b>30042158</b>	<b>30215772</b>	173614
Relative tiller number	id4010147	4	30215772	3.65	<b>30042158</b>	<b>30215772</b>	173614
Relative SPAD	id4010398	4	30708157	3.14	<b>30572064</b>	<b>30724662</b>	152598
Relative SPAD	wd4003148	4	30724662	4.12	<b>30572064</b>	<b>30724662</b>	152598
Relative SPAD	id4011239	4	32401691	2.77	32359551	32404251	44700
Relative plant height	id5000502	5	878185	3.10	873390	891285	17895
Relative SPAD	id5000798	5	1161078	3.83	1129010	1165808	36798
Relative SPAD	id5000894	5	1278055	2.88	none	none	0
Square-root transformed leaf bronzing score	id5000980	5	1506220	2.85	<b>1459590</b>	<b>1506761</b>	47171
Relative SPAD	id5000980	5	1506220	3.23	<b>1459590</b>	<b>1506761</b>	47171
Relative SPAD	id5000986	5	1545155	4.66	<b>1545155</b>	<b>1682431</b>	137276
Relative SPAD	id5000988	5	1546671	4.12	<b>1545155</b>	<b>1682431</b>	137276
Relative SPAD	id5001006	5	1613746	3.99	<b>1545155</b>	<b>1682431</b>	137276
Relative SPAD	id5001009	5	1614147	4.20	<b>1545155</b>	<b>1682431</b>	137276
Relative SPAD	id5001011	5	1615248	3.61	<b>1545155</b>	<b>1682431</b>	137276
Relative SPAD	id5001043	5	1680423	2.98	<b>1545155</b>	<b>1682431</b>	137276
Relative SPAD	id5001082	5	1870287	2.76	1870287	1896801	26514
Lignin content	id5001305	5	2261234	3.10	<b>2261234</b>	<b>2266858</b>	5624
Lignin content	id5001307	5	2266267	3.47	<b>2261234</b>	<b>2266858</b>	5624
Lignin content	ud5000116	5	2266858	3.15	<b>2261234</b>	<b>2266858</b>	5624
Relative SPAD	id5001358	5	2358432	2.98	<b>2335172</b>	<b>2530491</b>	195319
Relative SPAD	id5001368	5	2371020	2.98	<b>2335172</b>	<b>2530491</b>	195319
Relative SPAD	id5001424	5	2505482	2.90	<b>2335172</b>	<b>2530491</b>	195319
Relative SPAD	id5001426	5	2524224	3.22	<b>2335172</b>	<b>2530491</b>	195319
Relative SPAD	id5001439	5	2539180	3.48	<b>2532749</b>	<b>2540010</b>	7261
Relative SPAD	id5001440	5	2539289	4.17	<b>2532749</b>	<b>2540010</b>	7261
Relative SPAD	id5001443	5	2540010	3.50	<b>2532749</b>	<b>2540010</b>	7261
Relative SPAD	id5001447	5	2541735	3.19	none	none	0
Relative SPAD	id5001496	5	2614163	3.48	<b>2611736</b>	<b>2812540</b>	200804
Relative SPAD	id5001540	5	2773921	3.01	<b>2611736</b>	<b>2812540</b>	200804
Relative SPAD	id5001613	5	2860263	2.78	2812831	2860263	47432
Relative single panicle weight	id5001916	5	3308047	2.72	3231101	3483362	252261
Relative lignin content	id5002322	5	4326323	2.65	<b>4237117</b>	<b>4608778</b>	371661
Relative lignin content	id5002330	5	4329769	2.67	<b>4237117</b>	<b>4608778</b>	371661
Relative lignin content	id5002336	5	4403981	3.72	<b>4237117</b>	<b>4608778</b>	371661
Lignin content	id5002340	5	4405039	2.78	<b>4237117</b>	<b>4608778</b>	371661
Relative lignin content	id5002340	5	4405039	3.57	<b>4237117</b>	<b>4608778</b>	371661
Relative lignin content	id5002343	5	4406266	3.52	<b>4237117</b>	<b>4608778</b>	371661
Relative lignin content	id5002353	5	4560816	2.65	<b>4237117</b>	<b>4608778</b>	371661
Relative lignin content	id5002365	5	4565557	2.65	<b>4237117</b>	<b>4608778</b>	371661
Lignin content	id5004029	5	7965624	2.75	7722361	8035671	313310
Square-root transformed leaf bronzing score	id5006806	5	17081932	2.87	<b>17081932</b>	<b>17340893</b>	258961
Square-root transformed leaf bronzing score	id5006830	5	17097630	2.87	<b>17081932</b>	<b>17340893</b>	258961
Square-root transformed leaf bronzing score	id5006874	5	17175467	3.40	<b>17081932</b>	<b>17340893</b>	258961

## Appendices

Supplementary Table S11 (continued)

Trait	SNP marker ID	Chr	Position (MSU7)	-log10P value	LD block start (bp)	LD block end (bp)	LD block size (bp)
Square-root transformed leaf bronzing score	id5006882	5	17177287	3.37	<b>17081932</b>	<b>17340893</b>	258961
Square-root transformed leaf bronzing score	id5006917	5	17249762	4.09	<b>17081932</b>	<b>17340893</b>	258961
Square-root transformed leaf bronzing score	id5006921	5	17278368	3.54	<b>17081932</b>	<b>17340893</b>	258961
Square-root transformed leaf bronzing score	id5006957	5	17335310	3.04	<b>17081932</b>	<b>17340893</b>	258961
Relative dry weight	id5009204	5	21698191	3.06	<b>21520059</b>	<b>21765809</b>	245750
Relative dry weight	id5009236	5	21722470	3.10	<b>21520059</b>	<b>21765809</b>	245750
Relative dry weight	id5009252	5	21737217	2.86	<b>21520059</b>	<b>21765809</b>	245750
Relative dry weight	id5009260	5	21740567	3.29	<b>21520059</b>	<b>21765809</b>	245750
Relative dry weight	id5009270	5	21765809	3.38	<b>21520059</b>	<b>21765809</b>	245750
Relative dry weight	id5009271	5	21767927	2.89	none	none	0
Relative dry weight	id5009527	5	22260982	2.59	<b>21789734</b>	<b>23191534</b>	1401800
Relative dry weight	id5009533	5	22262597	2.53	<b>21789734</b>	<b>23191534</b>	1401800
Relative dry weight	id5009548	5	22294655	2.58	<b>21789734</b>	<b>23191534</b>	1401800
Relative dry weight	id5009553	5	22329739	2.59	<b>21789734</b>	<b>23191534</b>	1401800
Relative dry weight	id5010339	5	23196533	2.73	23192557	23238236	45679
Relative thousand kernel weight	id5011026	5	24112155	2.66	24073706	24153780	80074
Relative total panicle weight	id5013309	5	27413299	2.12	27413299	27419785	6486
Relative dry weight	id6001161	6	1587958	2.71	none	none	0
Relative dry weight	id6001169	6	1590614	2.89	1589859	1591489	1630
Square-root transformed leaf bronzing score	id6002500	6	3117393	2.84	<b>3079074</b>	<b>3245705</b>	166631
Relative plant height	id6002518	6	3138055	3.06	<b>3079074</b>	<b>3245705</b>	166631
Relative total panicle weight	id6002613	6	3245705	2.08	<b>3079074</b>	<b>3245705</b>	166631
Relative total panicle weight	id6002690	6	3290851	2.17	<b>3288039</b>	<b>3565083</b>	277044
Relative total panicle weight	id6002701	6	3313611	2.01	<b>3288039</b>	<b>3565083</b>	277044
Relative total panicle weight	id6002745	6	3331293	2.15	<b>3288039</b>	<b>3565083</b>	277044
Relative single panicle weight	id6002745	6	3331293	2.73	<b>3288039</b>	<b>3565083</b>	277044
Relative total panicle weight	id6002750	6	3331719	2.25	<b>3288039</b>	<b>3565083</b>	277044
Relative total panicle weight	id6002753	6	3333531	2.45	<b>3288039</b>	<b>3565083</b>	277044
Relative single panicle weight	id6002753	6	3333531	2.67	<b>3288039</b>	<b>3565083</b>	277044
Relative total panicle weight	id6002767	6	3365147	2.08	<b>3288039</b>	<b>3565083</b>	277044
Relative total panicle weight	id6002778	6	3378593	2.08	<b>3288039</b>	<b>3565083</b>	277044
Relative total panicle weight	id6002798	6	3409986	2.00	<b>3288039</b>	<b>3565083</b>	277044
Relative total panicle weight	id6002804	6	3415295	2.19	<b>3288039</b>	<b>3565083</b>	277044
Relative lignin content	id6003868	6	6102112	2.45	<b>5874707</b>	<b>6149929</b>	275222
Relative lignin content	ud6000288	6	6149929	2.54	<b>5874707</b>	<b>6149929</b>	275222
Relative lignin content	id6003878	6	6150705	2.68	<b>6150705</b>	<b>6181369</b>	30664
Relative lignin content	id6003886	6	6152443	2.57	<b>6150705</b>	<b>6181369</b>	30664
Square-root transformed leaf bronzing score	id6004094	6	6450686	2.78	6401217	6458990	57773
Relative tiller number	id6004657	6	7195418	2.68	<b>7195038</b>	<b>7500053</b>	305015
Relative dry weight	id6004689	6	7402624	2.86	<b>7195038</b>	<b>7500053</b>	305015
Relative tiller number	id6007211	6	11335701	2.72	<b>11333425</b>	<b>11335701</b>	2276
Relative total panicle weight	id6007211	6	11335701	2.05	<b>11333425</b>	<b>11335701</b>	2276
Relative SPAD	id6009229	6	16178354	3.09	14348413	16322729	1974316
Square-root transformed leaf bronzing score	id6010557	6	19997868	3.52	19867540	20037143	169603
Square-root transformed leaf bronzing score	id6010782	6	20676259	2.91	20167772	20789922	622150
Relative plant height	id6011457	6	21982423	3.19	<b>21594032</b>	<b>22083453</b>	489421
Relative plant height	id6011459	6	21983366	3.08	<b>21594032</b>	<b>22083453</b>	489421
Relative plant height	id6011784	6	22811564	3.23	22811036	22811564	528
Relative dry weight	id6013288	6	24913235	2.56	24805278	24985716	180438
Lignin content	id6014825	6	26634670	3.61	<b>26568040</b>	<b>26660888</b>	92848
Relative lignin content	id6014825	6	26634670	2.64	<b>26568040</b>	<b>26660888</b>	92848
Relative dry weight	id6015530	6	27382490	4.88	<b>27169002</b>	<b>27382490</b>	213488
Relative tiller number	id6015530	6	27382490	2.81	<b>27169002</b>	<b>27382490</b>	213488
Relative total panicle weight	id6015530	6	27382490	2.98	<b>27169002</b>	<b>27382490</b>	213488
Relative thousand kernel weight	id6016985	6	31003300	3.19	30876829	31209346	332517
Square-root transformed leaf bronzing score	id7000056	7	333762	2.79	130689	355220	224531
Relative lignin content	id7000076	7	412556	2.79	none	none	0
Relative SPAD	id7000612	7	4649633	2.74	3862042	4690279	828237
Relative tiller number	id7001442	7	7973082	2.60	7575084	9830107	2255023
Relative single panicle weight	id7001787	7	10065311	2.81	<b>9986580</b>	<b>11059439</b>	1072859
Relative single panicle weight	ud7000750	7	10069296	2.81	<b>9986580</b>	<b>11059439</b>	1072859
Relative SPAD	wd7001619	7	12383193	3.82	11621241	14609592	2988351
Relative plant height	id7002483	7	15705746	3.98	<b>15347454</b>	<b>15783982</b>	436528
Relative plant height	id7002504	7	15778441	3.29	<b>15347454</b>	<b>15783982</b>	436528
Relative plant height	id7002511	7	15783982	3.44	<b>15347454</b>	<b>15783982</b>	436528
Relative thousand kernel weight	id7002801	7	18131988	2.88	18112337	18131988	19651
Relative thousand kernel weight	id7002824	7	18203932	2.63	18133033	18340346	207313
Relative lignin content	id7003553	7	21690387	2.51	21690387	21691463	1076
Relative lignin content	id7003683	7	22106228	2.49	22087975	22106228	18253
Lignin content	id7004144	7	23352533	3.04	<b>23352533</b>	<b>23749170</b>	396637

## Appendices

Supplementary Table S11 (continued)

Trait	SNP marker ID	Chr	Position (MSU7)	-log10P value	LD block start (bp)	LD block end (bp)	LD block size (bp)
Lignin content	id7004145	7	23353153	3.15	23352533	23749170	396637
Lignin content	id7004147	7	23397917	3.14	23352533	23749170	396637
Lignin content	id7004152	7	23402064	3.02	23352533	23749170	396637
Lignin content	id7004236	7	23626884	3.12	23352533	23749170	396637
Relative thousand kernel weight	ud7001748	7	24070937	2.66	23902555	24217159	314604
Relative SPAD	id7005764	7	28748176	2.78	28748176	28866029	117853
Relative single panicle weight	ud8000441	8	7651501	2.89	7610150	7762348	152198
Relative single panicle weight	id8002341	8	7651801	2.70	7610150	7762348	152198
Relative plant height	id8002474	8	7946139	2.80	7880420	7990630	110210
Relative plant height	id8002490	8	7972601	3.21	7880420	7990630	110210
Relative plant height	id8002494	8	7984606	4.20	7880420	7990630	110210
Relative plant height	id8002513	8	8061366	3.58	none	none	0
Relative plant height	id8002514	8	8061532	3.72	8061532	8110168	48636
Relative plant height	id8002535	8	8107390	3.98	8061532	8110168	48636
Relative plant height	id8002538	8	8109057	3.10	8061532	8110168	48636
Relative plant height	id8002540	8	8110168	3.06	8061532	8110168	48636
Relative dry weight	id8002687	8	8761031	2.71	none	none	0
Relative dry weight	id8002877	8	9107117	4.18	9107117	9126757	19640
Relative total panicle weight	id8002959	8	9201517	2.01	9198147	9201580	3433
Relative total panicle weight	id8003259	8	10255023	2.28	10162063	10655137	493074
Relative total panicle weight	id8003440	8	10752334	2.48	10744639	12260698	1516059
Relative total panicle weight	id8003470	8	10904409	2.08	10744639	12260698	1516059
Relative plant height	id8004125	8	15361853	3.02	15280176	15631111	350935
Lignin content	id8004263	8	15715575	2.96	15715575	16031418	315843
Relative lignin content	id8004948	8	18676233	2.62	18572809	19027763	454954
Lignin content	id8005576	8	20431619	2.86	20427347	20431619	4272
Square-root transformed leaf bronzing score	id8005661	8	20766217	3.30	20708815	20928072	219257
Relative single panicle weight	id8006881	8	24803160	2.67	none	none	0
Relative plant height	id8007026	8	25732130	3.08	25681614	25861199	179585
Relative total panicle weight	id8007067	8	25902075	2.05	25889638	26138246	248608
Relative single panicle weight	id8007067	8	25902075	3.44	25889638	26138246	248608
Relative lignin content	id8007079	8	25956252	2.44	25889638	26138246	248608
Relative lignin content	id8007122	8	26106055	3.10	25889638	26138246	248608
Lignin content	ud8001738	8	26137272	2.77	25889638	26138246	248608
Lignin content	id8007129	8	26138246	2.76	25889638	26138246	248608
Lignin content	id8007136	8	26143127	2.96	26138443	26143395	4952
Lignin content	id8007143	8	26148673	2.94	26144377	26148673	4296
Relative single panicle weight	id8007277	8	26542005	2.91	26522932	26572534	49602
Relative single panicle weight	id8007280	8	26547937	3.01	26522932	26572534	49602
Relative single panicle weight	ud8001763	8	26572534	2.94	26522932	26572534	49602
Relative plant height	id8007408	8	27158102	3.42	27154863	27158102	3239
Relative lignin content	id8007614	8	27657121	2.45	27644713	27657121	12408
Lignin content	id9001200	9	4561489	3.06	4451839	4641583	189744
Lignin content	id9002928	9	10486881	2.85	none	none	0
Relative thousand kernel weight	id9003162	9	11513243	3.80	none	none	0
Relative thousand kernel weight	id9003164	9	11571873	2.93	none	none	0
Relative thousand kernel weight	id9003632	9	13167757	2.75	13161911	ND	ND
Relative total panicle weight	id9003632	9	13167757	2.49	13161911	ND	ND
Lignin content	id9004364	9	15282227	3.47	15245649	15567052	321403
Lignin content	id9004425	9	15335422	3.06	15245649	15567052	321403
Lignin content	id9004439	9	15339046	3.05	15245649	15567052	321403
Relative tiller number	id9007075	9	20028058	3.12	19948107	20126967	178860
Relative lignin content	id9007100	9	20157986	2.60	20157986	20717806	559820
Relative tiller number	id10000021	10	112886	2.91	65322	112886	47564
Relative tiller number	id10000023	10	112937	2.91	112937	116235	3298
Relative dry weight	id10000028	10	179097	2.53	147398	303254	155856
Relative tiller number	id10000028	10	179097	3.80	147398	303254	155856
Relative tiller number	id10000105	10	587378	2.94	587378	588693	1315
Relative tiller number	wd10000214	10	742505	2.85	680072	742505	62433
Relative lignin content	id10000212	10	1105635	2.86	1105635	1137829	32194
Relative lignin content	id10000237	10	1193146	2.63	1164189	1240092	75903
Relative tiller number	id10000559	10	2105294	2.59	2105294	2149319	44025
Relative tiller number	id10002079	10	6536152	2.59	6495219	6542749	47530
Relative plant height	wd10002654	10	12200062	3.05	12019245	13079689	1060444
Relative plant height	wd10002741	10	12405458	3.01	12019245	13079689	1060444
Relative plant height	id10003308	10	12477302	3.07	12019245	13079689	1060444
Relative plant height	id10003320	10	12480953	3.01	12019245	13079689	1060444
Relative plant height	wd10002922	10	12600440	3.05	12019245	13079689	1060444
Relative plant height	id10003329	10	12686147	3.18	12019245	13079689	1060444
Relative plant height	id10003331	10	12687964	3.02	12019245	13079689	1060444

## Appendices

Supplementary Table S11 (continued)

Trait	SNP marker ID	Chr	Position (MSU7)	-log10P value	LD block start (bp)	LD block end (bp)	LD block size (bp)
Relative plant height	wd10002947	10	12696271	3.07	12019245	13079689	1060444
Relative plant height	id10003354	10	12773018	3.03	12019245	13079689	1060444
Relative plant height	id10003364	10	12818896	3.15	12019245	13079689	1060444
Relative plant height	id10003368	10	12863056	3.01	12019245	13079689	1060444
Relative plant height	id10003371	10	12864656	3.00	12019245	13079689	1060444
Relative plant height	id10003380	10	12880441	3.08	12019245	13079689	1060444
Relative plant height	id10003381	10	12882675	2.96	12019245	13079689	1060444
Relative plant height	wd10003039	10	12942023	2.96	12019245	13079689	1060444
Relative plant height	id10003390	10	12975321	2.93	12019245	13079689	1060444
Relative single panicle weight	id10003623	10	13782039	2.89	13782039	14488618	706579
Relative lignin content	id10004685	10	16823791	2.47	16790136	16943046	152910
Relative single panicle weight	id10004934	10	17273846	3.03	17228916	17414240	185324
Relative single panicle weight	id10004953	10	17361778	3.20	17228916	17414240	185324
Relative single panicle weight	id10004968	10	17366969	4.27	17228916	17414240	185324
Relative total panicle weight	id11002940	11	7440741	2.68	7440741	7518809	78068
Relative thousand kernel weight	id11003505	11	9058117	2.93	9029858	9081750	51892
Relative dry weight	id11003918	11	10697135	2.61	10405648	10885796	480148
Relative thousand kernel weight	id11004739	11	14324286	2.90	10974127	14851997	3877870
Relative thousand kernel weight	id11004960	11	15174386	2.95	14886048	15390435	504387
Relative plant height	wd11002155	11	15874941	2.90	none	none	0
Relative dry weight	id11005541	11	16283771	2.85	16283395	16509939	226544
Relative dry weight	id11005911	11	16981957	2.97	16954234	17059195	104961
Relative lignin content	ud11001008	11	17634934	2.49	none	none	0
Relative dry weight	id11006506	11	18393512	3.83	18315964	18409258	93294
Relative lignin content	id11006547	11	18427872	2.43	18427872	18431966	4094
Relative lignin content	id11006569	11	18449220	2.45	18444663	18497286	52623
Relative lignin content	id11006588	11	18495915	2.72	18444663	18497286	52623
Relative total panicle weight	id11008601	11	22570666	2.14	22564193	22570666	6473
Relative total panicle weight	dd11000872	11	22571193	2.03	22571129	22571193	64
Relative tiller number	id11008635	11	22581569	3.16	22576805	22582906	6101
Square-root trans formed leaf bronzing score	id11001199	11	22648869	3.28	22647845	22650359	2514
Relative plant height	id11009406	11	24278047	3.68	24234277	24330376	96099
Relative SPAD	id11009575	11	24805317	3.19	24728131	24805317	77186
Lignin content	id11010050	11	25566515	3.75	25564335	25567092	2757
Relative lignin content	id11010112	11	25620382	2.77	25620382	25620728	346
Relative dry weight	id11010238	11	25961716	2.53	25909990	26028661	118671
Relative dry weight	id11010361	11	26318850	2.67	26318342	26318850	508
Relative dry weight	ud11001609	11	26327481	3.20	26326121	26327481	1360
Relative tiller number	id11010448	11	26475568	3.04	26453836	26476262	22426
Lignin content	id11010955	11	27594430	2.73	27584697	27594430	9733
Lignin content	id11011454	11	28735824	3.31	none	none	0
Relative lignin content	id11011672	11	28969154	2.79	28969154	28972941	3787
Relative lignin content	id11011686	11	28973574	2.49	none	none	0
Relative thousand kernel weight	id12000510	12	1157980	2.64	941087	ND	ND
Relative lignin content	id12001658	12	3876956	2.60	3321156	3937979	616823
Relative lignin content	ud12000260	12	4871704	2.76	4554103	5037545	483442
Relative dry weight	id12002594	12	6142005	2.65	5860219	6185402	325183
Relative SPAD	id12003671	12	ND	2.93	8757292	9184585	427293
Relative total panicle weight	ud12000566	12	9231272	2.04	9229978	9255373	25395
Relative lignin content	id12004099	12	10607918	2.53	10187067	10631970	444903
Relative single panicle weight	id12004298	12	11224533	2.74	11192933	13886605	2693672
Relative single panicle weight	id12005116	12	14179322	2.70	13891437	14218146	326709
Relative lignin content	id12005196	12	14394933	2.56	14234209	14491254	257045
Relative single panicle weight	id12005215	12	14491225	2.92	14234209	14491254	257045
Relative single panicle weight	id12005221	12	14492915	3.30	14492915	14547101	54186
Relative single panicle weight	id12005222	12	14493184	3.27	14492915	14547101	54186
Relative plant height	id12005228	12	14494269	3.28	14492915	14547101	54186
Relative plant height	id12005236	12	14496493	3.10	14492915	14547101	54186
Relative single panicle weight	id12005245	12	14547101	3.72	14492915	14547101	54186
Relative single panicle weight	id12005277	12	14831486	2.95	14770987	14832683	61696
Relative single panicle weight	id12005278	12	14831605	2.96	14770987	14832683	61696
Relative single panicle weight	id12005391	12	15239935	3.94	15156073	15453575	297502
Relative dry weight	id12005469	12	15453575	2.52	15156073	15453575	297502
Relative lignin content	id12005469	12	15453575	2.43	15156073	15453575	297502
Relative lignin content	id12005561	12	15843436	2.53	15778231	15864073	85842
Relative dry weight	wd12002971	12	15912775	3.49	15866816	15912775	45959
Relative total panicle weight	wd12003381	12	16905472	3.13	16500144	17003227	503083
Relative single panicle weight	wd12003381	12	16905472	3.36	16500144	17003227	503083
Relative total panicle weight	id12005779	12	17200196	2.07	17196296	17200196	3900
Relative tiller number	id12006261	12	18763833	2.88	18763833	18764104	271



## Appendices

Supplementary Table S11 (continued)

Trait	SNP marker ID	Chr	Position (MSU7)	$-\log_{10}P$ value	LD block start (bp)	LD block end (bp)	LD block size (bp)
Relative thousand kernel weight	id12006502	12	19470916	3.16	<b>19469816</b>	<b>19518299</b>	48483
Relative thousand kernel weight	id12006504	12	19472152	3.17	<b>19469816</b>	<b>19518299</b>	48483
Relative thousand kernel weight	id12006532	12	19492867	3.76	<b>19469816</b>	<b>19518299</b>	48483
Relative thousand kernel weight	id12006540	12	19495892	3.88	<b>19469816</b>	<b>19518299</b>	48483
Relative dry weight	id12006850	12	21209160	2.68	21205508	21209292	3784
Relative lignin content	id12007272	12	21906434	2.46	none	none	0
Relative dry weight	ud12001410	12	23628972	3.99	<b>23556025</b>	<b>23664806</b>	108781
Relative dry weight	id12008228	12	23661669	4.87	<b>23556025</b>	<b>23664806</b>	108781
Relative tiller number	id12008228	12	23661669	2.94	<b>23556025</b>	<b>23664806</b>	108781
Relative dry weight	id12009860	12	26768077	2.58	26761501	26768077	6576

A total of 50 SNPs which showed the highest  $-\log_{10}P$  values were collected from each trait, and the position,  $-\log_{10}P$  value and the corresponding LD block are shown. The SNPs were ordered according to the chromosomal position. The LD blocks were determined by using Haploview 4.2 applying the method of Gabriel (detailed in the Materials and Methods). The red colour shows SNP markers which are shared by more than one trait. ND indicates 'no data'. Boldface on the LD block indicates that the LD block contains multiple SNPs.

## Appendices

Supplementary Table S12: List of genes located within the identified candidate loci for all phenotypes.

Trait	Chr	Gene ID	Putative function	Closest <i>Arabidopsis</i> homologue
Square-root transformed leaf bronzing score	1	LOC_Os01g72560	expressed protein	At2g41200
Square-root transformed leaf bronzing score	5	LOC_Os05g29090	transposon protein, putative, CACTA, En/Spm sub-class, expressed	
Square-root transformed leaf bronzing score	5	LOC_Os05g29100	retrotransposon protein, putative, unclassified, expressed	
Square-root transformed leaf bronzing score	5	LOC_Os05g29110	retrotransposon protein, putative, unclassified, expressed	
Square-root transformed leaf bronzing score	5	LOC_Os05g29120	retrotransposon protein, putative, Ty3-gypsy subclass, expressed	
Square-root transformed leaf bronzing score	5	LOC_Os05g29130	retrotransposon protein, putative, unclassified, expressed	
Square-root transformed leaf bronzing score	5	LOC_Os05g29140	retrotransposon protein, putative, unclassified, expressed	
Square-root transformed leaf bronzing score	5	LOC_Os05g29150	expressed protein	At2g47560
Square-root transformed leaf bronzing score	5	LOC_Os05g29160	hypothetical protein	
Square-root transformed leaf bronzing score	5	LOC_Os05g29170	expressed protein	
Square-root transformed leaf bronzing score	5	LOC_Os05g29174	retrotransposon protein, putative, unclassified, expressed	
Square-root transformed leaf bronzing score	5	LOC_Os05g29676	RING-H2 finger protein, putative, expressed	At1g72200
Square-root transformed leaf bronzing score	5	LOC_Os05g29680	expressed protein	
Square-root transformed leaf bronzing score	5	LOC_Os05g29690	retrotransposon protein, putative, unclassified, expressed	
Square-root transformed leaf bronzing score	5	LOC_Os05g29700	retrotransposon, putative, centromere-specific, expressed	
Square-root transformed leaf bronzing score	5	LOC_Os05g29710	RING-H2 finger protein, putative, expressed	At5g10380
Square-root transformed leaf bronzing score	5	LOC_Os05g29720	retrotransposon protein, putative, Ty1-copia subclass, expressed	
Square-root transformed leaf bronzing score	5	LOC_Os05g29730	retrotransposon protein, putative, unclassified, expressed	
Square-root transformed leaf bronzing score	5	LOC_Os05g29735	expressed protein	
Square-root transformed leaf bronzing score	5	LOC_Os05g29740	invertase/pectin methylesterase inhibitor family protein, putative, expressed	
Square-root transformed leaf bronzing score	5	LOC_Os05g29750	cytochrome P450 71E1, putative, expressed	
Square-root transformed leaf bronzing score	5	LOC_Os05g29760	ferrochelatase-2, chloroplast precursor, putative, expressed	At2g30390
Square-root transformed leaf bronzing score	5	LOC_Os05g29770	expressed protein	
Square-root transformed leaf bronzing score	5	LOC_Os05g29780	retrotransposon protein, putative, unclassified, expressed	
Square-root transformed leaf bronzing score	5	LOC_Os05g29790	pectinesterase, putative, expressed	At4g02330
Square-root transformed leaf bronzing score	5	LOC_Os05g29800	expressed protein	At2g44020
Square-root transformed leaf bronzing score	5	LOC_Os05g29810	AP2 domain containing protein, expressed	At1g53910
Square-root transformed leaf bronzing score	5	LOC_Os05g29820	transposon protein, putative, CACTA, En/Spm sub-class, expressed	
Square-root transformed leaf bronzing score	5	LOC_Os05g29829	hypothetical protein	
Square-root transformed leaf bronzing score	5	LOC_Os05g29840	retrotransposon protein, putative, unclassified	
Square-root transformed leaf bronzing score	5	LOC_Os05g29850	transposon protein, putative, CACTA, En/Spm sub-class, expressed	
Square-root transformed leaf bronzing score	5	LOC_Os05g29860	mitochondrial carrier protein, putative, expressed	At4g39460
Square-root transformed leaf bronzing score	5	LOC_Os05g29870	basic salivary proline-rich protein 3 precursor, putative, expressed	
Square-root transformed leaf bronzing score	5	LOC_Os05g29880	3-hydroxyacyl-CoA dehydrogenase, putative, expressed	At3g06860
Square-root transformed leaf bronzing score	5	LOC_Os05g29900	expressed protein	At1g02816
Square-root transformed leaf bronzing score	5	LOC_Os05g29910	retrotransposon protein, putative, unclassified, expressed	
Square-root transformed leaf bronzing score	5	LOC_Os05g29920	expressed protein	At1g02816
Square-root transformed leaf bronzing score	5	LOC_Os05g29930	late embryogenesis abundant protein, putative, expressed	
Square-root transformed leaf bronzing score	5	LOC_Os05g29940	expressed protein	
Square-root transformed leaf bronzing score	5	LOC_Os05g29950	expressed protein	
Square-root transformed leaf bronzing score	5	LOC_Os05g29960	expressed protein	At2g47630
Square-root transformed leaf bronzing score	5	LOC_Os05g29974	lipase, putative, expressed	At3g62830
Relative plant height	8	LOC_Os08g13250	speckle-type POZ protein, putative, expressed	At3g06190
Relative plant height	8	LOC_Os08g13270	expressed protein	
Relative plant height	8	LOC_Os08g13280	expressed protein	
Relative plant height	8	LOC_Os08g13290	transposon protein, putative, CACTA, En/Spm sub-class, expressed	
Relative plant height	8	LOC_Os08g13300	transposon protein, putative, CACTA, En/Spm sub-class, expressed	
Relative plant height	8	LOC_Os08g13310	expressed protein	
Relative plant height	8	LOC_Os08g13320	expressed protein	At1g78890
Relative plant height	8	LOC_Os08g13330	retrotransposon protein, putative, Ty1-copia subclass, expressed	
Relative plant height	8	LOC_Os08g13340	retrotransposon protein, putative, Ty1-copia subclass, expressed	
Relative plant height	8	LOC_Os08g13350	expressed protein	At1g16860
Relative plant height	8	LOC_Os08g13360	kelch repeat protein, putative, expressed	At1g51550
Relative plant height	8	LOC_Os08g13380	expressed protein	
Relative plant height	8	LOC_Os08g13390	expressed protein	At2g15560
Relative plant height	8	LOC_Os08g13400	expressed protein	At4g29905
Relative plant height	8	LOC_Os08g13410	retrotransposon protein, putative, unclassified	
Relative plant height	8	LOC_Os08g13420	S-domain receptor-like protein kinase, putative, expressed	At5g60900
Relative dry weight	6	LOC_Os06g44940	retrotransposon protein, putative, unclassified, expressed	
Relative dry weight	6	LOC_Os06g44950	retrotransposon protein, putative, unclassified, expressed	
Relative dry weight	6	LOC_Os06g44960	retrotransposon protein, putative, unclassified, expressed	
Relative dry weight	6	LOC_Os06g44970	auxin efflux carrier component, putative, expressed	At5g57090
Relative dry weight	6	LOC_Os06g44980	expressed protein	At5g57123
Relative dry weight	6	LOC_Os06g44990	transposon protein, putative, Pong sub-class	
Relative dry weight	6	LOC_Os06g45000	ubiquitin-conjugating enzyme, putative, expressed	At5g05080
Relative dry weight	6	LOC_Os06g45010	expressed protein	At4g03390
Relative dry weight	6	LOC_Os06g45020	STRUBBELIG-RECEPTOR FAMILY 3 precursor, putative, expressed	
Relative dry weight	6	LOC_Os06g45030	transposon protein, putative, unclassified, expressed	
Relative dry weight	6	LOC_Os06g45040	B-box zinc finger family protein, putative, expressed	
Relative dry weight	6	LOC_Os06g45050	clathrin assembly protein, putative, expressed	At4g25940
Relative dry weight	6	LOC_Os06g45060	expressed protein	
Relative dry weight	6	LOC_Os06g45070	diphthamide biosynthesis protein 3, putative, expressed	At2g15910
Relative dry weight	6	LOC_Os06g45080	rabGAP/TBC domain-containing protein, putative, expressed	At4g29950
Relative dry weight	6	LOC_Os06g45090	expressed protein	
Relative dry weight	6	LOC_Os06g45100	FAD binding domain of DNA photolyase domain containing protein, expressed	At5g24850

## Appendices

Supplementary Table S12 (continued)

Trait	Chr	Gene ID	Putative function	Closest <i>Arabidopsis</i> homologue
Relative dry weight	6	LOC_Os06g45110	DNA binding protein, putative, expressed	At4g31350
Relative dry weight	6	LOC_Os06g45120	ATP synthase, putative, expressed	At1g78900
Relative dry weight	6	LOC_Os06g45130	expressed protein	
Relative dry weight	6	LOC_Os06g45140	bZIP transcription factor domain containing protein, expressed	At5g24800
Relative dry weight	6	LOC_Os06g45150	pollen allergen, putative, expressed	
Relative dry weight	6	LOC_Os06g45160	pollen allergen, putative, expressed	
Relative dry weight	6	LOC_Os06g45170	retrotransposon protein, putative, unclassified, expressed	
Relative dry weight	6	LOC_Os06g45180	pollen allergen, putative, expressed	
Relative dry weight	6	LOC_Os06g45184	retrotransposon protein, putative, Ty3-gypsy subclass, expressed	
Relative dry weight	6	LOC_Os06g45190	pollen allergen, putative, expressed	
Relative dry weight	6	LOC_Os06g45200	group 3 pollen allergen, putative, expressed	
Relative dry weight	6	LOC_Os06g45210	pollen allergen, putative, expressed	
Relative dry weight	6	LOC_Os06g45220	expressed protein	
Relative dry weight	6	LOC_Os06g45230	pollen allergen, putative, expressed	
Relative dry weight	6	LOC_Os06g45240	inactive receptor kinase At2g26730 precursor, putative, expressed	At1g50610
Relative dry weight	6	LOC_Os06g45250	tRNA pseudouridine synthase family protein, putative, expressed	At5g35400
Relative dry weight	6	LOC_Os06g45260	transposon protein, putative, unclassified, expressed	
Relative dry weight	6	LOC_Os06g45270	transposon protein, putative, unclassified, expressed	
Relative dry weight	6	LOC_Os06g45280	protein kinase APK1B, chloroplast precursor, putative, expressed	At2g07180
Relative dry weight	6	LOC_Os06g45290	pollen allergen, putative, expressed	
Relative dry weight	8	LOC_Os08g15070	GDU1, putative, expressed	At4g31730
Relative dry weight	8	LOC_Os08g15080	proline rich protein 3, putative, expressed	At3g21215
Relative dry weight	12	LOC_Os12g38400	MYB family transcription factor, putative, expressed	At2g37630
Relative dry weight	12	LOC_Os12g38410	TNP1, putative	
Relative dry weight	12	LOC_Os12g38420	expressed protein	
Relative dry weight	12	LOC_Os12g38430	SR repressor protein, putative, expressed	At3g55460
Relative dry weight	12	LOC_Os12g38440	XH domain containing protein, expressed	At1g15910
Relative dry weight	12	LOC_Os12g38450	exostosin family domain containing protein, expressed	At2g29040
Relative dry weight	12	LOC_Os12g38460	RNA recognition motif family protein, expressed	At3g28880
Relative dry weight	12	LOC_Os12g38470	expressed protein	
Relative dry weight	12	LOC_Os12g38480	expressed protein	
Relative dry weight	12	LOC_Os12g38490	SCARECROW, putative, expressed	At1g07530
Relative dry weight	12	LOC_Os12g38500	transposon protein, putative, unclassified, expressed	
Relative dry weight	12	LOC_Os12g38510	GRF zinc finger family protein	
Relative dry weight	12	LOC_Os12g38520	expressed protein	
Relative dry weight	12	LOC_Os12g38540	expressed protein	
Relative tiller number	1	LOC_Os01g72960	expressed protein	At5g09310
Relative tiller number	1	LOC_Os01g72970	DUF630/DUF632 domains containing protein, putative, expressed	At1g21740
Relative tiller number	1	LOC_Os01g72980	tRNA uridine 5-carboxymethylaminomethyl modification enzyme	
Relative single panicle weight	2	LOC_Os02g36090	gidA, putative, expressed	At2g13440
Relative single panicle weight	2	LOC_Os02g36100	expressed protein	
Relative single panicle weight	2	LOC_Os02g36110	retrotransposon protein, putative, Ty3-gypsy subclass, expressed	
Relative single panicle weight	2	LOC_Os02g36120	cytochrome P450, putative, expressed	At2g45570
Relative single panicle weight	2	LOC_Os02g36130	hypothetical protein	
Relative single panicle weight	2	LOC_Os02g36140	expressed protein	
Relative single panicle weight	2	LOC_Os02g36150	terpene synthase, putative, expressed	At1g79460
Relative single panicle weight	2	LOC_Os02g36160	cytochrome P450, putative, expressed	At5g25120
Relative single panicle weight	2	LOC_Os02g36170	transposon protein, putative, unclassified, expressed	
Relative single panicle weight	2	LOC_Os02g36180	retrotransposon protein, putative, Ty3-gypsy subclass	
Relative single panicle weight	2	LOC_Os02g36190	transposon protein, putative, unclassified, expressed	
Relative single panicle weight	2	LOC_Os02g36200	cytochrome P450, putative, expressed	At5g25120
Relative single panicle weight	2	LOC_Os02g36210	hypothetical protein	
Relative single panicle weight	2	LOC_Os02g36220	ent-kaurene synthase, chloroplast precursor, putative, expressed	At4g02780
Relative single panicle weight	2	LOC_Os02g36230	terpene synthase, putative, expressed	At1g79460
Relative single panicle weight	10	LOC_Os10g32920	ribosomal protein, putative, expressed	At3g04400
Relative single panicle weight	10	LOC_Os10g32930	expressed protein	
Relative single panicle weight	10	LOC_Os10g32940	expressed protein	
Relative single panicle weight	10	LOC_Os10g32950	retrotransposon protein, putative, unclassified, expressed	
Relative single panicle weight	10	LOC_Os10g32960	peroxisome assembly protein 12, putative, expressed	At3g04460
Relative single panicle weight	10	LOC_Os10g32970	eukaryotic translation initiation factor, putative, expressed	At5g35620
Relative single panicle weight	10	LOC_Os10g32980	CESA7 - cellulose synthase, expressed	At5g44030
Relative single panicle weight	10	LOC_Os10g32990	receptor-like protein kinase 2 precursor, putative, expressed	At1g35710
Relative single panicle weight	10	LOC_Os10g33000	retrotransposon protein, putative, unclassified, expressed	
Relative single panicle weight	10	LOC_Os10g33010	retrotransposon protein, putative, unclassified, expressed	
Relative single panicle weight	10	LOC_Os10g33020	expressed protein	
Relative single panicle weight	10	LOC_Os10g33030	expressed protein	At4g02210
Relative single panicle weight	10	LOC_Os10g33040	receptor-like protein kinase precursor, putative, expressed	At1g35710
Relative single panicle weight	10	LOC_Os10g33050	expressed protein	
Relative single panicle weight	10	LOC_Os10g33060	hcr2-5D, putative, expressed	At4g08850
Relative single panicle weight	10	LOC_Os10g33070	expressed protein	
Relative single panicle weight	10	LOC_Os10g33080	leucine-rich repeat receptor protein kinase EXS precursor, putative, expressed	At1g35710
Relative single panicle weight	10	LOC_Os10g33104	expressed protein	
Relative single panicle weight	10	LOC_Os10g33130	leucine-rich repeat receptor protein kinase EXS precursor, putative, expressed	At3g24240
Relative single panicle weight	10	LOC_Os10g33140	hcrVf2 protein, putative, expressed	At2g34930
Relative single panicle weight	10	LOC_Os10g33170	POT domain containing peptide transporter, putative, expressed	At5g46050
Relative single panicle weight	10	LOC_Os10g33190	expressed protein	

## Appendices

Supplementary Table S12 (continued)

Trait	Chr	Gene ID	Putative function	Closest <i>Arabidopsis</i> homologue
Relative single panicle weight	10	LOC_Os10g33200	expressed protein	
Relative single panicle weight	10	LOC_Os10g33204	hypothetical protein	
Relative SPAD	4	LOC_Os04g51610	calcium-transporting ATPase, plasma membrane-type, putative, expressed	At5g57110
Relative SPAD	4	LOC_Os04g51620	expressed protein	
Relative SPAD	4	LOC_Os04g51630	60S ribosomal protein L7, putative, expressed	At3g13580
Relative SPAD	4	LOC_Os04g51640	expressed protein	
Relative SPAD	4	LOC_Os04g51650	expressed protein	
Relative SPAD	4	LOC_Os04g51660	transferase family protein, putative, expressed	At3g29590
Relative SPAD	4	LOC_Os04g51680	expressed protein	At5g10695
Relative SPAD	4	LOC_Os04g51690	glycosyl hydrolase family 47 domain contain protein, expressed	At1g51590
Relative SPAD	4	LOC_Os04g51700	DNA ligase I, ATP-dependent family protein, expressed	At5g57160
Relative SPAD	4	LOC_Os04g51710	expressed protein	At1g16860
Relative SPAD	4	LOC_Os04g51720	retrotransposon protein, putative, unclassified, expressed	
Relative SPAD	4	LOC_Os04g51730	retrotransposon protein, putative, unclassified, expressed	
Relative SPAD	4	LOC_Os04g51740	retrotransposon protein, putative, Ty3-gypsy subclass	
Relative SPAD	4	LOC_Os04g51750	retrotransposon protein, putative, unclassified, expressed	
Relative SPAD	4	LOC_Os04g51760	expressed protein	
Relative SPAD	4	LOC_Os04g51770	expressed protein	At1g78890
Relative SPAD	4	LOC_Os04g51780	expressed protein	At4g29960
Relative SPAD	4	LOC_Os04g51786	containing DUF163, putative, expressed	At5g10620
Relative SPAD	4	LOC_Os04g51792	PAP fibrillin family domain containing protein, expressed	At5g19940
Relative SPAD	4	LOC_Os04g51794	DNA binding protein, putative, expressed	At4g31350
Relative SPAD	4	LOC_Os04g51796	DNA repair ATPase-related, putative, expressed	At2g24420
Relative SPAD	4	LOC_Os04g51800	MYB protein, putative, expressed	At4g09460
Relative SPAD	4	LOC_Os04g51809	expressed protein	
Relative SPAD	4	LOC_Os04g51820	OsHKT1;1 - Na <sup>+</sup> transporter, expressed	At4g10310
Relative SPAD	5	LOC_Os05g03620	TKL_IRAK_CR4L.4 - The CR4L subfamily has homology with Crinkly4, expressed	At3g55950
Relative SPAD	5	LOC_Os05g03630	dnaJ domain containing protein, expressed	At3g09810
Relative SPAD	5	LOC_Os05g03640	flavonol synthase/flavanone 3-hydroxylase, putative, expressed	At5g05600
Relative SPAD	5	LOC_Os05g03650	retrotransposon protein, putative, unclassified, expressed	
Relative SPAD	5	LOC_Os05g03660	retrotransposon protein, putative, unclassified, expressed	
Relative SPAD	5	LOC_Os05g03670	retrotransposon protein, putative, Ty3-gypsy subclass, expressed	
Relative SPAD	5	LOC_Os05g03680	retrotransposon protein, putative, unclassified, expressed	
Relative SPAD	5	LOC_Os05g03690	retrotransposon protein, putative, Ty3-gypsy subclass, expressed	
Relative SPAD	5	LOC_Os05g03700	hypothetical protein	
Relative SPAD	5	LOC_Os05g03710	retrotransposon protein, putative, unclassified	
Relative SPAD	5	LOC_Os05g03730	retrotransposon protein, putative, unclassified	
Relative SPAD	5	LOC_Os05g03740	transcription factor TF2, putative, expressed	At2g38250
Relative SPAD	5	LOC_Os05g03750	expressed protein	
Relative SPAD	5	LOC_Os05g03760	zinc finger family protein, putative, expressed	At5g58620
Relative SPAD	5	LOC_Os05g03770	expressed protein	
Relative SPAD	5	LOC_Os05g03780	cation efflux family protein, putative, expressed	At2g46800
Relative SPAD	5	LOC_Os05g03790	expressed protein	
Relative SPAD	5	LOC_Os05g05200	O-acyltransferase, putative, expressed	At1g57600
Relative SPAD	5	LOC_Os05g05210	WD domain, G-beta repeat domain containing protein, expressed	At4g03020

The trait, chromosome number, gene ID, putative function, closest *Arabidopsis* homologue and gene ontology (GO) are shown. All information was obtained from MSU rice genome database (<http://rice.plantbiology.msu.edu/>, as of March 2014). The closest homologue of *Arabidopsis* was listed only when available in the database. The gray colour means either the gene is a transposable element or not expressed.

Appendices

Supplementary Table S13: Heritability of each trait.

<b>Trait</b>	<b>Genetic variance</b>	<b>Residual variance</b>	<b>Heritability (<math>h^2</math>)</b>
Square-root transformed leaf bronzing score	0.09	0.18	0.33
Relative plant height	8.38	17.13	0.33
Relative dry weight	156.41	661.14	0.19
Relative tiller number	143.13	403.28	0.26
Relative thousand kernel weight	18.42	243.67	0.07
Relative total panicle weight	0.02	1798.91	0.00
Relative single panicle weight	487.36	833.63	0.37
Relative SPAD	21.66	47.40	0.31
Lignin content	0.07	0.03	0.74
Relative lignin content	14.54	150.24	0.09
Average			0.27

## Supplementary data for Chapter 5

### Supplementary Protocol S3

#### *Gene ontology (GO) enrichment analysis of microarray datasets*

An original microarray dataset was obtained from the study by Frei *et al.* (2010), where the cultivar Nipponbare was subjected to comparative microarray together with two chromosomal segment substitution lines (SL15 and SL41; detailed in Chapter 1). Only Nipponbare and SL41 were used for the GO enrichment analysis because of lack of detailed physiological studies with SL15. Statistical analyses were conducted again using only Nipponbare and SL41 as in Frei *et al.* (2010). Raw *P* values were used rather than adjusted false-discovery rate (FDR) to determine differentially expressed genes because too few genes showed significance after the FDR correction. Raw *P* value of 0.05 was considered significant. The genes which showed significant up-regulation in SL41, significant down-regulation in SL41, and a significant interaction between genotype and treatment were curated. The gene IDs in the original file (RAP-DB IDs) were converted to MSU IDs on RAP-DB website (<http://rapdb.dna.affrc.go.jp/>, as of November 2014) since only MSU ID was compatible with the subsequent analysis. GO enrichment analysis was conducted using Rice Oligonucleotide Array Database (<http://www.ricearray.org/index.shtml>, as of November 2014; Cao *et al.*, 2012). Each set of genes was loaded into the database, and the enriched GO terms were determined in the category of ‘Biological process’, ‘Cellular component’ and ‘Molecular function’. The calculated *P* values (Hyper *P* values) were corrected for multiple comparison according to the method of Benjamini and Hochberg (1995). Adjusted FDR of 0.05 was considered significant. Only over-represented GO terms were shown on the list.

The same analysis was conducted for another comparative microarray study using Nipponbare and SL46, which carry the biomass-related QTL *OzT8* from Kasalath. The experimental details are given in the table legend.

---

**Supplementary References**

- Benjamini Y, Hochberg Y.** 1995. Controlling the false discovery rate: A practical and powerful approach to multiple testing. *Journal of the Royal Statistical Society. Series B (Methodological)* **57**, 289–300.
- Booker F, Burkey K, Morgan P, Fiscus E, Jones A.** 2012. Minimal influence of G-protein null mutations on ozone-induced changes in gene expression, foliar injury, gas exchange and peroxidase activity in *Arabidopsis thaliana* L. *Plant, Cell and Environment* **35**, 668–681.
- Bradford MM.** 1976. A rapid and sensitive method for the quantitation of microgram quantities of protein utilizing the principle of protein-dye binding. *Analytical Biochemistry* **72**, 248–254.
- Cho K, Shibato J, Agrawal GK, et al.** 2008. Integrated transcriptomics, proteomics, and metabolomics analyses to survey ozone responses in the leaves of rice seedling. *Journal of Proteome Research* **7**, 2980–2998.
- Cao P, Jung K-H, Choi D, Hwang D, Zhu J, Ronald PC.** 2012. The Rice Oligonucleotide Array Database: an atlas of rice gene expression. *Rice* **5**, 17.
- Chujo T, Miyamoto K, Shimogawa T, et al.** 2013. OsWRKY28, a PAMP-responsive transrepressor, negatively regulates innate immune responses in rice against rice blast fungus. *Plant molecular biology* **82**, 23–37.
- Curtis MD, Grossniklaus U.** 2003. A gateway cloning vector set for high-throughput functional analysis of gene in planta. *Plant Physiology* **133**, 462–469.
- Frei M, Tanaka JP, Chen CP, Wissuwa M.** 2010. Mechanisms of ozone tolerance in rice: characterization of two QTLs affecting leaf bronzing by gene expression profiling and biochemical analyses. *Journal of Experimental Botany* **61**, 1405–1417.
- Ishihama N, Yamada R, Yoshioka M, Katou S, Yoshioka H.** 2011. Phosphorylation of the *Nicotiana benthamiana* WRKY8 transcription factor by MAPK functions in the defense response. *The Plant Cell* **23**, 1153–1170.
- Ke Y, Liu H, Li X, Xiao J, Wang S.** 2014. Rice OsPAD4 functions differently from Arabidopsis AtPAD4 in host-pathogen interactions. *The Plant Journal* **78**, 619–631.
- Kilian J, Whitehead D, Horak J, et al.** 2007. The AtGenExpress global stress expression data set: protocols, evaluation and model data analysis of UV-B light, drought and cold stress responses. *The Plant Journal* **50**, 347–363.
- Kyndt T, Nahar K, Haegeman A, De Vleeschauwer D, Höfte M, Gheysen G.** 2012. Comparing systemic defence-related gene expression changes upon migratory and sedentary nematode attack in rice. *Plant Biology* **14**, 73–82.
- Lima JC, Arenhart RA, Margis-Pinheiro M, Margis R.** 2011. Aluminum triggers broad changes in microRNA expression in rice roots. *Genetics and Molecular Research* **10**, 2817–2832.

- Lin Y, Gu X, Tang H, Hou Y, Yu D, Zhang X.** 2013. Cloning and expression analysis of an ascorbate oxidase (AO) gene from strawberry (*Fragaria×ananassa* cv. Toyonaka). *Journal of Agricultural Science* **5**, 14-22.
- Mao C, Wang S, Jia Q, Wu P.** 2006. *OsEIL1*, a rice homolog of the *Arabidopsis EIN3* regulates the ethylene response as a positive component. *Plant molecular biology* **61**, 141-152.
- McNally KL, Childs KL, Bohnert R, et al.** 2009. Genomewide SNP variation reveals relationships among landraces and modern varieties of rice. *Proceedings of the National Academy of Sciences of the United States of America* **106**, 12273–12278.
- Minh-Thu P-T, Hwang D-J, Jeon J-S, Nahm BH, Kim Y-K.** 2013. Transcriptome analysis of leaf and root of rice seedling to acute dehydration. *Rice* **6**, 38.
- Nahar K, Kyndt T, De Vleeschauwer D, Höfte M, Gheysen G.** 2011. The jasmonate pathway is a key player in systemically induced defense against root knot nematodes in rice. *Plant Physiology* **157**, 305–316.
- Oono Y, Kawahara Y, Yazawa T, et al.** 2013. Diversity in the complexity of phosphate starvation transcriptomes among rice cultivars based on RNA-seq profiles. *Plant molecular biology* **83**, 523–537.
- Ramonell K, Berrocal-Lobo M, Koh S, Wan J, Edwards H, Stacey G, Somerville S.** 2005. Loss-of-function mutations in chitin responsive genes show increased susceptibility to the powdery mildew pathogen *Erysiphe cichoracearum*. *Plant Physiology* **138**, 1027–1036.
- Rzewuski G, Sauter M.** 2008. Ethylene biosynthesis and signaling in rice. *Plant Science* **175**, 32–42.
- Szewczyk E, Nayak T, Oakley CE, et al.** 2006. Fusion PCR and gene targeting in *Aspergillus nidulans*. *Nature protocol* **1**, 3111–3120.
- Tamura K, Peterson D, Peterson N, Stecher G, Nei M, Kumar S.** 2011. MEGA5: Molecular evolutionary genetics analysis using maximum likelihood, evolutionary distance, and maximum parsimony methods. *Molecular Biology and Evolution* **28**, 2731–2739.
- Tintor N, Ross A, Kanehara K, et al.** 2013. Layered pattern receptor signaling via ethylene and endogenous elicitor peptides during *Arabidopsis* immunity to bacterial infection. *Proceedings of the National Academy of Sciences of the United States of America* **110**, 6211–6216.
- Tuomainen J, Betz C, Kangasjärvi J, Ernst D, Yin Z-H, Langebartels C, Sandermann H.** 1997. Ozone induction of ethylene emission in tomato plants: regulation by differential accumulation of transcripts for the biosynthetic enzymes. *The Plant Journal* **12**, 1151–1162.
- Varadaraj K, Skinner DM.** 1994. Denaturants or cosolvents improve the specificity of PCR amplification of a G+C-rich DNA using genetically engineered DNA polymerases. *Gene* **140**, 1–5.



- De Vos M, Van Oosten VR, Van Poecke RMP, et al.** 2005. Signal signature and transcriptome changes of *Arabidopsis* during pathogen and insect attack. *Molecular Plant-Microbe Interactions* **18**, 923-937.
- Walia H, Wilson C, Condamine P, et al.** 2005. Comparative transcriptional profiling of two contrasting rice genotypes under salinity stress during the vegetative growth stage. *Plant Physiology* **139**, 822–835.
- Widodo B, Broadley MR, Rose T, et al.** 2010. Response to zinc deficiency of two rice lines with contrasting tolerance is determined by root growth maintenance and organic acid exudation rates, and not by zinc-transporter activity. *New Phytologist* **186**, 400–414.
- Yau CP, Wang L, Yu M, Zee SY, Yip WK.** 2004. Differential expression of three genes encoding an ethylene receptor in rice during development, and in response to indole-3-acetic acid and silver ions. *Journal of Experimental Botany* **55**, 547-556.
- Yun K-Y, Park MR, Mohanty B, et al.** 2010. Transcriptional regulatory network triggered by oxidative signals configures the early response mechanisms of japonica rice to chilling stress. *BMC plant biology* **10**, 16.
- Zarivi O, Bonfigli A, Colafarina S, Aimola P, Ragnelli AM, Miranda M, Pacioni G.** 2013. Transcriptional, biochemical and histochemical investigation on laccase expression during *Tuber melanosporum* Vittad. development. *Phytochemistry* **87**, 23-29.
- Zhang Z, Schäffer AA, Miller W, Madden TL, Lipman DJ, Koonin EV, Altschul SF.** 1998. Protein sequence similarity searches using patterns as seeds. *Nucleic acids research* **26**, 3986-3990.
- Zhao K, Wright M, Kimball J, et al.** 2010. Genomic diversity and introgression in *O. sativa* reveal the impact of domestication and breeding on the rice genome. *PLoS one* **5**, e10780.

## Peer-review publications

**Ueda Y, Wu L, Frei M.** 2013. A critical comparison of two high-throughput ascorbate analyses methods for plant samples. *Plant Physiology and Biochemistry* **70**, 418–423.

Contribution: All the experiments except for iron stress treatment. Data analysis and manuscript preparation.

**Ueda Y, Frimpong F, Qi Y, Matthus E, Wu L, Höller S, Kraska T, Frei M.** 2015. Genetic dissection of ozone tolerance in rice (*Oryza sativa* L.) by genome-wide association study. *Journal of Experimental Botany* **66**, 293–306.

Contribution: Leading the experiment at the experimental site, large part of phenotyping (LBS measurement, lignin quantification, height measurement and tiller number counting), all the statistical and bioinformatic analyses and manuscript preparation.

**Ueda Y, Siddique S, Frei M.** 2015. A novel gene, *OZONE-RESPONSIVE APOPLASTIC PROTEINI*, enhances cell death in ozone stress in rice. *Plant Physiology* [In Press].

Contribution: All the experiments except for confocal microscope imaging and genotyping of rice mutants. Statistical and bioinformatic analyses and manuscript preparation.

**Matthus E, Wu L-B, Ueda Y, Höller S, Becker M, Frei M.** 2015. Loci, genes and mechanisms associated with tolerance to ferrous iron toxicity in rice (*Oryza sativa* L.). *Theoretical and Applied Genetics*. [In Press]

Contribution: Part of phenotyping (shoot/root length measurement and tiller number counting). Establishment of DNA sequencing protocol and mapping method. Q value computation and discussion.

**Höller S, Ueda Y, Wu L, Wang Y, Hejirezaei M-R, Ghaffari M-R, von Wirén N, Frei M.** 2015. Ascorbate biosynthesis in rice (*Oryza sativa* L.) and its involvement in stress tolerance and plant development. *Plant molecular biology* **88**, 545-560.

Contribution: System setup for ozone stress treatment and ozone concentration measurement.

**Wu L-B, Ueda Y, Lai S-K, Frei M.** 2015. Shoot tolerance mechanisms to iron toxicity in rice (*Oryza sativa* L.) – evidence for a pro-oxidant activity of ascorbate. *Under review*.

Contribution: Support in the greenhouse experiment, hypothesis testing experiments and part of qPCR experiments.

## Other scientific activities

### Conference participation

28th-31st January 2013: ICP Vegetation 26th Task Force Meeting. Halmstad, Sweden.

<Oral Presentation>

○ **Ueda Y, Wang Y, Wissuwa M, Frei M.** Genetic approaches to increase tolerance to ozone in rice. Abstract pp. 41.

17th-19th July 2013: 11th International POG Conference–Reactive Oxygen and Nitrogen Species in Plants. Warsaw, Poland.

<Poster Presentation>

○ **Ueda Y, Wang Y, Frei M.** The role of ascorbate oxidase under ozone stress in rice. Abstract pp. 199. (in *Journal of Biotechnology, Computational Biology and Bionanotechnology* **94**, 2013)

\* Best Poster Award

18th-21st May 2014: International Conference on Ozone and Plants. Beijing, China.

<Oral Presentation>

○ **Ueda Y, Frimpong F, Qi Y, Matthus E, Wu L, Höller S, Kraska T, Frei M.** A Genome-wide association study (GWAS) reveals genetic factors underlying ozone tolerance in rice (*Oryza sativa* L.). Abstract pp. S3–15.

24th-26th June 2015: 12th International Conference on Reactive Oxygen and Nitrogen Species in Plants: from model systems to field. Verona, Italy.

<Poster Presentation>

○ **Ueda Y, Siddique S, Frei M.** Characterization of OsORAP1, a novel positive regulator of cell death under ozone stress in rice (*Oryza sativa* L.). Abstract pp. 98.

### Research stay

3rd-16th March 2013: The International Rice Research Institute (IRRI). Los Baños, The Philippines.

## Curriculum Vitae

**Name:** Yoshiaki Ueda

**Place of Birth:** Okayama, Japan

**Nationality:** Japanese

**Education:**

April 2003–March 2006: Okayama-Asahi High School, Okayama

April 2006–March 2008: College of Arts and Sciences, The University of Tokyo

April 2008–March 2010: Faculty of Agriculture, The University of Tokyo

Bachelor thesis title: ‘The effect of ozone stress on the gene expression in rice (*Oryza sativa* L.) [In Japanese]’

April 2010–March 2012: Graduate School of Agricultural and Life Sciences, The University of Tokyo

Master thesis title: ‘How does ozone cause reactive oxygen formation and damage to photosystem II in rice leaves?–Elucidation of mechanisms’

May 2012–present: Institute of Crop Science and Resource Conservation (INRES), University of Bonn

**Work experience:**

April 2012: Research fellow, Laboratory of Plant Biotechnology, The University of Tokyo

**Awards:**

July 2013: Best poster award (POG President – Stanisław Karpiński Award) in *11th International POG conference (Reactive Oxygen and Nitrogen Species in Plants)*. Warsaw, Poland.

March 2013, May 2014: Conference travel grant. *Theodor-Brinkmann-Graduate School*. Bonn, Germany.